Systems, Structure and Control

Systems, Structure and Control

Edited by
Petr Husek

I-Tech

Published by In-Teh

In-Teh is Croatian branch of I-Tech Education and Publishing KG, Vienna, Austria.

www.in-teh.org
Additional copies can be obtained from:
publication@ars-journal.com

First published August 2008
Printed in Croatia

A catalogue record for this book is available from the University Library Rijeka under no. 111221000
System, Structure and Control, Edited by Petr Husek
p. cm.
ISBN 978-953-7619-05-3
1. Systems. 2. Control. I. Petr Husek

Preface

The title of the book System, Structure and Control encompasses broad field of theory and applications of many different control approaches applied on different classes of dynamic systems. Output and state feedback control include among others robust control, optimal control or intelligent control methods such as fuzzy or neural network approach, dynamic systems are e.g. linear or nonlinear with or without time delay, fixed or uncertain, onedimensional or multidimensional. The applications cover all branches of human activities including any kind of industry, economics, biology, social sciences etc. Naturally it is not purpose of this book in few chapters neither to provide a comprehensive survey of all the above mentioned disciplines nor to give a detailed study of any of them. Nevertheless, the following 11 chapters demonstrate that even today after several decades of intensive effort of many researchers and practitioners the area of control of dynamic systems still brings new challenging problems and produces solutions of many of them.

The brief outline of the volume is as follows.

In chapter 1 a new method for design of state-derivative feedback control of linear systems is presented. State–derivative feedback can be considered as a generalization of classical state feedback in those applications where state derivative is easier to obtain then the direct state, e.g. in vibration attenuation control of many mechanical systems including car suspension systems, bridge cables or landing gear components. In the contribution an extension of known methods for descriptor systems with polytopic parameter uncertainty is presented.

Chapter 2 is concerned with the problem of stability analysis of linear systems with time delays. Such systems naturally occur very often, e.g. in network control or remote control via satellite. Time-delayed systems are of great interest for many decades but still many questions remain unanswered or achieved results are too conservative. Here an improved time-domain delay-dependent (i.e. taking into account the magnitude of time delay) approach result for both continuous and discrete time systems is presented. The obtained result is also applied on stability analysis of large scale systems.

The problem of state observation of nonlinear systems using differential neural network is addressed in chapter 3. State observation is very important in those applications where we would like to use the advantages of state feedback but the states are not accessible. Many different techniques have been already used to solve the problem. In the contribution approximation properties of a class of dynamic neural networks are used for state observation of uncertain nonlinear systems affected by bounded external perturbations.

In chapter 4 sliding mode control is designed and applied on control of electric power systems. Such systems are modeled as complex large-scale systems which are difficult to control. Sliding mode control is one of the most used and effective control approaches to nonlinear systems, especially when disturbances and parameter variations are present. In the contribution combination of block control, integral sliding control and nested sliding mode control is applied.

Chapter 5 deals with the problem of robust stability analysis of linear systems with parametric uncertainty. The case is considered where the coefficients of characteristic polynomial depend polynomically on system parameters that are allowed to vary in prescribed mutually independent intervals. Such problem is generally difficult to solve due to its non-convexity. Here an iterative algorithm based on testing the value set is introduced.

Parameter estimation applied on fouling detection in ducts presented in chapter 6 demonstrates practical usability of theoretical methods. Electric pulses of ultrasonic transducers are transmitted through the pipelines and received, amplified and filtered. The ultrasonic pulses are modeled as a nonlinear process affected by Gaussian noise. The parameters of the model are estimated using nonlinear estimation methods.

In chapter 7 fuzzy controllers are designed for stabilization of nonlinear systems described by Takagi-Sugeno fuzzy models. Takagi-Sugeno fuzzy models proved to be a useful tool for modeling nonlinear systems which offers systematic way for analysis of their behavior. The feedback controllers and the controlled systems do not share the same membership functions that makes the controller design more complicated. The design is based on membership function dependent Lyapunov approach with common Lyapunov matrix considered for all subsystems.

Global synchronization of Kuramoto coupled oscillators is studied in chapter 8. Kuramoto models serve as good approximation of many systems in different fields, e.g. biology, physics or mechanics. In recent years much attention has been devoted to investigation of local stability properties but collective synchronization which is important in many applications has been studied only for last few years. The contribution stresses the importance of algebraic structure of interconnection graphs for ensuring the global attraction domain of coupled oscillators.

Chapter 9 is devoted to stability analysis of n-D systems that are widely used e.g. in modeling of parameter distributed systems. The contribution shows differences between stability definitions of univariate and multivariate polynomials and presents an algorithm for Schur stability test of bivariate polynomials. The algorithm is also used for Hurwitz stability analysis of continuous-time polynomials employing generalization of Moebius transformation.

In chapter 10 problem of tuning of fixed order and fixed structure controllers for linear systems in LQ and H2 framework is addressed. Tuning is employed by open loop frequency response shaping which is very popular because it guarantees not only stability of closed loop but also good performance even if some uncertainty is present. The method can be used e.g. for tuning of PID controllers – the most used controllers in industry.

Utilization of exponential holder together with sliding mode control for sampled data systems is the topic of chapter 11. The contribution demonstrates the advantage of exponential holder to zero order hold by ensuring asymptotic tracking of reference signal when the proposed controller is applied on the original continuous system. In this case ripple-free behavior of closed loop system even for nonconstant reference signal is guaranteed.

Editor

Petr Husek
Czech Technical University in Prague
Czech Republic

Contents

1

Control Designs for Linear Systems Using State-Derivative Feedback

Rodrigo Cardim, Marcelo C. M. Teixeira, Edvaldo Assunção and Flávio A. Faria
UNESP - São Paulo State University, Department of Electrical Engineering Brazil

1. Introduction

From classical control theory, it is well-known that state-derivative feedback can be very useful, and even in some cases essential to achieve a desired performance. Moreover, there exist some practical problems where the state-derivative signals are easier to obtain than the state signals. For instance, in the following applications: suppression of vibration in mechanical systems, control of car wheel suspension systems, vibration control of bridge cables and vibration control of landing gear components. The main sensors used in these problems are accelerometers. In this case, from the signals of the accelerometers it is possible to reconstruct the velocities with a good precision but not the displacements. Defining the velocities and displacement as the state variables, then one has available for feedback the state-derivative signals. Recent researches about state-derivative feedback design for linear systems have been presented. The procedures consider, for instance, the pole placement problem (Abdelaziz & Valášek, 2004; Abdelaziz & Valášek, 2005), and the design of a Linear Quadratic Regulator (Duan et al., 2005). Unfortunately these results are not applied to the control of uncertain systems or systems subject to structural failures. Another kind of control design is the use of state-derivative and state feedback. It has been used by many researches for applications in descriptor systems (Nichols et al., 1992; A. Bunse-Gerstner & Nichols, 1999; Duan et al., 1999; Duan & Zhang, 2003). However, usually these designs are more complex than the design procedures with only state or state-derivative feedback.
In this chapter two new control designs using state-derivative feedback for linear systems are presented. Firstly, considering linear descriptor plants, a simple method for designing a state-derivative feedback gain using methods for state feedback control design is proposed. It is assumed that the descriptor system is a linear, time-invariant, Single-Input (SI) or Multiple-Input (MI) system. The procedure allows that the designers use the well-known state feedback design methods to directly design state-derivative feedback control systems. This method extends the results described in (Cardim et al., 2007) and (Abdelaziz & Valášek, 2004) to a more general class of control systems, where the plant can be a descriptor system. As the first design can not be directly applied for uncertain systems, then a design considering LMI formulation is presented. This result can be used to solve systems with polytopic uncertainties in the plant parameters, or subject to structural failures. Furthermore, it can include as design specifications the decay rate and bounds on the output

peak, and on the state-derivative feedback matrix K. When feasible, LMI can be easily solved using softwares based on convex programming, for instance MATLAB. These new control designs allow new specifications, and also consider a broader class of plants than the related results available in the literature (Abdelaziz & Valášek, 2004; Duan et al., 2005; Assunção et al., 2007c). The proposed method extends the results presented in (Assunção et al., 2007c), because it can also be applied for the control of uncertain systems subject to structural failures. Examples illustrate the efficiency of these procedures.

2. Design of State-Derivative Feedback Controllers for Descriptor Systems Using a State Feedback Control Design

In this section, a simple method for designing a state-derivative feedback gain using methods for state feedback control design, where the plant can be a descriptor system, is proposed.

2.1 Statement of the Problem

Consider a controllable linear descriptor system described by

$$E\dot{x}(t) = Ax(t) + Bu(t), \qquad x(0) = x_0, \tag{1}$$

where $E \in \mathbb{R}^{n\times n}, x(t) \in \mathbb{R}^n$ is the state vector and $u(t) \in \mathbb{R}^m$ is the control input vector. It is assumed that $1 \le m \le n$, and also, $A \in \mathbb{R}^{n\times n}$ and $B \in \mathbb{R}^{n\times m}$ are time-invariant matrices. Now, consider the state-derivative feedback control

$$u(t) = -K_d \dot{x}(t)\,. \tag{2}$$

Then, the problem is to obtain a state-derivative feedback gain K_d, using state feedback techniques, such that the poles of the controlled system (1), (2) are arbitrarily specified by a set $\{\lambda_1, \lambda_2, ..., \lambda_n\}$, where $\lambda_i \in \mathbb{C}$ and $\lambda_i \neq 0$, $i = 1, 2, ..., n$, such that this closed-loop systems presents a suitable performance. The motivation of this study was to investigate the possibility of designing state-derivative gains using state feedback design methods. This procedure allows the designers to use well-known methods for pole-placement using state feedback, available in the literature, for state-derivative feedback design (Chen, 1999; Valášek & Olgac, 1995*a*; Valášek & Olgac, 1995*b*). To establish the proposed results, consider the following assumptions:

(A) $rank\,[E \mid B] = n$;
(B) $rank\,[A] = n$;
(C) $rank\,[B] = m$.

Remark 1. *It is known (Bunse-Gerstner et al, 1992; Duan et al, 1999) that if Assumption (A) holds, then there exists K_d such that:*

$$rank[E + BK_d] = n. \tag{3}$$

Assumption (B) was also considered in (Abdelaziz & Valášek, 2004) and, as will be described below, is important for the stability of the system (1), with the proposed method and the control law $u = -K_d\dot{x}$. Assumption (C) means that B is a full rank matrix. For K_d

such that (3) holds, then from (2) it follows that (1) can be rewrite such as a standard linear system, given by:

$$E\dot{x}(t) = Ax(t) - BK_d\dot{x}(t), \tag{4}$$

$$\dot{x}(t) = (E + BK_d)^{-1}Ax(t). \tag{5}$$

From (5) note that if *rank(A)* < *n*, then the controlled system (1), (2) given by (5) is unstable, because it presents at least one pole equal to zero. It is known that the stability problem for descriptor systems is much more complicated than for standard systems, because it is necessary to consider not only stability, but also regularity (Bunse-Gerstner et al., 1992; S. Xu & J. Lam, 2004). In this work, a descriptor system is regular if it has uniqueness in the solutions and avoid impulsive responses. In the next section, the proposed method is presented.

2.2 Design of State-Derivative Feedback Using a State Feedback Design

Lemma 1 below will be very useful in the analysis of the method that solves the proposed problem.

Lemma 1. *Consider a matrix* $Z \in \mathbb{R}^{n\times n}$ *, with rank(Z) = n and eigenvalues equal to* $\lambda_1, \lambda_2, \ldots, \lambda_n$ *. Then, the eigenvalues of* Z^{-1} *are the following*: $\lambda_1^{-1}, \lambda_2^{-1}, \ldots, \lambda_n^{-1}$.

Proof: For each eigenvalue $\lambda \in \{\lambda_1, \lambda_2, \ldots, \lambda_n\}$ of *Z*, there exists an eigenvector *v* such that

$$Zv = \lambda v\,. \tag{6}$$

Considering that *rank(Z)* = *n*, then $\lambda \neq 0$. Therefore, from (6),

$$v = Z^{-1}\lambda v \Rightarrow \lambda^{-1}v = Z^{-1}v\,, \tag{7}$$

and so λ^{-1} is an eigenvalue of Z^{-1} .

Remark 2. *Consider that* $\lambda = a + jb$ *is an eigenvalue of Z. Then, from Lemma 1,* $\lambda^{-1} = (a+jb)^{-1} = \frac{a}{a^2+b^2} - j\frac{b}{a^2+b^2}$ *is also an eigenvalue of* Z^{-1} *. Therefore, note that the real parts of the* λ *and* λ^{-1} *present the same signal. So, if Z is Hurwitz (it has all eigenvalues with negative real parts), then* Z^{-1} *will be also Hurwitz.*

Now, the main result of this section will be presented.

Theorem 1. *Define the matrices:*

$$A_n = A^{-1}E \qquad \text{and} \qquad B_n = -A^{-1}B \tag{8}$$

and suppose that (A_n, B_n) *is controllable. Let* K_d *be a state feedback gain, such that* {$\lambda_1^{-1}, \lambda_2^{-1}, \ldots, \lambda_n^{-1}$} *are the poles of the closed-loop system*

$$\dot{x}_n(t) = A_n x_n(t) + B_n u_n(t)\,, \tag{9}$$

$$u_n(t) = -K_d x_n(t)\,, \tag{10}$$

where $\lambda_i \in \mathbb{C}$ *and* $\lambda_i \neq 0$*, i = 1,2,...,n, are arbitrarily specified. Then, for this gain* K_d*,* $\{\lambda_1, \lambda_2, ..., \lambda_n\}$ *are the poles of the controlled system with state-derivative feddback (1), (2) and also, the condition (3) holds.*

Proof: Considering that (A_n, B_n) is controllable, then one can find a state feedback gain K_d such that the controlled system with state feedback (9), (10), given by

$$\dot{x}_n(t) = (A_n - B_n K_d) x_n(t) . \tag{11}$$

has poles equal to $\lambda_1^{-1}, \lambda_2^{-1}, ..., \lambda_n^{-1}$ (Chen, 1999). Now, from $A_n = A^{-1}E, B_n = -A^{-1}B$ and $\lambda_i \neq 0$, i = 1, 2,..., n, note that

$$(A_n - B_n K_d)^{-1} = [A^{-1}(E + BK_d)]^{-1} \tag{12}$$

$$= (E + BK_d)^{-1} A \tag{13}$$

and from (11) and Lemma 1, $\lambda_1, \lambda_2, ..., \lambda_n$ are the eigenvalues of $(E + BK_d)^{-1} A$. Therefore (3) holds, the state-derivative feedback system (1) and (2) can be described by (5) and presents poles equal to $\lambda_1, \lambda_2, ..., \lambda_n$.

This result is a generalization of the methods proposed in (Abdelaziz & Valášek, 2004) and (Cardim et al., 2007), because it can be applied in the control of descriptor systems (1), with $det(E) = 0$.

2.3 Examples

The effectiveness of the proposed methods designs is demonstrated by simulation results.

First Example

A simple electrical circuit, can be represented by the linear descriptor system below (Nichols et al, 1992):

$$\begin{bmatrix} 0 & 1 \\ 0 & 0 \end{bmatrix} \begin{bmatrix} \dot{x}_1(t) \\ \dot{x}_2(t) \end{bmatrix} = \begin{bmatrix} 1 & 0 \\ 0 & 1 \end{bmatrix} \begin{bmatrix} x_1(t) \\ x_2(t) \end{bmatrix} + \begin{bmatrix} 0 \\ 1 \end{bmatrix} u(t) , \tag{14}$$

where x_1 is the current and the x_2 is the potential of a capacitor. In this system one has:

$$E = \begin{bmatrix} 0 & 1 \\ 0 & 0 \end{bmatrix}, \qquad A = \begin{bmatrix} 1 & 0 \\ 0 & 1 \end{bmatrix}, \qquad B = \begin{bmatrix} 0 \\ 1 \end{bmatrix}, \tag{15}$$

Consider the pole placement as design technique, using the state derivative feedback (2) with the feedback gain matrix K_d. In this example, the suitable closed-loop poles for the controlled system (2) and (14) are the following:

$$\lambda_1 = -2 + 1i, \qquad \lambda_2 = -2 - 1i$$

Note that, the system (14) with the control signal (2) satisfies the Assumptions A, B and C. From (8) one has:

$$A_n = \begin{bmatrix} 0 & 1 \\ 0 & 0 \end{bmatrix}, \qquad B_n = \begin{bmatrix} 0 \\ -1 \end{bmatrix}, \tag{16}$$

and (A_n, B_n) is controllable.
From Theorem 1, the poles for the new closed-loop system with state feedback (9) and (10) with A_n and B_n given in (8) are the following:

$$\lambda_1^{-1} = -0.40 - 0.20i, \qquad \lambda_2^{-1} = -0.40 + 0.20i.$$

So, one can obtain by using the command *acker* of MATLAB (Ogata, 2002), the feedback gain matrix K_d below:

$$K_d = [\ -0.20 \quad -0.80\ ]. \tag{17}$$

Figures 1 and 2 show the simulation results of the controlled system (5) with the initial condition $x(0) = [1\ 0]^T$. In this example the validity and simplicity of the proposed method can be observed.
Example 2
Consider a linear descriptor MI system described by the following equations:

$$\begin{bmatrix} 0 & 0 \\ 1 & 0 \end{bmatrix}\begin{bmatrix} \dot{x}_1(t) \\ \dot{x}_2(t) \end{bmatrix} = \begin{bmatrix} -0.800 & 0.020 \\ -0.020 & 0 \end{bmatrix}\begin{bmatrix} x_1(t) \\ x_2(t) \end{bmatrix} + \begin{bmatrix} 0.050 & 1 \\ 0.001 & 0 \end{bmatrix} u(t), \tag{18}$$

where $u(t) = [u_1(t)\ \ u_2(t)]^T$.
The wanted poles for closed-loop system with the control law $u(t) = -K_d \dot{x}(t)$ are given by:

$$\lambda_1 = -2 + 1i, \qquad \lambda_2 = -2 - 1i\ .$$

Observe that, the system (18) with the control signal (2) satisfies the Assumptions A, B and C. From (8) one has:

$$A_n = \begin{bmatrix} -50 & 0 \\ -2000 & 0 \end{bmatrix}, \qquad B_n = \begin{bmatrix} 0.050 & 0 \\ -0.500 & -50 \end{bmatrix}, \tag{19}$$

and (A_n, B_n) is controllable.
From Theorem 1, the poles for the new closed-loop system with state feedback (11), with A_n and B_n given in (19) are the following:

$$\lambda_1^{-1} = -0.40 - 0.20i, \qquad \lambda_2^{-1} = -0.40 + 0.20i.$$

So, with these parameters, one can obtain with the command *place* of MATLAB, the feedback gain matrix K_d below:

$$K_d = \begin{bmatrix} -992.0000 & 4.0000 \\ 49.9240 & -0.0480 \end{bmatrix}. \tag{20}$$

Figures 3 and 4 show the simulation results of the controlled system with state-derivative feedback, given by (2), (18) and (20) that can be described by (5), with the initial condition $x_0 = [1\ 0]^T$.

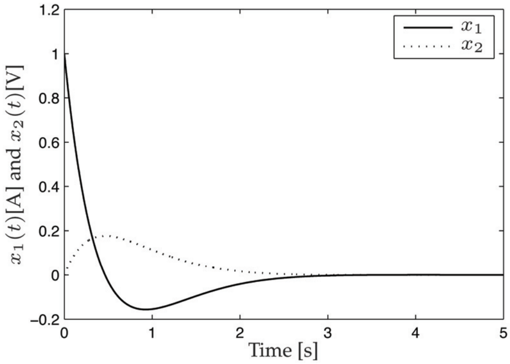

Figure 1. Transient response of the controlled system (Example 1), for $x_0 = [1\ 0]^T$

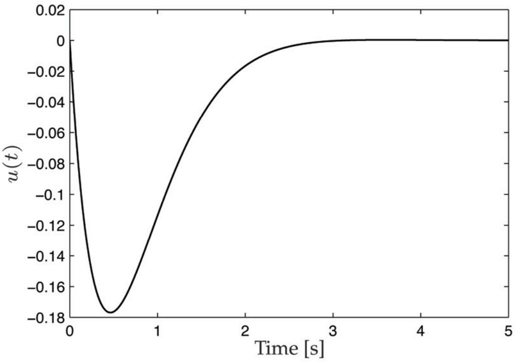

Figure 2. Control inputs of the controlled system (Example 1), for $x_0 = [1\ 0]^T$

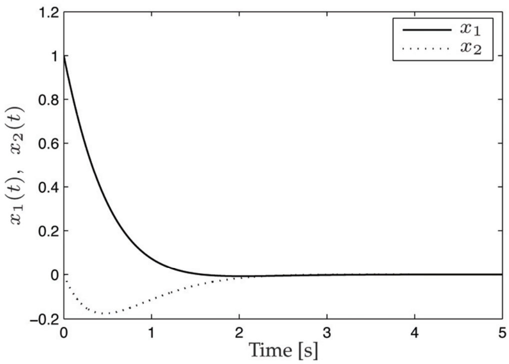

Figure 3. Transient response of the controlled system (Example 2), for $x_0 = [1\ 0]^T$

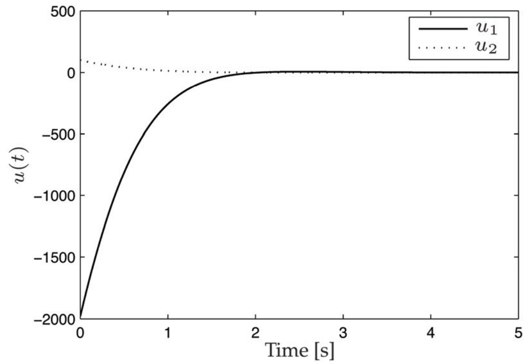

Figure 4. Control inputs of the controlled system (Example 2), for $x_0 = [1\ 0]^T$

Example 3

In this example, is considered that the matrix $E = I$. So, the system (1) is in the standard space state form. The idea was to show that, for the case where $det(E) \neq 0$, the proposed method is also valid.

Consider the mechanical system shown in Figure 5. It is a simple model of a controlled vibration absorber, in the sense of reducing the oscillations of the masses m_1 and m_2. In this case, the model contains two control inputs, $u_1(t)$ and $u_2(t)$. This system is described by the following equations (Cardim et al., 2007):

$$\begin{cases} m_1\ddot{y}_1(t) + b_1(\dot{y}_1(t) - \dot{y}_2(t)) + k_1 y_1(t) = u_1(t), \\ m_2\ddot{y}_2(t) + b_1(\dot{y}_2(t) - \dot{y}_1(t)) + k_2 y_2(t) = u_2(t). \end{cases} \tag{21}$$

The state space rorm of the mechanical system in Figure 5 is represented in equation (1) considering as state variables $x(t) = [x_1(t)\ x_2(t)\ x_3(t)\ x_4(t)]^T$, where $x_1(t) = y_1(t)$, $x_2(t) = \dot{y}_1(t)$, $x_3(t) = y_2(t)$, $x_4(t) = \dot{y}_2(t)$, $u(t) = [u_1(t)\ u_2(t)]^T$ and:

$$E = \begin{bmatrix} 1 & 0 & 0 & 0 \\ 0 & 1 & 0 & 0 \\ 0 & 0 & 1 & 0 \\ 0 & 0 & 0 & 1 \end{bmatrix}, A = \begin{bmatrix} 0 & 1 & 0 & 0 \\ \frac{-k_1}{m_1} & \frac{-b_1}{m_1} & 0 & \frac{b_1}{m_1} \\ 0 & 0 & 0 & 1 \\ 0 & \frac{b_1}{m_2} & \frac{-k_2}{m_2} & \frac{-b_1}{m_2} \end{bmatrix}, B = \begin{bmatrix} 0 & 0 \\ \frac{1}{m_1} & 0 \\ 0 & 0 \\ 0 & \frac{1}{m_2} \end{bmatrix}. \tag{22}$$

For a digital simulation of the control system, assume for instance that $m_1 = 10kg$, $m_2 = 30kg$, $k_1 = 2.5kN/m$, $k_2 = 1.5kN/m$ and $b_1 = 30Ns/m$. Consider the pole placement as design technique, and the following closed-loop poles for the controlled system:

$$\lambda_1 = -10, \qquad \lambda_2 = -15, \qquad \lambda_{3,4} = -2 \pm 10i.$$

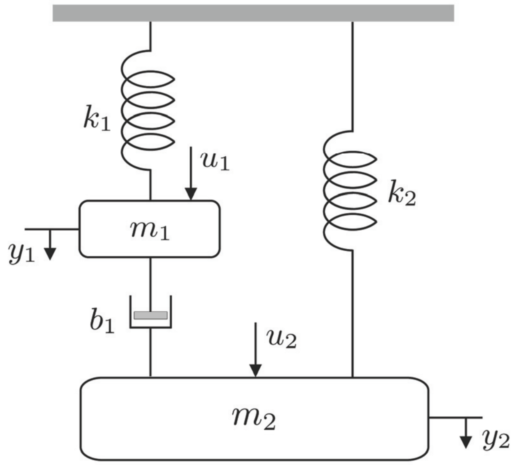

Figure 5. Multivariable (MI) mass-spring system with damping

With these parameters and from (8), one has:

$$A_n = \begin{bmatrix} -0.0120 & -0.0040 & 0.0120 & 0 \\ 1.0000 & 0 & 0 & 0 \\ 0.0200 & 0 & -0.0200 & -0.0200 \\ 0 & 0 & 1.0000 & 0 \end{bmatrix}, B_n = \begin{bmatrix} 0.4000\times10^{-3} & 0 \\ 0 & 0 \\ 0 & 0.6667\times10^{-3} \\ 0 & 0 \end{bmatrix}, \quad (23)$$

and (A_n, B_n) is controllable.

From Theorem 1, the poles for the new closed-loop system with state feedback (11), with A_n and B_n given in (23) are the following:

$$\lambda_1^{-1} = -0.1000, \qquad \lambda_2^{-1} = -0.0667, \qquad \lambda_{3,4}^{-1} = -0.0192 \pm 0.0962i.$$

So, with these parameters, one can obtain through the command *place* of MATLAB, the feedback gain matrix K_d below:

$$K_d = \begin{bmatrix} 178.9532 & -6.4647 & 323.3542 & 19.8478 \\ -79.6370 & -11.4321 & 152.3204 & -26.1863 \end{bmatrix}. \quad (24)$$

Figures 6 and 7 show the simulation results of the controlled system (1), (2), (22), (24), that can be given by (5), with the initial condition $x(0) = [0.1\ \ 0\ \ 0.1\ \ 0]^T$.

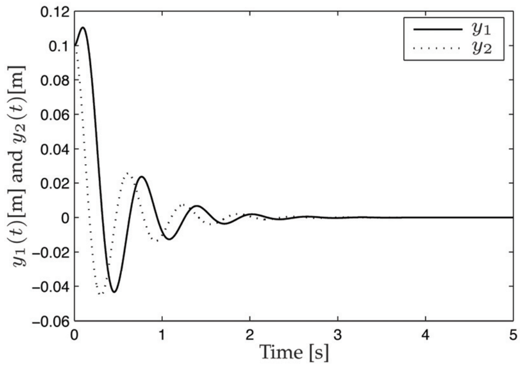

Figure 6. Transient response of the controlled system (Example 3), with $x(0) = [0.1\ \ 0\ \ 0.1\ \ 0]^T$

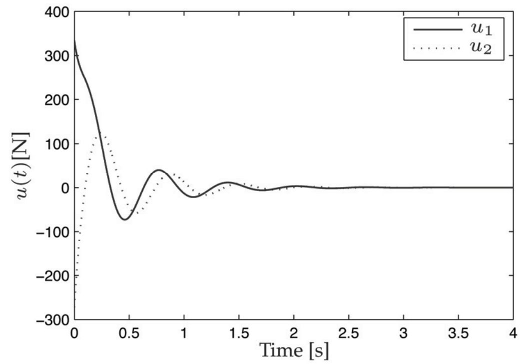

Figure 7. Control inputs of the controlled system (Example 3), with $x(0) = [0.1\ \ 0\ \ 0.1\ \ 0]^T$

3. LMI-Based Control Design for State-Derivative Feedback

Consider the linear time-invariant uncertain polytopic system, described as convex combinations of the polytope vertices:

$$\begin{aligned}\dot{x}(t) &= \sum_{i=1}^{r_a} \alpha_i A_i x(t) + \sum_{j=1}^{r_b} \beta_j B_j u(t),\\ &= A(\alpha)x(t) + B(\beta)u(t),\end{aligned} \tag{25}$$

and

$$\left.\begin{array}{lll}\alpha_i \geq 0, & i = 1,\ldots,r_a, & \displaystyle\sum_{i=1}^{r_a} \alpha_i = 1,\\ \beta_j \geq 0, & j = 1,\ldots,r_b, & \displaystyle\sum_{j=1}^{r_b} \beta_j = 1,\end{array}\right\} \tag{26}$$

where $x(t) \in \mathbb{R}^n$ is the state vector, $u(t) \in \mathbb{R}^m$ is the input vector, r_a and r_b are the numbers of polytope vertices of the matrices $A(\alpha)$ and $B(\beta)$, respectively. For $i = 1, \dots, r_a$ and $j = 1, \dots, r_b$ one has: $A_i \in \mathbb{R}^{n\times n}$ and $B_j \in \mathbb{R}^{n\times m}$ are constant matrices and α_i and β_j are constant and unknown real numbers.
From (8) and (25), one has:

$$A_n = A(\alpha)^{-1}E \quad \text{and} \quad B_n = -A(\alpha)^{-1}B(\beta), \tag{27}$$

Then, for the control design of the system (25) with Theorem 1, is necessary to know the real numbers α_i and β_j. However, in the practical problems these parameters are unknown. Therefore, Theorem 1 can not be directly applied in the control design of the system (25). For the solution of this problem, in this section sufficient Linear Matrix Inequalities (LMI) conditions for asymptotic stability of linear uncertain systems using state-derivative feedback are presented. The LMI formulation has emerged recently (Boyd et al., 1994) as an useful tool for solving a great number of practical control problems such as model reduction, design of linear, nonlinear, uncertain and delayed systems (Boyd et al., 1994; Assunção & Peres, 1999; Teixeira et al., 2001; Teixeira et al., 2002; Teixeira et al., 2003; Palhares et al., 2003; Teixeira et al., 2005; Assunção et al., 2007*a*; Assunção et al., 2007*b*; Teixeira et al., 2006). The main features of this formulation are that different kinds of design specifications and constraints that can be described by LMI, and once formulated in terms of LMI, the control problem, when it presents a solution, can be efficiently solved by convex optimization algorithms (Nesterov & Nemirovsky, 1994; Boyd et al., 1994; Gahinet et al., 1995; Sturm, 1999). The global optimum is found with polynomial convergence time (El Ghaoui & Niculescu, 2000). The state-derivative feedback has been examined with various approaches (Abdelaziz & Valášek, 2004; Kwak et al., 2002; Duan et al., 2005; Cardim et al., 2007), but neither them can be applied for uncertain systems or systems subject to structural failures (Isermann, 1997; Isermann & Ballé, 1997; Isermann, 2006). Robust state-derivative feedback LMI-based designs for linear time-invariant and time-varying systems were recently proposed in (Assunção et al., 2007c), but the results does not consider structural failures in the control design. Structural failures appear of natural form in the systems, for instance, in the following cases: physical wear of equipments, or short circuit of electronic components.
Recent researches for detection of the structural failures (or faults) in systems, have been presented in LMI framework (Zhong et al., 2003; Liu et al., 2005; D. Ye & G. H. Yang, 2006; S. S. Yang & J. Chen, 2006).
In this section, we will show that it is possible to extend the presented results in (Assunção et al., 2007c), for the case where there exist structural failures in the plant. A fault-tolerant design is proposed. The methods can include in the LMI-based control designs the specifications of bounds: on the decay rate, on the output peak, and on the state-derivative feedback matrix *K*. These design procedures allow new specifications and also, they consider a broader class of plants than the related results available in the literature.

3.1 Statement of the Problem

Consider a homogeneous linear time-invariant system given by

$$\dot{x}(t) = A_N x(t) \tag{28}$$

It is known from literature that the linear system (28) is asymptotically stable if there exist a symmetric matrix P satisfying the Lyapunov conditions (Boyd et al., 1994):

$$\left.\begin{array}{c} P > 0, \\ \text{and} \\ A_N' P + P A_N < 0. \end{array}\right\} \tag{29}$$

This result is useful for the design of the proposed controller.
In this work, structural failure is defined as a permanent interruption of the system's ability to perform a required function under specified operating conditions (Isermann & Ballé, 1997).
Systems subject to structural failures can be described by uncertain polytopic systems (25) (see Section 3.5 for details). Now, suppose that all poles of (25) are different from zero (the matrix $A(\alpha)$ must have a full rank). Then, the proposed problem is defined below.

Problem 1: Find a constant matrix $K \in \mathbb{R}^{m\times n}$ such that the following conditions hold:

1. $(I + B(\beta)K)$ has a full rank;
2. the closed-loop system (25) with the state-derivative feedback control

$$u(t) = -K\dot{x}(t), \tag{30}$$

   is asymptotically stable.

Note that from (25) and (30) it follows that

$$\dot{x}(t) = A(\alpha)x(t) - B(\beta)K\dot{x}(t)$$

or

$$(I + B(\beta)K)\dot{x}(t) = A(\alpha)x(t).$$

When $(I + B(\beta)K)$ has a full rank, the closed-loop system is well-defined and given by

$$\dot{x}(t) = (I + B(\beta)K)^{-1} A(\alpha)x(t). \tag{31}$$

This condition was also assumed in other related researches (Kwak et al., 2002; Abdelaziz & Valášek, 2004; Assunção et al., 2007c; Cardim et al., 2007).

3.2 Robust Stability Condition for State-derivative Feedback

The main results of this section is presented in the next theorem, that solves Problem 1 (Assunção et al., 2007c). For the proof of this theorem, the following result will be useful.

Remark 3. *Recall that for any nonsymetric matrix* $M\ (M \neq M'), M \in \mathbb{R}^{n\times n}$, *if* $M + M' < 0$, *then* M *has a full rank.*

Theorem 2. *A sufficient condition for the solution of Problem 1 is the existence of matrices* $Q = Q'$ *and* Y, *where* $Q \in \mathbb{R}^{n\times n}$ *and* $Y \in \mathbb{R}^{m\times n}$, *such that:*

$$Q > 0, \tag{32}$$

$$QA_i' + A_iQ + B_jYA_i' + A_iY'B_j' < 0 \tag{33}$$

where i = 1, ... ,r_a and j = 1, ... ,r_b. Furthermore, when (32) and (33) hold, a state-derivative feedback matrix that solves the Problem 1 is given by:

$$K = YQ^{-1} \tag{34}$$

Proof: Supposing that (32) and (33) hold, then multiplying both sides of (33) by $\alpha_i\beta_j$, for i = 1, ... , r_a and j = 1, ... , r_b and considering (26), it follows that

$$\begin{aligned}
&\alpha_i\beta_j(QA_i' + A_iQ + B_jYA_i' + A_iY'B_j') < 0, \qquad \forall i, j, \\
&\Leftrightarrow \sum_{i=1}^{r_a}\sum_{j=1}^{r_b}\alpha_i\beta_j(QA_i' + A_iQ + B_jYA_i' + A_iY'B_j') = \\
&Q\left(\sum_{i=1}^{r_a}\alpha_iA_i\right)' + \left(\sum_{i=1}^{r_a}\alpha_iA_i\right)Q + \left(\sum_{j=1}^{r_b}\beta_jB_j\right)Y\left(\sum_{i=1}^{r_a}\alpha_iA_i\right)' \\
&+\left(\sum_{i=1}^{r_a}\alpha_iA_i\right)Y'\left(\sum_{j=1}^{r_b}\beta_jB_j\right)' < 0
\end{aligned} \tag{35}$$

Then, from (25) one has

$$QA(\alpha)' + A(\alpha)Q + B(\beta)YA(\alpha)' + A(\alpha)Y'B(\beta)' < 0 .$$

Replacing $Y = KQ$ and $Q = P^{-1}$ one obtains

$$\begin{aligned}
&P^{-1}A(\alpha)' + A(\alpha)P^{-1} + B(\beta)KP^{-1}A(\alpha)' + A(\alpha)P^{-1}K'B(\beta)' = \\
&(I + B(\beta)K)P^{-1}A(\alpha)' + A(\alpha)P^{-1}(I + B(\beta)K)' < 0
\end{aligned} \tag{36}$$

From Remark 3, it follows that the matrix $((I + B(\beta)K)P^{-1}A(\alpha)'$ has a full rank, and so the matrices $(I + B(\beta)K)$ and $A(\alpha)'$ have a full rank too. Now, premultiply by $P(I + B(\beta)K)^{-1}$, posmultiply by $[(I + B(\beta)K)']^{-1}P$ in both sides of (36) and replace $A_N(\alpha,\beta) = (I + B(\beta)K)^{-1}A(\alpha)$ to obtain

$$\begin{aligned}
&A(\alpha)'[(I + B(\beta)K)']^{-1}P + P(I + B(\beta)K)^{-1}A(\alpha) = \\
&A_N(\alpha,\beta)'P + PA_N(\alpha,\beta) < 0
\end{aligned} \tag{37}$$

Observe that, when the LMI (32) and (33) hold, the system (31) satisfies the Lyapunov conditions (29), considering $A_N(\alpha,\beta) = (I + B(\beta)K)^{-1}A(\alpha)$. Therefore, when the LMI (32) and (33) hold the system (31) is asymptotically stable and a solution that solves Problem 1 is given by (34).

When (32) and (33) are feasible, they can be easily solved using available softwares, such as LMISol (de Oliveira et al, 1997), that is a free software, or MATLAB (Gahinet et al, 1995; Sturm, 1999). These algorithms have polynomial time convergence.

Remark 4. *From the analysis presented in the proof of Theorem 2, after equation (36), note that when (32) and (33) are feasible, the matrix* $A(\alpha)$*, defined in (25), has a full rank. Therefore,* $A(\alpha)$ *with a full rank is a necessary condition for the application of Theorem 2. Moreover, from (25), observe that for* $\alpha_i = 1$ *and* $\alpha_k = 0$*,* $i \neq k$*, i, k = 1, 2,... ,* r_a*, then* $A(\alpha) = A_i$*. So, if* $A(\alpha)$ *has a full rank, then* A_i*, i = 1, 2,... ,* r_a *has a full rank too.*

Usually, only the stability of a control system is insufficient to obtain a suitable performance. In the design of control systems, the specification of the decay rate can also be very useful.

3.3 Decay Rate Conditions

Consider, for instance, the controlled system (31). According to (Boyd et al., 1994), the decay rate is defined as the largest real constant $\gamma, \gamma > 0$, such that

$$lim_{t\to\infty} e^{\gamma t} \|x(t)\| = 0$$

holds, for all trajectories $x(t), t \geq 0$.

One can use the Lyapunov conditions (29) to impose a lower bound on the decay rate, replacing (29) by

$$P > 0, \quad and \quad A_N(\alpha,\beta)'P + PA_N(\alpha,\beta) < -2\gamma P. \tag{38}$$

where γ is a real constant (Boyd et al., 1994). Sufficient conditions for stability with decay rate for Problem 1 are presented in the next theorem (Assunção et al., 2007c).

Theorem 3. *The closed-loop system (31), given in Problem 1, has a decay rate greater or equal to* γ *if there exist a symmetric matrix* $Q \in \mathbb{R}^{n\times n}$ *and a matrix* $Y \in \mathbb{R}^{m\times n}$ *such that*

$$Q > 0 \tag{39}$$

$$\begin{bmatrix} QA_i' + A_iQ + B_jYA_i' + A_iY'B_j' & Q + B_jY \\ Q + Y'B_j' & -Q/(2\gamma) \end{bmatrix} < 0 \tag{40}$$

where i = 1, ... , r_a *and j = 1, ...,* r_b*. Furthermore, when (39) and (40) hold, then a robust state-derivative feedback matrix is given by:*

$$K = YQ^{-1}. \tag{41}$$

Proof: Following the same ideas of the proof of Theorem 2, multiply both sides of (40) by $\alpha_i\beta_j$, for *i* = 1, ... , r_a and *j* = 1, ..., r_b and consider (26), to conclude that

$$\begin{bmatrix} QA(\alpha)' + A(\alpha)Q + B(\beta)YA(\alpha)' + A(\alpha)Y'B(\beta)' & Q + B(\beta)Y \\ Q + Y'B(\beta)' & -Q/(2\gamma) \end{bmatrix} < 0$$

Now, using the Schur complement (Boyd et al., 1994), the equation above is equivalent to:

$$\begin{aligned} &QA(\alpha)' + A(\alpha)Q + B(\beta)YA(\alpha)' + A(\alpha)Y'B(\beta)' \\ &+(Q + B(\beta)Y)2\gamma Q^{-1}\left(Q + B(\beta)Y\right)' < 0 \end{aligned} \tag{42}$$

Replacing $Y = KQ$ and $Q = P^{-1}$ one obtains

$$\begin{aligned} &(I + B(\beta)K)P^{-1}A(\alpha)' + A(\alpha)P^{-1}(I + B(\beta)K)' \\ &+(I + B(\beta)K)P^{-1}(2\gamma P)P^{-1}(I + B(\beta)K)' = \\ &(I + B(\beta)K)P^{-1}A(\alpha)' + A(\alpha)P^{-1}(I + B(\beta)K)' \\ &+(I + B(\beta)K)(2\gamma P^{-1})(I + B(\beta)K)' < 0 \end{aligned} \tag{43}$$

Premultiplying by $P(I + B(\beta)K)^{-1}$, posmultiplying by $[(I + B(\beta)K)']^{-1}P$ in both sides of (43) and replacing $A_N(\alpha,\beta) = (I + B(\beta)K)^{-1}A(\alpha)$ one obtain

$$\begin{aligned} &A(\alpha)'[(I + B(\beta)K)']^{-1}P + P(I + B(\beta)K)^{-1}A(\alpha) + 2\gamma P < 0 \\ &\Leftrightarrow A_N(\alpha,\beta)'P + PA_N(\alpha,\beta) < -2\gamma P, \end{aligned} \tag{44}$$

that is equivalent to the Lyapunov condition (38). Then, when (39) and (40) hold, the system (31) satisfies the Lyapunov conditions (38), considering $A_N(\alpha,\beta) = (I + B(\beta)K)^{-1}A(\alpha)$. Therefore, the system (31) is asymptotically stable with a decay rate greater or equal to γ, and a solution for the problem can be given by (41).
Due to limitations imposed in the practical applications of control systems, many times it should be considered output constraints in the design.

3.4 Bounds on Output Peak

Consider that the output of the system (25) is given by:

$$y(t) = Cx(t), \tag{45}$$

where $y(t) \in \mathbb{R}^p$ and $C \in \mathbb{R}^{p\times n}$. Assume that the initial condition of (25) and (45) is $x(0)$. If the feedback system (31) and (45) is asymptotically stable, one can specify bounds on output peak as described below:

$$max\left\|y(t)\right\|_2 = max\sqrt{y'(t)y(t)} < \xi_0 \tag{46}$$

for $t \geq 0$, where ξ_0 is a known positive constant. From (Boyd et al., 1994), (46) is satisfied when the following LMI hold:

$$\begin{bmatrix} 1 & x(0)' \\ x(0) & Q \end{bmatrix} > 0, \tag{47}$$

$$\begin{bmatrix} Q & QC' \\ CQ & \xi_0^2 I \end{bmatrix} > 0, \tag{48}$$

and the LMI that guarantee stability (Theorem 2), given by (32) and (33), or stability and decay rate (Theorem 3), given by (39) and (40).
In some cases, the entries of the state-derivative feedback matrix K must be bounded. In (Assunção et al., 2007c) is presented an optimization procedure to obtain bounds on the state-derivative feedback matrix K, that can help the practical implementation of the controllers. The result is the following:

Theorem 4. *Given a constant $\mu_0 > 0$, then the specification of bounds on the state-derivative feedback matrix K can be described by finding the minimum value of $\beta, \beta > 0$, such that $KK' < \beta I / \mu_0^2$. The optimal value of β can be obtained by the solution of the following optimization problem:*

$$\min \beta$$
$$s.t.$$
$$\begin{bmatrix} \beta I & Y \\ Y' & I \end{bmatrix} > 0, \tag{49}$$

$$Q > \mu_0 I, \tag{50}$$

$$\textit{(Set of LMI)},$$

where the Set of LMI can be equal to (33), or (40), with or without the LMI (47) and (48).

Proof: See (Assunção et al., 2007c) for more details.
In the next section, a numerical example illustrates the efficiency of the proposed methods for solution of Problem 1.

3.5 Example

The presented methods are applied in the design of controllers for an uncertain mechanical system subject to structural failures. For the designs and simulations, the software MATLAB was used.

Active Suspension Systems

Consider the active suspension of a car seat given in (E. Reithmeier and G. Leitmann, 2003; Assunção et al., 2007c) with other kind of control inputs, shown in Figure 8. The model consists of a car mass M_c and a driver-plus-seat mass m_s. Vertical vibrations caused by a street may be partially attenuated by shock absorbers (stiffness k_1 and damping b_1). Nonetheless, the driver may still be subjected to undesirable vibrations. These vibrations, again, can be reduced by appropriately mounted car seat suspension elements (stiffness k_2 and damping b_2). Damping of vibration of the masses M_c and m_s can be increased by changing the control inputs $u_1(t)$ and $u_2(t)$. The dynamical system can be described by

$$\begin{bmatrix} \dot{x}_1(t) \\ \dot{x}_2(t) \\ \dot{x}_3(t) \\ \dot{x}_4(t) \end{bmatrix} = \begin{bmatrix} 0 & 0 & 1 & 0 \\ 0 & 0 & 0 & 1 \\ \dfrac{-k_1-k_2}{M_c} & \dfrac{k_2}{M_c} & \dfrac{-b_1-b_2}{M_c} & \dfrac{b_2}{M_c} \\ \dfrac{k_2}{m_s} & \dfrac{-k_2}{m_s} & \dfrac{b_2}{m_s} & \dfrac{-b_2}{m_s} \end{bmatrix} \begin{bmatrix} x_1(t) \\ x_2(t) \\ x_3(t) \\ x_4(t) \end{bmatrix} + \begin{bmatrix} 0 & 0 \\ 0 & 0 \\ \dfrac{1}{M_c} & \dfrac{-1}{M_c} \\ 0 & \dfrac{1}{m_s} \end{bmatrix} u(t), \tag{51}$$

$$\begin{bmatrix} y_1(t) \\ y_2(t) \end{bmatrix} = \begin{bmatrix} 1 & 0 & 0 & 0 \\ 0 & 1 & 0 & 0 \end{bmatrix} \begin{bmatrix} x_1(t) \\ x_2(t) \\ x_3(t) \\ x_4(t) \end{bmatrix}. \tag{52}$$

The state vector is defined by $x(t) = [x_1(t) \quad x_2(t) \quad \dot{x}_1(t) \quad \dot{x}_2(t)]^T$.
As in (E. Reithmeier and G. Leitmann, 2003), for feedback only the accelerations signals $\ddot{x}_1(t)$ and $\ddot{x}_2(t)$ are available (that are measured by accelerometer sensors). The velocities $\dot{x}_1(t)$ and $\dot{x}_2(t)$ are estimated from their measured time derivatives. Therefore the accelerations and velocities signals are available (derivative of states), and so one can use the proposed method to solve the problem.
Consider that the driver weight can assume values between 50kg and 100kg. Then the system in Figure 8 has an uncertain constant parameter m_s such that, 70kg $\leq m_s \leq$ 120kg. Additionally, suppose that can also happen a fail in the damper of the seat suspension (in other words, the damper can break after some time). The fault can be described by a polytopic uncertain system, where the system parameters without failure correspond to a vertice of the polytopic, and with failures, the parameters are in another vertice. Then, one can obtain the polytopic plant given in (25) and (26), composed by the polytopic sets due the failures and the uncertain plant parameters.

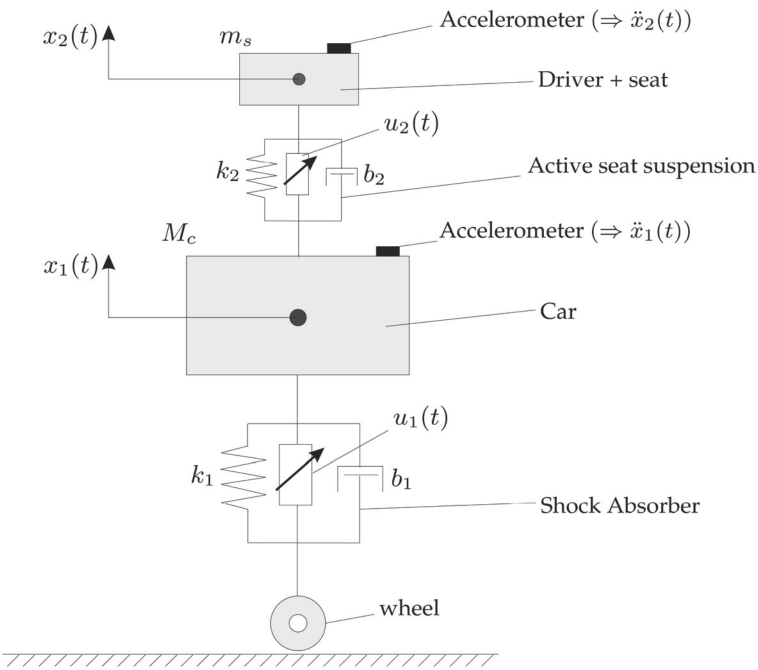

Figure 8. Active suspension of a car seat

The damper of the seat suspension b_2 can be considered as an uncertain parameter such that: b_2 = 5 x 10^2Ns/m while the damper is working and b_2 = 0 when the damper is broken. Hence, and supposing M_c = 1500kg (mass of the car), k_1 = 4 x 10^4N/m (stiffness), k_2 = 5 x 10^3N/m (stiffness) and b_1 = 4 x 10^3Ns/m (damping), the plant (51) and (52) can be described by equations (25), (26) and (45), and the matrices A_i and B_j, where r_a = 4, r_b, = 2, are given by:

$$A_1 = \begin{bmatrix} 0 & 0 & 1 & 0 \\ 0 & 0 & 0 & 1 \\ -30 & 3.33 & -3 & 0.33 \\ 71.43 & -71.43 & 7.143 & -7.143 \end{bmatrix}, A_2 = \begin{bmatrix} 0 & 0 & 1 & 0 \\ 0 & 0 & 0 & 1 \\ -30 & 3.33 & -3 & 0.33 \\ 41.67 & -41.67 & 4.167 & -4.167 \end{bmatrix},$$

while the damper is working (in this case b_2 = 5 x 10^2 Ns/m, m_s = 70kg in A_1 and m_s = 120kg in A_2),

$$A_3 = \begin{bmatrix} 0 & 0 & 1 & 0 \\ 0 & 0 & 0 & 1 \\ -30 & 3.33 & -2.67 & 0 \\ 71.43 & -71.43 & 0 & 0 \end{bmatrix}, A_4 = \begin{bmatrix} 0 & 0 & 1 & 0 \\ 0 & 0 & 0 & 1 \\ -30 & 3.33 & -2.67 & 0 \\ 41.67 & -41.67 & 0 & 0 \end{bmatrix},$$

when the damper is broken (in this case b_2 = 0, m_s = 70kg in A_3 and m_s = 120kg in A_4) and

$$B_1 = \begin{bmatrix} 0 & 0 \\ 0 & 0 \\ 6.67\times10^{-4} & -6.67\times10^{-4} \\ 0 & 1.43\times10^{-2} \end{bmatrix}, B_2 = \begin{bmatrix} 0 & 0 \\ 0 & 0 \\ 6.67\times10^{-4} & -6.67\times10^{-4} \\ 0 & 8.33\times10^{-3} \end{bmatrix},$$

because the input matrix $B(\beta)$ depends only on the uncertain parameter m_s (in this case m_s = 70kg in B_1 and m_s = 120kg in B_2). Specifying an output peak bound ξ_0 = 300, an initial condition $x(0) = [0.1\ \ 0.3\ \ 0\ 0]^T$ and using the MATLAB (Gahinet et al, 1995) to solve the LMI (32) and (33) from Theorem 2, with (47) and (48), the feasible solution was:

$$Q = \begin{bmatrix} 2.4006\times10^4 & 2.2812\times10^4 & -4.1099\times10^4 & -2.6578\times10^4 \\ 2.2812\times10^4 & 2.3265\times10^4 & -2.1628\times10^4 & -2.9019\times10^4 \\ -4.1099\times10^4 & -2.1628\times10^4 & 5.29\times10^5 & 8.3897\times10^4 \\ -2.6578\times10^4 & -2.9019\times10^4 & 8.3897\times10^4 & 1.8199\times10^5 \end{bmatrix},$$

$$Y = \begin{bmatrix} -7.9749\times10^6 & -3.0334\times10^7 & -4.4436\times10^6 & 6.5815\times10^8 \\ 1.7401\times10^6 & 2.2947\times10^6 & -8.0344\times10^6 & -1.616\times10^7 \end{bmatrix}.$$

From (34), we obtain the state-derivative feedback matrix below:

$$K = \begin{bmatrix} 2.894 \times 10^3 & 923.6 & -442.06 & 4.3902 \times 10^3 \\ -498.14 & 471.29 & -22.567 & -75.996 \end{bmatrix}. \quad (53)$$

The locations in the s-plane of the eigenvalues λ_i, for the eight vertices (A_i, B_j), i = 1, 2, 3, 4 and j = 1, 2, of the robust controlled system, are plotted in Figure 9. There exist four eigenvalues for each vertice.

Consider that driver weight is 70kg, and so m_s = 90kg. Using the designed controller (53) and the initial condition x(0) defined above, the controlled system was simulated. The transient response and the control inputs (30), of the controlled system, while the damper is working are presented in Figures 10 and 11. Now suppose that happen a fail in the damper of the seat suspension b_2 after 1s (in other words, $b_2 = 5 \times 10^2$Ns/m if $t \leq$ 1s and b_2 = 0 if $t >$ 1s). Then, the transient response and the control inputs (30), of the controlled system, are displayed in Figures 12 and 13. The required condition $max\sqrt{y'(t)y(t)} < \xi_0 = 300$ was satisfied.

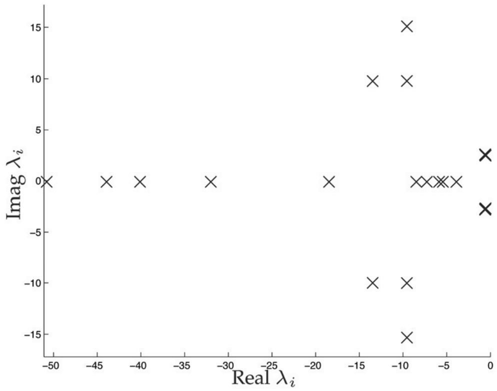

Figure 9. The eigenvalues in the eight vertices of the controlled uncertain system

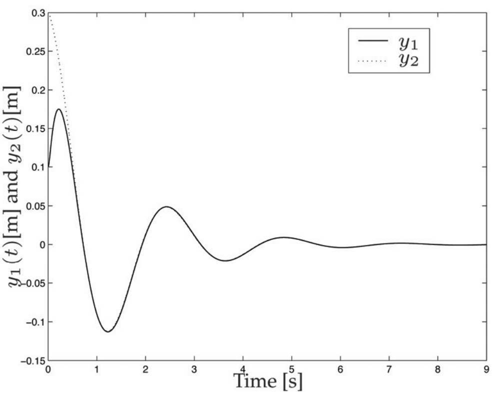

Figure 10. Transient response of the system with the damper working

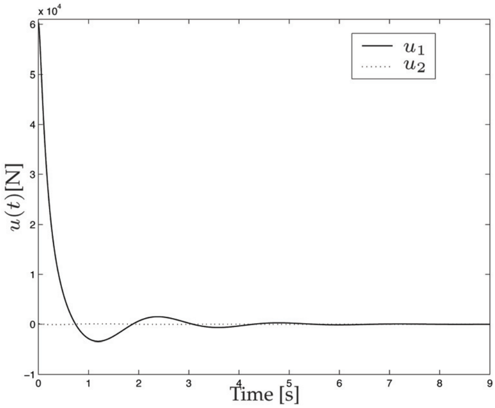

Figure 11. Control inputs of the controlled system with the damper working

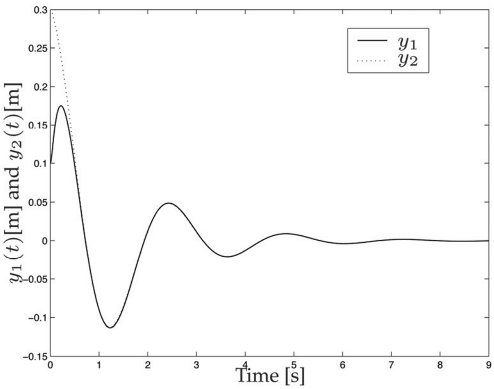

Figure 12. Transient response of the system with a fail in the damper b_2 after 1s

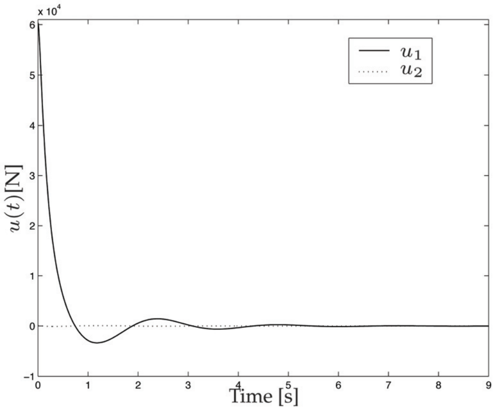

Figure 13. Control inputs of the controlled system with a fail in the damper b_2 after 1s

Observe in Figures 10 and 12, that the happening of a fail in the damper b_2 does not change the settling time of the controlled system, and had little influence in the control inputs. Furthermore, as discussed before, considering m_s = 90kg and the controller (53), the matrix $(I + B(\beta)K)$ has a full rank ($\det(I + B(\beta)K)$ = 0.85868 $\neq$ 0).

There exist problems where only the stability of the controlled system is insufficient to obtain a suitable performance. Specifying a lower bound for the decay rate equal γ = 3, to obtain a fast transient response, Theorem 3 is solved with (47) and (48) (ξ_0 = 300). The solution obtained with the software MATLAB was:

$$Q = \begin{bmatrix} 3.9195\times10^3 & 3.1064\times10^3 & -2.6316\times10^4 & -1.6730\times10^4 \\ 3.1064\times10^3 & 3.6868\times10^3 & -1.3671\times10^4 & -1.8038\times10^4 \\ -2.6316\times10^4 & -1.3671\times10^4 & 5.3775\times10^5 & 1.0319\times10^5 \\ -1.6730\times10^4 & -1.8038\times10^4 & 1.0319\times10^5 & 1.9587\times10^5 \end{bmatrix},$$

$$Y = \begin{bmatrix} 4.3933\times10^7 & 2.8021\times10^7 & -7.9356\times10^8 & -1.6408\times10^8 \\ 1.3888\times10^6 & 1.8426\times10^6 & -9.1885\times10^6 & -1.69\times10^7 \end{bmatrix}.$$

From (41), we obtain the state-derivative feedback matrix below:

$$K = \begin{bmatrix} -621 & 3.8664\times10^3 & -1.452\times10^3 & 230.33 \\ -313.58 & 365.55 & -8.79 & -74.77 \end{bmatrix} \tag{54}$$

The locations in the s-plane of the eigenvalues λ_i, for the eight vertices (A_i, B_j), i = 1, 2, 3, 4 and j = 1, 2, of the robust controlled system, are plotted in Figure 14. There exist four eigenvalues for each vertice.

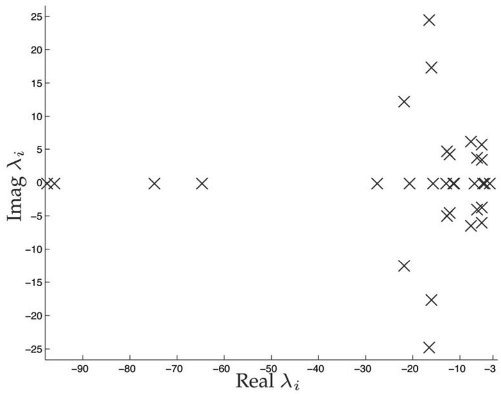

Figure 14. The eigenvalues in the eight vertices of the controlled uncertain system

From Figure 14, one has that all eigenvalues of the vertices have real part lower than $-\gamma = -3$. Therefore, the controlled uncertain system has a decay rate greater or equal to γ. Again, considering that m_s = 90kg and using the designed controller (54) the matrix $(I + B(\beta)K)$ has a full rank ($\det(I + B(\beta)K)$ = 0.026272). For the initial condition *x(0)* defined above, the controlled system was simulated. The transient response and the control inputs (30) of the controlled system are presented in Figures 15, 16, 17 and 18, respectively.

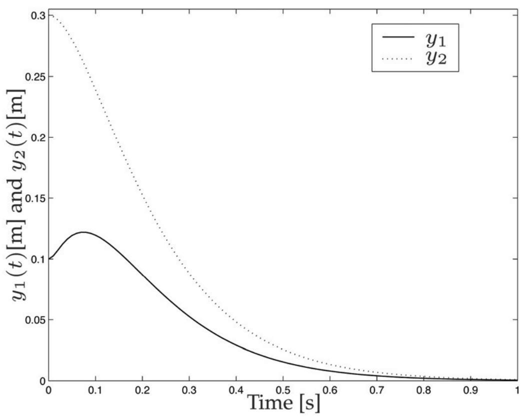

Figure 15. Transient response of the system with the damper working

Observe that, the settling time in Figures 15 and 17 are smaller than the settling time in Figures 10 and 12, where only stability was required and also, $max\sqrt{y'(t)y(t)}$ is equal to 0.31623 < $\xi_0 = 300$. Then, the specifications were satisfied by the designed controller (54). Moreover, the happening of a fail in the damper b_2 does not significantly change the settling time (Figures 15 and 17) of the controlled system. In spite of the change in the control inputs from Figures 16 and 18, the fail in the damper does not changed the maximum absolute value of the control signal ($u(t)$ = 1.1161 x 10^5N).

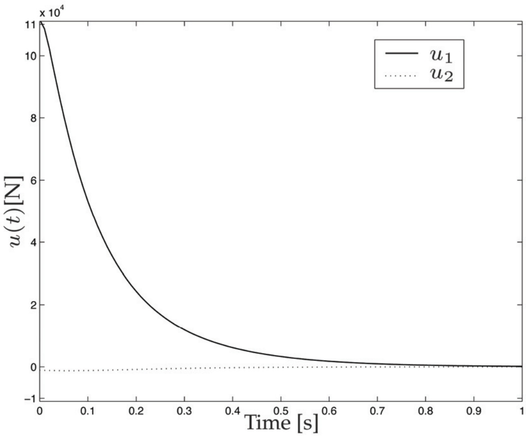

Figure 16. Control inputs of the controlled system with the damper working

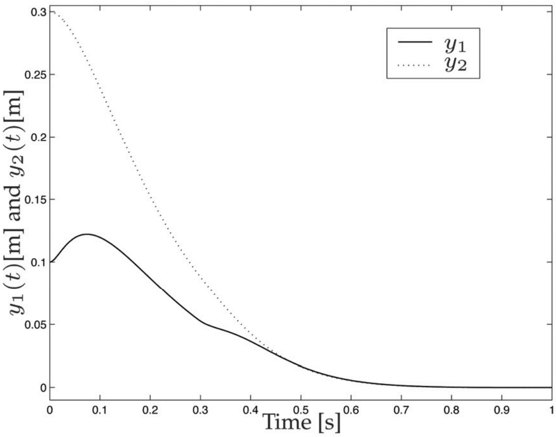

Figure 17. Transient response of the system with a fail in the damper b_2 after 0.3s

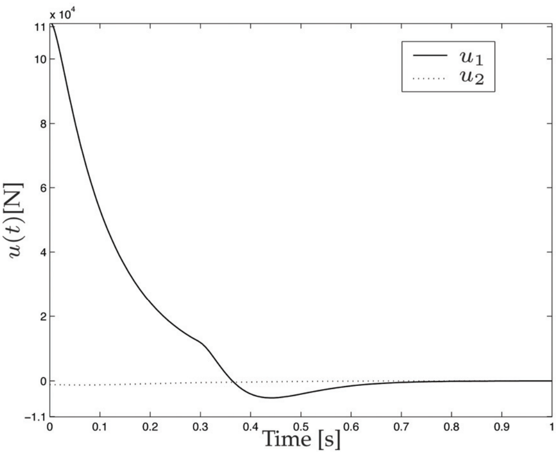

Figure 18. Control inputs of the controlled system with a fail in the damper b_2 after 0.3s

Note that some absolute values of the entries of (53) and (54) are great values and it could be a trouble for the practical implementation of the controller. For the reduction of this problem in the implementation of the controller, the specification of bounds on the state-derivative feedback matrix K can be done using the optimization procedure stated in Theorem 4, with $\mu_0 = 0.1$. The optimal values, obtained with the software MATLAB, for Theorem 4 considering: (33) for stability, or (40) for stability with bound on the decay rate ($\gamma = 3$), and (47) and (48) ($\xi_0 = 300$) are displayed in Table 1. Considering that m_s = 90kg and the initial condition $x(0)$ defined above, the transient response and the control inputs obtained by Theorem 4 considering (33) or (40), are displayed in Figures 19, 20, 21 and 22 respectively.

Theorem 4 with (33)	Theorem 4 with (40)
$Q=\begin{bmatrix} 1.2265 & 1.5357 & -1.667 & -5.8859 \\ 1.5357 & 2.5422 & 0.6289 & -5.1654 \\ -1.667 & 0.6289 & 27.177 & 30.007 \\ -5.8859 & -5.1654 & 30.007 & 67.502 \end{bmatrix}$	$Q=\begin{bmatrix} 0.16831 & 0.088439 & -0.52166 & -0.25122 \\ 0.088439 & 0.56992 & -0.07813 & -2.3703 \\ -0.52166 & -0.07813 & 5.1595 & -2.9849 \\ 0.25122 & -2.3703 & -2.9849 & 43.238 \end{bmatrix}$
$Y=\begin{bmatrix} 17.423 & 19.928 & -13.793 & 12.407 \\ -25.896 & 20.088 & -2.8711 & 0.69624 \end{bmatrix}$	$Y=\begin{bmatrix} 918.06 & 749.73 & -3.3745\times10^{3} & 204.86 \\ 30.057 & 468.97 & -102.46 & -3.5475\times10^{3} \end{bmatrix}$
$K=\begin{bmatrix} 39.536 & -6.5518 & -2.7229 & 4.3402 \\ -276.41 & 173.56 & -17.953 & -2.829 \end{bmatrix}$	$K=\begin{bmatrix} 4.7321\times10^{3} & 859.72 & -121.49 & 70.976 \\ -559.07 & 664.62 & -98.521 & -55.661 \end{bmatrix}$

Table 1. The solutions with Theorem 4

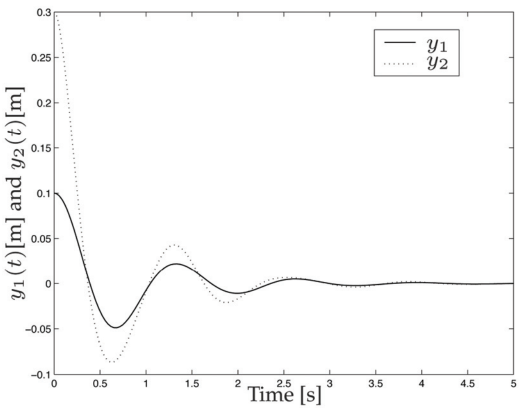

Figure 19. Transient response of the system with a fail in the damper b_2 after 1s, obtained with Theorem 4 and (33)

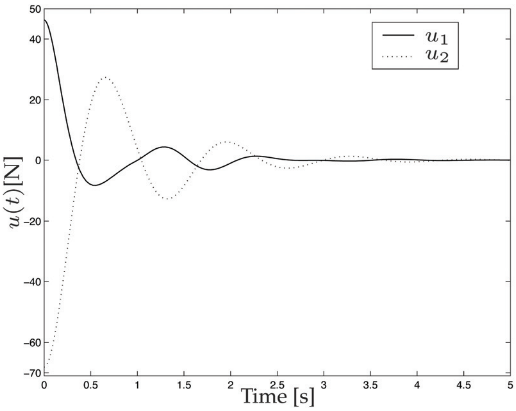

Figure 20. Control inputs of the controlled system with a fail in the damper b_2 after 1s

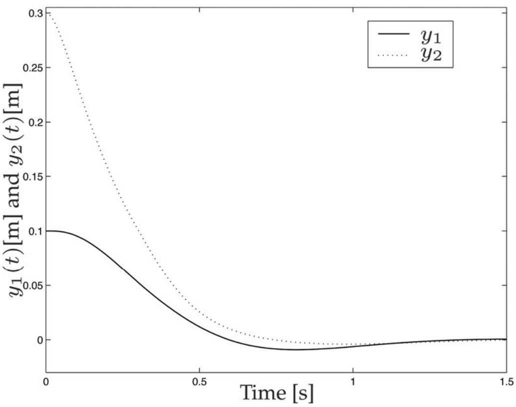

Figure 21. Transient response of the system with a fail in the damper b_2 after 0.3s, obtained with Theorem 4 and (40)

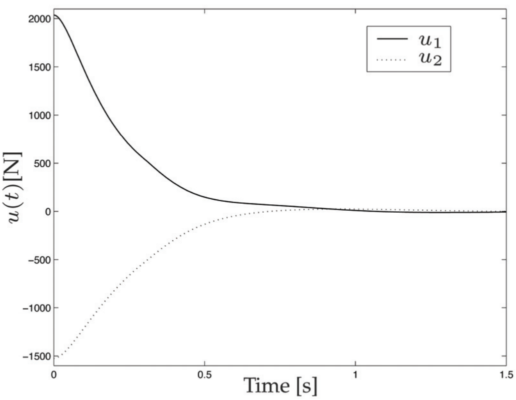

Figure 22. Control inputs of the controlled system with a fail in the damper b_2 after 0.3s

The matrix norm of the controller (53) obtained with Theorem 2 is equal to $\|K\|$ = 5.3628xl0[3] and the maximum absolute value of the control signal is $u(t)$ = 6.0356 x 10^4N, while that the matrix norm of the same controller obtained with Theorem 4 considering (33) is equal to $\|K\|$ = 328.96 and the maximum absolute value of the control signal is $u(t)$ = 68.111N.

Then, Theorem 4 was able to stabilize the controlled system with a smaller state-derivative feedback matrix gain. The similar form, the maximum absolute value of the control signal $u(t)$ from (54), obtained with Theorem 3 is $u(t)$ = 1.1161 x 10^5N, and of the same controller obtained with Theorem 4 considering (40) is $u(t)$ = 2.0362 x 10^3N. This example shows that the proposed methods are simple to use and it is easy to specify the constraints in the design.

4. Conclusions

In this chapter two new control designs using state-derivative feedback for linear systems were presented. Firstly, considering linear descriptor plants, a simple method for designing a state-derivative feedback gain (K_d) using methods for state feedback control design was proposed. The descriptor linear systems must be time-invariant, Single-Input (SI) or Multiple-Input (MI) system. The procedure allows that the designers use the well-known state feedback design methods to directly design state-derivative feedback control systems. This method extends the results described in (Cardim et al, 2007) and (Abdelaziz & Valášek, 2004) to a more general class of control systems, where the plant can be a descriptor system. As the first design can not be directly applied for uncertain systems, then a design considering sufficient stability conditions based on LMI for state-derivative feedback, that provide an extension of the methods presented in (Assunção et al., 2007c) were presented. The designers can include in the LMI-based control design, the specification of the decay rate and bounds on output peak and on state-derivative feedback gains. The plant can be subject to structural failures. So, in this case, one has a fault-tolerant design. Furthermore, the new design methods allow a broader class of plants and performance specifications, than the related results available in the literature, for instance in (E. Reithmeier and G. Leitmann, 2003; Abdelaziz & Valášek, 2004; Duan et al., 2005; Assunção et al., 2007c; Cardim et al., 2007). The presented method offers LMI-based designs for state-derivative feedback that, when feasible, can be efficiently solved by convex programming techniques. In Sections 2.3 and 3.5, the validity and simplicity of the new control designs can be observed with some numerical examples.

5. Acknowledgments

The authors acknowledge the financial support by FAPESP, CAPES and CNPq, from Brazil.

6. References

A. Bunse-Gerstner, R. Byers, V. M. & Nichols, N. (1999), Feedback design for regularizing descriptor systems, in *Linear Algebra and its Applications*, pp. 119-151.

Abdelaziz, T. H. S. & Valášek, M. (2005), Direct Algorithm for Pole Placement by State-Derivative Feedback for Multi-Input Linear Systems - Nonsingular Case, *Kybernetika* 41(5), 637-660.

Abdelaziz, T. H. S. & Valášek, M. (2004), Pole-placement for SISO Linear Systems by State-Derivative Feedback, *IEE Proceedings-Control Theory Applications* 151(4), 377-385.

Assunção, E., Andrea, C. Q. & Teixeira, M. C. M. (2007*a*), $\mathcal{H}_2$ and $\mathcal{H}_\infty$, -optimal control for the tracking problem with zero variation, *IET Control Theory Applications* 1(3), 682-688.

Assunção, E., Marchesi, H. E, Teixeira, M. C. M. & Peres, P. L. D. (2007*b*), Global Optimization for the H_∞-Norm Model Reduction Problem, *International Journal of Systems Science* 38(2), 125-138.

Assunção, E. & Peres, P. L. D. (1999), A global optimization approach for the $\mathcal{H}_2$-norm model reduction problem, in *Proceedings of the 38th IEEE Conference on Decision and Control*, Phoenix, AZ, USA, pp. 1857-1862.

Assunção, E., Teixeira, M. C. M., Faria, F. A., da Silva, N. A. P. & Cardim, R. (2007*c*), Robust State-Derivative Feedback LMI-Based Designs for Multivariable Linear Systems, *International Journal of Control* 80(8), 1260-1270.

Boyd, S., El Ghaoui, L., Feron, E. & Balakrishnan, V. (1994), *Linear Matrix Inequalities in Systems and Control Theory,* 2nd edn, SLAM Studies in Applied Mathematics, USA. http://www.stanford.edu/ boyd/lmibook/lmibook.pdf.

Bunse-Gerstner, A., Nichols, N. & Mehrmann, V. (1992), Regularization of Descriptor Systems by Derivative and Proportional State Feedback, in *SIAM J. Matrix Anal Appl.*, pp. 46-67.

Cardim, R., Teixeira, M. C. M., Assunção, E. & Covacic, M. R. (2007), Design of State-Derivative Feedback Controllers Using a State Feedback Control Design, in *3rd IFAC Symposium on System, Structure and Control*, Vol. 1, Iguassu Falls, PR, Brazil, pp. Article 135-6 pages.

Chen, C. T. (1999), *Linear System Theory and Design,* 2nd edn, Oxford University Press, New York.

D. Ye & G. H. Yang (2006), Adaptive fault-tolerant tracking control against actuator faults with application to flight control, *Control Systems Technology, IEEE Transactions on* 14(6), 1088-1096.

de Oliveira, M. C., Farias, D. P. & Geromel, J. C. (1997), *LMISol, User's guide,* UNICAMP, Campinas-SP, Brazil, http://www.dt.fee.unicamp.br/~mauricio/software.html.

Duan, G. R., Irwin, G. W. & Liu, G. P. (1999), Robust Stabilization of Descriptor Linear Systems via Proportional-plus-derivative State Feedback, in *Proceedings of the 1999 American Control Conference*, San Diego, CA, USA, pp. 1304-1308.

Duan, G. R. & Zhang, X. (2003), Regularizability of Linear Descriptor Systems via Output plus Partial State Derivative Feedback, *Asian Journal of Control* 5(3), 334-340.

Duan, Y. E, Ni, Y Q. & Ko, J. M. (2005), State-Derivative feedback control of cable vibration using semiactive magnetorheological dampers, *Computer-Aided Civil and Infrastructure Engineering* 20(6), 431-449.

E. Reithmeier and G. Leitmann (2003), Robust vibration control of dynamical systems based on the derivative of the state, *Archive of Applied Mechanics* 72(11-12), 856-864.

El Ghaoui & Niculescu, S. (2000), *Advances in Linear Matrix Inequalities Methods in Control,* SIAM Advances in Design and Control, USA.

Gahinet, P., Nemirovski, A., Laub, A. J. & Chilali, M. (1995), *LMI control toolbox - For use with Matlab,* The Math Works Inc.

Isermann, R. (1997), Supervision, fault-detection and fault-diagnosis methods - an introduction, *Control Engineering Practice* 5(5), 639-652.

Isermann, R. (2006), *Fault-Diagnosis systems: An introduction from fault detection to fault tolerance,* Springer, Berlin.

Isermann, R. & Ballé, P. (1997), Trends in the application of model-based fault detection and diagnosis of technical processes, *Control Engineering Practice* 5(5), 709-719.

Kwak, S. K., Washington, G. & Yedavalli, R. K. (2002), Acceleration-Based vibration control of distributed parameter systems using the "reciprocal state-space framework", *Journal of Sound and Vibration* 251(3), 543-557.

Liu, J., Wang, J. L. & Yang, G. H. (2005), An LM1 approach to minimum sensitivity analysis with application to fault detection, *Automatica* 41(11), 1995-2004.

Nesterov, Y. & Nemirovsky, A. (1994), *Interior-Point Polynomial Algorithms in Convex Programming,* SLAM Studies in Applied Mathematics, USA.

Nichols, N., Bunse-Gerstner, A. & Mehrmann, V. (1992), Regularization of descriptor systems by derivative and proportional state feedback, in *SIAM J. Matrix Anal. Appl.*, pp. 46-67.

Ogata, K. (2002), *Modern Control Engineering,* 4th edn, Prentice-Hall, New Jersey.

Palhares, R. M., Hell, M. B., Duraes, L. M., Ribeiro Neto, J. L., Teixeira, M. C. M. & Assunção, E. (2003), Robust H_∞ Filtering for a Class of State-delayed Nonlinear Systems in an LMI Setting, *International Journal Of Computer Research* 12(1), 115-122.

S. S. Yang & J. Chen (2006), Sensor faults compensation for MLMO fault-tolerant control systems, *Transactions of the Institute of Measurement and Control* 28(2), 187-205.

S. Xu & J. Lam (2004), Robust Stability and Stabilization of Discrete Singular Systems: An Equivalent Characterization, *IEEE Transactions on Automatic Control* 49(4), 568-574.

Sturm, J. (1999), Using SeDuMi 1.02, a MATLAB toolbox for optimization over symmetric cones, *Optimization Methods and Software* 11-12, 625-653. http://citeseer.ist.psu.edu/sturm99using.html.

Teixeira, M. C. M., Assunção, E. & Avellar, R. G. (2003), On relaxed LMI-based designs for fuzzy regulators and fuzzy observers, *IEEE Transactions on Fuzzy Systems* 11(5), 613-623.

Teixeira, M. C. M., Assunção, E. & Palhares, R. M. (2005), Discussion on: H_∞ Output Feedback Control Design for Uncertain Fuzzy Systems with Multiple Time Scales: An LMI Approach, *European Journal of Control* 11(2), 167-169.

Teixeira, M. C. M, Assunção, E. & Pietrobom, H. C. (2001), On Relaxed LMI-Based Design Fuzzy, in *Proceedings of the 6th European Control Conference*, Porto, Portugal, pp. 120-125.

Teixeira, M. C. M., Covacic, M., Assunção, E. & Lordelo, A. D. (2002), Design of SPR Systems and Output Variable Structure Controllers Based on LMI, in *7th IEEE International Workshop on Variable Structure Systems*, Vol. 1, Sarajevo, Bosnia, pp. 133-144.

Teixeira, M. C. M., Covacic, M. R. & Assunção, E. (2006), Design of SPR Systems with Dynamic Compensators and Output Variable Structure Control, in *International Workshop on Variable Structure Systems*, Vol. 1, Alghero-Italy, pp. 328-333.

Valášek, M. & Olgac, N. (1995a), An Efficient Pole-Placement Technique for Linear Time-Variant SISO System, *1EE Proceedings-Control Theory and Applications* 142(5), 451-458.

Valášek, M. & Olgac, N. (1995b), Efficient Eigenvalue Assignments for General Linear MIMO Systems, *Automatica* 31(11), 1605-1617.

Zhong, M., Ding, S. X., Lam, J. & Wang, H. (2003),'An LMI approach to design robust fault detection filter for uncertain LTI systems, *Automatica* 39(3), 543-550.

2

Asymptotic Stability Analysis of Linear Time-Delay Systems: Delay Dependent Approach

Dragutin Lj. Debeljkovic[1] and Sreten B. Stojanovic[2]
[1]University of Belgrade, Faculty of Mechanical Engineering
[2]University of Nis, Faculty of Technology
Serbia

1. Introduction

The problem of investigation of time delay systems has been exploited over many years. Time delay is very often encountered in various technical systems, such as electric, pneumatic and hydraulic networks, chemical processes, long transmission lines, etc. The existence of pure time lag, regardless if it is present in the control or/and the state, may cause undesirable system transient response, or even instability.
During the last three decades, the problem of stability analysis of time delay systems has received considerable attention and many papers dealing with this problem have appeared (Hale & Lunel, 1993). In the literature, various stability analysis techniques have been utilized to derive stability criteria for asymptotic stability of the time delay systems by many researchers (Yan, 2001; Su, 1994; Wu & Muzukami, 1995; Xu, 1994; Oucheriah, 1995; Kim, 2001). The developed stability criteria are classified often into two categories according to their dependence on the size of the delay: delay-dependent and delay-independent stability criteria (Hale, 1997; Li & de Souza, 1997; Xu et al., 2001). It has been shown that delay-dependent stability conditions that take into account the size of delays, are generally less conservative than delay-independent ones which do not include any information on the size of delays.
Further, the delay-dependent stability conditions can be classified into two classes: frequency-domain (which are suitable for systems with a small number of heterogeneous delays) and time-domain approaches (for systems with a many heterogeneous delays).
In the first approach, we can include the two or several variable polynomials (Kamen 1982; Hertz et al. 1984; Hale et al. 1985) or the small gain theorem based approach (Chen & Latchman 1994).
In the second approach, we have the comparison principle based techniques (Lakshmikantam & Leela 1969) for functional differential equations (Niculescu et al. 1995a; Goubet-Bartholomeus et al. 1997; Richard et al. 1997) and respectively the Lyapunov stability approach with the Krasovskii and Razumikhin based methods (Hale & Lunel 1993; Kolmanovskii & Nosov 1986). The stability problem is thus reduced to one of finding solutions to Lyapunov (Su 1994) or Riccati equations (Niculescu et al., 1994), solving linear matrix inequalities (LMIs) (Boyd et al. 1994; Li & de Souza, 1995; Niculescu et al., 1995b; Gu 1997) or analyzing eigenvalue distribution of appropriate finite-dimensional matrices (Su

1995) or matrix pencils (Chen et al., 1994). For further remarks on the methods see also the guided tours proposed by (Niculescu et al., 1997a; Niculescu et al., 1997b; Kharitonov, 1998; Richard, 1998; Niculescu & Richard, 2002; Richard, 2003).

It is well-known (Kolmanovskii & Richard, 1999) that the choice of an appropriate Lyapunov–Krasovskii functional is crucial for deriving stability conditions. The general form of this functional leads to a complicated system of partial differential equations (Malek-Zavareiand & Jamshidi, 1987). Special forms of Lyapunov–Krasovskii functionals lead to simpler delay-independent (Boyd et al., 1994; Verriest & Niculescu, 1998; Kolmanovskii & Richard, 1999) and (less conservative) delay-dependent conditions (Li & de Souza, 1997; Kolmanovskii et al., 1999; Kolmanovskii & Richard, 1999; Park, 1999; Lien et al., 2000; Niculescu, 2001). Note that the latter simpler conditions are appropriate in the case of unknown delay, either unbounded (delay-independent conditions) or bounded by a known upper bound (delay-dependent conditions).

In the delay-dependent stability case, special attention has been focused on the first delay interval guaranteeing the stability property, under some appropriate assumptions on the system free of delay. Thus, algorithms for computing optimal (or suboptimal) bounds on the delay size are proposed in (Chiasson, 1988; Chen et al., 1994) (frequency-based approach), in (Fu et al., 1997) (integral quadratic constraints interpretations), in (Li & de Souza, 1995; Niculescu et al., 1995b; Su, 1994) (Lyapunov-Razumikhin function approach) or in (Gu, 1997) (discretization schemes for some Lyapunov- Krasovskii functionals). For computing general delay intervals, see, for instance, the frequency based approaches proposed in (Chen, 1995).

In the past few years, there have been various approaches to reduce the conservatism of delay-dependent conditions by using new bounding for cross terms or choosing new Lyapunov–Krasovskii functional and model transformation. The delay-dependent stability criterion of (Park et al., 1998; Park, 1999) is based on a so-called Park's inequality for bounding cross terms. However, major drawback in using the bounding of (Park et al., 1998) and (Park, 1999) is that some matrix variables should be limited to a certain structure to obtain controller synthesis conditions in terms of LMIs. This limitation introduces some conservatism. In (Moon et al., 2001) a new inequality, which is more general than the Park's inequality, was introduced for bounding cross terms and controller synthesis conditions were presented in terms of nonlinear matrix inequalities in order to reduce the conservatism. It has been shown that the bounding technique in (Moon et al., 2001) is less conservative than earlier ones. An iterative algorithm was developed to solve the nonlinear matrix inequalities (Moon et al., 2001).

Further, in order to reduce the conservatism of these stability conditions, various model transformations have been proposed. However, the model transformation may introduce additional dynamics. In (Fridman & Shaked, 2003) the sources for the conservatism of the delay-dependent methods under four model transformations, which transform a system with discrete delays into one with distributed delays are analyzed. It has been demonstrated that descriptor transformation, that has been proposed in (Fridman & Shaked, 2002a), leads to a system which is equivalent to the original one, does not depend on additional assumptions for stability of the transformed system and requires bounding of fewer cross-terms. In order to reduce the conservatism, (Han, 2005a; Han, 2005b) proposed some new methods to avoid using model transformation and bounding technique for cross terms.

In (Fridman & Shaked, 2002b) both the descriptor system approach and the bounding technique using by (Moon et al., 2001) are utilized and the delay-dependent stability results are performed. The derived stability criteria have been demonstrated to be less conservative than existing ones in the literature.

Delay-dependent stability conditions in terms of linear matrix inequalities (LMIs) have been obtained for retarded and neutral type systems. These conditions are based on four main model transformations of the original system and application mentioned inequalities.

The majority of stability conditions in the literature available, of both continual and discrete time delay systems, are sufficient conditions. Only a small number of works provide both necessary and sufficient conditions, (Lee & Diant, 1981; Xu et al., 2001; Boutayeb & Darouach, 2001), which are in their nature mainly dependent of time delay. These conditions do not possess conservatism but often require more complex numerical computations. In our paper we represent some necessary and sufficient stability conditions.

Less attention has been drawn to the corresponding results for discrete-time delay systems (Verriest & Ivanov, 1995; Kapila & Haddad, 1998; Song et al., 1999; Mahmoud, 2000; Lee & Kwon, 2002; Fridman & Shaked, 2005; Gao et al., 2004; Shi et al., 2000). This is mainly due to the fact that such systems can be transformed into augmented high dimensional systems (equivalent systems) without delay (Malek-Zavarei & Jamshidi, 1987; Gorecki et al., 1989). This augmentation of the systems is, however, inappropriate for systems with unknown delays or systems with time varying delays. Moreover, for systems with large known delay amounts, this augmentation leads to large-dimensional systems. Therefore, in these cases the stability analysis of discrete time delay systems can not be to reduce on stability of discrete systems without delay.

In our paper we present delay-dependent stability criteria for particular classes of time delay systems: continuous and discrete time delay systems and continuous and discrete time delay large-scale systems. Thereat, these stability criteria are express in form necessary and sufficient conditions.

The organization of this chapter is as follows. In section 2 we present necessary and sufficient conditions for delay-dependent asymptotic stability of particular class of continuous and discrete time delay systems. Moreover, we show that in the paper of (Lee & Diant, 1981) there are some mistakes in formulation of particular theorems. We correct these errors and extend derived results on discrete time delay systems. Further extensions of these results to the class of continuous and discrete large scale time delay systems are presented in the section 3. All theoretical results are supported by suitable chosen numerical examples. And section 4 discuss and summarizes contributions.

2. Time delay systems

Throughout this chapter we use the following notation. $\mathbb{R}$ and $\mathbb{C}$ denote real (complex) vector space or the set of real (complex) numbers, $\mathbb{T}^+$ denotes the set of all non-negative integers, λ^* means conjugate of $\lambda \in \mathbb{C}$ and F^* conjugate transpose of matrix $F \in \mathbb{C}^{n \times n}$. Re(s) is the real part of $s \in \mathbb{C}$. The superscript T denotes transposition. For real matrix F the notation $F > 0$ means that the matrix F is positive definite. $\lambda_i(F)$ is the eigenvalue of matrix F. Spectrum of matrix F is denoted with $\sigma(F)$ and spectral radius with $\rho(F)$.

2.1 Continuous time delay systems

For the sake of completeness, we present the following result (Lee & Diant, 1981). Considers class of continuous time-delay systems described by

$$\dot{x}(t) = A_0 x(t) + A_1 x(t-\tau), \quad x(t) = \varphi(t), \ -\tau \le t < 0 \tag{1}$$

Theorem 2.1.1 (Lee & Diant, 1981) Let the system be described by (1). If for any given matrix $Q = Q^* > 0$ there exist matrix $P = P^* > 0$, such that

$$P\big(A_0 + T(0)\big) + \big(A_0 + T(0)\big)^T P = -Q \tag{2}$$

where $T(t)$ is continuous and differentiable matrix function which satisfies

$$\dot{T}(t) = \begin{cases} (A_0 + T(0))T(t), & 0 \le t \le \tau, \quad T(\tau) = A_1 \\ 0 & , \quad t > \tau \end{cases} \tag{3}$$

then the system (1) is asymptotically stable.

In paper (Lee & Diant, 1981) it is emphasized that the key to the success in the construction of a Lyapunov function corresponding to the system (1) is the existence of at least one solution $T(t)$ of (3) with boundary condition $T(\tau) = A_1$. In other words, it is required that the nonlinear algebraic matrix equation

$$e^{\left(A_0 + T(0)\right)\tau} T(0) = A_1 \tag{4}$$

has at least one solution for $T(0)$. It is asserted, there, that asymptotic stability of the system (*Theorem* 2.1.1) can be determined based on the knowledge of *only one* or *any*, solution of the particular nonlinear matrix equation.

We now demonstrate that *Theorem* 2.1.1 should be improved since it does not take into account all possible solutions for (4). The counterexample, based on our approach and supported by the Lambert function application, is given in (Stojanovic & Debeljkovic, 2006).

Conclusion 2.1.1 (Stojanovic & Debeljkovic, 2006) If we introduce a new matrix,

$$R \triangleq A_1 + T(0) \tag{5}$$

then condition (2) reads

$$PR + R^* P = -Q \tag{6}$$

which presents a well-known Lyapunov's equation for the system without time delay.

This condition will be fulfilled if and only if R is a stable matrix i.e. if

$$\operatorname{Re}\lambda_i(R) < 0 \tag{7}$$

holds.

Let Ω_T and Ω_R denote sets of all solutions of eq. (4) per T(0) and (6) per R, respectively.

Conclusion 2.1.2 (Stojanovic & Debeljkovic, 2006) Eq. (4) expressed through matrix R can be written in a different form as follows,

$$R - A_0 - e^{-R\tau} A_1 = 0 \tag{8}$$

and there follows

$$\det\left(R - A_0 - e^{-R\tau} A_1\right) = 0 \tag{9}$$

Substituting a matrix variable R by scalar variable s in (7), the characteristic equation of the system (1) is obtained as

$$f(s) = \det\left(sI - A_0 - e^{-s\tau} A_1\right) = 0 \tag{10}$$

Let us denote

$$\Sigma \triangleq \left\{ s \,|\, f(s) = 0 \right\} \tag{11}$$

a set of all characteristic roots of the system (1). The necessity for the correctness of desired results, forced us to propose new formulations of *Theorem* 2.1.1.

Theorem 2.1.2 (Stojanovic & Debeljkovic, 2006) Suppose that there exist(s) the solution(s) $T(0) \in \Omega_T$ of (4). Then, the system (1) is asymptotically stable if and only if any of the two following statements holds:

1. For any matrix $Q = Q^* > 0$ there exists matrix $P_0 = P_0^* > 0$ such that (2) holds for all solutions $T(0) \in \Omega_T$ of (4).
2. The condition (7) holds for all solutions $R = A_1 + T(0) \in \Omega_R$ of (8).

Conclusion 2.1.3 (Stojanovic & Debeljkovic, 2006) Statement *Theorem* 2.1.2 require that condition (2) is fulfilled for all solutions $T(0) \in \Omega_T$ of (4). In other words, it is requested that condition (7) holds for all solution R of (8) (especially for $R = R_{max}$, where the matrix $R_m \in \Omega_R$ is maximal solvent of (8) that contains eigenvalue with a maximal real part $\lambda_m \in \Sigma$: $\operatorname{Re}\lambda_m = \max\limits_{s \in \Sigma} \operatorname{Re} s$). Therefore, from (7) follows condition $\operatorname{Re}\lambda_i(R_m) < 0$. These matrix condition is analogous to the following known scalar condition of asymptotic stability: System (1) is asymptotically stable if and only if the condition $\operatorname{Re} s < 0$ holds for all solutions s of (10) (especially for $s = \lambda_m$).

On the basis of *Conclusion 2.1.3,* it is possible to reformulate *Theorem 2.1.2* in the following way.

Theorem 2.1.3 (Stojanovic & Debeljkovic, 2006) Suppose that there exists maximal solvent R_m of (8). Then, the system (1) is asymptotically stable if and only if any of the two following equivalent statements holds:

1. For any matrix $Q = Q^* > 0$ there exists matrix $P_0 = P_0^* > 0$ such that (6) holds for the solution $R = R_m$ of (8).
2. $\operatorname{Re}\lambda_i(R_m) < 0$.

2.2 Discrete time delay systems

2.2.1 Introduction

Basic inspiration for our investigation in this section is based on paper (Lee & Diant, 1981), however, the stability of discrete time delay systems is considered herein.

We propose necessary and sufficient conditions for delay dependent stability of discrete linear time delay system, which as distinguished from the criterion based on eigenvalues of the matrix of equivalent system (Gantmacher, 1960), use matrices of considerably lower dimension. The time-dependent criteria are derived by Lyapunov's direct method and are exclusively based on the maximal and dominant solvents of particular matrix polynomial equation. Obtained stability conditions do not possess conservatism but require complex numerical computations. However, if the dominant solvent can be computed by Traub's or Bernoulli's algorithm, it has been demonstrated that smaller number of computations are to be expected compared with a traditional stability procedure based on eigenvalues of matrix A_{eq} of equivalent (augmented) system (see (14)).

2.2.2. Preliminaries

A linear, discrete time-delay system can be represented by the difference equation

$$x(k+1) = A_0 x(k) + A_1 x(k-h) \tag{12}$$

with an associated function of initial state

$$x(\theta) = \psi(\theta), \qquad \theta \in \{-h, -h+1, \ldots, 0\} \tag{13}$$

The equation (12) is referred to as homogenous or the unforced state equation.

Vector $x(k) \in \mathbb{R}^n$ is a state vector and $A_0, A_1 \in \mathbb{R}^{n\times n}$ are constant matrices of appropriate dimensions, and pure system time delay is expressed by integers $h \in \mathbb{T}^+$. System (12) can be expressed with the following representation without delay, (Malek-Zavarei & Jamshidi, 1987; Gorecki et al., 1989).

$$\begin{gathered} x_{eq}(k) = \begin{bmatrix} x^T(k-h) & x^T(k-h+1) & \cdots x^T(k) \end{bmatrix} \in \mathbb{R}^N, \qquad N \triangleq n(h+1) \\ x_{eq}(k+1) = A_{eq} x_{eq}(k), \;\; A_{eq} = \begin{bmatrix} 0 & I_n & \cdots & 0 \\ \vdots & \vdots & \ddots & \vdots \\ 0 & 0 & \cdots & I_n \\ A_1 & 0 & \cdots & A_0 \end{bmatrix} \in \mathbb{R}^{N\times N} \end{gathered} \tag{14}$$

The system defined by (14) is called the equivalent (augmented) system, while matrix A_{eq}, the matrix of equivalent (augmented) system. Characteristic polynomial of system (12) is given with:

$$f(\lambda) \triangleq \det M(\lambda) = \sum_{j=0}^{n(h+1)} a_j \lambda^j, \quad a_j \in \mathbb{R}, \qquad M(\lambda) = I_n \lambda^{h+1} - A_0 \lambda^h - A_1 \tag{15}$$

Denote with

$$\Omega \triangleq \{\, \lambda \mid f(\lambda) = 0 \,\} = \lambda\left(A_{eq}\right) \tag{16}$$

the set of all characteristic roots of system (12). The number of these roots amounts to $n(h+1)$. A root λ_m of Ω with maximal module:

$$\lambda_m \in \Omega: \ |\lambda_m| = \max\left|\lambda\left(A_{eq}\right)\right| \tag{17}$$

let us call maximal root (eigenvalue). If scalar variable λ in the characteristic polynomial is replaced by matrix $X \in \mathbb{C}^{n\times n}$ the two following monic matrix polynomials are obtained

$$M(X) = X^{h+1} - A_0 X^h - A_1 \tag{18}$$

$$F(X) = X^{h+1} - X^h A_0 - A_1 \tag{19}$$

It is obvious that $F(\lambda) = M(\lambda)$. For matrix polynomial $M(X)$, the matrix of equivalent system A_{eq} represents block companion matrix.

A matrix $S \in \mathbb{C}^{n\times n}$ is a *right solvent* of $M(X)$ if

$$M(S) = 0 \tag{20}$$

If

$$F(R) = 0 \tag{21}$$

then $R \in \mathbb{C}^{n\times n}$ is a *left solvent* of $M(X)$, (Dennis et al., 1976).

We will further use matrix S to denote right solvent and matrix R to denote left solvent of $M(X)$.

In the present paper the majority of presented results start from left solvents of $M(X)$. In contrast, in the existing literature right solvents of $M(X)$ were mainly studied. The mentioned discrepancy can be overcome by the following *Lemma*.

Lemma 2.2.1 (Stojanovic & Debeljkovic, 2008.b). Conjugate transpose value of left solvent of $M(X)$ is also, at the same time, right solvent of the following matrix polynomial

$$\mathcal{M}(X) = X^{h+1} - A_0^T X^h - A_1^T \tag{22}$$

Conclusion 2.2.1 Based on *Lemma* 2.2.1, all characteristics of left solvents of $M(X)$ can be obtained by the analysis of conjugate transpose value of right solvents of $\mathcal{M}(X)$.

The following proposed factorization of the matrix $M(\lambda)$ will help us to better understand the relationship between eigenvalues of left and right solvents and roots of the system.

Lemma 2.2.2 (Stojanovic & Debeljkovic, 2008.b). The matrix $M(\lambda)$ can be factorized in the following way

$$M(\lambda) = \left(\lambda^h I_n + (S - A_0)\sum_{i=1}^{h} \lambda^{h-i} S^{i-1}\right)(\lambda I_n - S) = (\lambda I_n - R)\left(\lambda^h I_n + \sum_{i=1}^{h} \lambda^{h-i} R^{i-1}(R - A_0)\right) \tag{23}$$

Conclusion 2.2.2 From (15) and (23) follows $f(S)=f(R)=0$, e.g. the characteristic polynomial $f(\lambda)$ is *annihilating polynomial* for right and left solvents of $M(X)$. Therefore, $\lambda(S)\subset\Omega$ and $\lambda(R)\subset\Omega$ hold.

Eigenvalues and eigenvectors of the matrix have a crucial influence on the existence, enumeration and characterization of solvents of the matrix equation (20), (Dennis et al., 1976; Pereira, 2003).

Definition 2.2.1 (Dennis et al., 1976; Pereira, 2003). Let $M(\lambda)$ be a matrix polynomial in λ. If $\lambda_i \in \mathbb{C}$ is such that $\det M(\lambda_i)=0$, then we say that λ_i is a *latent root* or an *eigenvalue* of $M(\lambda)$. If a nonzero $v_i \in \mathbb{C}^n$ is such that $M(\lambda_i)v_i=0$ then we say that v_i is a (right) *latent vector* or a (right) *eigenvector* of $M(\lambda)$, corresponding to the eigenvalue λ_i.

Eigenvalues of matrix $M(\lambda)$ correspond to the characteristic roots of the system, i.e. eigenvalues of its block companion matrix A_{eq}, (Dennis et al., 1976). Their number is $n\cdot(h+1)$. Since $F^*(\lambda)=\mathcal{M}(\lambda^*)$ holds, it is not difficult to show that matrices $M(\lambda)$ and $\mathcal{M}(\lambda)$ have the same spectrum.

In papers (Dennis et al., 1976, Dennis et al., 1978; Kim, 2000; Pereira, 2003) some sufficient conditions for the existence, enumeration and characterization of right solvents of $M(X)$ were derived. They show that the number of solvents can be zero, finite or infinite.

For the needs of system stability (12) only the so called maximal solvents are usable, whose spectrums contain maximal eigenvalue λ_m. A special case of maximal solvent is the so called dominant solvent, (Dennis et al., 1976; Kim, 2000), which, unlike maximal solvents, can be computed in a simple way.

Definition 2.2.2 Every solvent S_m of $M(X)$, whose spectrum $\sigma(S_m)$ contains maximal eigenvalue λ_m of Ω is a *maximal solvent*.

Definition 2.2.3 (Dennis et al., 1976; Kim, 2000). Matrix A dominates matrix B if all the eigenvalues of A are greater, in modulus, then those of B. In particular, if the solvent S_1 of $M(X)$ dominates the solvents $S_2,\ldots,S_l$ we say it is a *dominant solvent*.

Conclusion 2.2.3 The number of maximal solvents can be greater than one. Dominant solvent is at the same time maximal solvent, too. The dominant solvent S_1 of $M(X)$, under certain conditions, can be determined by the Traub, (Dennis et al., 1978) and Bernoulli iteration (Dennis et al., 1978; Kim, 2000).

Conclusion 2.2.4 Similar to the definition of right solvents S_m and S_1 of $M(X)$, the definitions of both maximal left solvent, R_m, and dominant left solvent, R_1, of $M(X)$ can be provided. These left solvents of $M(X)$ are used in a number of theorems to follow. Owing to *Lemma* 2.2.1, they can be determined by proper right solvents of $\mathcal{M}(X)$.

2.2.3. Main results

Theorem 2.2.1 (Stojanovic & Debeljkovic, 2008.b). Suppose that there exists at least one left solvent of $M(X)$ and let R_m denote one of them. Then, linear discrete time delay system (12) is asymptotically stable if and only if for any matrix $Q = Q^* > 0$ there exists matrix $P = P^* > 0$ such that

$$R_m^* P R_m - P = -Q \tag{24}$$

Proof. *Sufficient condition.* Define the following vector discrete functions

$$x_k = x(k+\theta), \quad \theta \in \{-h, -h+1, \dots, 0\}, \quad z(x_k) = x(k) + \sum_{j=1}^{h} T(j) x(k-j) \tag{25}$$

where, $T(k) \in \mathbb{C}^{n \times n}$ is, in general, some time varying discrete matrix function. The conclusion of the theorem follows immediately by defining Lyapunov functional for the system (12) as

$$V(x_k) = z^*(x_k) P z(x_k), \quad P = P^* > 0 \tag{26}$$

It is obvious that $z(x_k) = 0$ if and only if $x_k = 0$, so it follows that $V(x_k) > 0$ for $\forall x_k \neq 0$. The forward difference of (26), along the solutions of system (12) is

$$\Delta V(x_k) = \Delta z^*(x_k) P z(k) + z^*(x_k) P \Delta z(x_k) + \Delta z^*(x_k) P \Delta z(x_k) \tag{27}$$

A difference of $\Delta z(x_k)$ can be determined in the following manner

$$\begin{aligned}
&\Delta z(x_k) = \Delta x(k) + \sum_{j=1}^{h} T(j) \Delta x(k-j), \quad \Delta x(k) = (A_0 - I_n) x(k) + A_1 x(k-h) \\
&\sum_{j=1}^{h} T(j) \Delta x(k-j) = T(1)\left[x(k) - x(k-1)\right] + \cdots + T(h)\left[x(k-h+1) - x(k-h)\right] \\
&\qquad = T(1) x(k) - T(h) x(k-h) + \left(T(2) - T(1)\right) x(k-1) + \cdots \\
&\qquad\quad + \left(T(h) - T(h-1)\right) x(k-h+1)
\end{aligned} \tag{28}$$

Define a new matrix R by

$$R = A_0 + T(1) \tag{29}$$

If

$$\Delta T(h) = A_1 - T(h) \tag{30}$$

then $\Delta z(x_k)$ has a form

$$\Delta z(x_k) = (R - I_n) x(k) + \sum_{j=1}^{h} \left[\Delta T(j) \cdot x(k-j)\right] \tag{31}$$

If one adopts

$$\Delta T(j) = (R - I_n) T(j), \quad j = 1, 2, \ldots, h \tag{32}$$

then (27) becomes

$$\Delta V(x_k) = z^*(x_k)\left(R^* P R - P\right) z(x_k) \tag{33}$$

It is obvious that if the following equation is satisfied

$$R^* P R - P = -Q, \quad Q = Q^* > 0 \tag{34}$$

then $\Delta V(x_k) < 0,\ x_k \neq 0$.

In the Lyapunov matrix equation (34), of all possible solvents *R* of $M(X)$, only one of maximal solvents is of importance, for it is the only one that contains maximal eigenvalue $\lambda_m \in \Omega$, which has dominant influence on the stability of the system. So, (24) represent stability sufficient condition for system given by (12).

Matrix $T(1)$ can be determined in the following way. From (32), follows

$$T(h+1) = R^h T(1) \tag{35}$$

and using (29)-(30) one can get (21), and for the sake of brevity, instead of matrix $T(1)$, one introduces simple notation T.

If solvent which is not maximal is integrated into Lyapunov equation, it may happen that there will exist positive definite solution of Lyapunov matrix equation (24), although the system is not stable.

Necessary condition. If the system (12) is asymptotically stable then all roots $\lambda_i \in \Omega$ are located within unit circle. Since $\sigma(R_m) \subset \Omega$, follows $\rho(R_m) < 1$, so the positive definite solution of Lyapunov matrix equation (24) exists.

Corollary 2.2.1 Suppose that there exists at least one maximal left solvent of $M(X)$ and let R_m denote one of them. Then, system (12) is asymptotically stable if and only if $\rho(R_m) < 1$, (Stojanovic & Debeljkovic, 2008.b).

Proof. Follows directly from *Theorem* 2.2.1.

Corollary 2.2.2 (Stojanovic & Debeljkovic, 2008.b) Suppose that there exists dominant left solvent R_1 of $M(X)$. Then, system (12) is asymptotically stable if and only if $\rho(R_1) < 1$.

Proof. Follows directly from *Corollary* 2.2.1, since dominant solution is, at the same time, maximal solvent.

Conclusion 2.2.5 In the case when dominant solvent R_1 may be deduced by Traub's or Bernoulli's algorithm, *Corollary* 2.2.2 represents a quite simple method. If aforementioned algorithms are not convergent but still there exists at least one of maximal solvents R_m, then one should use *Corollary* 2.2.1. The maximal solvents may be found, for example, using the concept of eigenpars, Pereira (2003). If there is no maximal solvent R_m, then proposed necessary and sufficient conditions *can not be used* for system stability investigation.

Conclusion 2.2.6 For some time delay systems it holds

$$\dim\left(R_1\right)=\dim\left(R_m\right)=\dim\left(A_i\right)=n \ll \dim\left(A_{eq}\right)=n\left(h+1\right)$$

For example, if time delay amounts to $h=100$, and the row of matrices of the system is $n=2$, then: $R_1, R_m \in \mathbb{C}^{2\times 2}$ and $A_{eq} \in \mathbb{C}^{202\times 202}$.

To check the stability by eigenvalues of matrix A_{eq}, it is necessary to determine 202 eigenvalues, which is not numerically simple. On the other hand, if dominant solvent can be computed by Traub's or Bernoulli's algorithm, *Corollary* 2.2.2 requires a relatively small number of additions, subtractions, multiplications and inversions of the matrix format of only 2×2.

So, in the case of great time delay in the system, by applying *Corollary* 2.2.2, a smaller number of computations are to be expected compared with a traditional procedure of examining the stability by eigenvalues of companion matrix A_{eq}. An accurate number of computations for each of the mentioned method require additional analysis, which is not the subject-matter of our considerations herein.

2.2.4. Numerical examples

Example 2.2.1 (Stojanovic & Debeljkovic, 2008.b). Let us consider linear discrete systems with delayed state (12) with

$$A_0=\begin{bmatrix} 7/10 & -1/2 \\ 1/2 & 17/10 \end{bmatrix},\quad A_1=\begin{bmatrix} 1/75 & 1/3 \\ -1/3 & -49/75 \end{bmatrix},$$

A. For $h=1$ there are two left solvents of matrix polynomial equation (21) ($R^2-RA_0-A_1=0$):

$$R_1=\begin{bmatrix} 19/30 & -1/6 \\ 1/6 & 29/30 \end{bmatrix},\quad R_2=\begin{bmatrix} 1/15 & -1/3 \\ 1/3 & 11/15 \end{bmatrix},$$

Since $\lambda(R_1)=\{4/5,4/5\}$, $\lambda(R_2)=\{2/5,2/5\}$, dominant solvent is R_1. As we have $V\left(R_1,R_2\right)$ nonsingular, Traub's or Bernoulli's algorithm may be used. Only after $(4+3)$ iterations for Traub's algorithm (Dennis et al., 1978) and 17 iterations for Bernoulli algorithm (Dennis et al., 1978), dominant solvent can be found with accuracy of 10^{-4}. Since $\rho(R_1)=4/5<1$, based on *Corollary* 2.2.2, it follows that the system under consideration is asymptotically stable.

B. For $h=20$ applying Bernoulli or Traub's algorithm for computation the dominant solvent R_1 of matrix polynomial equation (21) ($R^{21}-R^{20}A_0-A_1=0$), we obtain

$$R_1=\begin{bmatrix} 0.6034 & -0.5868 \\ 0.5868 & 1.7769 \end{bmatrix}$$

Based on *Corollary* 2.2.2, the system is not asymptotically stable because $\rho(R_1)=1.1902>1$.

Finally, let us check stability properties of the system using his maximal eigenvalue:

$$\lambda_{max}\left\{A_{eq}\right\}=\lambda_{max}\left[\begin{array}{c|c} 0_{40x2} & I_{40x40} \\ \hline A_0 & 0_{2x2}\ \ldots\ 0_{2x2}\ A_1 \end{array}\right]=1.1902>1$$

Evidently, the same result is obtained as above.

3. Large scale time delay systems

3.1 Continuous large scale time delay systems

3.1.1 Introduction

There exist many real-world systems that can be modeled as large-scale systems: examples are power systems, communication systems, social systems, transportation systems, rolling mill systems, economic systems, biological systems and so on. It is also well known that the control and analysis of large-scale systems can become very complicated owing to the high dimensionality of the system equation, uncertainties, and time-delays. During the last two decades, the stabilization of uncertain large-scale systems becomes a very important problem and has been studied extensively (Siljak, 1978; Mahmoud et al., 1985). Especially, many researchers have considered the problem of stability analysis and control of various large-scale systems with time-delays (Wu, 1999; Park, 2002 and references therein).

Recently, the stabilization problem of large-scale systems with delays has been considered by (Lee & Radovic, 1988; Hu, 1994; Trihn & Aldeen 1995a; Xu, 1995). However, the results in (Lee & Radovic, 1988; Hu, 1994) apply only to a very restrictive class of systems for which the number of inputs and outputs is equal to or greater than the number of states. Also, since the sufficient conditions of (Trinh & Aldeen 1995a; Xu, 1995) are expressed in terms of the matrix norm of the system matrices, usually the matrix norm operation makes the criteria more conservative.

The paper (Xu, 1995) provides a new criterion for delay-independent stability of linear large scale time delay systems by employing an improved Razumikhin-type theorem and M-matrix properties. In (Trinh & Aldeen, 1997), by employing a Razumikhin-type theorem, a robust stability criterion for a class of linear system subject to delayed time-varying nonlinear perturbations is given.

The basic aim of the above mentioned works was to obtain only sufficient conditions for stability of large scale time delay systems. It is notorious that those conditions of stability are more or less conservative.

In contrast, the major results of our investigations are necessary and sufficient conditions of asymptotic stability of continuous large scale time delay autonomous systems. The obtained conditions are expressed by nonlinear system of matrix equations and the Lyapunov matrix equation for an ordinary linear continuous system without delay. Those conditions of stability are delay-dependent and do not possess conservatism. Unfortunately, viewed mathematically, they require somewhat more complex numerical computations.

3.1.2 Main Results

Consider a linear continuous large scale time delay autonomous systems composed of N interconnected subsystems. Each subsystem is described as:

$$\dot{x}_i(t) = A_i x_i(t) + \sum_{j=1}^{N} A_{ij} x_j(t - \tau_{ij}),\ 1 \le i \le N \tag{36}$$

with an associated function of initial state $x_i(\theta) = \varphi_i(\theta)$, $\theta \in [-\tau_{m_i}, 0]$, $1 \le i \le N$. $x_i(t) \in \mathbb{R}^{n_i}$ is state vector, $A_i \in \mathbb{R}^{n_i \times n_i}$ denote the system matrix, $A_{ij} \in R^{n_i \times n_j}$ represents the interconnection matrix between the i-th and the j-th subsystems, and τ_{ij} is constant delay. For the sake of brevity, we first observe system (36) made up of two subsystems ($N = 2$). For this system, we derive new necessary and sufficient delay-dependent conditions for stability, by Lyapunov's direct method. The derived results are then extended to the linear continuous large scale time delay systems with multiple subsystems.

a) Large scale systems with two subsystems

Theorem 3.1.1. (Stojanovic & Debeljkovic, 2005). Given the following system of matrix equations (SME)

$$\mathcal{R}_1 - A_1 - e^{-\mathcal{R}_1 \tau_{11}} A_{11} - e^{-\mathcal{R}_1 \tau_{21}} S_2 A_{21} = 0 \tag{37}$$

$$\mathcal{R}_1 S_2 - S_2 A_2 - e^{-\mathcal{R}_1 \tau_{12}} A_{12} - e^{-\mathcal{R}_1 \tau_{22}} S_2 A_{22} = 0 \tag{38}$$

where A_1, A_2, A_{12}, A_{21} and A_{22} are matrices of system (36) for $N = 2$, n_i subsystem orders and τ_{ij} pure time delays of the system. If there exists solution of SME (37)-(38) upon unknown matrices $\mathcal{R}_1 \in C^{n_1 \times n_1}$ and $S_2 \in C^{n_1 \times n_2}$, then the eigenvalues of matrix $\mathcal{R}_1$ belong to a set of roots of the characteristic equation of system (36) for $N = 2$.

Proof. By introducing the time delay operator $e^{-\tau s}$, the system (36) can be expressed in the form

$$\dot{x}(t) = \begin{bmatrix} A_1 + A_{11} e^{-\tau_{11} s} & A_{12} e^{-\tau_{12} s} \\ A_{21} e^{-\tau_{21} s} & A_2 + A_{22} e^{-\tau_{22} s} \end{bmatrix} x(t) = A_e(s) x(t),\ x(t) = \begin{bmatrix} x_1^T(t) & x_2^T(t) \end{bmatrix}^T \tag{39}$$

Let us form the following matrix

$$F(s) = \left[F_{ij}(s)\right] = sI_{n_1+n_2} - A_e(s) = \begin{bmatrix} sI_{n_1} - A_1 - A_{11} e^{-\tau_{11} s} & -A_{12} e^{-\tau_{12} s} \\ -A_{21} e^{-\tau_{21} s} & sI_{n_2} - A_2 - A_{22} s^{-\tau_{22} s} \end{bmatrix} \tag{40}$$

Its determinant is

$$\begin{aligned} \det F(s) &= \det \begin{bmatrix} F_{11}(s) & F_{12}(s) \\ F_{21}(s) & F_{22}(s) \end{bmatrix} = \det \begin{bmatrix} F_{11}(s) + S_2 F_{21}(s) & F_{12}(s) + S_2 F_{22}(s) \\ F_{21}(s) & F_{22}(s) \end{bmatrix} \\ &= \det \begin{bmatrix} G_{11}(s, S_2) & G_{12}(s, S_2) \\ G_{21}(s) & G_{22}(s) \end{bmatrix} = \det G(s, S_2) \end{aligned} \tag{41}$$

$$G_{11}(s,S_2) = sI_{n1} - A_1 - A_{11}e^{-\tau_{11}s} - S_2A_{21}e^{-\tau_{21}s} \tag{42}$$

$$G_{12}(s,S_2) = sS_2 - S_2A_2 - A_{12}e^{-\tau_{12}s} - S_2A_{22}e^{-\tau_{22}s} \tag{43}$$

Transformational matrix S_2 is unknown for the time being, but condition determining this matrix will be derived in a further text.
The characteristic polynomial of system (36) for $N = 2$, defined by

$$f(s) \triangleq \det(sI_N - A_e(s)) = \det G(s,S_2) \tag{44}$$

is independent of the choice of matrix S_2, because the determinant of matrix $G(s,S_2)$ is invariant with respect to elementary row operation of type 3. Let us designate a set of roots of the characteristic equation of system (36) by $\Sigma \triangleq \{ s \,|\, f(s) = 0 \}$. Substituting scalar variable s by matrix X in $G(s,S_2)$ we obtain

$$G(X,S_2) = \begin{bmatrix} G_{11}(X,S_2) & G_{12}(X,S_2) \\ G_{21}(X) & G_{22}(X) \end{bmatrix} \tag{45}$$

If there exist transformational matrix S_2 and matrix $\mathcal{R}_1 \in C^{n_1 \times n_1}$ such that $G_{11}(\mathcal{R}_1,S_2) = 0$ and $G_{12}(\mathcal{R}_1,S_2) = 0$ is satisfied, i.e. if (37)-(38) hold, then

$$f(\mathcal{R}_1) = \det G_{11}(\mathcal{R}_1,S_2) \cdot \det G_{22}(\mathcal{R}_1) = 0 \tag{46}$$

So, the characteristic polynomial (44) of system (36) is annihilating polynomial (Lancaster & Tismenetsky, 1985) for the square matrix $\mathcal{R}_1$, defined by (37)-(38). In other words, $\sigma(\mathcal{R}_1) \subset \Sigma$.

Theorem 3.1.2 (Stojanovic & Debeljkovic, 2005) Given the following SME

$$\mathcal{R}_2 - A_2 - e^{-\mathcal{R}_2\tau_{12}} S_1A_{12} - e^{-\mathcal{R}_2\tau_{22}} A_{22} = 0 \tag{47}$$

$$\mathcal{R}_2S_1 - S_1A_1 - e^{-\mathcal{R}_2\tau_{11}} S_1A_{11} - e^{-\mathcal{R}_2\tau_{21}} A_{21} = 0 \tag{48}$$

where A_1, A_2, A_{12}, A_{21} and A_{22} are matrices of system (36) for $N = 2$, n_i subsystem orders and τ_{ij} time delays of the system. If there exists solution of SME (47)-(48) upon unknown matrices $\mathcal{R}_2 \in C^{n_2 \times n_2}$ and $S_1 \in C^{n_2 \times n_1}$, then the eigenvalues of matrix $\mathcal{R}_2$ belong to a set of roots of the characteristic equation of system (36) for $N = 2$.

Proof. Proof is similarly with the proof of *Theorem* 3.1.1.

Corollary 3.1.1 If system (36) is asymptotically stable, then matrices $\mathcal{R}_1$ and $\mathcal{R}_2$, defined by SME (37)-(38) and (47)-(48), respectively, are stable ($\mathrm{Re}\,\lambda(\mathcal{R}_i) < 0$, $1 \le i \le 2$).

Proof. If system (36) is asymptotically stable, then $\forall s \in \Sigma, \operatorname{Re} s < 0$. Since $\sigma(\mathcal{R}_i) \subset \Sigma$, $1 \le i \le 2$, it follows that $\forall \lambda \in \sigma(\mathcal{R}_i)$, $\operatorname{Re}\lambda < 0$, i.e. matrices $\mathcal{R}_1$ and $\mathcal{R}_2$ are stable.

Definition 3.1.1 The matrix $\mathcal{R}_1$ ($\mathcal{R}_2$) is referred to as *solvent* of SME (37)-(38) or (47)-(48).

Definition 3.1.2 Each root λ_m of the characteristic equation (44) of the system (36) which satisfies the following condition: $\operatorname{Re}\lambda_m = \max \operatorname{Re} s$, $s \in \Sigma$ will be referred to as *maximal root* (*eigenvalue*) of system (36).

Definition 3.1.3 Each solvent $\mathcal{R}_{1m}$ ($\mathcal{R}_{2m}$) of SME (37)-(38) or (47)-(48), whose spectrum contains maximal eigenvalue λ_m of system (36), is referred to as *maximal solvent* of SME (37) -(38) or (47)-(48).

Theorem 3.1.3 (Stojanovic & Debeljkovic, 2005) Suppose that there exists at least one maximal solvent of SME (47)-(48) and let $\mathcal{R}_{1m}$ denote one of them. Then, system (36), for $N = 2$, is asymptotically stable if and only if for any matrix $Q = Q^* > 0$ there exists matrix $P = P^* > 0$ such that

$$\mathcal{R}_{1m}^* P + P\mathcal{R}_{1m} = -Q \tag{49}$$

Proof. *Sufficient condition.* Similarly (Lee & Diant, 1981), define the following vector continuous functions

$$x_{ti} = x_i(t+\theta), \quad \theta \in \left[-\tau_{m_i}, 0\right], \quad z(x_{t1}, x_{t2}) = \sum_{i=1}^{2} S_i \left(x_i(t) + \sum_{j=1}^{2} \int_0^{\tau_{ji}} T_{ji}(\eta) x_i(t-\eta) d\eta \right) \tag{50}$$

where $T_{ji}(t) \in C^{n_i \times n_i}$, $j = 1,2$ are some time varying continuous matrix functions and $S_1 = I_{n_1}$, $S_2 \in C^{n_1 \times n_2}$.

The proof of the theorem follows immediately by defining Lyapunov functional for system (36) as

$$V(x_{t1}, x_{t2}) = z^*(x_{t1}, x_{t2}) P z(x_{t1}, x_{t2}), \quad P = P^* > 0 \tag{51}$$

Derivative of (51), along the solutions of system (36) is

$$\dot{V}(x_{t1}, x_{t2}) = \dot{z}^*(x_{t1}, x_{t2}) P z(x_{t1}, x_{t2}) + z^*(x_{t1}, x_{t2}) P \dot{z}(x_{t1}, x_{t2}) \tag{52}$$

$$\dot{z}(x_{t1}, x_{t2}) = \sum_{i=1}^{2} S_i \left(\dot{x}_i(t) + \sum_{j=1}^{2} \frac{d}{dt} \int_o^{\tau_{ji}} T_{ji}(\eta) x_i(t-\eta) d\eta \right) \tag{53}$$

$$\frac{d}{dt} \int_0^{\tau_{ji}} T_{ji}(\eta)\, x_i(t-\eta)\, d\eta = \int_0^{\tau_{ji}} T_{ji}'(\eta)\, x_i(t-\eta)\, d\eta + T_{ji}(0)\, x_i(t) - T_{ji}(\tau_{ji})\, x_i(t-\tau_{ji}) \tag{54}$$

Therefore

$$\dot{z}(x_{t1},x_{t2}) = \sum_{i=1}^{2}\left\{ S_i\left(A_i + \sum_{j=1}^{2} T_{ji}(0)\right)x_i(t) + \sum_{j=1}^{2}\left(S_jA_{ji} - S_iT_{ji}(\tau_{ji})\right)x_i(t-\tau_{ji}) + \sum_{j=1}^{2}\int_0^{\tau_{ji}} S_iT_{ji}{}'(\eta)x_i(t-\eta)d\eta \right\} \tag{55}$$

If we define new matrices

$$\mathcal{R}_i = A_i + \sum_{j=1}^{2} T_{ji}(0),\ i=1,2 \tag{56}$$

and if one adopts

$$S_iT_{ji}(\tau_{ji}) = S_jA_{ji}\ ,\ i,j=1,2 \tag{57}$$

$$S_iT_{ji}{}'(\eta) = \mathcal{R}_1S_iT_{ji}(\eta),\quad S_i\mathcal{R}_i = \mathcal{R}_1S_i,\quad i,j=1,2 \tag{58}$$

then

$$\dot{z}(x_{t1},x_{t2}) = \mathcal{R}_1z(x_{t1},x_{t2}),\quad \dot{V}(x_{t1},x_{t2}) = z^*(x_{t1},x_{t2})\left(\mathcal{R}_1{}^*P + P\mathcal{R}_1\right)z(x_{t1},x_{t2}) \tag{59}$$

It is obvious that if the following equation is satisfied

$$\mathcal{R}_1{}^*P + P\mathcal{R}_1 = -Q < 0\ , \tag{60}$$

then $\dot{V}(x_{t1},x_{t2}) < 0$, $\forall x_{ti} \neq 0$.
In the Lyapunov matrix equation (49), of all possible solvents $\mathcal{R}_1$ only one of maximal solvents $\mathcal{R}_{1m}$ is of importance, because it is containing maximal eigenvalue $\lambda_m \in \Sigma$, which has dominant influence on the stability of the system.
If a solvent, which is not maximal, is integrated into Lyapunov equation (49), it may happen that there will exist positive definite solution of this equation, although the system is not stable.
Necessary condition. Let us assume that system (36) for $N=2$ is asymptotically stable, i.e. $\forall s \in \Sigma$, $\operatorname{Re} s < 0$ hold. Since $\sigma(\mathcal{R}_{1m}) \subset \Sigma$ follows $\operatorname{Re}\lambda(\mathcal{R}_{1m}) < 0$ and the positive definite solution of Lyapunov matrix equation (49) exists.
From (57)-(58) follows

$$S_jA_{ji} = e^{\mathcal{R}_1\tau_{ji}}S_iT_{ji}(0),\ S_1 = I_{n_1},\quad i=1,2,\ j=1,2 \tag{61}$$

Using (56) and (61), for $i=1$, we obtain (37).
Multiplying (56) (for $i=2$) from the left by matrix S_2 and using (58) and (61) we obtain (38)

Taking a solvent with eigenvalue $\lambda_m \in \Sigma$ (if it exists) as a solution of the system of equations (37)-(38), we arrive at a maximal solvent $\mathcal{R}_{1m}$.

Theorem 3.1.4 (Stojanovic & Debeljkovic 2005) Suppose that there exists at least one maximal solvent of SME (47)-(48) and let $\mathcal{R}_{2m}$ denote one of them. Then, system (36), for $N = 2$, is asymptotically stable if and only if for any matrix $Q = Q^* > 0$ there exists matrix $P = P^* > 0$ such that

$$\mathcal{R}_{2m}^* P + P\mathcal{R}_{2m} = -Q \tag{62}$$

Proof. Proof is almost identical to that exposed for *Theorem* 3.1.3.

Conclusion 3.1.1 The proposed criteria of stability are expressed in the form of necessary and sufficient conditions and as such do not possess conservatism unlike the existing sufficient criteria of stability.

Conclusion 3.1.2 To the authors' knowledge, in the literature available, there are no adequate numerical methods for direct computations of maximal solvents $\mathcal{R}_{1m}$ or $\mathcal{R}_{2m}$. Instead, using various initial values for solvents $\mathcal{R}_i$, we determine $\mathcal{R}_{im}$ by applying minimization methods based on nonlinear least squares algorithms (see *Example* 3.1.1).

b) Large scale system with multiple subsystems

Theorem 3.1.5. (Stojanovic & Debeljkovic, 2005) Given the following system of matrix equations

$$\mathcal{R}_k S_i - S_i A_i - \sum_{j=1}^{N} e^{-\mathcal{R}_k \tau_{ji}} S_j A_{ji} = 0, \quad S_i \in C^{n_k \times n_i}, \quad S_k = I_{n_k}, \quad 1 \le i \le N \tag{63}$$

for a given k, $1 \le k \le N$, where A_i and A_{ji}, $1 \le i \le N$, $1 \le j \le N$ are matrices of system (36) and τ_{ji} is time delay in the system. If there is a solvent of (63) upon unknown matrices $\mathcal{R}_k \in C^{n_k \times n_k}$ and S_i, $1 \le i \le N$, $i \ne k$, then the eigenvalues of matrix $\mathcal{R}_k$ belong to a set of roots of the characteristic equation of system (36).

Proof. Proof of this theorem is a generalization of proof of *Theorem* 3.1.1 or *Theorem* 3.1.2.

Theorem 3.1.6 (Stojanovic & Debeljkovic, 2005) Suppose that there exists at least one maximal solvent of (63) *for given* k, $1 \le k \le N$ and let $\mathcal{R}_{km}$ denote one of them. Then, linear discrete large scale time delay system (36) is asymptotically stable if and only if for any matrix $Q = Q^* > 0$ there exists matrix $P = P^* > 0$ such that

$$\mathcal{R}_{km}^* P + P\mathcal{R}_{km} = -Q \tag{64}$$

Proof. Proof is based on generalization of proof for *Theorem* 3.1.3 and *Theorem* 3.1.4. It is sufficient to take arbitrary *N* instead of $N = 2$.

3.1.3 Numerical example

Example 3.1.1 Consider following continuous large scale time delay system with delay interconnections

$$\begin{aligned}\dot{x}_1(t) &= A_1x_1(t) + A_{12}x_2(t-\tau_{12})\\ \dot{x}_2(t) &= A_2x_2(t) + A_{21}x_1(t-\tau_{21}) + A_{23}x_3(t-\tau_{23})\\ \dot{x}_3(t) &= A_3x_3(t) + A_{31}x_1(t-\tau_{31}) + A_{32}x_2(t-\tau_{32})\end{aligned} \tag{65}$$

$$A_1 = \begin{bmatrix} -6 & 2 & 0 \\ 0 & -7 & 0 \\ 0 & 0 & -10.9 \end{bmatrix},\ A_{12} = \begin{bmatrix} 3 & -2 & 0 \\ 0 & 0 & 3 \\ -2 & 1 & 2 \end{bmatrix},\ A_2 = \begin{bmatrix} -1.87 & 4.91 & 10.30 \\ -2.23 & -16.51 & -24.11 \\ 1.87 & -3.91 & -10.30 \end{bmatrix},\ A_{21} = \begin{bmatrix} -1 & 0 & -2 \\ 3 & 0 & 5 \\ 1 & 0 & 2 \end{bmatrix},$$

$$A_{23} = \begin{bmatrix} -1 & -1 \\ 3 & 2 \\ 1 & 1 \end{bmatrix},\quad A_3 = \begin{bmatrix} -18.5 & -17.5 \\ -13.5 & -18.5 \end{bmatrix},\quad A_{31} = \begin{bmatrix} 4 & -2 & 1 \\ 2 & 0 & 1 \end{bmatrix},\quad A_{32} = \begin{bmatrix} 1 & 2 & -1 \\ 3 & 2 & 0 \end{bmatrix},$$

Applying *Theorem* 3.1.5 to a given system, for $k = 1$, the following SME is obtained

$$\begin{aligned}\mathcal{R}_1 - A_1 - e^{-\mathcal{R}_1\tau_{21}}S_2A_{21} - e^{-\mathcal{R}_1\tau_{31}}S_3A_{31} &= 0\\ \mathcal{R}_1S_2 - S_2A_2 - e^{-\mathcal{R}_1\tau_{12}}A_{12} - e^{-\mathcal{R}_1\tau_{32}}S_3A_{32} &= 0\\ \mathcal{R}_1S_3 - S_3A_3 - e^{-\mathcal{R}_1\tau_{23}}S_2A_{23} &= 0\end{aligned} \tag{66}$$

If for pure system time delays we adopt the following values: $\tau_{12} = 5$, $\tau_{21} = 2$, $\tau_{23} = 4$, $\tau_{31} = 5$ and $\tau_{32} = 3$, by applying the nonlinear least squares algorithms, we obtain a great number of solutions upon $\mathcal{R}_1$ which satisfy SME (66):
Among those solutions is a maximal solution:

$$\mathcal{R}_{1m} = \begin{bmatrix} -0.0484 & -0.0996 & 0.0934 \\ 0.2789 & -0.3123 & 0.2104 \\ 1.1798 & -1.1970 & -0.3798 \end{bmatrix}$$

The eigenvalues of matrix $\mathcal{R}_{1m}$ amount to: $\lambda_1 = -0.2517$, $\lambda_{2,3} = -0.2444 \pm j\ 0.3726$.

Therefore, for a maximal eigenvalue λ_m one of the values from the set $\{\lambda_2, \lambda_3\}$ can be adopted. Based on *Theorem* 3.1.6, it follows that the large scale time delay system is asymptotically stable.

3.2 Discrete large scale time delay systems

3.2.1 Introduction

Recently, the stability and stabilization problem of large-scale systems with delays has been considered by (Lee & Radovic, 1987, 1988), (Hu, 1994), (Trinh & Aldeen, 1995b), (Xu, 1995), (Huang et al., 1995), (Lee & Hsien 1997), (Wang & Mau 1997) and (Park, 2002).
Most related works treated the stabilization problem in the continuous-time case. Since most modern control systems are controlled by a digital computer, it is natural to deal with the problem in a discrete-time domain.

Based on the Lyapunov stability theorem associated with norm inequality techniques, in (Lee & Hsien, 1997) the stability testing problem for discrete large-scale uncertain systems with time delays in the interconnections is investigated. Three classes of uncertainties are treated: nonlinear, linear unstructured and linear highly structured uncertainties. A criterion to guarantee the robust stabilization and the state estimation for perturbed discrete time-delay large-scale systems is proposed in (Wang & Mau, 1997). This criterion is independent of time delay and does not need the solution of a Lyapunov equation or Riccati equation.

In paper (Park, 2002) the synthesis of robust decentralized controllers for uncertain large-scale discrete-time systems with time delays in the subsystem interconnections is considered. Based on the Lyapunov method, a sufficient condition for robust stability is derived in terms of a linear matrix inequality. Further, (Park et al., 2004) was discussed how to solve dynamic output feedback controller design problem for decentralized guaranteed cost stabilization of large-scale discrete-delay system by convex optimization. The problems of robust non-fragile control for uncertain discrete-delay large-scale systems under state feedback gain variations are investigated in (Park, 2004).

In this section the necessary and sufficient conditions for the asymptotic stability of a particular class of large-scale linear discrete time-delay systems are considered. The obtained conditions of stability are derived by Lyapunov's direct method and expressed by system of matrix polynomial equations. The conditions are not conservative against the majority of results reported in the literature available. In the case of great time delays in the system and a great number of subsystems, by applying the derived results it has been demonstrated that a smaller number of computations are to be expected compared with a classical stability criteria based on eigenvalues of matrix of equivalent system.

3.2.2. Preliminaries

Consider a large-scale linear discrete time-delay systems composed of N interconnected S_i. Each subsystem S_i, $1 \le i \le N$ is described as

$$S_i: \quad x_i(k+1) = A_i x_i(k) + \sum_{j=1}^{N} A_{ij} x_j\left(k - h_{ij}\right) \tag{67}$$

with an associated function of initial state

$$x_i(\theta) = \psi_i(\theta), \quad \theta \in \left\{-h_{m_i}, -h_{m_i}+1 \ , \ \dots \ , \ 0\right\} \tag{68}$$

where $x_i(k) \in \mathbb{R}^{n_i}$ is state vector, $A_i \in \mathbb{R}^{n_i \times n_i}$ denotes the system matrix, $A_{ij} \in \mathbb{R}^{n_i \times n_j}$ represents the interconnection matrix between the i-th and the j-th subsystems and the constant delay $h_{ij} \in \mathbb{T}^{+}$.

In the following lemma necessary and sufficient condition for asymptotic stability of system (67) has been given, expressed via eigenvalues the so called *equivalent matrix* $\mathcal{A}$. This condition is based upon the fact that the observed system is finite-dimensional. The order of this system is very high and time delay dependent.

Lemma 3.2.1 System (67) will be asymptotically stable if and only if

$$\rho(\mathcal{A}) < 1 \tag{69}$$

holds, where matrix

$$\mathcal{A}=\left[\mathcal{A}_{ij}\right]\in\mathbb{R}^{N_e\times N_e},\quad N_e=\sum_{i=1}^{N}N_i,\quad N_i=n_i\left(h_{m_i}+1\right),\quad h_{m_i}=\max_j h_{ji} \tag{70}$$

is defined in the following way

$$\mathcal{A}_{ii}=\begin{array}{c}\begin{array}{ccccccc}\overset{1}{\downarrow} & & \cdots & \overset{h_{ii}+1}{\downarrow} & & & \end{array}\\ \left[\begin{array}{cccccc|c} A_i & 0 & \cdots & A_{ii} & \cdots & 0 & 0\\ \hline I_{n_i} & 0 & \cdots & 0 & \cdots & 0 & 0\\ \vdots & \vdots & \cdots & \vdots & \cdots & \vdots & \vdots\\ 0 & 0 & \vdots & 0 & \vdots & I_{n_i} & 0\end{array}\right]\end{array}\in\mathbb{R}^{N_i\times N_i},\quad \mathcal{A}_{ij}=\begin{array}{c}\begin{array}{ccccc}\overset{1}{\downarrow} & \cdots & \overset{h_{ij}+1}{\downarrow} & & \end{array}\\ \left[\begin{array}{ccccc} 0 & \cdots & A_{ij} & \cdots & 0\\ \hline 0 & \cdots & 0 & \cdots & 0\\ \vdots & \vdots & \vdots & \ddots & \vdots\\ 0 & \cdots & 0 & \cdots & 0\end{array}\right]\end{array}\in\mathbb{R}^{N_i\times N_i} \tag{71}$$

where A_i and A_{ij}, $1\le i\le N$, $1\le j\le N$, are matrices of system (67).

Proof. It is not difficult to demonstrate that system (67) can be given in the following equivalent form

$$\begin{gathered}\hat{x}(k+1)=\mathcal{A}\hat{x}(k),\quad \hat{x}(k)=\left[\hat{x}_1^T(k)\quad \hat{x}_2^T(k)\quad\cdots\quad \hat{x}_N^T(k)\right]^T\qquad 1\le i\le N\\ \hat{x}_i(k)=\left[x_i^T(k)\quad x_i^T(k-1)\quad\cdots\quad x_i^T\left(k-h_{m_i}\right)\right]^T\end{gathered} \tag{72}$$

wherefrom a given condition for asymptotic stability follows directly.

3.2.3. Main results

Using Lyapunov's direct method, necessary and sufficient conditions for delay-dependent stability for system (67), are derived.

Prior to it, we demonstrate that the spectrum of matrix, which is integrated into Lyapunov equation, is a subset of spectrum of matrix $\mathcal{A}$, i.e. a set of characteristic roots of system (67).

Theorem 3.2.1. (Stojanovic & Debeljkovic, 2008.a) Given the following system of monic matrix polynomial equations (SMPE)

$$\mathcal{R}_\ell^{h_{m_i}+1}S_i-\mathcal{R}_\ell^{h_{m_i}}S_iA_i-\sum_{j=1}^{N}\mathcal{R}_\ell^{h_{m_i}-h_{ji}}S_jA_{ji}=0,\quad S_i\in\mathbb{C}^{n_\ell\times n_i},\quad S_\ell=I_{n_\ell} \tag{73}$$

for a given ℓ, $1\le\ell\le N$, , where A_i and A_{ji}, $1\le i\le N$, $1\le j\le N$ are matrices of system (67) and h_{ji} is time delay in the system, $h_{m_i}=\max_j h_{ji}$, $1\le i\le N$.

If there is a solution of SMPE (73) upon unknown matrices $\mathcal{R}_\ell\in\mathbb{C}^{n_\ell\times n_\ell}$ and S_i, $1\le i\le N$, $i\ne\ell$, then $\lambda(\mathcal{R}_\ell)\subset\lambda(\mathcal{A})$ holds, where matrix $\mathcal{A}$ is defined by (70)-(71).

Proof. By introducing time-delay operator z^{-h}, system (67) can be expressed in the following form

$$x(k+1)=A_e(z)x(k),\quad x(k)=\begin{bmatrix} x_1^T(k) & x_2^T(k) & \cdots & x_N^T(k)\end{bmatrix}^T$$
$$A_e(z)=\begin{bmatrix} A_1+A_{11}z^{-h_{11}} & \cdots & A_{1N}z^{-h_{1N}} \\ \vdots & \ddots & \vdots \\ A_{N1}z^{-h_{N1}} & \cdots & A_N+A_{NN}z^{-h_{NN}} \end{bmatrix} \tag{74}$$

Let us form the following matrix.

$$F(z)=zI_{N_e}-A_e(z)=\left[F_{ij}(z)\right]=\begin{bmatrix} zI_{n_1}-A_1-A_{11}z^{-h_{11}} & \cdots & -A_{1N}z^{-h_{1N}} \\ \vdots & \ddots & \vdots \\ -A_{N1}z^{-h_{N1}} & \cdots & zI_{n_N}-A_N-A_{NN}z^{-h_{NN}} \end{bmatrix} \tag{75}$$

If we add to the arbitrarily chosen ℓ - th block row of this matrix the rest of its block rows previously multiplied from the left by the matrices $S_j \neq 0$, $1 \le j \le N$, $j \neq \ell$ respectively, we obtain

$$\det F(z)=\det\begin{bmatrix} F_{11}(z) & \cdots & F_{1N}(z) \\ \vdots & \cdots & \vdots \\ F_1(z)+\sum\limits_{\substack{j=1\\ j\neq\ell}}^{N} S_jF_{j1}(z) & \cdots & F_{\ell N}(z)+\sum\limits_{\substack{j=1\\ j\neq\ell}}^{N} S_jF_{jN}(z) \\ \vdots & \ddots & \vdots \\ F_{N1}(z) & \cdots & F_{NN}(z) \end{bmatrix} \tag{76}$$

After multiplying i -th of the block column, $1 \le i \le N$, of the preceding matrix by $z^{h_{m_i}}$ and after integrating the matrix $S_\ell = I_{n_\ell}$, the determinant of matrix $F(z)$ equals

$$z^{\sum\limits_{i=1}^{N} n_i h_{m_i}} \det F(z)=$$
$$=\det\begin{bmatrix} z^{h_{m_1}}F_{11}(z) & \cdots & z^{h_{m_N}}F_{1N}(z) \\ \vdots & \vdots & \vdots \\ z^{h_{m_1}}\sum\limits_{j=1}^{N} S_jF_{j1}(z) & \cdots & z^{h_{m_N}}\sum\limits_{j=1}^{N} S_jF_{jN}(z) \\ \vdots & \ddots & \vdots \\ z^{h_{m_1}}F_{N1}(z) & \cdots & z^{h_{m_N}}F_{NN}(z) \end{bmatrix}=\det\begin{bmatrix} G_{11}(z) & \cdots & G_{1N}(z) \\ \vdots & \vdots & \vdots \\ G_{\ell 1}(z,S) & \cdots & G_{\ell N}(z,S) \\ \vdots & \vdots & \vdots \\ G_{N1}(z) & \cdots & G_{NN}(z) \end{bmatrix} \tag{77}$$
$$=\det G(z,S),\ S=\{S_1,\cdots,S_N\}$$

The ℓ -th block row of the $N\times N$ block matrix $G(z,S)$ is defined by

$$G_{\ell i}(z,S)=z^{h_{m_i}+1}S_i - z^{h_{m_i}}S_iA_i - \sum_{j=1}^{N} z^{h_{m_i}-h_{ji}}S_jA_{ji}, \quad 1\le i\le N, \quad S_\ell = I_{n_\ell} \tag{78}$$

The relation (76) was obtained by applying a finite sequence of elementary row operations of type 3 over matrix $F(z)$, (Lancaster & Tismenetsky, 1985). Transformation matrices $S_1,\cdots,S_N$, with the exception of matrix $S_\ell = I_{n_\ell}$, are unknown for the time being, but in a further text a condition will be derived that the unknown matrices are determined upon. The characteristic polynomial of system (67), (Gorecki et al., 1989)

$$g(z) \hat{=} \det G(z,S) = \sum_{j=0}^{N_e} a_j z^j, \quad N_e = \sum_{i=1}^{N} n_i\left(h_{m_i}+1\right), a_j \in \mathbb{R}, 0\le j\le N_e \tag{79}$$

does not depend on the choice of transformation matrices $S_1,\cdots,S_N$), (Lancaster & Tismenetsky, 1985).
Let us denote

$$\Sigma \hat{=} \{ z \,|\, g(z)=0 \} \tag{80}$$

a set of all characteristic roots of system (67). This set of roots equals the set $\lambda(\mathcal{A})$. Substituting a scalar variable z by matrix $X\in\mathbb{C}^{n_\ell\times n_\ell}$ in $G(z,S)$, a new block matrix is obtained $G(X,S)$. If there exist the transformation matrices S_i, $1\le i\le N$, $i\ne\ell$ and solvent $\mathcal{R}_\ell\in\mathbb{C}^{n_\ell\times n_\ell}$ such that for the ℓ-th block row of $G(X,S)$ holds $G_{\ell i}(\mathcal{R}_\ell,S)=0, \quad 1\le i\le N$ i.e. holds (73), then

$$g(\mathcal{R}_\ell)=0 \tag{81}$$

Therefore, the characteristic polynomial of system (67) is annihilating polynomial for the square matrix $\mathcal{R}_\ell$ and $\lambda(\mathcal{R}_\ell)\subset\Sigma$ holds. The mentioned assertion holds $\forall\ell, \quad 1\le\ell\le N$.

Definition 3.2.1 The matrix $\mathcal{R}_\ell$ is referred to as *solvent* of equations (73) for the given ℓ, $1\le\ell\le N$.

From (73) for the given ℓ, $1\le\ell\le N$, transformation matrices S_j $1\le j\le N$ and solvent $\mathcal{R}_\ell$ are computed, the latter being used further for examining the stability of system (67).

Definition 3.2.2 The characteristic root λ_m of system (67) with maximal module:

$$\lambda_m\in\Sigma: \quad |\lambda_m| = \max|\Sigma| = \max_i|\lambda_i(\mathcal{A})| \tag{82}$$

will be referred to as *maximal root* (*eigenvalue*) of system (67).

Definition 3.2.3 Each solvent $\mathcal{R}_{\ell m}$ of SMPE (73), for the given ℓ, $1\le\ell\le N$, whose spectrum contains maximal eigenvalue λ_m of system (67), is referred to as *maximal solvent* of (73).

Theorem 3.2.2 (Stojanovic & Debeljkovic, 2008.a) Suppose that there exist at least one ℓ, $1 \le \ell \le N$, that there exists *at least one* maximal solvent of SMPE (73) and let $\mathcal{R}_{\ell m}$ denote one of them. Then, linear discrete large-scale time-delay system (67) is asymptotically stable if and only if for any matrix $Q = Q^* > 0$ there exists matrix $P = P^* > 0$ such that

$$\mathcal{R}_{\ell m}^* \, P \, \mathcal{R}_{\ell m} - P = -Q \,. \tag{83}$$

Proof. *Sufficient condition.* Define the following vector discrete functions

$$v\left(x_{k1},\cdots,x_{kN}\right) = \sum_{i=1}^{N} S_i \left[x_i(k) + \sum_{j=1}^{N} \sum_{l=1}^{h_{ji}} T_{ji}(l) x_i(k-l) \right],\ x_{ki} = x_i(k+\theta),\ \theta \in \left\{-h_{m_i}, \dots, 0\right\} \tag{84}$$

where $T_{ji}(k) \in \mathbb{C}^{n_i \times n_i}$, $1 \le j \le N$, $1 \le i \le N$ are, in general, some time-varying discrete matrix functions and $S_\ell = I_{n_\ell}$, $S_i \in \mathbb{C}^{n_\ell \times n_i}$, $1 \le i \le N$, $i \ne \ell$. The conclusion of the theorem follows immediately by defining Lyapunov functional for system (67) as

$$V\left(x_{k1},\cdots,x_{kN}\right) = v^*(\cdot,\cdots,\cdot) P v(\cdot,\cdots,\cdot),\quad P = P^* > 0 \tag{85}$$

It is obvious that $V(\cdot,\cdots,\cdot) > 0$ for $\forall x_{ki} \ne 0$, $1 \le i \le N$. The forward difference of (85), along the solutions of system (67) is

$$\Delta V(\cdot,\cdots,\cdot) = \Delta v^*(\cdot,\cdots,\cdot)\, P\, v(\cdot,\cdots,\cdot) + v^*(\cdot,\cdots,\cdot)\, P\, \Delta v(\cdot,\cdots,\cdot) + \Delta v^*(\cdot,\cdots,\cdot)\, P\, \Delta v(\cdot,\cdots,\cdot) \tag{86}$$

A difference of $v(\cdot,\cdots,\cdot)$ can be determined in the following manner

$$\Delta v(\cdot,\cdots,\cdot) = \sum_{i=1}^{N} S_i \left[\Delta x_i(k) + \sum_{j=1}^{N} \sum_{l=1}^{h_{ji}} T_{ji}(l)\, \Delta x_i(k-l) \right] \tag{87}$$

$$\Delta x_i(k) = \left(A_i - I_{n_i}\right) x_i(k) + \sum_{j=1}^{N} A_{ij} x_j\left(k - h_{ij}\right) \tag{88}$$

Then

$$\begin{aligned} \Delta v(\cdot,\cdots,\cdot) = \sum_{i=1}^{N} S_i \Bigg[& \left(A_i - I_{n_i} + \sum_{j=1}^{N} T_{ji}(1) \right) x_i(k) + \sum_{j=1}^{N} T_{ji}\left(h_{ji}\right) x_i\left(k - h_{ji}\right) \\ & + \sum_{j=1}^{N} \sum_{l=1}^{h_{ji}-1} \Delta T_{ji}(l) x_i(k-l) + \sum_{j=1}^{N} A_{ij} x_j\left(k - h_{ij}\right) \Bigg] \end{aligned} \tag{89}$$

If we define new matrices

$$\mathcal{R}_i = A_i + \sum_{j=1}^{N} T_{ji}(1), \ 1 \le i \le N \tag{90}$$

then $\Delta v(\cdot,\cdots,\cdot)$ has a form

$$\begin{aligned}\Delta v(\cdot,\cdots,\cdot) = \sum_{i=1}^{N} \Bigg[& S_i \left(\mathcal{R}_i - I_{n_i}\right) x_i(k) + \sum_{j=1}^{N} \left(S_j A_{ji} - S_i T_{ji}\left(h_{ji}\right)\right) x_i\left(k - h_{ji}\right) \\ & + \sum_{j=1}^{N} \sum_{l=1}^{h_{ji}-1} S_i \Delta T_{ji}(l) x_i(k-l) \Bigg]\end{aligned} \tag{91}$$

If

$$S_j A_{ji} - S_i T_{ji}\left(h_{ji}\right) = S_i \Delta T_{ji}\left(h_{ji}\right), \quad 1 \le i \le N, \quad 1 \le j \le N \tag{92}$$

$$S_i \left(\mathcal{R}_i - I_{n_i}\right) = \left(\mathcal{R}_\ell - I_{n_\ell}\right) S_i, \quad 1 \le i \le N \tag{93}$$

$$S_i \Delta T_{ji}(l) = \left(\mathcal{R}_\ell - I_{n_\ell}\right) S_i\, T_{ji}(l), \ \ 1 \le i \le N, \quad 1 \le j \le N \tag{94}$$

then

$$\Delta v(\cdot,\cdots,\cdot) = \left(\mathcal{R}_\ell - I_{n_\ell}\right) v(\cdot,\cdots,\cdot), \quad \Delta V(\cdot,\cdots,\cdot) = v^*(\cdot,\cdots,\cdot)\left(\mathcal{R}_\ell^{\,*} P\, \mathcal{R}_\ell - P\right) v(\cdot,\cdots,\cdot) \tag{95}$$

It is obvious that if the following equation is satisfied

$$\mathcal{R}_\ell^{\,*} P\, \mathcal{R}_\ell - P = -Q, \qquad Q = Q^* > 0 \tag{96}$$

then $\Delta V(\cdot,\cdots,\cdot) < 0$, $\forall x_{ki} \ne 0$, $1 \le i \le N$.

In the Lyapunov matrix equation (83), of all possible solvents $\mathcal{R}_\ell$ of (73), only one of maximal solvents $\mathcal{R}_{\ell m}$ is of importance, for it is the only one that contains maximal eigenvalue $\lambda_m \in \Sigma$ (*Definition* 3.2.3), which has dominant influence on the stability of the system. If a solvent which is not maximal is integrated into Lyapunov equation (83), it may happen that there will exist a positive definite solution of this equation, although the system is not stable. Accordingly, condition (83) represents sufficient condition of the stability of system (67).

If it exists, maximal solvent $\mathcal{R}_{\ell m}$ can be determined in the following way. From (92) and (94) we obtain

$$S_j A_{ji} = \mathcal{R}_\ell^{\,h_{ji}} S_i T_{ji}(1), \quad S_\ell = I_{n_\ell}, \quad 1 \le i \le N, \ \ 1 \le j \le N \tag{97}$$

Multiplying i-th equation of the system of matrix equations (90) from the left by matrix $\mathcal{R}_\ell^{\,h_{mi}} S_i$ and using (93) and (97), we obtain equation (73). Taking solvent with eigenvalue

$\lambda_m \in \Sigma$ (if it exists) as a solution of the system of equations (73), we arrive at maximal solvent $\mathcal{R}_{\ell m}$.

Necessary condition. If system (67) is asymptotically stable, then $\forall \lambda_i \in \Sigma$, $|\lambda_i| < 1$. Since $\lambda(\mathcal{R}_{\ell m}) \subset \Sigma$,it follows that $\rho(\mathcal{R}_{\ell m}) < 1$, therefore the positive definite solution of Lyapunov matrix equation (67) exists.

Corollary 3.2.1 Suppose that for the given ℓ, $1 \le \ell \le N$, there exists matrix $\mathcal{R}_\ell$ being solution of SMPE (73). If system (67) is asymptotically stable, then matrix $\mathcal{R}_\ell$ is discrete stable ($\rho(\mathcal{R}_\ell) < 1$).

Proof. If system (67) is asymptotically stable, then $\forall z \in \Sigma$ $|z| < 1$. Since $\lambda(\mathcal{R}_\ell) \subset \Sigma$, it follows that $\forall \lambda \in \lambda(\mathcal{R}_\ell)$, $|\lambda| < 1$, i.e. matrix $\mathcal{R}_\ell$ is discrete stable.

Conclusion 3.2.1 It follows from the aforementioned, that it makes no difference which of the matrices $\mathcal{R}_{\ell m}$, $1 \le \ell \le N$ we are using for examining the asymptotic stability of system (67). The only condition is that there exists at least one matrix for at least one ℓ. Otherwise, it is impossible to apply *Theorem* 3.2.2.

Conclusion 3.2.2 The dimension of system (67) amounts to $N_e = \sum_{j=1}^{N} n_j \left(h_{m_j} + 1 \right)$. Conversely, if there exists a maximal solvent, the dimension of $\mathcal{R}_{\ell m}$ is multiple times smaller and amounts to n_ℓ. That is why our method is superior over a traditional procedure of examining the stability by eigenvalues of matrix $\mathcal{A}$.

The disadvantage of this method reflects in the probability that the obtained solution need not be a maximal solvent and it can not be known ahead if maximal solvent exists at all.

Hence the proposed methods are at present of greater theoretical than of practical significance.

3.2.4 Numerical example

Example 3.2.1 Consider a large-scale linear discrete time-delay systems, consisting of three subsystems described by Lee, Radovic (1987)

$$S_1:\ x_1(k+1) = A_1 x_1(k) + B_1 u_1(k) + A_{12} x_2(k - h_{12}),$$

$$S_2:\ x_2(k+1) = A_2 x_2(k) + B_2 u_2(k) + A_{21} x_1(k - h_{21}) + A_{23} x_3(k - h_{23}),$$

$$S_3:\ x_3(k+1) = A_3 x_3(k) + B_3 u_3(k) + A_{31} x_1(k - h_{31}),$$

$$A_1 = \begin{bmatrix} 0.8 & 0.6 \\ 0.4 & 0.9 \end{bmatrix}, A_2 = \begin{bmatrix} 0.7 & 0 & -0.5 \\ -0.1 & 6 & -0.1 \\ -0.6 & 1 & 0.8 \end{bmatrix}, B_1 = \begin{bmatrix} 0.1 \\ 0.1 \end{bmatrix}, A_{12} = \begin{bmatrix} 0.1 & 0 & 0.1 \\ 0.1 & 0 & 0.1 \end{bmatrix}, B_2 = \begin{bmatrix} 0 & -0.1 \\ 0.1 & 0.2 \\ 0 & 0.1 \end{bmatrix},$$

$$A_{21} = \begin{bmatrix} -0.1 & -0.2 \\ 0.3 & 0.1 \\ 0.1 & 0.2 \end{bmatrix}, A_{23} = \begin{bmatrix} -0.1 & 0 \\ 0.2 & -0.2 \\ 0.1 & 0 \end{bmatrix}, A_3 = \begin{bmatrix} 1 & 0.1 \\ -0.1 & 0.8 \end{bmatrix}, B_3 = \begin{bmatrix} 0.1 & 0 \\ 0 & 0.1 \end{bmatrix}, A_{31} = \begin{bmatrix} 0.1 & 0.2 \\ 0.1 & 0.2 \end{bmatrix},$$

The overall system is stabilized by employing a local memory-less state feedback control for each subsystem

$$u_i(k) = K_i x_i(k)\,,\ K_1 = \begin{bmatrix}-6 & -7\end{bmatrix}, K_2 = \begin{bmatrix}-7 & -45 & 10\\ 4 & -4 & -4\end{bmatrix}, K_3 = \begin{bmatrix}-5 & -1\\ 1 & -4\end{bmatrix}$$

Substituting the inputs into this system, we obtain the equivalent closed loop system representations

$$S_i:\ x_i(k+1) = \hat{A}_i\, x_i(k) + \sum_{j=1}^{3} A_{ij} x_j\left(k - h_{ij}\right),\ \ 1 \le i \le 3\,,\quad \hat{A}_i = A_i + B_i K_i$$

For time delay in the system, let us adopt: $h_{12} = 5$, $h_{21} = 2$, $h_{23} = 4$ and $h_{31} = 5$. Applying *Theorem* 3.2.1 to a given closed loop system, we obtain the following SMPE for $\ell = 1$

$$\mathcal{R}_1{}^6 - \mathcal{R}_1{}^5 \hat{A}_1 - \mathcal{R}_1{}^3 S_2 A_{21} - S_3 A_{31} = 0\,,$$

$$\mathcal{R}_1{}^6 S_2 - \mathcal{R}_1{}^5 S_2 \hat{A}_2 - A_{12} = 0\,,$$

$$\mathcal{R}_1{}^5 S_3 - \mathcal{R}_1{}^4 S_3 \hat{A}_3 - S_2 A_{23} = 0\,.$$

Solving this SMPE by minimization methods, we obtain

$$\mathcal{R}_1 = \begin{bmatrix}0.6001 & 0.3381\\ 0.6106 & 0.3276\end{bmatrix},\quad S_2 = \begin{bmatrix}0.0922 & 1.3475 & 0.5264\\ 0.0032 & 1.3475 & 0.4374\end{bmatrix},\quad S_3 = \begin{bmatrix}0.6722 & -0.3969\\ 1.3716 & -1.0963\end{bmatrix}.$$

Eigenvalue with maximal module of matrix $\mathcal{R}_1$ equals 0.9382. Since eigenvalue λ_m of $\mathcal{A} \in \mathbb{R}^{40\times 40}$ also has the same value, we conclude that solvent $\mathcal{R}_1$ is maximal solvent ($\mathcal{R}_{1m} = \mathcal{R}_1$). Applying *Theorem* 3.2.2, we arrive at condition $\rho(\mathcal{R}_{1m}) = 0.9382 < 1$ wherefrom we conclude that the observed closed loop large-scale time-delay system is asymptotically stable.

The difference in dimensions of matrices $\mathcal{R}_1 \in \mathbb{R}^{2\times 2}$ and $\mathcal{A} \in \mathbb{R}^{40\times 40}$ is rather high, even with relatively small time delays (the greatest time delay in our example is 5). So, in the case of great time delays in the system and a great number of subsystems N, by applying the derived results, a smaller number of computations are to be expected compared with a traditional procedure of examining the stability by eigenvalues of matrix $\mathcal{A}$.

An accurate number of computations for each of the mentioned method require additional analysis, which is not the subject-matter of our considerations herein.

4. Conclusion

In this chapter, we have presented new, necessary and sufficient, conditions for the asymptotic stability of a particular class of linear continuous and discrete time delay systems. Moreover, these results have been extended to the large scale systems covering the cases of two and multiple existing subsystems.

The time-dependent criteria were derived by Lyapunov's direct method and are exclusively based on the maximal and dominant solvents of particular matrix polynomial equation. It can be shown that these solvents exist only under some conditions, which, in a sense, limits the applicability of the method proposed. The solvents can be calculated using generalized Traub's or Bernoulli's algorithms. Both of them possess significantly smaller number of computation than the standard algorithm.

Improving the converging properties of used algorithms for these purposes, may be a particular research topic in the future.

5. References

Boutayeb M., M. Darouach (2001) Observers for discrete-time systems with multiple delays, *IEEE Transactions on Automatic Control*, Vol. 46, No. 5, 746-750.

Boyd S., El Ghaoui L., Feron E., and Balakrishnan V. (1994) *Linear matrix inequalities in system and control theory*, SIAM Studies in Applied Mathematics, 15. (Philadelphia, USA).

Chen J., and Latchman H.A. (1994) Asymptotic stability independent of delays: simple necessary and sufficient conditions, *Proceedings of American Control Conference*, Baltimore, USA, 1027-1031.

Chen J., Gu G., and Nett C.N. (1994) A new method for computing delay margins for stability of linear delay systems, *Proceedings of 33rd IEEE Conference on Decision and Control*, Lake Buena Vista, Florida, USA, 433-437.

Chen J. (1995) On computing the maximal delay intervals for stability of linear delay systems, *IEEE Transactions on Automatic Control*, Vol. 40, 1087-1093.

Chiasson J. (1988) A method for computing the interval of delay values for which a differential-delay system is stable, *IEEE Transactions on Automatic Control*, 33, 1176-1178.

Debeljkovic D.Lj., S.A. Milinkovic, S.B. Stojanovic (2005) *Stability of Time Delay Systems on Finite and Infinite Time Interval*, Cigoja press, Belgrade.

Debeljkovic Lj. D., S. A. Milinkovic (1999) *Finite Time Stability of Time Delay Systems*, GIP Kultura, Belgrade.

Dennis J. E., J. F. Traub, R. P. Weber (1976) The algebraic theory of matrix polynomials, *SIAM J. Numer. Anal.*, Vol. 13 (6), 831-845.

Dennis J. E., J. F. Traub, R. P. Weber (1978) Algorithms for solvents of matrix polynomials, *SIAM J. Numer. Anal.*, Vol. 15 (3), 523-533

Fridman E. (2001) New Lyapunov–Krasovskii functionals for stability of linear retarded and neutral type systems, *Systems and Control Letters*, Vol. 43, 309–319.

Fridman E. (2002) Stability of linear descriptor systems with delay: a Lyapunov-based approach, *Journal of Mathematical Analysis and Applications*, 273, 24–44.

Fridman E., and Shaked U. (2002a) A descriptor system approach to $H\infty$ control of linear time-delay systems, *IEEE Transactions on Automatic Control*, Vol. 47, 253–270.

Fridman E., and Shaked U. (2002b) An improved stabilization method for linear time-delay systems, *IEEE Transactions on Automatic Control*, Vol. 47, 1931–1937.

Fridman E., and Shaked U. (2003) Delay-dependent stability and $H\infty$ control: Constant and time-varying delays, *International Journal of Control*, Vol. 76, 48–60.

Fridman E., and Shaked U. (2005) Delay-Dependent $H\infty$ Control of Uncertain Discrete Delay Systems, *European Journal of Control* , Vol. 11, 29–37.

Fu M., Li H., and Niculescu S.-I. (1997) *Robust stability and stabilization of time-delay system via integral quadratic constraint approach*. In L. Dugard and E. I. Verriest (Eds.), Stability and Control of Time-Delay Systems, LNCIS, 228, (London: Springer-Verlag), 101-116.

Gantmacher F. (1960) *The theory of matrices*, Chelsea, New York.

Gao H., Lam J., Wang C. and Wang Y. (2004) Delay dependent output-feedback stabilization of discrete time systems with time-varying state delay, *IEE Proc.-Control Theory A*, Vol. 151, No. 6, 691-698.

Golub G.H., and C.F. Van Loan, (1996) *Matrix computations*, Jons Hopkins University Press, Baltimore.

Gorecki H., S. Fuksa, P. Grabovski and A. Korytowski (1989) *Analysis and synthesis of time delay systems*, John Wiley & Sons, Warszawa.

Goubet-Bartholomeus A., Dambrine M., and Richard J.-P. (1997) Stability of perturbed systems with time-varying delays, *Systems and Control Letters*, Vol. 31, 155- 163.

Gu K. (1997) Discretized LMI set in the stability problem of linear uncertain time-delay systems, *International Journal of Control*, Vol. 68, 923-934.

Hale J.K. (1977) *Theory of functional differential equations* (Springer- Verlag, New York,

Hale J.K., Infante E.F., and Tsen F.S.P. (1985) Stability in linear delay equations, *Journal on Mathematical Analysis and Applications*, Vol. 105, 533-555.

Hale J.K., and Lunel S.M. (1993) *Introduction to Functional Differential Equations, Applied Mathematics Sciences Series*, 99, (New York: Springer-Verlag).

Han Q.-L. (2005a) On stability of linear neutral systems with mixed time-delays: A discretized Lyapunov functional approach, *Automatica* Vol. 41, 1209–1218.

Han Q.-L. (2005b) A new delay-dependent stability criterion for linear neutral systems with norm-bounded uncertainties in all system matrices, *Internat. J. Systems Sci.*, Vol. 36, 469–475.

Hertz D., Jury E. I., and Zeheb E. (1984) Stability independent and dependent of delay for delay differential systems. *Journal of Franklin Institute*, 318, 143-150.

Hu Z. (1994) Decentralized stabilization of large scale interconnected systems with delays, *IEEE Transactions on Automatic Control*, Vol. 39, 180-182.

Huang S., H. Shao, Z. Zhang (1995) Stability analysis of large-scale system with delays, *Systems & Control Letters*, Vol. 25, 75-78.

Kamen E.W. (1982) Linear systems with commensurate time delays: Stability and stabilization independent of delay. *IEEE Transactions on Automatic Control*, Vol. 27, 367-375; corrections in *IEEE Transactions on Automatic Control*, Vol. 28, 248-249, 1983.

Kapila V., Haddad W. (1998) Memoryless $H\infty$ controllers for discrete-time systems with time delay, *Automatica,* Vol. 34, 1141-1144.

Kharitonov V. (1998) Robust stability analysis of time delay systems: A survey, *Proceedings of 4th IFAC System Structure and Control Conference*, Nantes, France, July.

Kim H. (2000) Numerical methods for solving a quadratic matrix equation, *Ph.D. dissertation*, University of Manchester, Faculty of Science and Engineering.

Kim H. (2001) Delay and its time-derivative dependent robust stability of time delayed linear systems with uncertainty, *IEEE Transactions on Automatic Control* 46 789–792.

Kolla S. R., J. B. Farison (1991) Analysis and design of controllers for robust stability of interconnected continuous systems, *Proceedings Amer. Contr. Conf.*, Boston, MA, 881-885.

Kolmanovskii V. B., and Nosov V. R. (1986) Stability *of Functional Differential Equations* (New York: Academic Press)

Kolmanovskii V., and Richard J. P. (1999) Stability of some linear systems with delays. *IEEE Transactions on Automatic Control*, 44, 984–989.

Kolmanovskii V., Niculescu S.-I., and Richard J. P., (1999) On the Lyapunov–Krasovskii functionals for stability analysis of linear delay systems. *International Journal of Control*, Vol. 72, 374–384.

Lakshmikantam V., and Leela S. (1969) *Differential and integral inequalities* (New York: Academic Press).

Lancaster P., M. Tismenetsky (1985) *The theory of matrices, 2nd Edition*, Academic press, New York.

Lee C., and Hsien T. (1997) Delay-independent Stability Criteria for Discrete uncertain Large-scale Systems with Time Delays, *J. Franklin Inst.*, Vol. 33 4B, No. 1, 155-166.

Lee T.N., and Radovic U. (1987) General decentralized stabilization of large-scale linear continuous and discrete time-delay systems, *Int. J. Control*, Vol. 46, No. 6, 2127-2140.

Lee T.N., and Radovic U. (1988) Decentralized Stabilization of Linear Continuous and Discrete-Time Systems with Delays in Interconnections, *IEEE Transactions on Automatic Control*, Vol. 33, 757–761.

Lee T.N., and S. Diant (1981) Stability of time-delay systems, *IEEE Transactions on Automatic Control*, Vol. 26, No. 4, 951-953.

Lee Y.S., and Kwon W.H. (2002) Delay-dependent robust stabilization of uncertain discrete-time state-delayed systems. *Preprints of the 15th IFAC World Congress*, Barcelona, Spain,

Li X., and de Souza, C. (1995) LMI approach to delay dependent robust stability and stabilization of uncertain linear delay systems. *Proceedings of 34th IEEE Conference on Decision and Control*, New Orleans, Louisiana, USA, 3614-3619.

Li X., and de Souza, C. (1997) Criteria for robust stability and stabilization of uncertain linear systems with state delay, *Automatica*, Vol. 33, 1657–1662.

Lien C.-H., Yu K.-W., and Hsieh J.-G., (2000) Stability conditions for a class of neutral systems with multiple time delays. *Journal of Mathematical Analysis and Applications*, 245, 20–27.

Mahmoud M, Hassen M, and Darwish M. (1985) *Large-scale control system: theories and techniques*. New York: Marcel-Dekker.

Mahmoud M. (2000) Robust H∞ control of discrete systems with uncertain parameters and unknown delays, *Automatica* Vol. 36, 627-635.

Malek-Zavarei M., and Jamshidi M. (1987) *Time-Delay Systems, Analysis, Optimization and Applications,* Systems and Control Series, Vol. 9 (North-Holland).

Moon Y.S., Park P.G., Kwon W.H., and Lee Y.S. (2001). Delay-dependent robust stabilization of uncertain state-delayed systems, *International Journal of Control*, Vol. 74(14), 1447–1455.

Niculescu S.-I., de Souza C. E., Dion J.-M., and Dugard L., (1994), Robust stability and stabilization for uncertain linear systems with state delay: Single delay case (I). *Proceedings of IFAC Workshop on Robust Control Design*, Rio de Janeiro, Brazil, 469-474.

Niculescu S.-I., de Souza C. E., Dugard L., and Dion J.-M. (1995a), Robust exponential stability of uncertain linear systems with time-varying delays. *Proceedings of 3rd European Control Conference*, Rome, Italy, 1802-1807.

Niculescu S.-I., Trofino-Neto A., Dion J.-M., and Dugard L. (1995b), Delay-dependent stability of linear systems with delayed state: An L.M.I. approach. *Proceedings of 34th IEEE Conference on Decision and Control*, New Orleans, Louisiana, USA, 1495-1497.

Niculescu S.-I., Dion J.-M., Dugard L., and Li H. (1997a) Stability of linear systems with delayed state: An L.M.I. approach. JESA, *special issue on "Analysis and control of time-delay systems"*, 31, 955-970.

Niculescu S.I., Verriest E. I., Dugard L., and Dion J. M. (1997b) *Stability and robust stability of time-delay systems: A guided tour. Lecture notes in control and information sciences*, Vol. 228 (1–71). London: Springer.

Niculescu S.-I., (2001), On delay-dependent stability under model transformations of some neutral linear systems, *International Journal of Control*, Vol. 74, 609–617.

Niculescu S.I., and Richard J.P. (2002) Analysis and design of delay and propagation systems, *IMA Journal of Mathematical Control and Information*, 19(1–2), 1–227 (special issue).

Oucheriah S. (1995) Measure of robustness for uncertain time-delay linear system, *ASME Journal of Dynamic Systems, Measurement, and Control* 117 633–635.

Park J.H. (2002) Robust Decentralized Stabilization of Uncertain Large-Scale Discrete-Time Systems with Delays, *Journal of Optimization Theory and Applications*, Vol. 113, No. 1, 105–119.

Park J.H. (2004) Robust non-fragile control for uncertain discrete-delay large-scale systems with a class of controller gain variations, *Applied Mathematics and Computation,* Vol. 149, 147–164.

Park J.H., Jung Ho Y., Park J.I., Lee S.G. (2004) Decentralized dynamic output feedback controller design for guaranteed cost stabilization of large-scale discrete-delay systems, *Applied Mathematics and Computation*, Vol. 156, No 2, 307-320.

Park P., Moon Y S., & Kwon W H. (1998) A delay-dependent robust stability criterion for uncertain time-delay systems, *In Proceedings of the American control conference,* 1963–1964.

Park P. (1999) A delay-dependent stability criterion for systems with uncertain time-invariant delays. *IEEE Transactions on Automatic Control*, Vol. 44, 876–877.

Pereira E. (2003) On solvents of matrix polynomials, *Applied numerical mathematics*, Vol. 47, 197-208.

Richard J.-P., Goubet- Bartholomeus A., Tchangani, Ph. A., and Dambrine M. (1997) *Nonlinear delay systems: Tools for quantitative approach to stabilization. L. Dugard and E. I. Verriest, (Eds.), Stability and Control of Time-Delay Systems*, LNCIS, 228, (London: Springer-Verlag), 218-240.

Richard J.-P. (1998) Some trends and tools for the study of time delay systems. *Proceedings of CESA98 IMACS/IEEE Multi conference*, Hammamet, Tunisia, 27-43.

Richard J.P. (2003) Time-delay systems: an overview of some recent advances and open problems, *Automatica* Vol. 39, 1667–1694.

Shi P., Agarwal R.K., Boukas E.-K., Shue S.-P. (2000) Robust $H\infty$ state feedback control of discrete timedelaylinear systems with norm-bounded uncertainty, *Internat. J. Systems Sci.*, Vol. 31 409- 415.

Siljak D. (1978) *Large-scale dynamic systems: stability and structure*, Amsterdam: North Holland.
Song S., Kim J., Yim C., Kim H. (1999) H∞ control of discrete-time linear systems with time-varying delays in state, *Automatica* Vol. 35, 1587-1591.
Stojanovic S.B., Debeljkovic D.Lj. (2005) Necessary and Sufficient Conditions for Delay-Dependent Asymptotic Stability of Linear Continuous Large Scale Time Delay Autonomous Systems, *Asian Journal of Control*, Vol. 7, No. 4, 414 - 418.
Stojanovic S.B., Debeljkovic D.Lj. (2006) Comments on Stability of Time-Delay Systems, *IEEE Transactions on Automatic Control* (submitted).
Stojanovic S.B., Debeljkovic D.Lj. (2008.a) Delay–Dependent Stability of Linear Discrete Large Scale Time Delay Systems: Necessary and Sufficient Conditions, *International Journal of Information & System Science*, Vol. 4, No. 2, 241 – 250.
Stojanovic S.B., Debeljkovic D.Lj. (2008.b) Necessary and Sufficient Conditions for Delay-Dependent Asymptotic Stability of Linear Discrete Time Delay Autonomous Systems, *Proceedings of 17th IFAC World Congress*, Seoul, Korea, July 06–10.
Su J.H. (1994) Further results on the robust stability of linear systems with a single delay, *Systems and Control Letters*, Vol. 23, 375-379.
Su J.H. (1995) The asymptotic stability of linear autonomous systems with commensurate delays. *IEEE Transactions on Automatic Control*, Vol. 40, 1114-1118.
Suh H., Z. Bein (1982) On stabilization by local state feedback for continuous-time large-scale systems with delays in interconnections, *IEEE Transactions on Automatic Control*, Vol. AC-27, 964-966.
Trinh H., and Aldeen M. (1995a) A Comment on Decentralized Stabilization of Large-Scale Interconnected Systems with Delays, *IEEE Transactions on Automatic Control*, Vol. 40, 914–916.
Trinh H., M. Aldeen (1995b) A comment on Decentralized stabilization of large scale interconnected systems with delays, *IEEE Transactions on Automatic Control*, Vol. 40, 914-916.
Trinh H., M. Aldeen (1997) On Robustness and Stabilization of Linear Systems with Delayed Nonlinear Perturbations, *IEEE Transactions on Automatic Control*, Vol. 42, 1005-1007.
Verriest E., Ivanov A. (1995) Robust stability of delay difference equations, *Proceedings IEEEE Conf. on Dec. and Control*, New Orleans, LA 386-391.
Verriest E., and Niculescu S.-I. (1998) *Delay-independent stability of linear neutral systems: a Riccati equation approach. In L. Dugard and E. Verriest (eds) Stability and Control of Time-Delay Systems*, Vol. 227 (London: Springer-Verlag), 92–100.
Wang W. J., R. J. Wang, and C. S. Chen (1995) Stabilization, estimation and robustness for continuous large scale systems with delays, *Contr. Theory Advan. Technol.*, Vol. 10, No. 4, 1717-1736.
Wang W. and, L. Mau (1997) Stabilization and estimation for perturbed discrete time-delay large-scale systems, *IEEE Transactions on Automatic Control*, Vol. 42, No. 9, 1277-1282.
Wu H. and K. Muzukami (1995) Robust stability criteria for dynamical systems in delayed perturbations, *IEEE Transactions on Automatic Control,* Vol. 40, 487–490.
Wu H. (1999) Decentralized Stabilizing State Feedback Controllers for a Class of Large-Scale Systems Including State Delays in the Interconnections, *Journal of optimization theory and applications*, Vol. 100. No. 1, 59-87.

Xu B. (1995) On delay-Independent and stability of large-scale systems with time delays, *IEEE Transactions on Automatic Control*, Vol. 40, 930-933.

Xu B., (1994) Comments on robust stability of delay dependence for linear uncertain systems, *IEEE Transactions on Automatic Control,* Vol. 39 2365.

Xu S., Lam J., and Yang C. (2001) H∞ and positive real control for linear neutral delay systems, *IEEE Transactions on Automatic Control*, Vol. 46, 1321–1326

Yan J.J. (2001) Robust stability analysis of uncertain time delay systems with delay-dependence, *Electronics Letters* Vol. 37, 135–137.

3

Differential Neural Networks Observers: development, stability analysis and implementation

Alejandro García[1], Alexander Poznyak[1], Isaac Chairez[2] and Tatyana Poznyak[2]
[1]Department of Automatic Control, CINVESTAV-IPN,
[2]Superior School of Chemical Engineering National Polytechnic Institute (ESIQIE-IPN)
México

1. Introduction

The control and possible optimization of a dynamic process usually requires the complete on-line availability of its state-vector and parameters. However, in the most of practical situations only the input and the output of a controlled system are accessible: all other variables cannot be obtained on-line due to technical difficulties, the absence of specific required sensors or cost (Radke & Gao, 2006). This situation restricts possibilities to design an effective automatic control strategy. To this matter many approaches have been proposed to obtain some numerical approximation of the entire set of variables, taking into account the current *available* information. Some of these algorithms assume a complete or partial knowledge of the system structure (mathematical model). It is worth mentioning that the influence of possible disturbances, uncertainties and nonlinearities are not always considered.

The aforementioned researching topic is called *state estimation, state observation* or, more recently, *software sensors design*. There are some classical approaches dealing with same problem. Among others there are a few based on the Lie-algebraic method (Knobloch et. al., 1993), Lyapunov-like observers (Zak & Walcott, 1990), the high-gain observation (Tornambe 1989), optimization-based observer (Krener & Isidori 1983), the reduced-order nonlinear observers (Nicosia et. al.,1988), recent structures based on sliding mode technique (Wang & Gao, 2003), numerical approaches as the set-membership observers (Alamo et. al., 2005) and etc. If the description of a process is incomplete or partially known, one can take the advantage of the function approximation capacity of the Artificial Neural Networks (ANN) (Haykin, 1994) involving it in the observer structure designing (Abdollahi et. al., 2006), (Haddad, et. al. 2007), (Pilutla & Keyhani, 1999).

There are known two types of ANN: *static* one, (Haykin, 1994) and *dynamic* neural networks (DNN). The first one deals with the class of global optimization problems trying to adjust the weights of such ANN to minimize an identification error. The second approach, exploiting the feedback properties of the applied Dynamic ANN, permits to avoid many problems related to global extremum searching. Last method transforms the learning process to an adequate feedback design (Poznyak et. al., 2001). Dynamic ANN's provide an effective instrument to attack a wide spectrum of problems, such as parameter identification, state estimation, trajectories tracking, and etc. Moreover, DNN demonstrates remarkable identification properties in the presence of uncertainties and external disturbances or, in other words, provides the *robustness* property.

In this chapter, we discuss the application of a special type of observers (based on the DNN) for the state estimation of a class of uncertain nonlinear system, which output and state are affected by bounded external perturbations. The chapter comprises four sections. In the first section the fundamentals concerning state estimation are included. The second section introduces the structure of the considered class of Differential Neural Network Observers (DNNO) and their main properties. In the third section the main result concerning the stability of estimation error, with its analysis based on the Lyapunov-Like method and Linear Matrix Inequalities (LMI) technique is presented. Moreover, the DNN dynamic weights boundedness is stated and treated as a second level of the learning process (the first one is the learning laws themselves). In the last section the implementation of the suggested technique to the chemical soil treatment by ozone is considered in details.

2. Fundamentals

2.1 Estimation problem

Consider the nonlinear continuous-time model given by the following ODE:

$$\begin{gathered}\frac{d}{dt}x(t) = f\left(x(t),u(t)\right) + \xi(t),\ x(0)\ \text{is fixed} \\ y(t) = Cx(t) + \eta(t)\end{gathered} \tag{1}$$

where

$x(t) \in \Re^n$	-	state-vector at time $t \geq 0$,
$y(t) \in \Re^m$	-	corresponding measurable output,
$C \in \Re^{m \times n}$	-	the known matrix defining the state-output transformation,
$u(t) \in \Re^r$	-	the bounded control action $(r \leq n)$ belonging to the following admissible set

$$U^{adm} := \left\{u(t)\ :\ \left\|u(t)\right\| \leq \Upsilon_u < \infty\right\},$$

$\xi(t)$ and $\eta(t)$	-	noises in the state dynamics and in the output, respectively, $f : \Re^{n \times r} \to \Re^n$.

The software sensor design, also called *state estimation (observation) problem,* consists in designing a vector-function $\hat{x}(t) \in \Re^n$, called *"estimation vector"*, based only the available data information (measurable) $\left\{y(t), u(t)\right\}_{\tau \in [0,t]}$ in such a way that it would be "closed" to its real (but non-measurable) state-vector $x(t)$. The measure of that "closeness" depends on the accepted assumptions on the state dynamics as well as the noise effects. The most of observers usually have ODE-structure:

$$\frac{d}{dt}\hat{x}(t)=F\left(\hat{x}(t),u(t),y_{\tau\in[0,t]}t\right),\ \hat{x}_0 \text{ is a fixed vector} \tag{2}$$

Here the mapping $F:\Re^n\times\Re^r\times L^m\times\Re^+\to\Re^n$ defines the structure of the observer to be implemented.

2.2 Physical Constraints of the state vector

To realize the state observation objective, many authors have taken advantages of the physical state constraints. Some examples of these techniques employing *"a priori"* information on states are: interval observers (Dochain, 2003) and moving horizon state estimation (Valdes-González et. al., 2003). In the present study, some physical restrictions are considered and using previous results given in (García, et. al. 2007). The main property of an observer, which are looked for, is to keep the generated state estimates $\hat{x}(t)$ within the given compact set X (even in the presence of noise), that is:

$$\hat{x}(t)\in X \tag{3}$$

In different problems the *compact set* X has a concrete physical sense. For example, the dynamic behaviors of some reagents, participating in chemical reactions, always keep their nonnegative current values. Similar remark seems to be true for other physical variables such as temperature, pressure, light intensity and etc. To complete (3) the next *projectional observer* is proposed:

$$\hat{x}(t)=\pi_X\left\{\hat{x}(t-h(t))+\int_{\tau=t-h(t)}^{t}F\left(\hat{x}(\tau),u(\tau),y_{s\in[0,\tau]}\tau\right)d\tau\right\},\ t>h(0) \tag{4}$$

Here $h(t)\in C^1$ fulfills $\dot{h}(t)\le 0$. The operator $\pi_X\{\cdot\}$ is the projector to the given convex compact set X possessing the property

$$\left\|\pi_X\{x\}-z\right\|\le\left\|x-z\right\| \tag{5}$$

for any $x\in\Re^n$ and any $z\in X$. The operator $\pi_X\{\cdot\}$ may be defined by different ways. Two examples of $\pi_X\{\}$ are given below.

Example 1 (Saturation function):

$$\pi_X\{x\}=\left[sat(x_1)\ \ \dots\ \ sat(x_n)\right]^{\mathrm{T}} \tag{6}$$

where for any i=1..n

$$sat(x_i):=\begin{cases}(x_i)^- & x_i\le(x_i)^-\\ x_i & (x_i)^-<x_i<(x_i)^+\\ (x_i)^+ & x_i\ge(x_i)^+\end{cases} \tag{7}$$

with $(x_i)^- < (x_i)^+$ as an extreme point *a priori* known.

Example 2 (Simplex): If X is the n-simplex, i.e.,

$$X = \left\{ z \in R^n \ : \ z_i \geq 0 \ (i = 1, \ldots, n), \ \sum_{i=1}^{n} z_i = 1 \right\} \tag{8}$$

then $\pi_X\{x\}$ can be found numerically by at least within n-steps. The case $n = 3$ is illustrated by Figure 1.

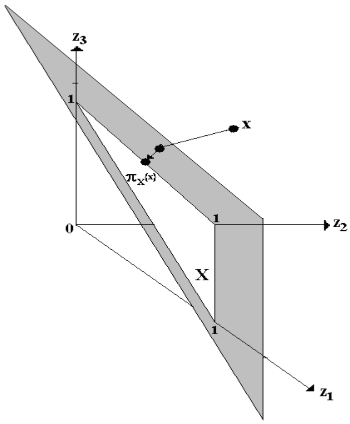

Figure 1. Projectional operator over a simplex (n=3)

An important point is that with the projectional operator implementations the trajectories $\{\hat{x}(t)\}$, generated by (4), are not differentiable for any $t \geq h(t) > 0$.

3 Structures of DNN Observers

3.1 State estimation under complete information

If the right-hand side $f(x(t))$ of the dynamics (1) is known then the structure F of the observer (4) is usually selected in the, so-called, Luenberger-type form:

$$F(\hat{x}(t), u(t), y(t), t) = f(\hat{x}(t), u(t)) + K(t)(y(t) - C\hat{x}(t)) \tag{9}$$

So, it repeats the dynamics of the plant and, additionally, contains the correction term, proportional to the output error (see, for example Yaz & Azemi, 1994; Poznyak, 2004). The adequate selection of the matrix-gain $K(t)$ provides a good-enough state estimation.

3.2 Differential Neural Network Observer, the "grey-box" case

In the case when the right-hand side $f(x,u)$ of the dynamics (1) is unknown, there is suggested to apply some guessing of it, say, $\bar{f}(x(t), u(t) \mid W(t))$ where $\bar{f} \in \Re^n$ defines the approximating map depending on the time-varying parameters $W(t)$, which should be adjusted by a "*adaptation law*" suggested by a designer or derived, using some stability analysis method. According to the DNN-approach (Poznyak et. al., 2001) we may decompose $\bar{f}(x(t),u(t)\,|\,W(t))$ in two parts: first one, approximates the linear dynamics part by a *Hurwitz* fixed matrix $A\in\Re^{n\times n}$ (selected by the designer) and the second one, uses the ANN reconstruction property for the nonlinear part by means of variable time parameters $W_{1,2}(t)$ with a set of basis functions, that is,

$$\begin{gathered}\bar{f}\left(x(t),u(t)\,|\,W_{1,2}(t)\right) := Ax(t)+W_1(t)\sigma(x(t))+W_2(t)\varphi(x(t))u(t)\\ A\in\Re^{n\times n},\ W_1(t)\in\Re^{n\times p},\ \sigma(\cdot)\in\Re^{p\times 1}\\ W_2(t)\in\Re^{n\times q},\ \varphi(\cdot)\in\Re^{q\times r}\end{gathered}\tag{10}$$

The activation vector (the basis) function $\sigma(\cdot)$ and matrix-function $\varphi(\cdot)$ are usually selected as functions with *sigmoid-type components*, i.e.:

$$\sigma_j(x(t)) := a_j\left(1+b_j\,exp\left(-\sum_{j=1}^{n} c_j x_j(t)\right)\right)^{-1},\ j=\overline{1,n}\tag{11}$$

and

$$\varphi_{i,j}(x(t)) := a_{i,j}\left(1+b_{i,j}\,exp\left(-\sum_{s=1}^{n} c_{i,s}\,x_s(t)\right)\right)^{-1},\ i=\overline{1,q};\ j=\overline{1,r}\tag{12}$$

It is easy to see that the activation functions satisfy the following sector conditions

$$\left\|\sigma(x(t))-\sigma(x'(t))\right\|^2_{\Lambda_\sigma}\le L_\sigma\left\|x(t)-x'(t)\right\|^2_{\Lambda_\sigma}\tag{13}$$

$$\left\|\varphi(x(t))-\varphi(x'(t))\right\|^2_{\Lambda_\varphi}\le L_\varphi\left\|x(t)-x'(t)\right\|^2_{\Lambda_\varphi}\tag{14}$$

and stay bounded on $\Re^n$. In (10), the constant parameter A, as well as the time-varying parameters $W_{1,2}(t)$, should be properly adjusted to guarantee a good state approximation. Notice that for any fixed matrices $W_{1,2}(t)=\hat{W}_{1,2}$ the dynamics (1) always could be represented as

$$\begin{gathered}\frac{d}{dt}x(t)=Ax(t)+\hat{W}_1\sigma(x(t))+\hat{W}_2\varphi(x(t))u(t)+\tilde{f}(t)+\xi(t)\\ \tilde{f}(t) := f(x(t))-\bar{f}\left(x(t)\,|\,\hat{W}_{1,2}\right)\end{gathered}\tag{15}$$

where $\tilde{f}(t)$ is referred to as a modeling error vector-field called the "*unmodelled dynamics*". In view of the corresponding boundedness property, the following inequality for the unmodelled dynamics $\tilde{f}(t)$ takes place:

$$\left\|\tilde{f}(t)\right\|^2_{\Lambda_f} \le \tilde{f}_0 + \tilde{f}_1 \left\|x(t)\right\|^2_{\Lambda^1_{\tilde{f}}}$$
$$\tilde{f}_0, \tilde{f}_1 > 0;\ \Lambda_f, \Lambda^1_{\tilde{f}} > 0,\ \Lambda_f = \Lambda_f^T,\ \Lambda^1_{\tilde{f}} = \left(\Lambda^1_{\tilde{f}}\right)^T \tag{16}$$

3.3 Structure DNN observers considering state physical constraints

Introduce the following projectional DNNO:

$$\hat{x}(t) = \pi_X \left\{ \hat{x}(t-h(t)) + \int_{\tau = t-h(t)}^{t} \left[A\hat{x}(\tau) + W_1(\tau)\sigma(\hat{x}(\tau)) + W_2(\tau)(\varphi(x(\tau))u(\tau) + Ke(\tau)\right] d\tau \right\}$$
$$e(t) := y(t) - C\hat{x}(t) \tag{17}$$

Here the weights matrices $W_1(t)$ and $W_2(t)$ supply the adaptive behavior to this class of observers if they are adjusted by an adequate manner. We derived (see Appendix) the following nonlinear weight *updating* laws based on the Lyapunov-like stability analysis:

$$\left.\begin{array}{c} \dfrac{d}{dt} W_1(t) = -\dfrac{k_1^{-1}(t)}{2} P\Omega(t)\sigma^T(\hat{x}(t)) - \dfrac{dk_1(t)}{dt}\tilde{W}_1(t) \\ \Omega(t) := \Pi\tilde{W}(t)\sigma(\hat{x}(t)) + 2N_{\varpi}C^T e(t-h(t));\quad \tilde{W}_1(t) := W_1(t) - \hat{W}_1; \\ \Pi = \left(N_{\varpi}\left(\varpi\Lambda_3 + C^T\Lambda_2 C\right)N_{\varpi}P + I\right) \end{array}\right\} \tag{18}$$

$$\left.\begin{array}{c} \dfrac{d}{dt} W_2(t) = -\dfrac{k_2^{-1}(t)}{2} P\Phi(t)u^T(\tau)\varphi^T(\hat{x}(\tau)) - \dfrac{dk_2(t)}{dt}\tilde{W}_2(t) \\ \Phi(t) := \Xi\tilde{W}_2(\tau)(\varphi(\hat{x}(\tau))u(\tau) + 2N_{\varpi}C^T e(t-h(t));\quad \tilde{W}_2(t) := W_2(t) - \hat{W}_2; \\ \Xi = \left(N_{\varpi}\left(\varpi\Lambda_7 + C^T\Lambda_6 C\right)N_{\varpi}P + I\right) \end{array}\right\} \tag{19}$$

where:

$$N_{\varpi} = \left(C^T C + \varpi I\right)^{-1},\ \varpi > 0$$

To improve the behavior of this adaptive laws, the matrix $\hat{W}_{1,2}$ can be "provided" by one of the, so-called, *training algorithms* (see, for example, Chairez et. al., 2006; Stepanyan & Hovakimyan, 2007). Both present least square solutions considering some identification structure for possible set of fictitious values or even an available set of directly measured data of the process.

4. DNN Observers Stability

4.1 Behavior of weights dynamics

Here we wish to show that under the adapting weights laws (18) and (19) the weights $W_1(t)$ and $W_2(t)$ are bounded.

Theorem 1 (bounded adaptive weights): If $k_i(t)$ $(\mathrm{i}=1,2)$ in (18) and (19) satisfy

$$\begin{aligned} \frac{d}{dt}k_1(t) &\leq -\frac{2(k_1(t))^2\left|tr\left\{\widetilde{W}_1^T(t)P\Omega(t)\sigma^T(\hat{x}(t))\right\}\right|}{tr\left\{\widetilde{W}_1^T(t)\widetilde{W}_1(t)\right\}+ck_1(t)\left[k_1(t)-k_{1min}\right]} \\ \frac{d}{dt}k_2(t) &\leq -\frac{2(k_2(t))^2\left|tr\left\{\widetilde{W}_2(t)P\Phi(t)u^T(t)\varphi^T(\hat{x}(t))\right\}\right|}{tr\left\{\widetilde{W}_2(t)^T\widetilde{W}_2(t)\right\}+ck_2(t)\left(k_2(t)-k_{2,min}\right)} \end{aligned} \tag{20}$$

then $tr\left\{\widetilde{W}_1^T(t)\widetilde{W}_1(t)\right\}$ is monotonically non-increasing function.

Proof: Considering the dynamics for the weight matrix $\widetilde{W}_1(t)$ and the following candidate Lyapunov function $V_w(t)$.

$$V_w(t) := \frac{1}{2}tr\left\{\widetilde{W}_1^T(t)\widetilde{W}_1(t)\right\}+\frac{c}{4}\left[k_1(t)-k_{1min}\right]_+^2 \tag{21}$$

where

$$[z(t)]_+ := \begin{cases} z(t) & z(t)\geq 0 \\ 0 & z(t)<0 \end{cases} \tag{22}$$

Then, one has

$$\frac{d}{dt}V_w(t) := tr\left\{\widetilde{W}_1^T(t)\left(\frac{d}{dt}W_1(t)\right)\right\}+2^{-1}c\frac{d(k_1(t))}{dt}\left[k_1(t)-k_{1min}\right]_+^2 \tag{23}$$

By (18) it follows

$$\begin{aligned} &\frac{d}{dt}V_w(t) = tr\left\{\widetilde{W}_1^T(t)\left(-\frac{k_1^{-1}(t)}{2}\left[P\Omega(t)\sigma^T(\hat{x}(t))-\frac{d(k_1(t))}{dt}\widetilde{W}_1(t)\right]\right)\right\}+ \\ &2^{-1}c\frac{d(k_1(t))}{dt}\left[k_1(t)-k_{1min}\right]_+ \leq \frac{k^{-1}(t)}{2}\left|tr\left\{\widetilde{W}_1^T(t)P\Omega(t)\sigma^T(\hat{x}(t))\right\}\right|+ \\ &2^{-1}\frac{d(k_1(t))}{dt}\left(k_1^{-1}(t)tr\left\{\widetilde{W}_1^T(t)\widetilde{W}_1(t)\right\}+2^{-1}c\left[k_1(t)-k_{1min}\right]_+\right) \end{aligned} \tag{24}$$

The property $\frac{d}{dt}V_w(t)\leq 0$ results from (20).

Some examples of $k_i(t)$ $(i=1,2)$ are given below

a. Introduce the following auxiliary function

$$s\left(\tilde{W}_1^T(t), e(t-h(t))\right) := \frac{k_1^{-1}(t)\left|tr\left\{\tilde{W}_1^T(t)P\Omega(t)\sigma^T(\hat{x}(t))\right\}\right|}{c\left[k_1(t)-k_{1,min}\right]_+}$$

And select

$$k_1(t) := \frac{k(0)}{1+a\left(\tilde{W}_1^T(t), e(t-h(t))\right)exp(bt)} + k_{min,j}, \quad k_{min,j} > 0$$

$$\frac{d(k_1(t))}{dt} := -k_1(0)\frac{a\left(\tilde{W}_1^T(t), e(t-h(t))\right)b_j\,exp(bt)}{1+a\left(\tilde{W}_1^T(t), e(t-h(t))\right)exp\left(b_j t\right)} < -s\left(\tilde{W}_1^T(t), e(t-h(t))\right)$$

Leading to

$$a\left(\tilde{W}_1^T(t), e(t-h(t))\right)exp(bt)\left(k(0)b - s\left(\tilde{W}_1^T(t), e(t-h(t))\right)\right) > s\left(\tilde{W}_1^T(t), e(t-h(t))\right)$$

The last inequality is fulfilled if the weight dependent parameter $a\left(\tilde{W}_1^T(t), e(t))\right)$ is selected as

$$a\left(\tilde{W}_1^T(t), e(t-h(t))\right) > s\left(\tilde{W}_1^T(t), e(t-h(t))\right)exp(-bt)\Psi^{-1}$$
$$\Psi := k(0)b - s\left(\tilde{W}_1^T(t), e(t-h(t))\right)$$

b. Analogously, for $\tilde{W}_2^T(t)$:

$$s\left(\tilde{W}_2^T(t), e(t-h(t))\right) := \frac{k_2^{-1}(t)\left|tr\left\{\tilde{W}_2^T(t)P\Phi(t)u^T(\tau)\varphi^T(\hat{x}(\tau))\right\}\right|}{c\left[k_2(t)-k_{2,min}\right]_+}$$

$$k_2(t) := \frac{k(0)}{1+a\left(\tilde{W}_2^T(t), e(t-h(t))\right)exp(bt)} + k_{min,j}, \quad k_{min,j} > 0$$

$$\frac{d}{dt}k_2(t) := -k_2(0)\frac{a\left(\tilde{W}_2^T(t), e(t-h(t))\right)b_j\,exp(bt)}{1+a\left(\tilde{W}_2^T(t), e(t-h(t))\right)exp\left(b_j t\right)} < -s\left(\tilde{W}_2^T(t), e(t-h(t))\right)$$

It is worth to notice that the learning law (18) and (19) must be realized on-line in parallel with the gain-parameter adaptation procedure (20). By this reason, this structure can be considered as a second adaptation level.

4.2 Main theorem on an upper bound for the observation error

For the stability analysis of the proposed DNNO, the next assumptions are accepted:

A1) the function $f:\Re^{n}\rightarrow\Re^{n}$ is Lipschitz continuous in $x\in X$, that is, for all $x,x'\in X$ there exist constants $L_{1,2}$ such that

$$\begin{gathered}\left\|f(x,u,t)-f(y,v,t)\right\|\leq L_1\left\|x-y\right\|+L_2\left\|u-v\right\| \\ \left\|f(0,0,t)\right\|^2\leq C_1;\ x,y\in\Re^{n};\ u,v\in\Re^{m};\ 0\leq L_1,L_2<\infty\end{gathered}\tag{25}$$

A2) The pair (A,C) is observable, that is, there exists a gain matrix $K\in\Re^{n\times m}$ such that matrix

$$\tilde{A}(K):=A-KC\tag{26}$$

is stable (Hurwitz).

A3) The noises $\xi(t)$ and $\eta(t)$ in the system (1) are uniformly (on t) bounded such that

$$\left\|\xi(t)\right\|^2_{\Lambda_\xi}\leq\Upsilon_\xi,\ \left\|\eta(t)\right\|^2_{\Lambda_\eta}\leq\Upsilon_\eta\tag{27}$$

where Λ_ξ and Λ_η are known "normalizing" non-negative definite matrices, which permit to operate with vectors having components of different physical nature (for example, meters, voltage and etc.).

Theorem *(Upper error for DNNO)***.** Under assumptions *A1-A3* and if there exist matrices $\Lambda_i=\Lambda_i^T>0$, $\Lambda_i\in\Re^{n\times n}$, $i=1\ldots10$, $Q_0\in\Re^{n\times n}$, $K\in\Re^{n\times m}$ and positive parameters ϖ, μ_1,μ_2 and μ_3 such that the following LMI

$$\begin{bmatrix}\begin{matrix}-\Gamma(K,\varpi,\mu_1,\mu_2) & P\\ P & R\end{matrix} & 0 & 0 & 0\\ 0 & \begin{matrix}\Theta_1 & \tilde{A}^T(K)P\\ P\tilde{A}(K) & \mu_1 P\end{matrix} & 0 & 0\\ 0 & 0 & \begin{matrix}\Theta_2 & \hat{W}_1^T(K)P\\ P\hat{W}_1 & \mu_2 P\end{matrix} & 0\\ 0 & 0 & 0 & \begin{matrix}\Theta_3 & \hat{W}_2^T(K)P\\ P\hat{W}_2 & \mu_3 P\end{matrix}\end{bmatrix}>0\tag{28}$$

with $tr\{\Theta_i\}<1,\quad i=1,2,3$ and

$$\Gamma(K,\delta,\mu_1,\mu_2) = \left[\tilde{A}^T(K)P + P\tilde{A}(K) + Q\left(\delta,\mu_1,\mu_2,\mu_3\right)\right]$$
$$R^{-1} = \Lambda_1^{-1} + \Lambda_9^{-1} + \Lambda_{10}^{-1} + \hat{W}_1\Lambda_5^{-1}\left(\hat{W}_1\right)^T + \hat{W}_2\Lambda_8^{-1}\left(\hat{W}_2\right)^T$$
$$Q\left(\delta,\mu_1,\mu_2,\mu_3\right) = \left[\left\|\Lambda_5\right\|L_\sigma + \left\|\Lambda_8\right\|L_\varphi\Upsilon_u^2 + \mu_1 + \mu_2 L_\sigma + \mu_3\Upsilon_u^2 L_\varphi\right]I$$
$$+\varpi\left(\Lambda_3^{-1} + \Lambda_7^{-1}\right) + Q_0$$

has positive definite solution **P**, then the projectional DNNO, with the weight's learning laws, given by (18), (19), (20) and with $h(t)$ satisfying

$$\lim_{t\to\infty} h(t) \to \varepsilon, 0 < \varepsilon << 1 \tag{29}$$

Provides the following upper bound for the "averaged estimation" error

$$\begin{aligned}
&\overline{\lim_{T\to\infty}} \frac{1}{T}\int_{\tau=0}^{T}\left(\delta^T(\tau-h(\tau))Q_0\delta(\tau-h(\tau)\right)d\tau \le \\
&\left\|\Lambda_9\right\|\left(\left(\left\|K\right\|\left\|\Lambda_\eta^{-1}\right\|^{1/2}\Upsilon_\eta + \left\|\Lambda_\xi^{-1}\right\|^{1/2}\Upsilon_\xi\right)\right)^2 \\
&+\left\|\Lambda_{10}\right\|\left\|\Lambda_{\tilde{f}}^{-1}\right\|\left[\tilde{f}_0 + \tilde{f}_1\left\|x(t)\right\|^2_{\Lambda_{\tilde{f}}^1}\right] + \left\|K\right\|^2\left\|P\right\|\left\|\Lambda_\eta^{-1}\right\|^{1/2}\Upsilon_\eta \\
&+\left\|P\right\|\left\|\Lambda_{\tilde{f}}^{-1}\right\|\left[\tilde{f}_0 + \tilde{f}_1\left\|\Lambda_{\tilde{f}}^1\right\|\mathtt{Diam}(x)^2\right] + \left\|P\right\|\left\|\Lambda_\xi^{-1}\right\|\Upsilon_\xi + 2\Upsilon_\eta
\end{aligned} \tag{30}$$

where $Diam(x) = \sup_{x,z\in X}\left\|x-z\right\|$, and $\delta(t) := \hat{x}(t) - x(t)$ is the state estimation error. The proof of this theorem is presented in the appendix A.

Remark 1: It is easy to see that in the absence of noises ($\eta(t) = \xi(t) = 0$) and unmodelled dynamics ($\tilde{f} = 0$), we can prove that:

$$\overline{\lim_{T\to\infty}} \frac{1}{T}\int_{\tau=0}^{T}\left(\delta^T(\tau-h(\tau))Q_0\delta(\tau-h(\tau)\right)d\tau \to 0 \tag{31}$$

5. Numerical Example Implementation

5.1 Algorithm of Implementation

As it follows from the presentation above, to realized the suggested approach one needs to fulfill the following steps:

- Define the projector.
- Select Matrices A and $\hat{W}$ (some hints are given in Chairez, et. al. 2006; Stepanyan & Hovakimyan, 2007).
- Select K such that $A - KC$ is stable, with C defined by the output of the system.

- Find P as the solution of the LMI problem (28).
- Introduce P into the adapting weight law (18), (19) and (20) and realized them on-line.

5.2 DNNO implementation (Contaminated Soil Treatment by Ozonation)

High oxidation process employing ozone is one of the most recent approaches in the treatment of the contaminated soil with chemical compounds such as polyaromatic hydrocarbons. The next simplified model (32) describes the ozonization of one contaminant in the solid and gas phases in a semi-continuous reactor (Poznyak T., et. al. 2007).

$$
\begin{aligned}
\frac{d}{dt}x_1(t) &= V_{gas}^{-1}\left[W_{gas}C^{in} - W_{gas}x_1(t) - k_1 x_{4,t}x_3(t) - K_t^{abs}\left(Q_{max}^{free\_abs} - x_2(t)\right)\right] \\
\frac{d}{dt}x_2 &= K_t^{abs}\left(Q_{max}^{free\_abs} - x_2(t)\right) \\
\frac{d}{dt}x_{3,t} &= k_1 x_4(t)x_3(t) \\
\frac{d}{dt}x_4(t) &= -k_1 G^{-1}x_4(t)x_3(t)
\end{aligned}
\tag{32}
$$

Here in (32) $y(t) = x_1(t) + \eta(t)$ (see Figures 2 and 3) is the ozone concentration (mole/L) at the output of the reactor assumed to be on-line measurable, $x_2(t)$ (mole) is the ozone amount absorbed by the soil, which is not reacting with the contaminant, $x_3(t)$ (mole) is the ozone amount absorbed by the soil and reacting with the contaminant, and $x_4(t)$ (mole/g) is the current contaminant concentration, C^{in} is the ozone concentration at the reactor input (mole/L), $Q_{max}^{free\_abs}$ is the maximum amount of ozone, which can be absorbed by the soil, $Wgas$ is the gas flow (L/s) (established as a constant value), $Vgas$ is the volume of the gas phase.

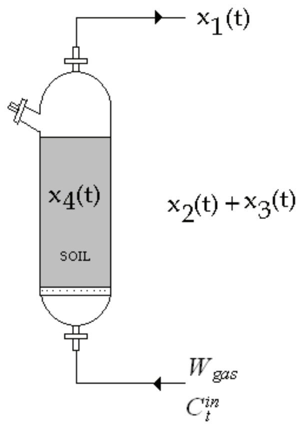

(L).

Figure 2. Contaminated soil ozonation procedure in a semi-continuous batch reactor

It is worth notice that the model is employed only as a data source; any structural information (mathematical model) has been used in the projectional DNNO design.
The convex compact set X according to the physical system constrictions is given as:

$$X := \left\{ \begin{array}{c} 0 \le x_1(t) \le x_1(t) \\ 0 \le x_2(t) \le Q_{max}^{free\_abs} \\ 0 \le x_3(t) \le V_{gas} C^{in} \\ 0 \le x_4(t) \le x_4(t) \end{array} \right\} \tag{33}$$

Projectional operator is defined as in (6), and the corresponding observer parameters are defined by:

$$A = \begin{bmatrix} -2.6 & 0 & 0 & 0 \\ 0 & -1.6 & 0 & 0 \\ 0 & 0 & -2.24 & 0 \\ 0 & 0 & 0 & -0.46 \end{bmatrix}, K = \begin{bmatrix} 0.01 \\ 0.01 \\ -0.0001 \\ -0.1 \end{bmatrix} \tag{34}$$

Figures 4-7 represent the results of x_3 and x_4 estimation from the measurable output. We have compared the projectional DNNO against a DNNO without projection operator, it means, with and without considering physical restrictions in the DNNO structure. Simulation have been realized in the presence of "quasi-white noise" $\eta(t)$ (amplitude $= 0.6 \times 10^{-5}$) and with the same initial conditions in both cases.

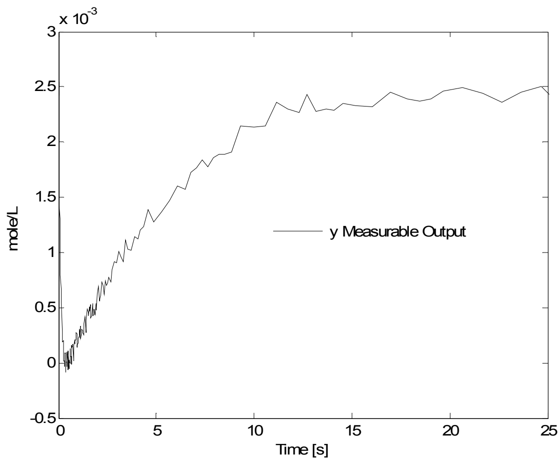

Figure 3. Measurable output (available information)

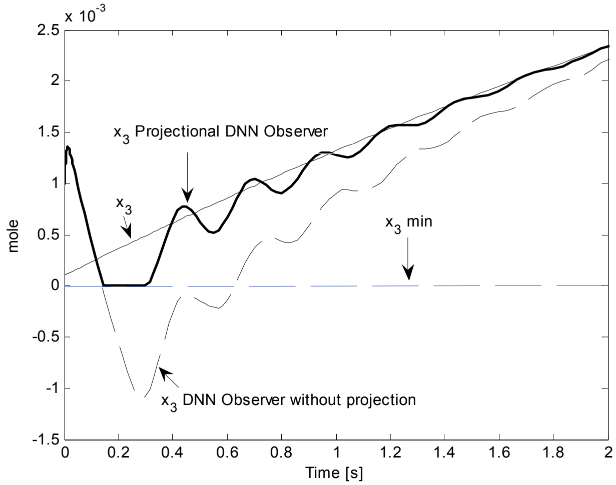

Figure 4. Estimation of $x_3(t)$ (2 s)

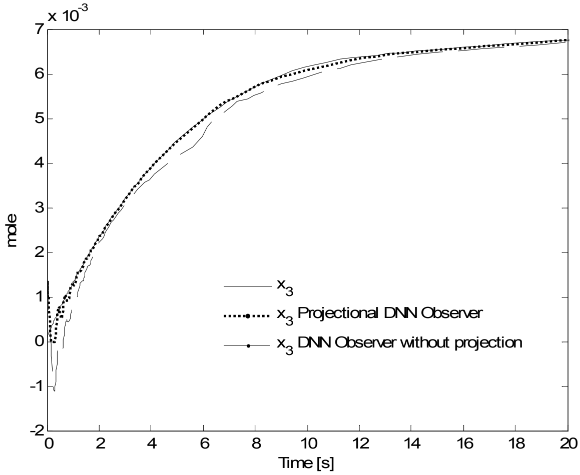

Figure 5. Estimation of $x_3(t)$ (20 s)

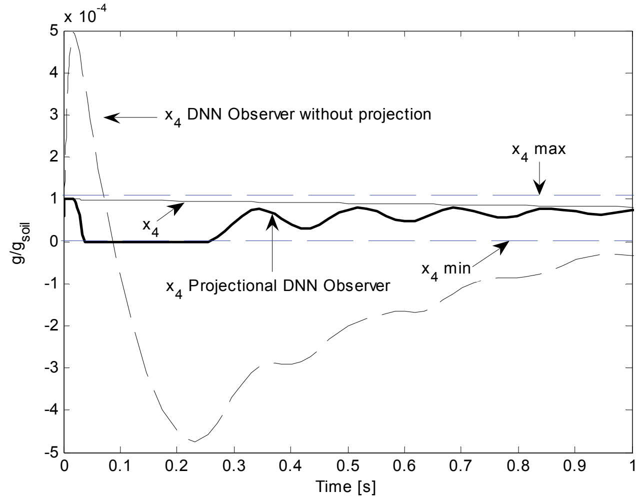

Figure 6. Estimation of $x_4(t)$ (1 s)

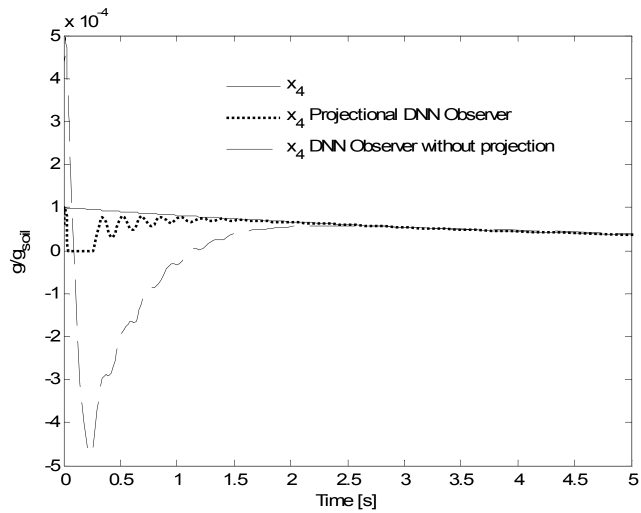

Figure 7. Estimation of $x_4(t)$ (5 s)

As it can be seen, the projectional DNNO has significantly better quality in state estimation, especially in the beginning of the process, when negative values and over-estimation have been obtained by a non-projectional DNNO.

6. Conclusion and future work

The complete convergence analysis for this class of adaptive observer is presented. Also the boundedness property of the adaptive weights in DNN was proven. Since the projection method leads to discontinuous trajectories in the estimated states, a nonstandard Lyapunov - Krasovski functional is applied to derive the upper bound for estimation error (in "average sense"), which depends on the noise power (output and dynamics disturbances) and on an unmodelled dynamic. It is shown that the asymptotic stability is attained when both of these uncertainties are absent. The illustrative example confirms the advantages, which the suggested observers have being compared with traditional ones.

Appendix (proof of Theorem 2)

Evidently that

$$\|\delta(t') - \delta(t-h)\| \le L_\delta \|t' - (t - h(t))\|$$

$$\|\eta(t)\| = \sqrt{\left(\Lambda_\eta^{1/2}\eta(t), \Lambda_\eta^{-1}\Lambda_\eta^{1/2}\eta(t)\right)} \le \sqrt{\left\|\Lambda_\eta^{-1}\right\| \|\eta(t)\|^2_{\Lambda_\eta}} \le \left\|\Lambda_\eta^{-1}\right\|^{1/2} \Upsilon_\eta$$

$$\|\xi(t)\| \le \left\|\Lambda_\xi^{-1}\right\|^{1/2} \Upsilon_\xi$$

$$\|\tilde{f}(t)\| \le \left\|\Lambda_{\tilde{f}}^{-1}\right\|^{1/2} \left[\tilde{f}_0 + \tilde{f}_1 \|x(t)\|^2_{\Lambda^1_{\tilde{f}}}\right]^{1/2}$$

where $\delta(t') := \hat{x}(t') - x(t')$ is the state estimation error at time t.
Consider the next "nonstandard" Lyapunov-Krasovskii ("energetic") function

$$V(t) = \int_{t-h(t)}^{t} \left[\|\delta(\tau)\|_p^2 + k(\tau) tr\left\{\tilde{W}^T(\tau)\tilde{W}(\tau)\right\}\right] d\tau$$

where $\tilde{W}(\tau\tau) = W(\tau(- \hat{W}$. Since the problem under consideration contains uncertainties and external output disturbances we won't demonstrate that the time-derivative of this energetic function is strictly negative. Instead, we will use it to obtain an upper bound for the averaged state estimation error. Taking time derivative of Lyapunov-Krasovski function and considering the property (5), the assumption $A2$, and in view of (29) we have:

$$
\begin{gathered}
\frac{d}{dt}V(t)\le \\
\left\| \pi_X\left\{ \hat{x}(t-h(t)) + \int_{\tau=t-h(t)}^{t} \left[A\hat{x}(\tau) + W_1(\tau)\sigma(\hat{x}(\tau)) + W_2(\tau)(\varphi(\hat{x}(\tau))u(\tau) + K(Cx(\tau)+\eta(\tau)-C\hat{x}(t))) \right] d\tau \right\} \right. \\
\left. -x(t) \right\|_p^2 - \\
\left\| \delta(t-h(t)) \right\|_p^2 + \\
k_1(t)\mathbf{tr}\left\{ \tilde{W}_1^T(t)\tilde{W}_1(t) \right\} - k_1(t-h(t))\mathbf{tr}\left\{ \tilde{W}_1^T(t-h(t))\tilde{W}_1(t-h(t)) \right\} + \\
k_2(t)\mathbf{tr}\left\{ \tilde{W}_2^T(t)\tilde{W}_2(t) \right\} - k_2(t-h(t))\mathbf{tr}\left\{ \tilde{W}_2^T(t-h(t))\tilde{W}_2(t-h(t)) \right\} \le \\
\left\| \hat{x}(t-h(t)) + \int_{\tau=t-h(t)}^{t} \left[A\hat{x}(\tau) + W_1(\tau)\sigma(\hat{x}(\tau)) + W_2(\tau)(\varphi(\hat{x}(\tau))u(\tau) + K(\eta(\tau)-C\delta(\tau)) \right] d\tau \right. \\
\left. -x(t-h(t)) - \int_{\tau=t-h(t)}^{t} \left[Ax(t) + \hat{W}_1\sigma(x(t)) + \hat{W}_2(\varphi(x(\tau))u(\tau) + \tilde{f}(\tau) + \xi(\tau) \right] d\tau \right\|_p^2 - \left\| \delta(t-h(t)) \right\|_p^2 \\
+k_1(t)\mathbf{tr}\left\{ \tilde{W}_1^T(t)\tilde{W}_1(t) \right\} - k_1(t-h(t))\mathbf{tr}\left\{ \tilde{W}_1^T(t-h(t))\tilde{W}_1(t-h(t)) \right\} \\
+k_2(t)\mathbf{tr}\left\{ \tilde{W}_2^T(t)\tilde{W}_2(t) \right\} - k_2(t-h(t))\mathbf{tr}\left\{ \tilde{W}_2^T(t-h(t))\tilde{W}_2(t-h(t)) \right\}
\end{gathered}
$$

Taking into account that

$$
\|a+b\|_P^2 = \|a\|_P^2 + \|b\|_P^2 + 2(Pa,b)
$$

Defining:

$$
\begin{gathered}
\tilde{A} \ := A - KC, \\
\tilde{W}_i(t) := W_i(t) - \hat{W}_i \quad i = 1,2 \\
\tilde{\sigma}(t) := \sigma(\hat{x}(t)) - \sigma(x(t)) \\
\tilde{\varphi}(t) \ := \varphi(\hat{x}(t)) - \varphi(x(t))
\end{gathered}
$$

we derive

$$
\begin{gathered}
\dot{V} \le a(t) + \beta(t) + \\
k_1(t)tr\left\{ \tilde{W}_1^T(t)\tilde{W}_1(t) \right\} - k_1(t-h(t))tr\left\{ \tilde{W}_1^T(t-h(t))\tilde{W}_1(t-h(t)) \right\} + \\
k_2(t)tr\left\{ \tilde{W}_2^T(t)\tilde{W}_2(t) \right\} - k_2(t-h(t))tr\left\{ \tilde{W}_2^T(t-h(t))\tilde{W}_2(t-h(t)) \right\}
\end{gathered}
$$

where:

$$
\begin{gathered}
\alpha(t) := \left\| \int_{\tau=t-h(t)}^{t} \left[\tilde{A}\delta(\tau) + \tilde{W}_1(\tau)\sigma(\hat{x}(\tau)) + \hat{W}_1\tilde{\sigma}(\tau) + \tilde{W}_2(\tau)(\varphi(\hat{x}(\tau))u(\tau) + \right. \right. \\
\left. \left. \hat{W}_2\tilde{\varphi}(\tau)u(\tau) + K\eta(\tau) - \xi(\tau) - \tilde{f}(\tau) \right] d\tau \right\|_2^P \\
\beta(t) := \left(2P\delta(t-h), \int_{\tau=t-h(t)}^{t} \left[\tilde{A}\delta(\tau) + \tilde{W}_1(\tau)\sigma(\hat{x}(\tau)) + \hat{W}_1\tilde{\sigma}(\tau) + \tilde{W}_2(\tau)(\varphi(\hat{x}(\tau))u(\tau) \right. \right. \\
\left. \left. + \hat{W}_2\tilde{\varphi}(\tau)u(\tau) + K\eta(\tau) - \xi(\tau) - \tilde{f}(\tau) \right] d\tau \right)
\end{gathered}
$$

The term $\beta(t)$ is expanded as

$$\beta(t)=2\left(P\delta(t-h(t)),\int_{\tau=t-h(t)}^{t}\tilde{A}\delta(\tau)d\tau\right)+$$
$$2\left(P\delta(t-h(t)),\int_{\tau=t-h(t)}^{t}\tilde{W}(\tau)\sigma\hat{x}(\tau)d\tau\right)+2\left(P\delta(t-h(t)),\int_{\tau=t-h(t)}^{t}\hat{W}_1\tilde{\sigma}(\tau)d\tau\right)$$
$$+2\left(P\delta(t-h(t)),\int_{\tau=t-h(t)}^{t}\tilde{W}_2(\tau)(\varphi(\hat{x}(\tau))u(\tau)d\tau\right)$$
$$+2\left(P\delta(t-h(t)),\int_{\tau=t-h(t)2}^{t}\hat{W}_2\tilde{\varphi}(\tau)u(\tau)d\tau\right)$$
$$+2\left(P\delta(t-h(t)),\int_{\tau=t-h(t)}^{t}(K\eta(\tau)-\xi(\tau))d\tau\right)-2\left(P\delta(t-h(t)),\int_{\tau=t-h(t)}^{t}\tilde{f}(\tau)d\tau\right)$$

Similarly, we can estimate α_t by the Jensen's inequality we get

$$\alpha(t):=\left\|\int_{\tau=t-h(t)}^{t}\left[\tilde{A}\delta(\tau)+\tilde{W}_1(\tau)\sigma(\hat{x}(\tau))+\hat{W}_1\tilde{\sigma}(\tau)+\tilde{W}_2(\tau)(\varphi(\hat{x}(\tau))u(\tau)\right.\right.$$
$$\left.\left.+\hat{W}_2\tilde{\varphi}(\tau)u(\tau)+K\eta(\tau)-\xi(\tau)-\tilde{f}(\tau)\right]d\tau\right\|_2^P\leq$$
$$8\left\{\int_{\tau=t-h(t)}^{t}\left(\left\|\tilde{A}\delta(\tau)\right\|_p^2+\left\|\tilde{W}_1(\tau)\sigma(\hat{x}(\tau))\right\|_p^2+\left\|\hat{W}_1\tilde{\sigma}(\tau)\right\|_p^2+\left\|\tilde{W}_2(\tau)(\varphi(\hat{x}(\tau))u(\tau)\right\|_p^2\right)d\tau\right.$$
$$\left.+\int_{\tau=t-h(t)}^{t}\left(\left\|\hat{W}_2\tilde{\varphi}(\tau)u(\tau)\right\|_p^2+\left\|K\eta(\tau)\right\|_p^2+\left\|\tilde{f}(\tau)\right\|_p^2+\left\|\xi(\tau)\right\|_p^2\right)d\tau\right\}$$

Each term of α_t and $\beta(t)$ is upper bounded, next facts are used. Norm inequality $\|AB\|\leq\|A\|\|B\|$ and the matrix inequality

$$XY^T+YX^T\leq X\Lambda\Lambda^T+Y\Lambda^{-1}Y^T$$

valid for any $X,Y\in R^{r\times s}$ and any $0<\Lambda=\Lambda^T\in R^{s\times s}$ (Poznyak, 2001).
It also necessary to represents the state estimation error δ_t as a function of the available output, the estimation error e_t :

$$\begin{gathered}-e(t)=\hat{y}(t)-y(t)=C\hat{x}(t)-Cx(t)-\eta(t)\\ -C^Te(t)=C^T(C\delta(t)-\eta(t))\\ -C^Te(t)+C^T\eta(t)=C^TC\delta(t)+\varpi\delta(t)-\varpi\delta(t)\\ -C^Te(t)+C^T\eta(t)+\varpi\delta(t)=\left(C^TC+\varpi I\right)\delta(t)\end{gathered}$$

Giving

$$\delta(t)=N_{\varpi}\left(-C^Te(t)+C^T\eta(t)+\varpi\delta(t)\right)$$

where:

$$N_{\varpi} := \left(C^T C + \varpi I\right)^{-1}$$

and ϖ is a small positive scalar. Taking into account all these facts next estimation is obtained:

$$\frac{d}{dt}V(t) \le h(t)\delta_{t-h(t)}^T \Big[\tilde{A}^T P + P\tilde{A} +$$
$$P\left(\Lambda_1^{-1} + \hat{W}_1 \Lambda_5^{-1} (\hat{W}_1)^T + \hat{W}_2 \Lambda_8^{-1} (\hat{W}_2)^T + \Lambda_9^{-1} + \Lambda_{10}^{-1} \right) P + \Big)$$
$$\left(\|\Lambda_5\| L_\sigma + \|\Lambda_8\| L_\varphi \Upsilon_u^2 + \mu_1 + \mu_2 L_\sigma + \mu_3 \Upsilon_u^2 L_\varphi \right) I + \varpi\left(\Lambda_3^{-1} + \Lambda_7^{-1} \right) + Q_0 \Big] \delta_{t-h(t)} +$$

$$h(t)^3 \left[\|\Lambda_1\| \|\tilde{A}\|^2 \frac{L_\delta^2}{4} + \|\Lambda_5\| \frac{L_\sigma L_\delta^2}{3} + \mu_2 \frac{L_\sigma L_\delta^2}{3} + \mu_1 \frac{L_\delta^2}{3} + \mu_3 \frac{\Upsilon_u^2 L_\varphi L_\delta^2}{3} + \|\Lambda_8\| \frac{L_\varphi \Upsilon_u^2 L_\delta^2}{3} \right] +$$
$$h(t) \left[\|\Lambda_9\| \left(\left(\|K\| \left\|\Lambda_\eta^{-1}\right\|^{1/2} \Upsilon_\eta + \left\|\Lambda_\xi^{-1}\right\|^{1/2} \Upsilon_\xi \right) \right)^2 + \|\Lambda_{10}\| \left\|\Lambda_{\tilde{f}}^{-1}\right\| \left[\tilde{f}_0 + \tilde{f}_1 \|x(t)\|_{\Lambda_{\tilde{f}}^1}^2 \right] + \right.$$
$$\left. \|K\|^2 \|P\| \left\|\Lambda_\eta^{-1}\right\|^{1/2} \Upsilon_\eta + \|P\| \left\|\Lambda_{\tilde{f}}^{-1}\right\| \left[\tilde{f}_0 + \tilde{f}_1 \left\|\Lambda_{\tilde{f}}^1\right\| Diam(x)^2 \right] + \right)$$
$$\|P\| \left\|\Lambda_\xi^{-1}\right\| \Upsilon_\xi + 2\Upsilon_\eta - \delta_{t-h(t)}^T Q_0 \delta_{t-h(t)} \Big] + \int_{\tau=t-h(t)}^{t} 2\left(e^T(t-h(t)) C N_\varpi P \tilde{W}_1(\tau) \sigma(\hat{x}(\tau)) \right) d\tau$$
$$+ \int_{\tau=t-h(t)}^{t} \left[\sigma^T(\hat{x}(\tau)) \tilde{W}_1^T(\tau) P N_\varpi \left(C\Lambda_2 C + \varpi \Lambda_3 \right) N_\varpi P \tilde{W}_1(\tau) \sigma(\hat{x}(\tau)) \right] d\tau$$

$$+ \int_{\tau=t-h(t)}^{t} \sigma^T(\hat{x}_\tau) \tilde{W}_1^T(\tau) P \tilde{W}_\tau \sigma(\hat{x}_\tau) d\tau + k_1(t) tr\left\{ \tilde{W}_1^T(t) \tilde{W}_1(t) \right\} -$$
$$k_1(t-h(t)) tr\left\{ \tilde{W}_1^T(t-h(t)) \tilde{W}_1(t-h(t)) \right\} +$$
$$\int_{\tau=t-h(t)}^{t} 2\left(e^T(t-h(t)) C N_\varpi P \tilde{W}_2(\tau) (\varphi(\hat{x}(\tau)) u(\tau) \right) d\tau$$
$$+ \int_{\tau=t-h(t)}^{t} u^T(\tau) \varphi^T(\hat{x}(\tau)) \tilde{W}_2^T(\tau) P N_\varpi \left(C^T \Lambda_6 C + \varpi \Lambda_7 \right) N_\varpi P \tilde{W}_2(\tau) (\varphi(\hat{x}(\tau)) u(\tau) d\tau$$
$$+ \int_{\tau=t-h(t)}^{t} u^T(\tau) (\varphi(\hat{x}(\tau))^T \tilde{W}_2^T(\tau) P \tilde{W}_2(\tau) (\varphi(\hat{x}(\tau)) u(\tau) d\tau +$$
$$k_2(t) tr\left\{ \tilde{W}_2^T(t) \tilde{W}_2(t) \right\} - k_2(t-h(t)) tr\left\{ \tilde{W}_2^T(t-h(t)) \tilde{W}_2(t-h(t)) \right\}$$

Considering

$$\begin{gathered}
\widetilde{A}^{T}(K)P + P\widetilde{A}(K) + PR^{-1}P + Q(\delta,\mu_1,\mu_2,\mu_3) \le 0 \\
R^{-1} = \Lambda_1^{-1} + \hat{W}_1\Lambda_5^{-1}(\hat{W}_1)^T + \hat{W}_2\Lambda_8^{-1}(\hat{W}_2)^T + \Lambda_9^{-1} + \Lambda_{10}^{-1} \\
Q(\delta,\mu_1,\mu_2,\mu_3) = \left[\|\Lambda_5\|L_{\sigma} + \|\Lambda_8\|L_{\varphi}\Upsilon_u^2 + \mu_1 + \mu_2 L_{\sigma} + \mu_3\Upsilon_u^2 L_{\varphi}\right]I \\
+\varpi\left(\Lambda_3^{-1} + \Lambda_7^{-1}\right) + Q_0
\end{gathered}$$

implies:

$$\begin{gathered}
\int_{\tau=t-h(t)}^{t} tr\left\{\widetilde{W}_1^T(\tau)P\left[2N_{\varpi}C^T e(t-h(t)) + N_{\varpi}\left(\varpi\Lambda_3 + C^T\Lambda_2 C\right)N_{\varpi}P\widetilde{W}_1(\tau)\sigma(\hat{x}(\tau))\right.\right. \\
\left.\left. + \widetilde{W}_1(\tau)\sigma(\hat{x}(\tau))\right]\sigma^T(\hat{x}(\tau))\right\}d\tau \\
+ k_1(t)tr\left\{\widetilde{W}_1^T(t)\widetilde{W}_1(t)\right\} - k_1(t-h(t))tr\left\{\widetilde{W}_1^T(t-h(t))\widetilde{W}_1(t-h(t))\right\} = 0
\end{gathered}$$

that can be obtained selecting

$$\begin{gathered}
\frac{d}{dt}W_1(t) = \\
-\frac{k_1(t)^{-1}}{2}\left\{P\left[2N_{\varpi}C^T e(t\text{-}h(t)) + N_{\varpi}\left(\varpi\Lambda_3 + C^T\Lambda_2 C\right)N_{\varpi}P\widetilde{W}_1(\tau)\sigma(\hat{x}(\tau)) + \right.\right. \\
\left. \widetilde{W}_1(\tau)\sigma(\hat{x}(\tau))\right]\sigma^T(\hat{x}(\tau)) - \\
\left.\frac{dk_1(t)}{dt}\widetilde{W}_1(t)\right\}
\end{gathered}$$

Analogously, for the second adaptive law

$$\begin{gathered}
\int_{\tau=t-h(t)}^{t} \mathbf{tr}\left\{\widetilde{W}_2^T(\tau)P\left[2N_{\varpi}C^T e(t-h(t)) + N_{\varpi}\left(C^T\Lambda_6 C + \varpi\Lambda_7\right)N_{\varpi}P\widetilde{W}_1(\tau)(\varphi(\hat{x}(\tau))u(\tau)\right.\right. \\
\left.\left. + \widetilde{W}_2(\tau)(\varphi(\hat{x}(\tau))u(\tau)\right]u^T(\tau)\varphi^T(\hat{x}(\tau))\right\}d\tau \\
+ k_2(t)\mathbf{tr}\left\{\widetilde{W}_2^T(t)\widetilde{W}_2(t)\right\} - k_2(t-h(t))\mathbf{tr}\left\{\widetilde{W}_2^T(t-h(t))\widetilde{W}_2(t-h(t))\right\} = 0
\end{gathered}$$

leading to

$$\begin{gathered}
\frac{d}{dt}W_2(t) = \\
-\frac{k_2(t)^{-1}}{2}\left\{P\left[2N_{\varpi}C^T e(t-h(t)) + N_{\varpi}\left(C^T\Lambda_6 C + \varpi\Lambda_7\right)N_{\varpi}P\widetilde{W}_1(\tau)(\varphi(\hat{x}(\tau))u(\tau) + \right.\right. \\
\left. \widetilde{W}_2(\tau)(\varphi(\hat{x}(\tau))u(\tau)\right]u^T(\tau)\varphi^T(\hat{x}(\tau)) \\
\left. -\frac{dk_2(t)}{dt}\widetilde{W}_2(t)\right\}
\end{gathered}$$

Finally:

$$\begin{aligned}\frac{d}{dt}V(t)\le h(t)^3\Bigg[&\|\Lambda_1\|\|\tilde{A}\|^2\frac{L_\delta^2}{4}+\|\Lambda_5\|\frac{L_\sigma L_\delta^2}{3}+\mu_2\frac{L_\sigma L_\delta^2}{3}+\mu_1\frac{L_\delta^2}{3}+\mu_3\frac{\Upsilon_u^2 L_\varphi L_\delta^2}{3}+\|\Lambda_8\|\frac{L_\varphi \Upsilon_u^2 L_\delta^2}{3}\Bigg]\\
&+h(t)\Bigg[\|\Lambda_9\|\left(\left(\|K\|\left\|\Lambda_\eta^{-1}\right\|^{1/2}\Upsilon_\eta+\left\|\Lambda_\xi^{-1}\right\|^{1/2}\Upsilon_\xi\right)\right)^2+\|\Lambda_{10}\|\left\|\Lambda_{\tilde{f}}^{-1}\right\|\left[\tilde{f}_0+\tilde{f}_1\|x(t)\|^2_{\Lambda^1_{\tilde{f}}}\right]\\
&+\|K\|^2\|P\|\left\|\Lambda_\eta^{-1}\right\|^{1/2}\Upsilon_\eta+\|P\|\left\|\Lambda_{\tilde{f}}^{-1}\right\|\left[\tilde{f}_0+\tilde{f}_1\left\|\Lambda^1_{\tilde{f}}\right\|Diam(x)^2\right]\\
&+\|P\|\left\|\Lambda_\xi^{-1}\right\|\Upsilon_\xi+2\Upsilon_\eta-\delta^T_{t-h(t)}Q_0\delta_{t-h(t)}\Bigg]\end{aligned}$$

or in the short form:

$$\frac{d}{dt}V(t)\le h(t)\left(h(t)^2 a+b-\delta^T(t-h(t))Q_0\delta(t-h(t))\right)$$

where

$$\begin{aligned}a &:= \|\Lambda_1\|\|\tilde{A}\|^2\frac{L_\delta^2}{4}+\|\Lambda_5\|\frac{L_\sigma L_\delta^2}{3}+\mu_2\frac{L_\sigma L_\delta^2}{3}+\mu_1\frac{L_\delta^2}{3}+\mu_3\frac{\Upsilon_u^2 L_\varphi L_\delta^2}{3}+\|\Lambda_8\|\frac{L_\varphi \Upsilon_u^2 L_\delta^2}{3}\\
b &:= \|\Lambda_9\|\left(\left(\|K\|\left\|\Lambda_\eta^{-1}\right\|^{1/2}\Upsilon_\eta+\left\|\Lambda_\xi^{-1}\right\|^{1/2}\Upsilon_\xi\right)\right)^2+\|\Lambda_{10}\|\left\|\Lambda_{\tilde{f}}^{-1}\right\|\left[\tilde{f}_0+\tilde{f}_1\|x(t)\|^2_{\Lambda^1_{\tilde{f}}}\right]\\
&+\|K\|^2\|P\|\left\|\Lambda_\eta^{-1}\right\|^{1/2}\Upsilon_\eta+\|P\|\left\|\Lambda_{\tilde{f}}^{-1}\right\|\left[\tilde{f}_0+\tilde{f}_1\left\|\Lambda^1_{\tilde{f}}\right\|Diam(x)^2\right]+\|P\|\left\|\Lambda_\xi^{-1}\right\|\Upsilon_\xi+2\Upsilon_\eta\end{aligned}$$

So,

$$\delta^T(t-h(t))Q_0\delta(t-h(t))\le\left(ah(t)^2+b\right)-\frac{dV(t)}{dt}\frac{1}{h(t)}$$

And integrating, we obtain

$$\int_{\tau=0}^{T}\delta^T(\tau-h(\tau))Q_0\delta(\tau-h(t)(\tau))d\tau\le\int_{\tau=0}^{T}\left[\left(ah(\tau)^2+b\right)-\frac{dV(t)}{dt}\frac{1}{h(\tau)}\right]d\tau$$

And hence,

$$\begin{aligned}-\int_{\tau=0}^{T}\frac{dV_\tau}{h(\tau)}=-\int_{\tau=0}^{T}d\left(\frac{V_\tau}{h(\tau)}\right)+\int_{\tau=0}^{T}\frac{V_\tau}{h(\tau)^2}h(\tau)d\tau\le\\
-\int_{\tau=0}^{T}d\left(\frac{V_\tau}{h(\tau)}\right)=-\frac{V_t}{h(t)}+\frac{V_0}{h(0)}\le\frac{V_0}{h(0)}\end{aligned}$$

This implies

$$\int_{\tau=0}^{T}\delta^T(\tau-h(t)(\tau))Q_0\delta(\tau-h(t)(\tau))d\tau\le a\int_{\tau=0}^{T}h(t)^2d\tau+bT+\frac{V_0}{h(0)}$$

Dividing by T and taking the upper limit we finally get (30).

8. References

Abdollahi, F. Talei, A., & Patel R. (2006). A stable neural network based observer with application to flexible joint manipulators. *IEEE Transactions on Neural Networks.* Vol 17. No 1 pp 118-129.

Alamo, T., Bravo, J. M. & Camacho, E. F. (2005). Guaranteed state estimation by zonotopes. *Automatica* vol 41 pp 1035-1043.

Chairez, I., Poznyak, A. & Poznyak, T. (2006). New Sliding mode learning law for Dynamic Neural Network Observer. *IEEE Transactions on Circuits Systems II*. Vol 53. Pp 1338-1342.

Dochain, D. (2003). State and parameter estimation in chemical and biochemical processes: a tutorial. *Journal of Process Control*. Vol 13. pp 801-818.

García, A., Poznyak, A., Chairez, I. & Poznyak T. (2007) Projectional dynamic neural network observer. *In proceedings 3rd IFAC symposium on system, structure and control*. Brazil.

Haddad, W. Bailey, J., Hayakawa T., & Hovakimnayan, N. (2007). Neural Network adaptive output feedback control for intensive care unit sedation and intraoperative anesthesia. *IEEE Transactions on Neural Networks*. Vol 18 pp. 1049-1065.

Haykin, S (1994). *Neural Networks, A comprehensive foundation*. IEEE Press New York.

Knobloch, H., Isidori, A. & Flocherzi, D. (1993). *Topics in Control Theory*, Birkhauser Verlag, Basel-Boston Berlin.

Krener, A. J. & Isidori (1983). Linearization by output injection and nonlinear observers. *System an Control Letters* Vol3, pp 47-52

Nicosia, S., Tomei, P. & A. Tornambe (1988), A nonlinear observer for elastic robot, *IEEE Journal of Robotics and Automation*, v.4,pp 45-52.

Pilutla, S. & Keyhani, A. (1999). Neural Network observers for on-line tracking of synchronous generator parameters. *IEEE Transactions on Energy Conversion*. Vol 14. pp 23-30.

Poznyak, A., Sanchez, E. & Wen Y. (2001). *Differential Neural Networks for robust nonlinear control*. World Scientific.

Poznyak, A. (2004). Deterministic output noise effects in sliding mode observation. In *variable structure system: from principles to implementation*. IEE Control Engineering series. pp 45-80.

Poznyak, T., García, A., Chairez, I., Gómez M & Poznyak, A. (2007). Application of the differential neural network observer to the kinetic parameters identification of the anthracene degradation contaminated model soil. *Journal of Hazardous Materials*. Vol 146, pp 661-667.

Radke, A. & Gao, Z.(2006). A survey of state an disturbance observers for practitioners, *Proceedings of the American Control Conference,* Minneapolis, Minnesota USA, pp 5183-5188

Stepanyan, V. & Hovakimyan, N. (2007). Robust Adaptive Observer Design for uncertain systems with bounded disturbances. *IEEE Transactions on Neural Networks*. Vol. 18, pp 1392-1403.

Tornambe, :A..(1989), Use of asymptotic observers having high-gains in the state and parameter estimation, In *Proc. 28th Conf. Dec. Control*, Tampa, Florida ·, pp 1791-1794.

Valdes-González, H., Flaus, J., Acuña G. (2003). Moving horizon state estimation with global convergence using interval techniques: application to biotechnological processes. *Journal of Process Control*. Vol 13. pp 325-336.

Wang, W., & Gao, Z. (2003). A comparison study of advanced state observer design techniques, *In Proceedings of the American Control Conference*. Pp 4754-4759.

Yaz E. & AzemiA. (1994). Robust-adaptive observers for systems having uncertain functions with unknown bounds, *Proceedings of Amer.Contr.Conf.*, NY, USA, v.1,pp. 73-74.

Zak H., & B. L.Walcott. (1990). State observation of nonlinear control systems via the method of Lyapunov. in Zinober, A.S.I. (ed.), *Deterministic Control of Uncertain Systems*, pp 333-350 Peter Peregrinus, Stevenage UK, 1990.

4

Integral Sliding Modes with Block Control of Multimachine Electric Power Systems

Héctor Huerta, Alexander Loukianov and José M. Cañedo
Centro de Investigación y de Estudios Avanzados del Instituto Politécnico Nacional, Unidad Guadalajara
Jalisco, México

1. Introduction

Over last 15 years the problem of rotor angle stability of electric power systems (EPS) has received a great attention. A fundamental problem in the design of feedback controllers for EPS is that of robust stabilizing both rotor angle and voltage magnitude, and achieving a specified transient behavior. Robustness implies operation with adequate stability margins and admissible performance level in spite of plant parameters variations and in the presence of external disturbances.

The EPS have nonlinearities and are subject to variations as a result of a change in the systems loading and/or configuration. Then, the EPS are modeled as complex large-scale nonlinear systems and the generators may be interconnected over several kilometers in very large power systems. Thus, the controller design is a challenging problem. A complete centralized control scheme could be difficult to implement in EPS, due to the reliability and distortion in information transfer. On the other hand, accurate prediction of system responses and system robustness to disturbances under different operation conditions are guarantee by robust decentralized control schemes. The decentralized controllers are locally implemented, so do not need system information communication among subsystems. In each subsystem, the effects of the other subsystems are considered as a disturbance. To design decentralized control schemes for EPS, a controller is designed for each generator connected to the system.

The control schemes of power systems are commonly based on reduced order linearized model and classical control algorithms that ensure asymptotic stability of the equilibrium point under small perturbations (Anderson & Fouad, 1994, DeMello & Concordia, 1969). Improvements on linear techniques have been analyzed in (Wang et al., 1998, Djukanovic et at., 1998a, Djukanovic et al., 1998b). Nevertheless, these controllers have been designed by using linear models. To analyze the EPS entire operation region, nonlinear control design techniques are more appropriate. Various nonlinear techniques have been implemented, e.g., control based on direct Lyapunov method (Machowsky et al., 1999), feedback linearization (FL) technique (Akhkrif, et al, 1999, Wu & Malik, 2006,) including backstepping (Jung et al., 2005 King et al., 1994), intelligent neural networks (Venayagamoorthy et al., 2003, Mohagheghi et al., 2007), fuzzy logic (Yousef & Mohamed, 2004) and normal form analysis (Kshatriya, et al., 2005, Liu et al., 2006).

All of the mentioned controllers provide larger stability margins with respect to traditional ones. But these control schemes were designed for reduced order plant. The unmodelled electrical dynamics can affect the electromechanical dynamics in case of large perturbations. The detailed 7-th order model of synchronous machine (five equations for electrical dynamics and two for mechanical dynamics) has been considered and a nonlinear controller using this model and FL technique has been designed to enhance transient stability (Akhkrif, et al., 1999). The proposed nonlinear control law is a function of all plant parameters and disturbances. In practice some of these parameters are subjected to variations as a result of a change in the system loading and/or configuration. Since the detailed model is so involved, a direct use of the FL technique results in a computationally expensive control algorithm. Moreover, this control scheme does not take into account practical limitation on the magnitude of the excitation voltage, and an observer design problem was not solved.

On the other hand, sliding mode control (SMC), (Utkin, et al., 1999) is one of the most effective strategies to deal with robust nonlinear controllers. SMC enables high accuracy and robustness to disturbances and plant parameter variations. Moreover, the control variables of the basic sliding mode control law rapidly switch between extreme limits, which are ideal for the direct operation of the switched mode power converters of synchronous generators. Sliding mode controllers for power systems have been designed in (Dash et al., 1996, Bandal et al., 2005), however for reduced order plants only, the best of our knowledge. Application of these controllers to full order plant would cause undesirable chattering, since unmodelled dynamics can be excited.

In (Loukianov et al., 2004) it was designed a sliding mode controller to regulate the terminal voltage and power angle for a single machine infinite-bus system, based on the eighth order generator model (two equations for mechanical dynamics and six equations for electrical ones for thermo electrical power system). In this case, an information about the power angle reference, δ_{ref}, is required. To overcome this restriction, in (Loukianov et al., 2006) a decentralized robust sliding mode control scheme was proposed to regulate the voltages and stabilize the speed in a multi machine power system.

In this paper an eighth order model for each generator of the multimachine power systems is considered. Sliding mode controller is designed by using the combination of three techniques: block control (Loukianov, 1998), integral sliding mode control (Utkin *et al.*, 1999), and nested sliding mode control (Adhami-Mirhosseini and Yazdanpanah, 2005). The block control technique is used to design a nonlinear sliding surface in such a way that the sliding mode dynamics are represented by a linear system with desired eigenvalues. The integral sliding mode control combined with nested control technique are applied to reject perturbations. The controller designed in this way is computationally low demanding and takes into account structural constraints of the control input. The main feature of the proposed control scheme is robustness with respect to the both matched and unmatched perturbations and only local information is required. Moreover, a nonlinear observer for the unmeasureable estates of the systems such as the rotor fluxes of the generators is presented.

This chapter is organized as follows. Section 2 presents a general mathematical description of the EPS (nonlinear eight order electrical generator, electrical network and loads models). Section 3 deals with the problem of nonlinear robust controller for the class of the nonlinear systems represented in the nonlinear block controllable form, the Integral Sliding Modes with Block Control technique is analyzed. Section 4 shows the design of a nonlinear robust control scheme for EPS, as well as a generator rotor fluxes observer. The results of the simulations in an equivalent of the WSCC, that illustrates the properties of the controller designed, can be found in section 5, followed by conclusions in section 6.

2. EPS Model

This section copes with the mathematical description of the EPS. The multimachine EPS model considers the generators model, the electrical network model and loads.

2.1 Generator model

The electrical dynamics comprised the field winding, rotor and stator windings, after the Park's transformation, can be expressed as follows (Anderson & Fouad, 1994):

$$\begin{bmatrix} d\boldsymbol{\lambda}_1/dt \\ d\mathbf{i}/dt \end{bmatrix} = \mathbf{A}(\omega)\cdot\begin{bmatrix} \boldsymbol{\lambda}_1 \\ \mathbf{i} \end{bmatrix} + \mathbf{T}\begin{bmatrix} \mathbf{v}_1 \\ \mathbf{v} \end{bmatrix} \tag{1}$$

where $\boldsymbol{\lambda}_1 = (\lambda_f, \lambda_g, \lambda_{kd}, \lambda_{kq})^T$, $\mathbf{i} = (i_d, i_q)^T$, $\mathbf{v} = (v_d, v_q)^T$, $\mathbf{v}_1 = (v_f,\ 0,\ 0,\ 0)^T$, λ_f is the field flux, λ_{kd}, λ_{kq} and λ_g are the direct-axis and quadrature-axis damper windings fluxes respectively, i_d and i_q are the stator currents, ω is the angular speed, v_f is the excitation control input, v_d and v_q are the direct-axis and quadrature-axis terminal voltages, respectively. The matrices $\mathbf{A}(\omega) = -\mathbf{T}\left[\mathbf{R}\cdot\mathbf{L}^{-1} + \mathbf{W}(\omega)\right]\mathbf{T}^{-1}$, $\mathbf{T}, \mathbf{R}, \mathbf{L}$ and $\mathbf{W}(\omega)$ are defined in *Appendix*.

The complete mathematical description includes also the swing equation given by

$$\begin{aligned} d\delta/dt &= \omega - \omega_b \\ d\omega/dt &= (\omega_b/2H)(T_m - T_e) \end{aligned} \tag{2}$$

where δ is the power angle, ω_b is the rated synchronous speed, H is the inertia constant, T_m is the mechanical torque applied to the shaft, and T_e is the electromagnetic torque, expressed in terms of the linked fluxes and currents as follows:

$$T_e = a_1\lambda_f i_q - a_2\lambda_g i_d + a_3\lambda_{kd} i_q - a_4\lambda_{kq} i_d - a_5 i_d i_q \tag{3}$$

where $a_1,\ldots,a_5$ are constants defined in *Appendix*. The mechanical torque T_m it is assumed to be a slowly varying and bounded function of time. Thus:

$$\dot{T}_m = 0\,. \tag{4}$$

Since the multimachine EPS has at least one more differential equation than is needed to solve the system, then, it is possible to define the angle relative to the generator 1 of the form:

$$\hat{\delta}_i = \delta_i - \delta_1, \quad i = 1, 2, \ldots, n$$

where n is the number of generators in the system. Thus

$$\frac{d\hat{\delta}_1}{dt}=0, \qquad \frac{d\hat{\delta}_i}{dt}=\omega_i-\omega_1, \qquad i=2,3,\ldots,n\,. \tag{5}$$

From (1)-(5), the nonlinear state-space presentation of the i^{th} generator in the multimachine power system is derived of the form

$$\begin{bmatrix}\dot{\mathbf{x}}_{1i}\\ \dot{\mathbf{x}}_{2i}\end{bmatrix}=\begin{bmatrix}\mathbf{f}_{1i}(\mathbf{x}_i,\ \mathbf{i}_i)\\ \mathbf{f}_{2i}(\mathbf{x}_i,\ \mathbf{i}_i)\end{bmatrix}+\begin{bmatrix}\mathbf{b}_{1i}\\ 0\end{bmatrix}v_{fi}+\begin{bmatrix}\mathbf{g}_i(\mathbf{x}_i,\ \mathbf{i}_i,\ T_{mi})\\ 0\end{bmatrix} \tag{6}$$

$$\mu\frac{d}{dt}\mathbf{i}_i=\mathbf{A}_{zi}(x_{2i})\mathbf{i}_i+\mathbf{f}_{zi}(\mathbf{x}_i)+\mathbf{b}_{zi}v_{fi}+\mathbf{H}_i\mathbf{v}_i \tag{7}$$

where $\mu=1/\omega_b$ is a small parameter, $\mathbf{x}_i=(\mathbf{x}_{1i}\ \mathbf{x}_{2i})^T$, $\mathbf{x}_{1i}=(x_{1i},x_{2i},x_{3i})^T=(\hat{\delta}_i,\ \omega_i,\ \lambda_{fi})^T$, $\mathbf{x}_{2i}=(x_{4i},x_{5i},x_{6i})^T=(\lambda_{gi},\lambda_{kdi},\lambda_{kqi})^T$, $\mathbf{i}_i=(i_{di},i_{qi})^T$, $\mathbf{f}_{1i}=\begin{bmatrix}x_{2i}-\omega_b\\ f_{\omega i}(\mathbf{x}_i,\mathbf{i}_i,T_{mi})-q_i(\mathbf{x}_i,\mathbf{i}_i)x_{3i}\\ b_{i1}x_{3i}+b_{i2}x_{5i}+b_{i3}i_{di}\end{bmatrix}$, $\mathbf{f}_{2i}(\mathbf{x}_i,\ \mathbf{i}_i)=\mathbf{A}_{2i}\mathbf{x}_{2i}+\mathbf{d}_{i1}x_{3i}+\mathbf{D}_i\mathbf{i}_i$,

$f_{\omega i}(\cdot)=-d_{mi}(-a_{i2}x_{4i}i_{di}+a_{i3}x_{5i}i_{qi}-a_{i4}x_{6i}i_{di}+a_{i5}i_{di}i_{qi})$, $q_i(\cdot)=a_{i1}d_{m_i}i_{qi}$, $d_m=\dfrac{\omega_b}{2H}$,

$\mathbf{d}_{i1}=\begin{bmatrix}0\\0\\d_{i1}\end{bmatrix}$, $\mathbf{D}_i=\begin{bmatrix}0&c_{i3}\\d_{i3}&0\\0&e_{i3}\end{bmatrix}$, $\mathbf{A}_{2i}=\begin{bmatrix}c_{i1}&0&c_{i2}\\0&d_{i2}&0\\r_{i1}&0&r_{i2}\end{bmatrix}$ $\mathbf{b}_{1i}=\begin{bmatrix}0\\0\\1\end{bmatrix}$, $\mathbf{A}_{zi}=\begin{bmatrix}h_{i7}&k_{i6}x_{2i}\\h_{i6}x_{2i}&k_{i7}\end{bmatrix}$, $\mathbf{H}_i=\begin{bmatrix}h_{i1}&0\\0&k_{i1}\end{bmatrix}$,

$\mathbf{b}_{zi}=\begin{bmatrix}0\\h_{i8}\end{bmatrix}$, $\mathbf{f}_{zi}(\mathbf{x}_i)=\begin{bmatrix}h_{i2}x_{3i}+h_{i3}x_{5i}+h_{i4}x_{2i}x_{4i}+h_{i5}x_{2i}x_{6i}\\k_{i2}x_{4i}+k_{i3}x_{6i}+k_{i4}x_{2i}x_{3i}+k_{i5}x_{2i}x_{5i}\end{bmatrix}$, $\mathbf{v}_i=[v_{di},\ v_{qi}]^T$,

$\mathbf{g}_i(\mathbf{x}_i,\mathbf{i}_i,\ T_{mi})=[0,\ g_{2i}(\mathbf{x}_i,\mathbf{i}_i,\ T_{mi}),\ 0]^T$. The perturbation term $g_{2i}(\cdot)$ includes variations of the generator parameters in the function $f_{\omega i}(\cdot)$ and the mechanical torque T_{mi} (external disturbance), i. e.

$$g_{2i}(\cdot)=d_mT_{mi}-[\Delta a_{i2}x_{4i}i_{di}+\Delta a_{i3}x_{5i}i_{qi}+\Delta a_{i4}x_{6i}i_{di}+\Delta a_{i5}i_{di}i_{qi}],\ a_{ij}=a_{ij,n}+\Delta a_{ij},\ j=2,\ldots,5,$$

where $a_{ij,n}$ and Δa_{ij} are the nominal value and variation, respectively, of the parameter a_{ij}. Moreover $rank\{\mathbf{A}_{zi}\}=2$ for all admissible values of x_{2i}.

To neglect the fast dynamics in the electric networks that in turn permits to simplify and simulate the complete power system by a differential algebraic equation (DAE) (Anderson & Fouad, 1994) we use the singular perturbation technique (Khalil, 1996). Thus, setting $\mu=0$ in (7) results in

$$0=\mathbf{A}_{zi}(x_{2i})\mathbf{i}_i+\mathbf{f}_{zi}(\mathbf{x}_i)+\mathbf{H}_i\mathbf{v}_i \tag{8}$$

The solution of (8) for $\mathbf{i}_i$ is calculated as

$$\mathbf{i}_i = \mathbf{g}_{zi}(\mathbf{x}_i, \mathbf{v}_i) \tag{9}$$

where $\mathbf{g}_{zi} = -\mathbf{A}_{zi}^{-1}(x_{2i})\left(\mathbf{f}_{zi}(\mathbf{x}_i) + \mathbf{H}_i \mathbf{v}_i\right)$. Finally, equations (6) and (9) give the following DAE system for the i^{th} generator:

$$\dot{\mathbf{x}}_{1i} = \mathbf{f}_{1i}\left(\mathbf{x}_i, \mathbf{i}_i, T_{mi}\right) + \mathbf{b}_{1i} v_{fi} + \mathbf{g}_i\left(\mathbf{x}_i, \mathbf{i}_i, T_{mi}\right) \tag{10}$$

$$\dot{\mathbf{x}}_{2i} = \mathbf{f}_{2i}\left(\mathbf{x}_i, \mathbf{i}_i\right) \tag{11}$$

$$\mathbf{i}_i = \mathbf{g}_{zi}(\mathbf{x}_i, \mathbf{v}_i). \tag{12}$$

2.2 Electrical network model

Since the fast dynamics reduction for the generator was achieved in the last subsection, it is possible to neglect the dynamics of the loads and transmission lines. Then, considering the loads as constant impedances, the electrical network can be modeled using the phasorial nodal method. Moreover, all the nodes, except for the generator ones, can be reduced (Kron's reduction). Therefore the network algebraic equation can be expressed as (Anderson & Fouad, 1994)

$$\bar{\mathbf{I}} = \bar{\mathbf{Y}}(\delta_1, \ldots, \delta_n)\bar{\mathbf{V}} \tag{13}$$

where $\bar{\mathbf{V}} = \left[v_{d1} + jv_{q1}, \cdots, v_{dn} + jv_{qn}\right]^T$ and $\bar{\mathbf{I}} = \left[i_{d1} + ji_{q1}, \cdots, i_{dn} + ji_{qn}\right]^T$ are the complex terminal generators voltages and currents, respectively, $\bar{\mathbf{Y}}(\cdot)$ is the reduced transformed admittance matrix and its entry *jk* is given by:

$$\bar{\mathbf{Y}}_{jk} = \mathbf{Y}_{jk} e^{(\delta_j - \delta_k)}$$

with the elements $\mathbf{Y}_{jk}$ calculated by using the nodal method. It is more convenient to express the equation (13) of the form

$$\mathbf{I} = \tilde{\mathbf{Y}}(\delta_1, \ldots, \delta_n)\mathbf{V}, \ \ \tilde{\mathbf{Y}}(\cdot) \in R^{2n\times 2n} \tag{14}$$

where $\mathbf{V} = \left[v_{d1}, v_{q1}, \ldots, v_{dn}, v_{qn}\right]^T$ and $\mathbf{I} = \left[\mathbf{i}_1^T \ldots \mathbf{i}_n^T\right]^T = \left[i_{d1}, i_{q1}, \ldots, i_{dn}, i_{qn}\right]^T$ are the phasors components of the voltages and currents, respectively. Thus, the multimachine EPS model is given by (10)-(12) and (14). It is important to note that the vector $\mathbf{I}$ coincides with the generator currents i_{di} and i_{qi}.

3. Integral Sliding Modes with Block Control

The Integral Sliding Modes with Block Control (ISM) technique (Huerta-Avila et al., 2007a, Huerta-Avila et al., 2007b) is shown in this section. The description of the ISM is presented in generic terms to show the generality of the approach. In the next section a robust controller for the electrical power system will be designed by using this methodology.

3.1 Problem statement

In this work, the class of nonlinear systems presented in the NBC (nonlinear block controllable) form is studied. The NBC form consist of *r* blocks (Loukianov, 1998):

$$\begin{aligned} \dot{\mathbf{x}}_i &= \mathbf{f}_i(\overline{\mathbf{x}}_i) + \mathbf{B}_i(\overline{\mathbf{x}}_i)\mathbf{x}_{i+1} + \mathbf{g}_i(t,\mathbf{x}) \\ \dot{\mathbf{x}}_r &= \mathbf{f}_r(\mathbf{x}) + \mathbf{B}_r(\mathbf{x})\mathbf{u} + \mathbf{g}_r(t,\mathbf{x}), \quad i = 1,\ldots,r-1, \\ \mathbf{y} &= \mathbf{x}_1 \end{aligned} \tag{15}$$

where, $\mathbf{x} = [\mathbf{x}_1 \ldots \mathbf{x}_r]^T \in R^n$ is the state vector, $\mathbf{x}_i \in R^{n_i}$, $\overline{\mathbf{x}}_i = [\mathbf{x}_1 \ldots \mathbf{x}_i]^T$; $\mathbf{u} \in R^m$ is the control vector. Moreover, $\mathbf{f}(\cdot)$ and the columns of $\mathbf{B}(\cdot)$ are smooth vector fields, $\mathbf{g}_i(\cdot)$ is a bounded unknown perturbation term due to parameter variations and external disturbances, and

$$rank\left[\mathbf{B}_i(\mathbf{x}_1,\ldots,\mathbf{x}_i)\right] = n_i, \ \forall \mathbf{x}.$$

The integers $n_1,\ldots,n_r$ define the dimension of the i^{th} block (system structure) and satisfy

$$n_1 \le n_2 \le \cdots \le n_r = m, \quad \sum_{i=1}^{r} n_i = n.$$

The control objective is to design a controller such that the output $\mathbf{y}$ in (15) tracks a desired reference $\mathbf{x}_{ref}(t)$ with bounded derivatives, in spite of unknown but bounded perturbations. To induce quasi sliding mode in the i^{th} block of the system (15), the continuously differentiable sigmoid function $sigm(\upsilon/\varepsilon)$ defined as

$$sigm(\upsilon/\varepsilon) = \tanh(\upsilon/\varepsilon), \qquad \tanh(\upsilon/\varepsilon) = \frac{e^{\upsilon/\varepsilon} - e^{-\upsilon/\varepsilon}}{e^{\upsilon/\varepsilon} + e^{-\upsilon/\varepsilon}}$$

where $1/\varepsilon$ is the slope of the sigmoid function at $\upsilon = 0$, will be used since

$$\lim_{\varepsilon \to 0} sigm(\upsilon/\varepsilon) = sign(\upsilon).$$

3.2 Control design

According to the block control technique (Loukianov, 1998), the state $\mathbf{x}_{i+1}$, $i = 1, \ldots, r-1$ is considered as a virtual control vector in the i^{th} block of the system (15). The design procedure is described in *r* steps.

Step 1. The control error in the first block of the system (15) is defined as

$$\mathbf{z}_1 = \mathbf{x}_1 - \mathbf{x}_{ref} := \boldsymbol{\psi}_1(\mathbf{x}_1)$$

then

$$\dot{\mathbf{z}}_1 = \mathbf{f}_1(\mathbf{x}_1) + \mathbf{B}_1(\mathbf{x}_1)\mathbf{x}_2 + \overline{\mathbf{g}}_1(t,\mathbf{x}) \tag{16}$$

with $\overline{\mathbf{g}}_1(t,\mathbf{x}) = \mathbf{g}_1(t,\mathbf{x}) - \dot{\mathbf{x}}_{ref}$.

And the virtual control $\mathbf{x}_2$ in (16) is redefined of the form

$$\mathbf{x}_2 = \mathbf{x}_{2,0} + \mathbf{x}_{2,1} \tag{17}$$

where the nominal part, $\mathbf{x}_{2,0}$ is selected to eliminate the old dynamics in (16) and introduce the new desired ones, $k_1\mathbf{z}_1$, $k_1 > 0$, i. e.

$$\mathbf{x}_{2,0} = -\mathbf{B}_1^+(\mathbf{x}_1)\left(\mathbf{f}_1(\mathbf{x}_1) + k_1\mathbf{z}_1 - \mathbf{E}_1\mathbf{z}_2\right), \quad k_1 > 0 \tag{18}$$

where $\mathbf{z}_2 \in R^{n_2}$ is a new variables vector, $\mathbf{E}_1 = \left[\mathbf{I}_{n_1} \; 0\right] \in R^{n_1 \times n_2}$ and $\mathbf{B}_1^+$ is the right pseudo-inverse of $\mathbf{B}_1$, defined as $\mathbf{B}_1^+ = \mathbf{B}_1^T(\mathbf{B}_1\mathbf{B}_1^T)^{-1}$.
In order to reject the perturbation term $\overline{\mathbf{g}}_1(t,\mathbf{x})$ in (16), the second part of the virtual control (17), $\mathbf{x}_{2,1}$ is designed by using the integral sliding mode technique (Utkin et al., 1999). The pseudo-sliding manifold $\mathbf{s}_1$ is chosen as

$$\mathbf{s}_1 = \mathbf{z}_1 + \boldsymbol{\sigma}_1 = 0 \ , \qquad \mathbf{s}_1, \ \boldsymbol{\sigma}_1 \in R^{n_1} . \tag{19}$$

Then, from (16)-(19) it follows

$$\dot{\mathbf{s}}_1 = -k_1\mathbf{z}_1 + \mathbf{E}_1\mathbf{z}_2 + \mathbf{B}_1(\mathbf{x}_1)\mathbf{x}_{2,1} + \overline{\mathbf{g}}_1(t,\mathbf{x}) + \dot{\boldsymbol{\sigma}}_1 . \tag{20}$$

Choosing the dynamics for the integral variable $\boldsymbol{\sigma}_1$ of the form

$$\dot{\boldsymbol{\sigma}}_1 = k_1\mathbf{z}_1 - \mathbf{E}_1\mathbf{z}_2, \quad \boldsymbol{\sigma}_1(0) = -\mathbf{z}_1(0) \tag{21}$$

the equation (20) becomes

$$\dot{\mathbf{s}}_1 = \mathbf{B}_1(\mathbf{x}_1)\mathbf{x}_{2,1} + \overline{\mathbf{g}}_1(t,\mathbf{x}) . \tag{22}$$

The control input $\mathbf{x}_{2,1}$ in (22) is selected as follows:

$$\mathbf{x}_{2,1} = -\rho_1(\mathbf{x}_1)\mathbf{B}_1^+ sigm(\mathbf{s}_1/\varepsilon_1) \tag{23}$$

where $sigm(\mathbf{s}_1/\varepsilon_1) = \left[sigm(s_{1,1}/\varepsilon_1),\ldots,sigm(s_{1,n_1}/\varepsilon_1)\right]^T$. Substituting (17), (18) and (23) in (16) results in

$$\dot{\mathbf{z}}_1 = -k_1\mathbf{z}_1 + \mathbf{E}_1\mathbf{z}_2 - \rho_1(\mathbf{x}_1)sigm(\mathbf{s}_1/\varepsilon_1) + \overline{\mathbf{g}}_1(t,\mathbf{x}) . \tag{24}$$

If the matrix $\mathbf{M}_1(\mathbf{x}_1) \in R^{(n_2-n_1)\times n_2}$ is chosen such that the square matrix $\tilde{\mathbf{B}}_2(\mathbf{x}_1) = \left[\mathbf{B}_1(\mathbf{x}_1) \;\; \mathbf{M}_1(\mathbf{x}_1)\right]^T$ has full rank, the new variables vector $\mathbf{z}_2$ can be obtained from equations (17), (18) and (23) as

$$\mathbf{z}_2 = \tilde{\mathbf{B}}_2\mathbf{x}_2 + \begin{bmatrix} \mathbf{f}_1(\mathbf{x}_1) - k_1\boldsymbol{\psi}_1(\mathbf{x}_1) - \rho_1(\mathbf{x}_1)sigm\left(\dfrac{\mathbf{s}_1}{\varepsilon_1}\right) \\ 0 \end{bmatrix} := \boldsymbol{\psi}_2(\overline{\mathbf{x}}_2) \tag{25}$$

where $\bar{\mathbf{x}}_2 = [\mathbf{x}_1 \ \mathbf{x}_2]^T$. The procedure describe above can be achieved in the i^{th} block of (15) as follows.

Step i. At this step, the dynamics of the transformed i^{th} block of the system (15) are given by

$$\dot{\mathbf{z}}_i = \bar{\mathbf{f}}_i(\bar{\mathbf{x}}_i) + \bar{\mathbf{B}}_i(\bar{\mathbf{x}}_i)\mathbf{x}_{i+1} + \bar{\mathbf{g}}_i(t,\mathbf{x}) \tag{26}$$

where $\mathbf{z}_i \in R^{n_i}$ is a new variables vector, $\bar{\mathbf{g}}_i(t,\mathbf{x}) = \bar{\mathbf{g}}_{i-1}(t,\mathbf{x}) - d/dt\left[\rho_{i-1}(\bar{\mathbf{x}}_{i-1}) sigm(\mathbf{s}_{i-1}/\varepsilon_{i-1})\right]$, $\mathbf{z}_i = \boldsymbol{\psi}_i(\bar{\mathbf{x}}_i)$ and $\bar{\mathbf{B}}_i = \tilde{\mathbf{B}}_i\mathbf{B}_i$. The virtual control $\mathbf{x}_{i+1}$ in (26) is redefined as

$$\mathbf{x}_{i+1} = \mathbf{x}_{i+1,0} + \mathbf{x}_{i+1,1} \,. \tag{27}$$

Taking into account the procedure achieved in *step 1*, $\mathbf{x}_{i+1,0}$ and $\mathbf{x}_{i+1,1}$ are selected, respectively, of the form

$$\mathbf{x}_{i+1,0} = -\bar{\mathbf{B}}_i^{+}(\bar{\mathbf{x}}_i)\left(\bar{\mathbf{f}}_i(\bar{\mathbf{x}}_i) + k_i\mathbf{z}_i - \mathbf{E}_i\mathbf{z}_{i+1}\right), \quad k_i > 0 \tag{28}$$

$$\mathbf{x}_{i+1,1} = -\rho_i(\bar{\mathbf{x}}_i)\mathbf{B}_i^{+} sigm(\mathbf{s}_i/\varepsilon_i), \quad \rho_i > 0 \tag{29}$$

where $\mathbf{z}_{i+1} \in R^{n_{i+1}}$ is a new variables vector, $\mathbf{E}_i = \left[\mathbf{I}_{n_i} \ \ 0\right] \in R^{n_i \times n_{i+1}}$ and $\bar{\mathbf{B}}_i^{+} = \bar{\mathbf{B}}_i^{T}(\bar{\mathbf{B}}_i\bar{\mathbf{B}}_i^{T})^{-1}$. The proposed pseudo-sliding manifold and its derived dynamics, respectively, are:

$$\mathbf{s}_i = \mathbf{z}_i + \boldsymbol{\sigma}_i = 0 \ , \qquad \mathbf{s}_i,\ \boldsymbol{\sigma}_i \in R^{n_i} \ ,$$

$$\dot{\mathbf{s}}_i = -k_i\mathbf{z}_i + \mathbf{E}_i\mathbf{z}_{i+1} + \bar{\mathbf{B}}_i(\bar{\mathbf{x}}_i)\mathbf{x}_{i+1,1} + \bar{\mathbf{g}}_i(t,\mathbf{x}) + \dot{\boldsymbol{\sigma}}_i \,. \tag{30}$$

If $\boldsymbol{\sigma}_i$ satisfies

$$\dot{\boldsymbol{\sigma}}_i = k_i\mathbf{z}_i - \mathbf{E}_i\mathbf{z}_{i+1}, \ \ \boldsymbol{\sigma}_i(0) = -\mathbf{z}_i(0) \tag{31}$$

the equation (30) can be rewritten as

$$\dot{\mathbf{s}}_i = -\rho_i(\bar{\mathbf{x}}_i) sigm(\mathbf{s}_i/\varepsilon_i) + \bar{\mathbf{g}}_i(t,\mathbf{x}), \quad \rho_i(\bar{\mathbf{x}}_i) > 0 \,.$$

The substitution of (28) and (29) in the block (26) yields

$$\dot{\mathbf{z}}_i = -k_i\mathbf{z}_i + \mathbf{E}_i\mathbf{z}_{i+1} - \rho_i(\bar{\mathbf{x}}_i) sigm(\mathbf{s}_i/\varepsilon_i) + \bar{\mathbf{g}}_i(t,\mathbf{x}) \,.$$

Again, choosing a $(n_{i+1} - n_i) \times n_{i+1}$ matrix $\mathbf{M}_i(\bar{\mathbf{z}}_i)$ such that the square matrix $\tilde{\mathbf{B}}_{i+1}(\bar{\mathbf{x}}_i) = \left[\bar{\mathbf{B}}_i(\bar{\mathbf{x}}_i) \ \ \mathbf{M}_i(\bar{\mathbf{x}}_i)\right]^T$ has full rank, the new variables vector $\mathbf{z}_{i+1}$ can be obtained from equations (26)-(29) as

$$\begin{aligned}\mathbf{z}_{i+1} &= \tilde{\mathbf{B}}_{i+1}\mathbf{x}_{i+1} + \begin{bmatrix} \bar{\mathbf{f}}_i(\bar{\mathbf{x}}_i) - k_i\boldsymbol{\psi}_i(\bar{\mathbf{x}}_i) - \rho_i(\bar{\mathbf{x}}_i) sigm\left(\dfrac{\mathbf{s}_i}{\varepsilon_i}\right) \\ 0 \end{bmatrix}, \ i = 2,\ldots,r-1, \\ &:= \boldsymbol{\psi}_{i+1}(\bar{\mathbf{x}}_{i+1}).\end{aligned}$$

Step r. At the last step, the transformed complete system can be presented in the new variables $\mathbf{z}_1,\ldots,\mathbf{z}_r$ as

$$\begin{aligned}
\dot{\mathbf{z}}_i &= -k_i\mathbf{z}_i + \mathbf{E}_i\mathbf{z}_{i+1} - \rho_i(\overline{\mathbf{x}}_i)sigm(\mathbf{s}_i/\varepsilon_i) + \overline{\mathbf{g}}_i(t,\mathbf{x}) \\
\dot{\mathbf{s}}_i &= -\rho_i(\overline{\mathbf{x}}_i)sigm(\mathbf{s}_i/\varepsilon_i) + \overline{\mathbf{g}}_i(t,\mathbf{x}) \\
\dot{\mathbf{z}}_r &= \overline{\mathbf{f}}_r(\mathbf{x}) + \overline{\mathbf{B}}_r(\mathbf{x})\mathbf{u} + \overline{\mathbf{g}}_r(t,\mathbf{x}),\ \ i=1,\ldots,r-1
\end{aligned} \tag{32}$$

where $\overline{\mathbf{B}}_r(\cdot) = \tilde{\mathbf{B}}_{r-1}(\cdot)\mathbf{B}_r(\cdot)$ has full rank since $n_r = m$. Design the control input $\mathbf{u}$ in (32) as

$$\mathbf{u} = \mathbf{u}_0 + \mathbf{u}_1 \tag{33}$$

and define a sliding variable $\mathbf{s}_r \in R^{n_r}$ of the form

$$\mathbf{s}_r = \mathbf{z}_r + \boldsymbol{\sigma}_r,\ \ \boldsymbol{\sigma}_r \in R^{n_r}\ . \tag{34}$$

Then

$$\dot{\mathbf{s}}_r = \overline{\mathbf{f}}_r(\mathbf{x}) + \overline{\mathbf{B}}_r(\mathbf{x})\mathbf{u}_0 + \overline{\mathbf{B}}_r(\mathbf{x})\mathbf{u}_1 + \overline{\mathbf{g}}_r(t,\mathbf{x}) + \dot{\boldsymbol{\sigma}}_r\ . \tag{35}$$

Choosing

$$\dot{\boldsymbol{\sigma}}_r = -\overline{\mathbf{f}}_r(\mathbf{x}) - \overline{\mathbf{B}}_r(\mathbf{x})\mathbf{u}_0,\quad \boldsymbol{\sigma}_r(0) = -\mathbf{z}_r(0)$$

simplifies the equation (35) to

$$\dot{\mathbf{s}}_r = \overline{\mathbf{B}}_r(\mathbf{x})\mathbf{u}_1 + \overline{\mathbf{g}}_r(t,\mathbf{x})\ . \tag{36}$$

The second part of the control input (33) is selected as

$$\mathbf{u}_1 = -\rho_r(\mathbf{x})\overline{\mathbf{B}}_r^{-1}sign(\mathbf{s}_r),\ \ \rho_r(\mathbf{x}) > 0\ . \tag{37}$$

Under the condition $\rho_r(\mathbf{x}) > \left\|\overline{\mathbf{B}}_r^{-1}(\mathbf{x})\overline{\mathbf{g}}_r(t,\mathbf{x})\right\|$ sliding mode occurs on the manifold $\mathbf{s}_r = 0$ (34) in a finite time. Solving (36) for $\mathbf{u}_{r,1}$, formally setting $\dot{\mathbf{s}}_r = 0$, shows

$$\mathbf{u}_{1\mathrm{eq}} = \overline{\mathbf{B}}_r^{-1}(\mathbf{x})\overline{\mathbf{g}}_r(t,\mathbf{x})$$

where $\mathbf{u}_{1\mathrm{eq}}(t,\mathbf{x})$ is the equivalent control (Utkin et al., 1999). Therefore, the integral control (37) rejects the perturbation term $\overline{\mathbf{g}}_r(t,\mathbf{x})$ in the last block of (32):

$$\dot{\mathbf{z}}_r = \overline{\mathbf{f}}_r(\mathbf{x}) + \overline{\mathbf{B}}_r(\mathbf{x})\mathbf{u}_0 + \overline{\mathbf{B}}_r(\mathbf{x})\mathbf{u}_{1eq} + \overline{\mathbf{g}}_r(t,\mathbf{x})$$

and we have

$$\dot{\mathbf{z}}_r = \overline{\mathbf{f}}_r(\mathbf{x}) + \overline{\mathbf{B}}_r(\mathbf{x})\mathbf{u}_0\ .$$

Now, choosing

$$\mathbf{u}_0 = -\bar{\mathbf{B}}_r^{-1}(\mathbf{x})\left[\bar{\mathbf{f}}_r(\mathbf{x}) + k_r\mathbf{z}_r\right],\ k_r > 0$$

the sliding mode dynamics are described by

$$\begin{aligned}
\dot{\mathbf{z}}_i &= -k_i\mathbf{z}_i + \mathbf{E}_i\mathbf{z}_{i+1} - \rho_i(\bar{\mathbf{x}}_i)sigm(\mathbf{s}_i/\varepsilon_i) + \bar{\mathbf{g}}_i(t,\mathbf{x}) \\
\dot{\mathbf{s}}_i &= -\rho_i(\bar{\mathbf{x}}_i)sigm(\mathbf{s}_i/\varepsilon_i) + \bar{\mathbf{g}}_i(t,\mathbf{x}) \\
\dot{\mathbf{z}}_r &= -k_r\mathbf{z}_r, \quad i = 1,\dots,r-1.
\end{aligned} \tag{38}$$

Now, it is possible to establish the following result:
Theorem 1. If
H1) the unmatched $\bar{\mathbf{g}}_1(\cdot),\dots,\bar{\mathbf{g}}_{r-1}(\cdot)$ *and matched* $\bar{\mathbf{g}}_r(\cdot)$ *perturbations are bounded, i.e., there exist a known scalar function* $\beta_i(\mathbf{x})$ *such that*

$$\|\bar{\mathbf{g}}_i(t,\mathbf{x})\| \le \beta_i(\mathbf{x}),\quad i = 1,\dots,r$$

then, there exist constants $h_1,\dots,h_{r-1}$ *such that the states of the system (38), are uniformly bounded, i. e.*

$$\|\mathbf{z}_i(t)\| \le h_i,\ i = 1,\dots r-1.$$

Moreover the perturbed system (38) reaches to a neighborhood of the output $\mathbf{y} = \mathbf{x}_1$ *in finite time and remains in this neighborhood.*
Proof. The proof is constructive and consists of *r* steps, begin with the step *r*.
Step r. First, the sliding variable $\mathbf{s}_r$ stability is analyzed. Considering the Lyapunov function $\mathbf{V}_r = \mathbf{s}_r^T\mathbf{s}_r$, it follows:

$$\dot{\mathbf{V}}_r = \mathbf{s}_r^T\left[-\rho_r(\mathbf{x})sign(\mathbf{s}_r) + \bar{\mathbf{g}}_r(t,\mathbf{x})\right]. \tag{39}$$

Under the assumption H1, the equation (39) can be written as

$$\begin{aligned}
\dot{\mathbf{V}}_r &= \mathbf{s}_r^T\left[-\rho_r(\mathbf{x})sign(\mathbf{s}_r) + \beta_r(\mathbf{x})\right] \\
&\le \|\mathbf{s}_r\|\left[-\rho_r(\mathbf{x}) + \|\beta_r(\mathbf{x})\|\right].
\end{aligned} \tag{40}$$

From (40) it is easy to see that under the condition

$$\rho_r(\mathbf{x}) > \|\beta_r(\mathbf{x})\|$$

the derivative $\dot{\mathbf{V}}_r$ is definite negative and the equivalent control $\mathbf{u}_{r,1\mathrm{eq}}(t,\mathbf{x})$ satisfies

$$\mathbf{u}_{r,1\mathrm{eq}} = -\bar{\mathbf{g}}_r(t,\mathbf{x})$$

rejecting the perturbation term $\bar{\mathbf{g}}_r(t,\mathbf{x})$ in the last block of (38). Now, it is necessary to analyze the stability of the last block. Using the Lyapunov function $\mathbf{V}_r = \frac{1}{2}\mathbf{z}_r^T\mathbf{z}_r$, leads to

$$\dot{\mathbf{V}}_r \le -k_r\|\mathbf{z}_r\|^2,\ k_r > 0\ .$$

Thus, the trajectories of the last variables vector $\mathbf{z}_r$ are asymptotically stable.

Step r-1. Proceeding in similar way as in previous step, the Lyapunov function $\mathbf{V}_{r-1} = \mathbf{s}_{r-1}{}^T \mathbf{s}_{r-1}$ is proposed, then

$$\dot{\mathbf{V}}_{r-1} = \mathbf{s}_{r-1}{}^T \left[-\rho_{r-1}(\bar{\mathbf{x}}_{r-1}) sigm(\mathbf{s}_{r-1}) + \bar{\mathbf{g}}_{r-1}(t,\mathbf{x}) \right]. \tag{41}$$

In the region $\|\mathbf{s}_{r-1}\| > \varepsilon_{r-1}$ the equation (41) becomes

$$\begin{aligned} \dot{\mathbf{V}}_{r-1} &= \mathbf{s}_{r-1}{}^T \left[-\rho_{r-1}(\bar{\mathbf{x}}_{r-1}) sign(\mathbf{s}_{r-1}) + \bar{\mathbf{g}}_{r-1}(t,\mathbf{x}) \right] \\ &\le \|\mathbf{s}_{r-1}\| \left[-\rho_{r-1}(\bar{\mathbf{x}}_{r-1}) + \|\bar{\mathbf{g}}_{r-1}(t,\mathbf{x})\| \right] \end{aligned}. \tag{42}$$

Moreover, under the condition $\rho_{r-1}(\bar{\mathbf{x}}_{r-1}) > \|\bar{\mathbf{g}}_{r-1}(t,\mathbf{z})\|$, $\|\mathbf{s}_{r-1}\|$ will be decreasing until it reaches the set $\{\|\mathbf{s}_{r-1}\| \le \varepsilon_{r-1}\}$ in a finite time and it remains inside. The upper bound of this reaching time can be calculated by using the comparison lemma (Khalil, 1996) as follows:

$$t_{r-1} \le \|\mathbf{s}_{r-1}(0)\| - \varepsilon_{r-1}.$$

Furthermore the equivalent control $\mathbf{x}_{r-1,1eq}$ fulfills

$$\dot{\mathbf{s}}_{r-1} = \mathbf{x}_{r-1,1eq} + \bar{\mathbf{g}}_{r-1}(t,\mathbf{z}) = \varepsilon_{r-1}\boldsymbol{\gamma}_{r-1} \tag{43}$$

where $\varepsilon_{r-1}\boldsymbol{\gamma}_{r-1}$ is the error introduced by using the control law (29). To analyze the stability of the *r-1* block of the system (38), the Lyapunov function $\mathbf{V}_{r-1} = \frac{1}{2}\mathbf{z}_{r-1}{}^T \mathbf{z}_{r-1}$ is considered and its time derivative is given by

$$\begin{aligned} \dot{\mathbf{V}}_{r-1} &= \mathbf{z}_{r-1}{}^T \left[-k_{r-1}\mathbf{z}_{r-1} + \mathbf{E}_{r-1}\mathbf{z}_r - \rho_{r-1}(\bar{\mathbf{x}}_{r-1}) sigm\left(\mathbf{s}_{r-1}/\varepsilon_{r-1} \right) + \bar{\mathbf{g}}_{r-1}(t,\mathbf{z}) \right] \\ &\le -k_{r-1}\|\mathbf{z}_{r-1}\|^2 + \|\mathbf{z}_{r-1}\| \left[\|\mathbf{z}_r\| - \rho_{r-1}(\bar{\mathbf{x}}_{r-1}) sigm\left(\mathbf{s}_{r-1}/\varepsilon_{r-1} \right) + \bar{\mathbf{g}}_{r-1}(t,\mathbf{z}) \right]. \end{aligned}$$

In the region $\|\mathbf{s}_{r-1}\| > \varepsilon_{r-1}$, the derivative $\dot{\mathbf{V}}_{r-1}$ becomes

$$\begin{aligned} \dot{\mathbf{V}}_{r-1} &\le -k_{r-1}\|\mathbf{z}_{r-1}\|^2 + \|\mathbf{z}_{r-1}\| \left[\|\mathbf{z}_r\| - \rho_{r-1} sign\left(\mathbf{s}_{r-1}/\varepsilon_{r-1} \right) + \bar{\mathbf{g}}_{r-1}(t,\mathbf{z}) \right] \\ &\le -k_{r-1}\|\mathbf{z}_{r-1}\|^2 + \|\mathbf{z}_{r-1}\| \left[\|\mathbf{z}_r\| + \dot{\mathbf{s}}_{r-1} \right] \end{aligned}$$

and considering (43), it can be rewritten as

$$\dot{\mathbf{V}}_{r-1} \le -k_{r-1}\|\mathbf{z}_{r-1}\|^2 + \|\mathbf{z}_{r-1}\| \left[\|\mathbf{z}_r\| + \varepsilon_{r-1}\boldsymbol{\gamma}_{r-1} \right]. \tag{44}$$

Suppose that $\varepsilon_{r-1}\boldsymbol{\gamma}_{r-1}$ satisfies the following bound:

$$\varepsilon_{r-1}\boldsymbol{\gamma}_{r-1} \le \alpha_{r-1}\|\mathbf{z}_{r-1}\| + \beta_{r-1},\ \alpha_{r-1},\ \beta_{r-1} \in R.$$

Then it is possible to present the equation (44) of the form

$$\begin{aligned}\dot{\mathbf{V}}_{r-1} &\le -k_{r-1}\|\mathbf{z}_{r-1}\|^2 + \|\mathbf{z}_{r-1}\|\left[\|\mathbf{z}_r\| + \alpha_{r-1}\|\mathbf{z}_{r-1}\| + \beta_{r-1}\right] \\ &\le -\|\mathbf{z}_{r-1}\|\left[(k_{r-1}-\alpha_{r-1})\|\mathbf{z}_{r-1}\| - \|\mathbf{z}_r\| - \beta_{r-1}\right]\end{aligned}$$

which is negative in the region

$$\|\mathbf{z}_{r-1}\| > \delta_{r-1}\|\mathbf{z}_r\| + \lambda_{r-1} \tag{45}$$

where $\delta_{r-1} = \dfrac{1}{k_{r-1}-\alpha_{r-1}}$ and $\lambda_{r-1} = \dfrac{\beta_{r-1}}{k_{r-1}-\alpha_{r-1}}$. Moreover δ_{r-1} and λ_{r-1} are positive for $k_{r-1} > \alpha_{r-1}$. Thus the trajectories of the vector state enter ultimately in the region defined by

$$\|\mathbf{z}_{r-1}\| \le \delta_{r-1}\|\mathbf{z}_r\| + \lambda_{r-1}.$$

Step i. The step *r-1* can be generalized for the block *i*, with *i=r-1, r-2, …, 1.*
In the region $\|\mathbf{s}_i\| > \varepsilon_i$ the derivative of the Lyapunov function $\mathbf{V}_i = \mathbf{s}_i^T\mathbf{s}_i$, is calculated as

$$\begin{aligned}\dot{\mathbf{V}}_i &= \mathbf{s}_i^T\left[-\rho_i(\overline{\mathbf{x}}_i)sign(\mathbf{s}_i) + \overline{\mathbf{g}}_i(t,\mathbf{x})\right] \\ &\le \|\mathbf{s}_i\|\left[-\rho_i(\overline{\mathbf{x}}_i) + \|\overline{\mathbf{g}}_i(t,\mathbf{x})\|\right].\end{aligned} \tag{46}$$

Again, under the condition $\rho_i(\overline{\mathbf{x}}_i) > \|\overline{\mathbf{g}}_i(t,\mathbf{z})\|$, $\mathbf{s}_i$ enter in the region $\{\|\mathbf{s}_i\| \le \varepsilon_i\}$ in a finite time given by

$$t_i \le \|\mathbf{s}_i(0)\| - \varepsilon_i.$$

The equivalent control $\mathbf{x}_{i,1eq}$ satisfies

$$\dot{\mathbf{s}}_i = \mathbf{x}_{i,1eq} + \overline{\mathbf{g}}_i(t,\mathbf{z}) = \varepsilon_i\boldsymbol{\gamma}_i. \tag{47}$$

Considering the function $\mathbf{V}_i = \frac{1}{2}\mathbf{z}_i^T\mathbf{z}_i$ inside the subspace $\|\mathbf{s}_i\| > \varepsilon_i$, it follows

$$\begin{aligned}\dot{\mathbf{V}}_i &\le -k_i\|\mathbf{z}_i\|^2 + \|\mathbf{z}_i\|\left[\|\mathbf{z}_{i+1}\| - \rho_i(\overline{\mathbf{x}}_i)sign\left(\mathbf{s}_i/\varepsilon_i\right) + \overline{\mathbf{g}}_i(t,\mathbf{z})\right] \\ &\le -k_i\|\mathbf{z}_i\|^2 + \|\mathbf{z}_i\|\left[\|\mathbf{z}_{i+1}\| + \dot{\mathbf{s}}_i\right]\end{aligned}$$

and with (47), $\dot{\mathbf{V}}_i$ becomes

$$\dot{\mathbf{V}}_i \le -k_i\|\mathbf{z}_i\|^2 + \|\mathbf{z}_i\|\left[\|\mathbf{z}_{i+1}\| + \varepsilon_i\boldsymbol{\gamma}_i\right]$$

Supposing that $\varepsilon_i\boldsymbol{\gamma}_i$ fulfills

$$\varepsilon_i\boldsymbol{\gamma}_i \le \alpha_i\|\mathbf{z}_i\| + \beta_i,\ \alpha_i,\ \beta_i \in R$$

then

$$\dot{\mathbf{V}}_i \le -\|\mathbf{z}_i\|\left[(k_i - \alpha_i)\|\mathbf{z}_i\| - \|\mathbf{z}_{i+1}\| - \beta_i\right]$$

which is negative in the region

$$\|\mathbf{z}_i\| > \delta_i \|\mathbf{z}_{i+1}\| + \lambda_i$$

where $\delta_i = \dfrac{1}{k_i - \alpha_i}$ and $\lambda_i = \dfrac{\beta_i}{k_i - \alpha_i}$, which are positive for $k_i > \alpha_i$. Therefore a solution for $\mathbf{z}_i$ is ultimately bounded by

$$\|\mathbf{z}_i\| \le \delta_i \|\mathbf{z}_{i+1}\| + \lambda_i .$$

Then with the bound

$$\varepsilon_i \boldsymbol{\gamma}_i \le \alpha_i \|\mathbf{z}_i\| + \beta_i,\ i = 1, 2, ..., r-1$$

the convergence region is defined by:

$$\begin{aligned}
&\|\mathbf{z}_{r-1}\| > \delta_{r-1} \|\mathbf{z}_r\| + \lambda_{r-1} := h_{r-1} \\
&\|\mathbf{z}_{r-2}\| > \delta_{r-2} \|\mathbf{z}_{r-1}\| + \lambda_{r-2} := h_{r-2} \\
&\vdots \\
&\|\mathbf{z}_1\| > \delta_1 \|\mathbf{z}_2\| + \lambda_1 := h_1.
\end{aligned}$$

4. PES control design

Since the subsystem (10) has the NBC form, the ISM technique will be applied to design a robust controller for EPS. First, the rotor speed stability will be achieved. Secondly, the terminal voltage generator controller is outlined. Then, a switching logic is proposed to coordinate the operation of both controllers. Finally, an EPS observer is introduced.

4.1 Integral Sliding Mode Speed Stabilizer (ISMSS)

To achieve the first control objective, that is, the rotor speed stability enhancement, define the control error as (Huerta-Avila et al., 2007a, Huerta-Avila et al., 2007b)

$$z_{2i} = x_{2i} - \omega_b . \tag{48}$$

Taking the time derivative of (48) along the trajectories of (10) yields

$$\dot{z}_{2i} = f_{\omega i}(\mathbf{x}_i, \mathbf{v}_i) - q_i(\mathbf{x}_i, \mathbf{v}_i) x_{3i} + g_{2i}(\mathbf{x}_i, \mathbf{v}_i, T_{mi}) \tag{49}$$

where $\mathbf{x}_i = \left(\mathbf{x}_{1i}\ \mathbf{x}_{2i}\right)^T$, $q_i(t) > 0,\ \forall t > 0$.

Redefine the virtual control, x_{3i} in (49) as

$$x_{3i} = x_{3i,0} + x_{3i,1} . \tag{50}$$

The desired dynamics for z_{2i} is chosen of the form

$$\dot{z}_{2i} = -k_i z_{2i} + z_{3i} + q_i(\mathbf{x}_i, \mathbf{v}_i) x_{3i,1} + g_{2i}(\mathbf{x}_i, \mathbf{v}_i, T_{mi}),\ k_i > 0 \tag{51}$$

These dynamics can be obtained by choosing $x_{3i,0}$ as

$$x_{3i,0} = -\left[q_i(\mathbf{x}_i, \mathbf{v}_i)\right]^{-1}\left[f_{\omega i}(\mathbf{x}_i, \mathbf{v}_i) + k_i z_{2i} - z_{3i}\right] \tag{52}$$

where z_{3i} is a new variable. To design the second part of (50), $x_{3i,1}$, define a pseudo-sliding variable s_{2i} as

$$s_{2i} = z_{2i} + \sigma_{2i}$$

with the integral variable σ_{2i}. Using (49)-(51), it follows

$$\dot{s}_{2i} = -k_{0i} z_{2i} + z_{3i} + q_i(\mathbf{x}_i, \mathbf{v}_i) x_{3i,1} + g_{2i}(\mathbf{x}_i, \mathbf{v}_i, T_{mi}) + \dot{\sigma}_{2i} \tag{53}$$

Choosing

$$\dot{\sigma}_{2i} = k_{2i} z_{2i} - z_{3i}, \qquad \sigma_{2i}(0) = -z_{2i}(0)$$

the equation (53) becomes

$$\dot{s}_{2i} = g_{2i}(\mathbf{x}_i, \mathbf{v}_i, T_{mi}) + q_i(\mathbf{x}_i, \mathbf{v}_i) x_{3i,1} .$$

Select $x_{3i,1}$ of the form

$$x_{3i,1} = -\rho_{2i}\, sigm(s_{2i} / \varepsilon_i), \quad \rho_{2i} > 0 . \tag{54}$$

Then, the sliding variable $s_{\omega i} = z_{3i}$ is defined from (50), (52) and (54) of the form

$$s_{\omega i} = f_{\omega i}(\mathbf{x}_i, \mathbf{v}_i) + q_i(\mathbf{x}_i, \mathbf{v}_i) x_{3i} + k_{0i} z_{2i} + \rho_{2i} sigm(s_{2i} / \varepsilon_i) . \tag{55}$$

Thus, straightforward algebra reveals

$$\dot{s}_{\omega i} = f_{si}(\mathbf{x}_i, \mathbf{v}_i) + b_{si}(\mathbf{x}_i, \mathbf{v}_i) v_{fi} \tag{56}$$

where $f_{si}(\cdot)$ is a continuous function and $b_{si}(\cdot) = q_i(\cdot) b_{i4}$.
Considering (56), under the condition

$$k_{gi} > \left| b_{si}^{-1}(\mathbf{x}_i, \mathbf{v}_i) f_{si}(\mathbf{x}_i, \mathbf{v}_i) \right|$$

the proposed discontinuous control law

$$v_{fi} = -k_{gi} sign(s_{\omega i}), \qquad k_{gi} > 0 \tag{57}$$

ensures the convergence of the state to the manifold $s_{\omega i} = z_{3i} = 0$ (55) in a finite time (Utkin et al., 1999). The sliding mode motion on this manifold is governed by the reduced order system

$$\begin{aligned}
\dot{x}_{1i} &= z_{2i}, \\
\dot{z}_{2i} &= -k_{0i} z_{2i} - \rho_{2i}\, sigm(s_{2i} / \varepsilon_i) + g_{2i}(\mathbf{x}_i, \mathbf{v}_i, T_{mi}) \\
\dot{s}_{2i} &= -\rho_{2i}\, sigm(s_{2i} / \varepsilon_i) + g_{2i}(\mathbf{x}_i, \mathbf{v}_i, T_{mi})
\end{aligned} \tag{58}$$

$$\dot{\mathbf{x}}_{2i} = \mathbf{A}_{2i}\mathbf{x}_{2i} + \tilde{\mathbf{f}}_{2i}\left(\mathbf{x}_i, \mathbf{v}_i\right) \tag{59}$$

Now, choosing ε_i be sufficiently small and under the condition

$$\rho_{2i} > \left| g_{2i}\left(\mathbf{x}_i, \mathbf{v}_i, T_{mi}\right)\right|$$

a quasi sliding mode motion is enforced in a small ε_i-vicinity of $s_{2i} = 0$. Thus, if $\varepsilon_i \to 0$ then the perturbation term $g_{2i}\left(\mathbf{x}_i, \mathbf{v}_i, T_{mi}\right)$ in (59) is rejected, and the linearized mechanical dynamics can be represented as

$$\begin{aligned} \dot{x}_{1i} &= z_{2i} \\ \dot{z}_{2i} &= -k_{0i} z_{2i} \end{aligned} \tag{60}$$

with the desired eigenvalue $-k_{0i}$.

The equation (59) represents the rotor flux internal dynamics. The matrix $\mathbf{A}_{2i}$ is Hurwitz and the nonvanishing perturbation $\tilde{\mathbf{f}}_{2i}\left(\mathbf{x}_i, \mathbf{V}_i\right)$ is a continuous function. Therefore there exists an admissible region where a solution $\mathbf{x}_{2i}(t)$ of (60) is ultimately bounded (Khalil, 1996). Moreover, the control error z_{2i} (48) tends exponentially to zero, and the angle x_{1i} tends to a constant steady state, δ_{ssi}.

Remark: Since the initial conditions of the EPS are availabe, it is possible to apply the integral sliding modes technique.

4.2 Sliding Mode Voltage Regulator

In this subsection, the voltage regulation problem is studied. The terminal voltage, v_{gi}, is defined as

$$v_{gi}{}^2 = v_{di}{}^2 + v_{qi}{}^2 . \tag{61}$$

Using (8), v_{di} and v_{qi} are calculated of the form

$$\mathbf{v}_i = \begin{bmatrix} v_{di} \\ v_{qi} \end{bmatrix} = -\mathbf{H}_i^{-1}[\mathbf{A}_{zi}\mathbf{i}_i + \mathbf{f}_{zi}(\mathbf{x}_i)] . \tag{62}$$

Then, the dynamics for terminal voltage, v_{gi} can be obtained from (61), (62), (6), and (7) as (Loukianov, et al., 2006)

$$\dot{v}_{gi} = f_{vi}(\mathbf{x}_i, \mathbf{i}_i) + b_{vi}v_{fi} + g_{vi}(\mathbf{x}_i, \mathbf{i}_i, T_{mi}) \tag{63}$$

where $f_{vi}(\mathbf{x}_i, \mathbf{i}_i)$ is the nominal part of the voltage dynamics and the perturbation term $g_{vi}(\mathbf{x}_i, \mathbf{i}_i, T_{mi})$ contains parameter variations and external disturbances, $b_{vi} = h_{i2}b_{i4}$, $b_{vi}(t),\ \forall t \geq 0$. For the details see *Appendix*.

Defining the voltage control error

$$e_{vi} = v_{gi} - v_{refi}$$

and the control input v_{fi}

$$v_{fi} = v_{fi,0} + v_{fi,1} \tag{64}$$

we have

$$\dot{e}_{vi} = f_{vi}(\mathbf{x}_i, \mathbf{i}_i) + b_{vi} v_{fi,0} + b_{vi} v_{fi,1} + g_{vi}(\mathbf{x}_i, \mathbf{i}_i, T_{mi}) \tag{65}$$

where v_{refi} is the constant reference voltage. To design a robust controller we use the integral sliding mode approach (Utkin et al., 1999). In order to reject the perturbation term $g_{vi}(\mathbf{x}_i, \mathbf{i}_i, T_{mi})$ in (65) a sliding variable $s_{vi} \in R$ is formulated as

$$s_{vi} = e_{vi} + \sigma_{vi} \tag{66}$$

with the integral variable $\sigma_{vi} \in R$. Then from (65) and (66) it follows

$$\dot{s}_{vi} = f_{vi}(\mathbf{x}_i, \mathbf{i}_i) + b_{vi} v_{fi,0} + b_{vi} v_{fi,1} + g_{vi}(\mathbf{x}_i, \mathbf{i}_i, T_{mi}) + \dot{\sigma}_{vi} \tag{67}$$

Choosing

$$\dot{\sigma}_{vi} = -f_{vi}(\mathbf{x}_i, \mathbf{i}_i) - b_{vi} v_{fi,0}, \quad \sigma_{vi}(0) = -e_{vi}(0)$$

results in

$$\dot{s}_{vi} = b_{vi} v_{fi,1} + g_{vi}(\mathbf{x}_i, \mathbf{i}_i, T_{mi}) \tag{68}$$

Select $v_{fi,1}$ in (68) as

$$v_{fi,1} = -\rho_{2i}\, sign(s_{vi}), \ \rho_{2i} > 0 \,. \tag{69}$$

From (68), under the condition $\rho_{2i} > \left| b_{vi}^{-1} g_{vi}(\mathbf{x}_i, \mathbf{i}_i, T_{mi}) \right|$ a sliding mode is enforced on the manifold $s_{vi} = 0$ (66) from the initial time instant $t = 0$. The equivalent control

$$v_{fi,1eq} = -b_{vi}^{-1} g_{vi}(\mathbf{x}_i, \mathbf{i}_i, T_{mi})$$

calculated as a solution of $\dot{s}_{vi} = 0$ (67), compensates exactly the perturbation term $g_{vi}(\mathbf{x}_i, \mathbf{i}_i, T_{mi})$ in (63) (Utkin et al., 1999), and the sliding mode motion is described by the unperturbed system

$$\dot{e}_{vi} = f_{vi}(\mathbf{x}_i, \mathbf{i}_i) + b_{vi} v_{fi,0} \,. \tag{70}$$

Now, it is necessary to achieve the terminal voltage regulation, i. e. the control input $v_{fi,0}$ in (70) is selected of the form

$$v_{fi,0} = -k_g\, sign(e_{vi}) \tag{71}$$

From (70) and (71), we have

$$\dot{e}_{vi} = f_{vi}(\mathbf{x}_i, \mathbf{i}_i) - k_g b_{vi} sign\left(e_{vi}\right). \tag{72}$$

Then, under the condition

$$k_g > \left| b_{vi}^{-1} f_{vi}(\mathbf{x}_i, \mathbf{i}_i) \right| \tag{73}$$

the terminal voltage control error e_{vi} tends to zero in a finite time (Utkin et al., 1999).

4.3 Control logic

There are two control objectives: the rotor speed stabilization and the terminal voltage regulation for each generator in the EPS. However, only one control input is available, the excitation voltage v_{fi}. Then, the following control logic is proposed:

$$v_{fi} = \begin{cases} -k_{gi} sign(s_{\omega i}), & if \quad |s_{\omega i}| > \beta_i \\ -k_g sign\left(e_{vi}\right) - \rho_{2i} sign(s_{vi}), & if \quad |s_{\omega i}| \le \beta_i \end{cases}, \quad \beta_i = \begin{cases} \beta_{1i} & if \quad |\beta_{vi}| > \beta_{3i} \\ \beta_{2i} & if \quad |\beta_{vi}| \le \beta_{3i} \end{cases} \tag{74}$$

with $\beta_{2i} < \beta_{1i}$. Basically, a hierarchical control action through the proposed logic (74) is presented. First, the mechanical dynamics is stabilized by means of the ISMSS, yielding the stabilization of the speed switching manifold $s_{\omega i}$. When $s_{\omega i}$ reaches to a region defined by β_{1i}, the control resources are dedicated to stabilize the terminal voltage error β_{vi}. After the convergence of β_{vi} such that $|\beta_{vi}| \le \beta_{3i}$, the control logic reduces the $s_{\omega i}$ boundary layer width from β_{1i} to β_{2i}. Thus, the controller maintains the value of $s_{\omega i}$ within desired accuracy $|s_{\omega i}| \le \beta_{2i}$ and $|e_{vi}| \le \beta_{3i}$. Figure 1 shows the schematic diagram of the proposed controller.

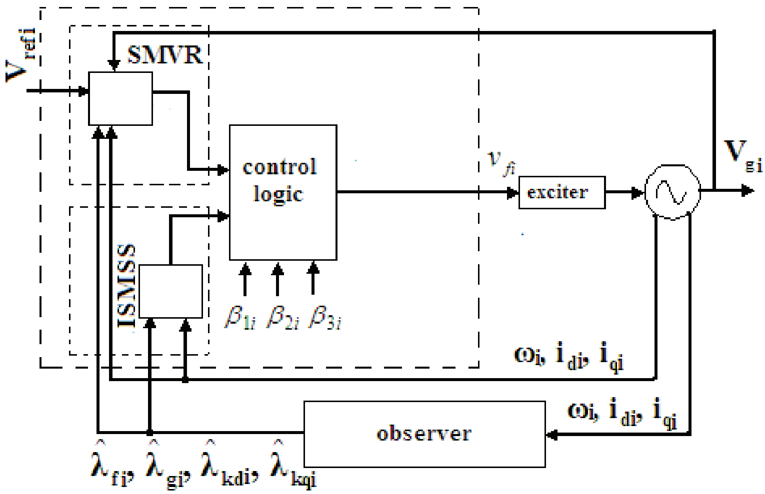

Figure 1. Proposed controller schematic diagram

4.4 EPS observer

Since the control scheme (74) needs the values of the rotor fluxes, it is neccesary to design a observer for the EPS. Assume that the power angle, x_{1i}, rotor speed, x_{2i} and stator currents i_{di} and i_{qi} can be measured.

The rotor fluxes x_{3i}, x_{4i}, x_{5i} and x_{6i} can be estimated by means of the following observer:

$$\begin{bmatrix} \dot{\hat{x}}_{3i} \\ \dot{\hat{x}}_{4i} \\ \dot{\hat{x}}_{5i} \\ \dot{\hat{x}}_{6i} \end{bmatrix} = \begin{bmatrix} b_{i1}\hat{x}_{3i} + b_{i2}\hat{x}_{5i} + b_{i3}i_{di} \\ c_{i1}\hat{x}_{4i} + c_{i2}\hat{x}_{6i} + c_{i3}i_{qi} \\ d_{i1}\hat{x}_{3i} + d_{i2}\hat{x}_{5i} + d_{i3}i_{di} \\ r_{i1}\hat{x}_{4i} + r_{i2}\hat{x}_{6i} + r_{i3}i_{qi} \end{bmatrix} + \begin{bmatrix} b_{i4} \\ 0 \\ 0 \\ 0 \end{bmatrix} v_{fi} \tag{75}$$

where $\hat{\mathbf{x}}_i = [\hat{x}_{3i},\ \hat{x}_{4i}, \hat{x}_{5i},\ \hat{x}_{6i}]^T$ are the estimate of the rotor fluxes. The convergence of the observer (75) can be analyzed by the error dynamics obtained from (75) and (6), given by the linear system:

$$\dot{\mathbf{e}}_i = \mathbf{A}_{0i} \tag{76}$$

with $\mathbf{e}_i = [e_{3i},\ldots,e_{6i}]$, $e_{ji} = x_{ji} - \hat{x}_{ji}$, $j = 3,\ldots,6$, $\mathbf{A}_{0i} = \begin{bmatrix} b_{i1} & 0 & b_{i2} & 0 \\ 0 & c_{i1} & 0 & c_{i2} \\ d_{i1} & 0 & d_{i2} & 0 \\ 0 & r_{4i} & 0 & r_{i2} \end{bmatrix}$.

The eigenvalues of the matrix $\mathbf{A}_{0i}$ calculated as

$$p_{1,2i} = \frac{1}{2}(c_{i1} + r_{i2}) \pm \frac{1}{2}\sqrt{c_{i1}{}^2 + r_{i2}{}^2 - 2c_{i1}r_{i2} + 4c_{i2}r_{i1}},$$
$$p_{3,4i} = \frac{1}{2}(b_{i1} + d_{i2}) \pm \frac{1}{2}\sqrt{b_{i1}{}^2 + d_{i2}{}^2 - 2b_{i1}d_{i2} + 4b_{i2}d_{i1}}$$

are real and negative. Therefore, the solution of the subsystem (76) is exponentially stable. The resulting estimates rotor fluxes are employed in the control logic (74) instead of the real variables.

5. Simulations results

The proposed control algorithm was tested on the equivalent model of the WSCC, (Western System Coordinating Council, Nine buses, three generators, three loads), fig. 2, (Anderson & Fouad, 1994). The parameters of the generators and network used in the simulation were taken from (Anderson & Fouad, 1994) (see *Appendix*).

Figures 3-8 depict results under four different events:

a. at t = 1 s, experienced a pulse 0.5 p.u. for 1 s in the generator 2,
b. at t = 4 s until t = 4.15 s, a three-phase short circuit is simulated in the terminals of generator 1,
c. at t = 10 s, a three-phase short circuit during 150 *ms* is applied in the line 5-7 (see fig. 2); the fault is cleared by opening the line, and

d. at *t=15 s*, it was introduced a parametric variations, by incrementing up to 25% the parameters L_{mi} in the generators.

Figures 3 and 5 show the relative angles and speed response of the close-loop system, respectively with a type I excitation system with PSS (Anderson & Fouad, 1994, EPRI, 1977). Figure 8 show the proposed observer converge in spite of perturbations.
Figures 4-7 reveal some important aspects:

1. The state variables fastly reach a steady state condition after small and large disturbances, showing the robust stability of the closed-loop system.
2. The controller is able to improve both, the power system stabilization and the post-fault terminal voltage regulation.

Comparing the transient speed response of the generators in case of ISMSS /SMVR and AVR/ PSS controllers shown in Figures 6 and 5 respectively, we have some important observations:

1. The traditional AVR/PSS stabilizes the system. However, the transient response of the classical controller is more oscillatory than the response given by the proposed nonlinear ISMSS /SMVR one since the latter adds significantly better damping in the power oscillations. It is possible to observe that the overshoot and settling time are reduced as well.
2. The performance of the ISMSS /SMVR is robust under different operating conditions. Figures 4 and 6 show clearly that the robustness of the controller under generators parameters variations and changes on the network configuration, such as disconnection of lines and incrementing and /or decrementing of loads. Thus the performance of the proposed ISMSS /SMVR controller tends to be unaffected.
3. Since the ISMSS /SMVR adds additional damping, the transient response controller is better compared to other ones (see for instance (Ahmed at al., 1996)). With the ISMSS /SMVR, the settling time is lesser and the overshot is shorter than the shown by the suboptimal robust controller presented in (Ahmed at al., 1996).

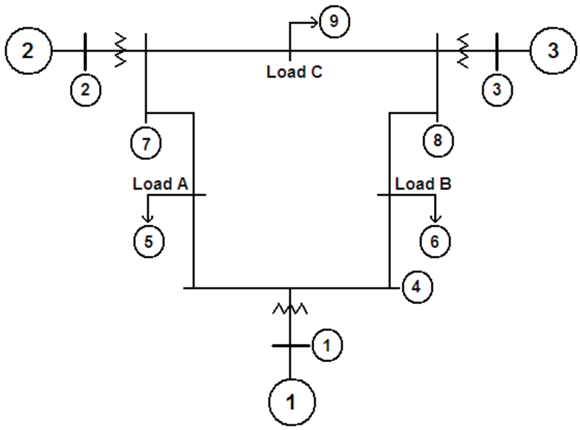

Figure 2. WSCC diagram

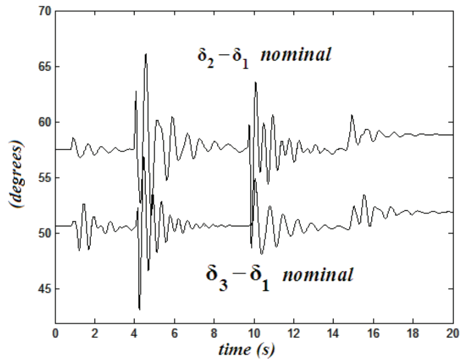

Figure 3. Relative angles response with classical control

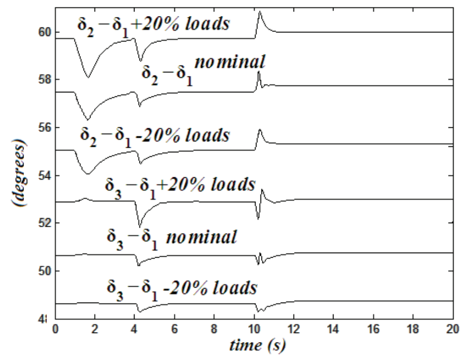

Figure 4. Relative angles response with the proposed controller

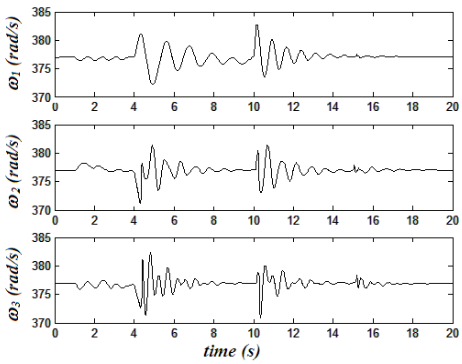

Figure 5. Speed of the three generators response with classical control

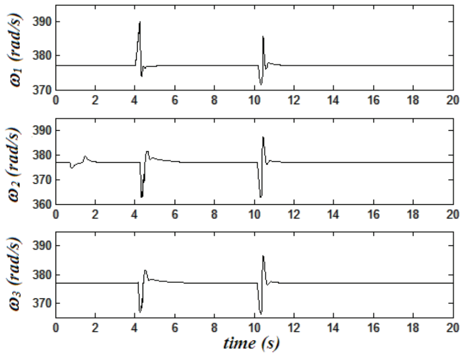

Figure 6. Speed of the three generators response with the proposed controller

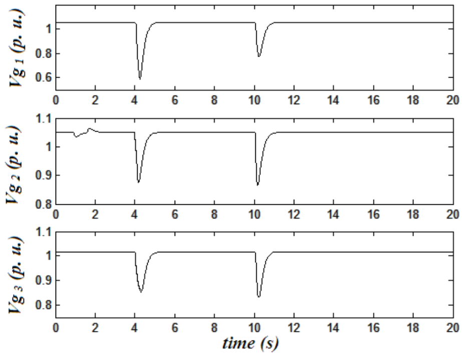

Figure 7. Terminal voltage of the three generators response with the proposed controller

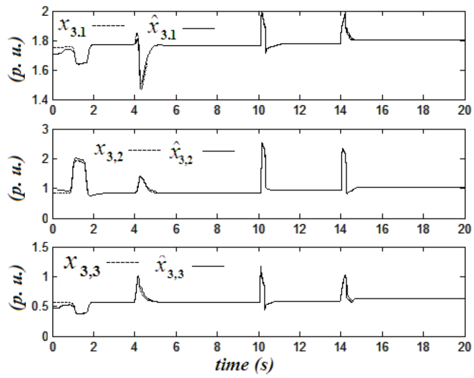

Figure 8. Field flux of the three generators response

6. Conclusions

The ISM with block control technique as a novel nonlinear control technique for the class of nonlinear systems presented in the NBC form was presented. The control methodology was explained step-by-step, and the stability conditions were found for each step. The ISM technique is robust under unknown but bounded matched and/or unmatched perturbations.
Then, in order to test the effectiveness of the ISM technique, a controller for EPS was designed. A plant model used for control is fully detailed nonlinear, and this model takes into account all interactions in power system between the electrical and mechanical dynamics and load constraints. With the proposed control scheme, the only local information is required. The stability analysis of the closed-loop EPS controller, including an observer was carried out. The designed ISMSS/SMVR was tested through simulation under the most important perturbations in the EPS:

1. Variation of the mechanical torque.
2. Large fault (a 150 ms short circuit).
3. Loads variations.
4. Generator parameter variations.

The simulation results show that the sliding mode controller with the proposed logic is able to achieve the mechanical dynamics and the generator terminal voltages robust stability under small and large disturbances.
The proposed performance of the nonlinear ISMSS/ SMVR control system (74) is independent from the operating point of the system. It is important to note that the proposed nonlinear control scheme ensures cancellation of the interactions between the subsystems provided an additional damping with respect to classical controllers.

7. References

Abidi, K. & Šabanovic, A., (2007). Sliding-mode control for high-precision motion of a piezostage, *IEEE Trans. on Industrial Electronics*, vol. 54, no. 1, pp. 629-637, 2007.

Adhami-Mirhosseini, A. & Yazdanpanah, M. J., (2005). Robust Tracking of perturbed systems by nested sliding mode control. *Proc. of ICCA2005*, Budapest, Hungary, June 2005.

Aggoune, M. E., Boudjeman, F., Bensenouci, A., Hellal, A., Elmesai, M.R., & Vadari, S.V., (1994). Design of Variable Structure Voltage Regulator Using Pole Assignment Technique, *IEEE Transaction on Automatic Control*, Vol. 39, No. 10, October 1994.

Ahmed, S. S., Chen, L. and Petroianu, A., (1996), *Design of Suboptimal H∞ Excitation Controller*, IEEE Trans. on Power Systems, Vol. 11, No. 1, February, 1996.

Akhkrif, O., Okou, F., Dessaint, L., & Champagne, R., (1999). Application of Multivariable Feedback Linearization Scheme for Rotor Angle Stability and Voltage Regulation of Power System, *IEEE Trans. Power Syst.*, Vol.14, No.2, pp.620-628, 1999.

Anderson, P. M., & Fouad, A., (1994). *Power System Control and Stability*, IEEE Press New York, 1994.

Bandal, V., Bandyopadhyay, B., & Kulkarni, A. M., (2005). Decentralized Sliding Mode Control Technique Based Power System Stabilizer (PSS) for Multimachine Power System, *Proc. Conference on Control Applications*, Toronto, Canada, August, 2005.

Dash, P., Sahoo, N., Elangovan, S., & Liew, A., (1996). Sliding Mode Control of a Static Controller for Synchronous Generator Stabilization, *Electrical Power & Energy Systems*, Vol. 18, pp. 55-64, 1996.

DeMello, F. P. & Concordia, C., (1969). Concepts of Synchronous Machine Stability as Affected by Excitation Control, *IEEE Trans., PAS-88*, Apr. 1969, 316-329.

Djukanovic, M., Khammash, M. and Vittal, V. (1998a), *Application of the structured value theory for robust stability and control analysis in multimachine power systems, Part I: Framework development*, IEEE, Trans. on Power Systems, Vol. 13, No. 4, November 1998.

Djukanovic, M., Khammash, M. and Vittal, V. (1998b), *Application of the structured value theory for robust stability and control analysis in multimachine power systems, Part II: Numerical simulations and results*, IEEE, Trans. on Power Systems, Vol. 13, No. 4, November 1998.

EPRI report, (1977). *Power System Dynamic Analysis Phase I*, EPRI EL-484, Project 670-1, July 1977

Huerta-Avila, H. (2005). *Control no lineal robusto de sistemas eléctricos de gran escala por modos deslizante,* M. Sc. Thesis, Scientific advisors: A. G. Loukianov and J. M. Cañedo, CINVESTAV, Unidad Guadalajara, México, September 2005.

Huerta-Avila, H., Loukianov, A. G., & Cañedo, J. M. (2007a). Nested Integral Sliding Mode Control of Multimachine Power Systems, *Proc. of SSSC07*, Iguazu, Brazil, October 2007.

Huerta-Avila, H., Loukianov, A. G., & Cañedo, J. M. (2007b). Nested Integral Sliding Mode Control of Large-Scale Power Systems, *Proc. of CDC07*, New Orleans, EUA, December 2007.

Jung, K., Kim, K., Yoon, T. & Jang, G. (2005). Decentralized Control for Multimachine Power Systems with Nonlinear Interconnections and Disturbances, *International Journal of Control, Automation, and Systems,* Vol 3, No. 2 (especial edition), pp. 270-277, June 2005.

Khalil, H. K., (1996). Nonlinear systems, Prentice Hall, Inc. Simon and Schuster, New Jersey, 1996.

King, C. A., Chapman, J. W. & Ilic, M. D., (1994). *Feedback linearizing excitation control on a full scale power system model,* IEEE Trans. Power Systems, 9, 1102-1109, 1994.

Kshatriya, N., Annakkage, U. D., Gole, A. M. & Fernando, I. T., (2005). Improving the Accuracy of Normal Forma Analysis, *IEEE Trans. on Power Systems*, Vol. 20, No. 1, February 2005.

Liu, S., Messina, A. R., & Vittal, V., (2006). A Normal Form Analysis Approach to Siting Power System Stabilizers (PSSs) and Assesing Power System Nonlinear Behavior, *IEEE Trans. on Power Systems*, Vol. 21, No. 4, November 2006.

Loukianov, A.G., (1998), Nonlinear Block Control with Sliding Mode, *Automation and Remote Control*, Vol.59, No.7, pp. 916-933, 1998.

Loukianov, A. G., Cañedo, J. M., Utkin, V. I. & Cabrera-Vázquez, J., (2004). Discontinuos Controller for Power Systems: Sliding-Mode Block Control Approach, *Trans. on Industrial Electronics*, Vol., No. 51, No. 2, April 2004, pp. 340-353.

Loukianov, A, G., Cañedo, J. M., & Huerta, H., (2006) *Decentralized Sliding Mode Block Control of Power Systems,* Proc. of PES General meeting 2006, Montreal, Quebec, Canada, June, 2006.

Machowsky, J., Robak, S., Bialek, J. W., Bumby, J. R., & Abi-Samra, N., (2000). Decentralized Stability-Enhancing Control of Synchronous Generator, *IEEE Transactions on Power Systems*, Vol. 15, No. 4, November 2000.

Mohagheghi, S., Valle, Y., Venayagamoorthy, G. K., & Harley, R. G., (2007). *A proportional-integrator type adaptive critic design-based neurocontroller for a static compensator in a multimachine power system*, IEEE, Trans. On Industrial Electronics, Vol. 54, No. 1, February, 2007.

Topalov, A.V., Cascella, G.L., Giordano, V., Cupertino, F., & Kaynak, O., (2007). Sliding mode neuro-adaptive control of electric drives, *IEEE Trans. on Industrial Electronics*, vol. 54, no. 1, pp. 671-679, 2007.

Utkin, V. I., Guldner, J., & Shi, J., (1999). Sliding Mode Control in Electromechanical Systems, Taylor & Francis, London, 1999.

Venayagamoorthy, G. K., Harley, R. G., & Wunsch, D. C., (2003). Dual Heuristic Programming Excitation Neruocontrol for Generators in a Multimachine Power System, *IEEE Trans on Industry Applications*, Vol. 39, No. 2, March/April 2003.

Wang, Y., Hill, D. J., & Guo, G., (1998). Robust Decentralized Control for Multimachine Power Systems, *IEEE Trans on Circuits and Systems-I:Fundamental Theory and Applications*, Vol. 45, No. 3, March 1998, pp 271-279..

Wu, B. & Malik, P., (2006). Multivariable Adaptive Control of Synchronous Machines in a Multimachine Power System, *IEEE Trans on Power Systems*, Vol. 21, No. 4, November 2006.

Xie, W., (2007). Sliding-mode-observer-based adaptive control for servo actuator with friction, *IEEE Trans. on Industrial Electronics*, vol. 54, no. 3, pp. 1517-1527, 2007.

Yildiz, Y., Šabanovic, A., & Abidi, K., (2007). Sliding mode neuro-controller for uncertain systems, *IEEE Trans. on Industrial Electronics*, vol. 54, no. 3, pp. 1676-1685, 2007

Yousef, A. M. & Mohamed, M. A., (2004). Multimachine Power System Stabilizer Based on Efficient Two-Layered Fuzzy Logic Controller, *Transactions on Engineering and Technology V3*, December 2004, pp.137-140.

8. Appendix

8.1 Matrices used in generator model (1)

$$\mathbf{R} = diag\left[R_f \; R_g \; R_{kd} \; R_{kq} - R_s - R_s\right], \mathbf{L} = \begin{bmatrix} \mathbf{L}_{11} & \mathbf{L}_{12} \\ \mathbf{L}_{21} & \mathbf{L}_{22} \end{bmatrix}, \mathbf{W}(\omega) = \begin{bmatrix} 0 & 0 \\ 0 & I(\omega) \end{bmatrix} \in R^{6\times 6},$$

$$I(\omega) = \begin{bmatrix} 0 & -\omega \\ \omega & 0 \end{bmatrix}, \begin{bmatrix} \mathbf{L}_{11} & \mathbf{L}_{12} \\ \mathbf{L}_{21} & \mathbf{L}_{22} \end{bmatrix} = \begin{bmatrix} \begin{pmatrix} L_f & 0 & L_{md} & 0 \\ 0 & L_g & 0 & L_{mq} \\ L_{md} & 0 & L_{kd} & 0 \\ 0 & L_{mq} & 0 & L_{kq} \end{pmatrix} & \begin{pmatrix} -L_{md} & 0 \\ 0 & -L_{mq} \\ -L_{md} & 0 \\ 0 & -L_{mq} \end{pmatrix} \\ \begin{pmatrix} L_{md} & 0 & L_{md} & 0 \\ 0 & L_{mq} & 0 & L_{mq} \end{pmatrix} & \begin{pmatrix} -L_d & 0 \\ 0 & -L_q \end{pmatrix} \end{bmatrix}.$$

L_d and L_q are the direct-axis and quadrature-axis self-inductances, L_f is the field self-inductance, L_g, L_{kd} and L_{kq} are the damper windings self-inductances, L_{md} and L_{mq} are the direct-axis and quadrature-axis magnetizing inductances

$\mathbf{T}=\begin{bmatrix}\mathbf{I}_4 & 0\\ \mathbf{T}_{21} & \mathbf{T}_{22}\end{bmatrix}$, $\begin{array}{l}\mathbf{T}_{21}=-[\mathbf{I}_2-\mathbf{L}_{22}^{-1}\mathbf{L}_{21}\mathbf{L}_{11}^{-1}\mathbf{L}_{12}]^{-1}\mathbf{L}_{22}^{-1}\mathbf{L}_{21}\mathbf{L}_{11}^{-1},\\ \mathbf{T}_{22}=-[\mathbf{I}_2-\mathbf{L}_{22}^{-1}\mathbf{L}_{21}\mathbf{L}_{11}^{-1}\mathbf{L}_{12}]^{-1}\mathbf{L}_{22}^{-1},\end{array}$, $\mathbf{I}_2$ and $\mathbf{I}_4$ are identity matrices of dimension 2 and 4, respectively.

8.2 Generators parameters

$$a_{i1}=\frac{L''_{di}-l_{ai}}{l_{fi}},a_{i2}=-\frac{L''_{qi}-l_{ai}}{l_{gi}},a_{i3}=\frac{L''_{di}-l_{ai}}{l_{kdi}},\ a_{i4}=-\frac{L''_{qi}-l_{ai}}{l_{kqi}},\ a_{i5}=L''_{qi}-L''_{di},$$

$$b_{i1}=-\frac{1}{\tau'_{d0i}}\left(1+L_{mdi}\frac{L''_{di}-l_{ai}}{l_{kdi}l_{fi}}\right),b_{i2}=\frac{L_{mdi}}{\tau'_{d0i}}\frac{L''_{di}-l_{ai}}{(L'_{di}-l_{ai})l_{kdi}},\ b_{i3}=-\frac{L_{mdi}}{\tau'_{d0i}}\frac{L''_{di}-l_{ai}}{L'_{di}-l_{ai}},\ b_{i4}=\omega_s,$$

$$c_{i1}=-\frac{1}{\tau'_{q0i}}\left(1+\frac{L''_{qi}-l_{ai}}{l_{kqi}l_{gi}}L_{mqi}\right),c_{i2}=\frac{L''_{q}-l_{a}}{\left(L'_{q}-l_{a}\right)l_{kq}}\frac{L_{mq}}{\tau'_{q0}},c_{i3}=-\frac{L_{mqi}}{\tau'_{q0i}}\left(\frac{L''_{qi}-l_{ai}}{L'_{qi}-l_{ai}}\right),d_{i1}=\frac{L'_{di}-l_{ai}}{\tau''_{d0i}l_{fi}},$$

$$d_{i2}=-\frac{1}{\tau''_{d0i}},d_{i3}=-\frac{L'_{di}-l_{ai}}{\tau''_{d0i}},r_{i1}=\frac{L'_{qi}-l_{ai}}{\tau''_{q0i}l_{gi}},\ r_{i2}=-\frac{1}{\tau''_{q0i}},r_{i3}=-\frac{L'_{qi}-l_{ai}}{\tau''_{q0i}},h_{i1}=-\frac{\omega_s}{L''_{di}},$$

$$h_{i2}=-\frac{1}{L''_{di}\tau'_{d0i}}\left(1+L_{mdi}\frac{L'_{di}-l_{ai}}{l_{fi}l_{kdi}}\right)\frac{L'_{di}-l_{ai}}{l_{fi}}+\frac{1}{L''_{di}\tau''_{d0i}}\frac{L''_{di}-l_{ai}}{L''_{di}l_{kdi}}\frac{L'_{di}-l_{ai}}{l_{fi}},\ h_{i4}=-\frac{1}{L''_{di}}\frac{L''_{qi}-l_{ai}}{l_{gi}},$$

$$h_{i5}=-\frac{L''_{qi}-l_{ai}}{L''_{di}l_{kqi}},h_{i3}=\frac{L_{mdi}}{L''_{di}\tau'_{d0i}}\frac{L''_{di}-l_{ai}}{\left(L'_{di}-l_{ai}\right)l_{kdi}}\frac{L''_{di}-l_{ai}}{l_{fi}}-\frac{1}{L''_{di}\tau''_{d0i}}\frac{L''_{di}-l_{ai}}{L''_{di}l_{kdi}},\ h_{i6}=\frac{L''_{qi}}{L''_{di}},\ h_{i8}=\frac{\omega_s(L''_{di}-l_{ai})}{L''_{di}l_{fi}},$$

$$k_{i1}=-\frac{\omega_s}{L''_{di}},\ h_{i7}=-\frac{\omega_s r_{ai}}{L''_{di}}-\frac{L_{mdi}}{L''_{di}\tau'_{d0i}}\frac{L''_{di}-l_{ai}}{l_{fi}}\frac{L'_{di}-l_{ai}}{l_{fi}}\frac{L''_{di}-l_{ai}}{L'_{di}-l_{ai}}-\frac{\left(L'_{di}-l_{ai}\right)}{L''_{di}\tau'_{d0i}}\frac{L''_{di}-l_{ai}}{L''_{di}l_{kdi}},$$

$$k_{i4}=-\frac{1}{L''_{qi}}\frac{L''_{qi}-l_{ai}}{l_{gi}}\frac{L'_{qi}-l_{ai}}{l_{fi}},k_{i2}=\frac{L_{mqi}}{L''_{qi}\tau'_{q0i}}\frac{L''_{qi}-l_{ai}}{\left(L'_{qi}-l_{ai}\right)l_{kqi}}\frac{L''_{qi}-l_{ai}}{l_{gi}}-\frac{1}{L''_{qi}\tau''_{q0i}}\frac{L''_{qi}-l_{ai}}{L''_{qi}l_{kdi}},$$

$$k_{i5}=-\frac{1}{L''_{qi}}\frac{L''_{qi}-l_{ai}}{L''_{qi}l_{kdi}},k_{i6}=\frac{L''_{di}}{L''_{qi}},$$

$$k_{i3}=-\frac{\omega_s r_{ai}}{L''_{qi}}-\frac{L_{mqi}}{L''_{qi}\tau'_{q0i}}\frac{L''_{qi}-l_{ai}}{l_{gi}}\frac{L'_{qi}-l_{ai}}{l_{gi}}\frac{L''_{qi}-l_{ai}}{L'_{qi}-l_{ai}}-\frac{1}{L''_{qi}\tau'_{q0i}}\left(L'_{qi}-l_{ai}\right)\frac{L''_{qi}-l_{ai}}{L''_{qi}l_{kdi}},$$

$$k_{i7}=-\frac{1}{L''_{qi}\tau'_{q0i}}\left(1+L_{mqi}\frac{L'_{qi}-l_{ai}}{l_{gi}l_{kqi}}\right)\frac{L'_{qi}-l_{ai}}{l_{gi}}+\frac{1}{L''_{qi}\tau''_{q0i}}\frac{L''_{qi}-l_{ai}}{L''_{qi}l_{kdi}}\frac{L'_{qi}-l_{ai}}{l_{gi}}.$$

Generator	1	2	3
MVA	247.5	192.0	128.0
kV	16.5	18.0	13.8
P.F.	1.0	0.85	0.85
Type	Hydro	Steam	Steam
Speed	180 r/min	3600 r/min	3600 r/min
X_d	0.1460	0.8958	1.3125
X_q	0.0969	0.8645	1.2587
X_d'	0.0608	0.1198	0.1813
X_q'	0.0969	0.1969	0.2500
τ_{d0}'	8.9600	6.0000	5.8900
τ_{q0}'	0.0000	0.5350	0.6000
X_d''	0.0400	0.0600	0.0800
X_q''	0.0400	0.0600	0.0800
τ_{d0}''	0.2000	0.3000	0.4000
τ_{q0}''	0.2000	0.3000	0.4000
X_l	0.0336	0.0521	0.0742
r_a	0.0000	0.0000	0.0000
H	23.6400	6.4000	3.0100

Table 1. Parameters of generator model (6)-(7)

	Gen. 1	Gen. 2	Gen. 3		Gen. 1	Gen. 2	Gen. 3
a_1	0.1003	0.1644	0.0945	e_3	-5.000	-4.0	-2.5
a_2	1.13	1.1787	0.9458	h_1	-1256	-9424	-4712
a_3	0.0403	0.0119	0.0203	h_2	273.4	863.6	141.3
a_4	1.2552	1.0145	1.0239	h_3	0.5	-6.6	3.2
a_5	0.020	0.01	0.010	h_4	-31	-50.2	-16.4
b_1	-0.017	-0.0251	-0.0114	h_5	18.8	97.1	29.7
b_2	0.522	2.4483	1.8567	h_6	-0.1	-0.3	-0.3
b_3	-0.5075	-2.4185	-1.8659	h_7	-4.2	-25.4	-12.8
b_4	376.991	376.991	376.991	h_8	0.1	1.3	0.9
c_1	-0.07	-0.022	-0.0472	k_1	-1885	-7539	-5385
c_2	0.6453	10.6390	11.4979	k_2	1.7	11.8	6.4
c_3	-0.5348	-10.611	-11.4581	k_3	5.1	6.9	34.5
d_1	0.1360	-0.2257	0.2267	k_4	31.5	8.37	39.9
d_2	-3.79	-3.0659	-2.2838	k_5	0.5	3.3	0.7
d_3	-3.33	-3.333	-2.5	k_6	-5.7	-23.6	-13.5
e_1	0.2665	0.5792	0.4395	k_7	-0.1	-0.8	-1.1
e_2	-0.7899	-3.2871	-2.1290				

Table 2. Generators parameters

	Gen. 1	Gen. 2	Gen. 3		Gen. 1	Gen. 2	Gen. 3
a_1	0.2175	0.0916	0.03	e_3	-5.000	-4.0	-2.5
a_2	1.1324	1.1787	0.9458	h_1	-1256	-9424	-4712
a_3	0.0403	0.0119	0.0203	h_2	126.1	1549	233.1
a_4	1.2552	1.0145	1.0239	h_3	5	-6.8	3.2
a_5	0.020	0.010	0.010	h_4	-14.5	-100.3	-25.8
b_1	-0.003	-0.005	-0.0023	h_5	19	108.3	28.4
b_2	0.1044	0.4897	0.3713	h_6	-0.1	-0.3	-0.3
b_3	-0.0601	-0.0844	-0.0358	h_7	-3.2	-25.4	-12.8
b_4	376.991	376.991	376.991	h_8	1	1.3	0.9
c_1	-0.07	-0.022	-0.0472	k_1	-1885	-7539	-5385
c_2	0.6453	10.6390	11.4979	k_2	1.7	11.8	6.4
c_3	-0.5348	-10.611	-11.4581	k_3	5.1	69.2	34.5
d_1	0.1360	-0.2257	0.2267	k_4	31.5	83.7	39.9
d_2	-8.2182	-1.7090	-1.3842	k_5	1.1	1.8	0.4
d_3	-5.0	-3.333	-2.5	k_6	-5.7	-23.6	-13.5
e_1	0.2665	0.5792	0.4395	k_7	-0.1	-0.8	-1.1
e_2	-0.7899	-3.2871	-2.1290				

Table 3. Perturbed generators parameters

	Generator 1	Generator 2	Generator 3
k_{gi}	0.02	0.02	0.03
k_{0i}	7.5	5	6
ρ_{2i}	8	10	9
e_1	0.9	0.8	1.2
e_2	0.01	0.03	0.02
e_3	0.001	0.002	0.001

Table 4. Controllers parameters

8.3 Functions used in controllers design

$$f_{vi}(\mathbf{x}_i,\mathbf{i}_i)=v_{di}(\mathbf{x}_i,\mathbf{i}_i)\varphi_{1i}(\mathbf{x}_i,\mathbf{i}_i)+v_{qi}(\mathbf{x}_i,\mathbf{i}_i)\varphi_{2i}(\mathbf{x}_i,\mathbf{i}_i),\ b_{vi}=\left(h_{i2}b_{i4}+\frac{1}{k_{i1}}k_{i4}b_{i4}x_{2i}\right),$$

$$\varphi_{1i}(\mathbf{x}_i,\mathbf{i}_i)=-\frac{1}{h_{i1}}\left[\begin{array}{l}h_{i2}\left(b_{i1}x_{3i}+b_{i2}x_{5i}+b_{i3}i_{di}\right)+h_{i3}\left(d_{i1}x_{3i}+d_{i2}x_{5i}+d_{i3}i_{1i}\right)+\\ h_{i4}\left(\begin{array}{l}x_{2i}\left(c_{i1}x_{4i}+c_{i2}x_{6i}+c_{i3}i_{2i}\right)+\\ \left(f_{\omega i}(\mathbf{x}_i,\mathbf{i}_i,T_{mi})-q_i(\mathbf{x}_i,\mathbf{i}_i)x_{3i}\right)x_{4i}\end{array}\right)+h_{i5}\left(\begin{array}{l}x_{2i}\left(r_{i1}x_{4i}+r_{i2}x_{6i}+r_{i3}i_{2i}\right)+\\ \left(f_{\omega i}(\mathbf{x}_i,\mathbf{i}_i,T_{mi})-q_i(\mathbf{x}_i,\mathbf{i}_i)x_{3i}\right)x_{6i}\end{array}\right)\end{array}\right],$$

$$\varphi_{2i}(\mathbf{x}_i,\mathbf{i}_i)=-\frac{1}{k_{i1}}\left[\begin{array}{l}k_{i2}\dot{x}_{4i}+k_{i3}\left(r_{i1}x_{4i}+r_{i2}x_{6i}+r_{i3}i_{2i}\right)+\\ k_{i4}\left(x_{2i}\left(b_{i1}x_{3i}+b_{i2}x_{5i}+b_{i3}i_{1i}\right)+\left(f_{\omega i}(\mathbf{x}_i,\mathbf{i}_i,T_{mi})-q_i(\mathbf{x}_i,\mathbf{i}_i)x_{3i}\right)x_{3i}\right)\\ +k_{i5}\left(x_{2i}\left(d_{i1}x_{3i}+d_{i2}x_{5i}+d_{i3}i_{1i}\right)+\left(f_{\omega i}(\mathbf{x}_i,\mathbf{i}_i,T_{mi})-q_i(\mathbf{x}_i,\mathbf{i}_i)x_{3i}\right)x_{5i}\right)\end{array}\right],$$

$$g_{vi}(\mathbf{x}_i,\mathbf{i}_i)=h_{i6}\frac{d}{dt}i_{di}+h_{i7}\left(x_{2i}\frac{d}{dt}i_{qi}+\dot{x}_{2i}i_{qi}\right)+k_{i6}\left(x_{2i}\frac{d}{dt}i_{di}+\dot{x}_{2i}\right)+k_{i7}\frac{d}{dt}i_{qi}+h_{i8}\frac{d}{dt}v_{fi}+\Delta f_{vi}.$$

5

Stability Analysis of Polynomials with Polynomic Uncertainty

Petr Hušek
Dept. of Control Engineering, Faculty of Electrical Engineering, Czech Technical University in Prague
Czech Republic

1. Introduction

When dealing with systems with parameter uncertainty most attention is paid to robustness analysis of linear time-invariant systems. In literature the most often investigated topic of analysis of linear time-invariant systems with parametric uncertainty is the problem of stability analysis of polynomials whose coefficients depend on uncertain parameters. The aim is to verify that all roots of such a polynomial are located in some prescribed set in complex plane or to find a bound within that uncertain parameters can vary from nominal ones preserving stability. The former problem is studied in this contribution.

The formulations of basic robustness problems and their first solutions for special cases are very old. For example, in the work (Neimark, 1949) some effective techniques for small number of parameters are presented. A powerful result concerning the stability analysis of polynomials with multilinear dependency of its coefficients is given in the book (Zadeh & Desoer, 1963). Also in Siljak's book (Siljak, 1969) special classes of robust stability analysis problems with parametric uncertainty are studied. Nevertheless, the starting point of an intensive interest in this area was the celebrated Kharitonov theorem (Kharitonov, 1978) dealing with interval polynomials. This elegant theorem with surprisingly simple result is considered as the biggest achievement in control theory in last century. When analysing stability of a polynomial with some dependency of its coefficients on interval parameters the solution becomes more complicated. The Edge theorem (Bartlett et al., 1988) claims that for linear (affine) dependency it is sufficient to check polynomials on exposed edges, the Mapping theorem (Zadeh & Desoer, 1963) provides a simplified sufficient stability condition for systems with multilinear parameter dependency.

To date there are only few results solving the problem of robust stability of polynomials with polynomic structure of coefficients (polynomic interval polynomials) that occur very often e.g. as characteristic polynomials in feedback control of uncertain plant with a fixed controller. None of the results is as elegant as those mentioned earlier. There are two basic approaches – algebraic and geometric. The first one is based on utilization of criteria commonly used for stability analysis of fixed polynomials – Hurwitz or Routh criterion – and their generalization for uncertain polynomials. The second one transforms the multidimensional problem in twodimensional test of frequency plot of the polynomial in

complex plane using zero exclusion principle. Very interesting algorithm using the latter approach is based on Bernstein expansion of a multivariate polynomial (Garloff, 1993).
In this chapter an algorithm for stability analysis of polynomials with polynomic parameter dependency based on geometric approach is presented. It consists in determination of a convex polygon overbounding the value set for each frequency and simple performance of the zero exclusion test. The method provides a sufficient stability condition for a continuous-time polynomial with polynomic coefficient dependency. An arbitrary stability region can be chosen.
The presented procedure is demonstrated and compared with the known results on benchmark example - control of Fiat Dedra engine corresponding to 7-th order polynomial with 7 uncertain parameters.

2. State of the art

There is no elegant result on robust stability of polynomic interval polynomial in comparison with interval, affine linear interval or multilinear interval polynomials. There are only few methods, which solve the problem, however almost all of them treat a little different problem and/or are applicable for polynomials dependent only on small number of parameters or polynomials of lower degree.
(De Gaston and Safonov, 1988) determine the stability margin of a multivariate feedback system with uncertainties entering independently into each feedback loop (which corresponds to multilinear parameter uncertainty) using the Mapping theorem. The box of uncertainties is iteratively splitted so that the value of stability margin is improved. The extension to the case of repeated parameters (polynomic parameter uncertainty) is due to (Sideris and de Gaston, 1986). A computational improvement of this method was done by (Sideris and Sanchez Pena, 1989). The algorithm is based on positivity testing of elements appearing in the first column of Routh table. This leads to determination of roots of multivariate polynomial which causes big numerical problems if the number of uncertain parameters and/or degree of the polynomial is even moderate. An improvement of the algorithm using frequency domain splitting is presented in (Chen & Zhou, 2003).
(Vicino et. al., 1990) suggested an algorithm for computing the stability margin in the l_∞ norm, i.e. the radius of the maximal ball in parameter space centered at a stable nominal point preserving stability, for uncertain systems affected by polynomially correlated perturbations. The original constrained nonlinear programming problem, which is generally nonconvex and may admit local extremes, is transformed into a signomial programming problem. An iterative procedure determining a sequence of lower and upper bounds converging to the global extreme is applied.
(Walter and Jaulin, 1994) characterize the set of all the values of the parameters of a linear time-invariant model that are associated with a stable behaviour. A formal Routh table is used to formulate the problem as one of set inversion, which is solved approximately but globally with tools borrowed from interval analysis.
(Kaesbauer, 1993) computes the stability radius for polynomic interval polynomial by solving a system of algebraic equations numerically using the Groebner basis. The method can be practically used up to five or six parameter case.
The most effective algorithm treating the problem of checking stability of polynomials with polynomic parameter uncertainty seems to be the one based on Bernstein expansion (Garloff, 1993) and its improvements (Garloff et al., 1997; Zettler & Garloff, 1998). The

procedure uses suitable properties of the Bernstein form of a multivariate polynomial and test stability by successive subdivision of the original parameter domain and checking positivity of a multivariate polynomial. It can be used in both algebraic (checking positivity of Hurwitz determinant) or geometric (testing the value set) approaches.
Conceptually the same approach is adopted by (Siljak and Stipanovic, 1999). They check robust stability by positivity test of the magnitude of frequency plot by searching minorizing polynomials and using Bernstein expansion. Methods of interval arithmetic are employed in (Malan et al., 1997). Solution of the problem using soft computing methods is presented in (Murdoch et al., 1991).

3. Backgrounds

At first let us introduce the basic terms and general results used in robust stability analysis of linear systems with parametric uncertainty.

DEFINITION 1 (Fixed polynomial) A polynomial $p(s)$ is said to be fixed polynomial of degree n, if

$$p(s)=\sum_{j=0}^{n}a_j s^j = a_n s^n + \cdots + a_1 s + a_0 \,. \tag{1}$$

DEFINITION 2 (Uncertain parameter) An l-dimensional column vector $\mathbf{q}=[q_1,\ldots,q_l]^T \in Q$ represents uncertain parameter. Q is called the uncertainty bounding set. In the whole work

$$Q=\left\{\mathbf{q}\in\Re^l : q_i^- \le q_i \le q_i^+ \ \text{ for } \ i=1,2,\ldots,l\right\}, \tag{2}$$

where $q_i^-, q_i^+,\ i=1,2,\ldots,l$ are the specified bounds for the i-th component q_i of $\mathbf{q}$. Such a Q is called a box.

DEFINITION 3 (Uncertain polynomial) A polynomial

$$p(s,\mathbf{q})=\sum_{j=0}^{n}a_j(\mathbf{q})s^j = a_n(\mathbf{q})s^n + \cdots + a_1(\mathbf{q})s + a_0(\mathbf{q});\ \mathbf{q}\in Q \,. \tag{3}$$

is called an uncertain polynomial.

DEFINITION 4 (Polynomic uncertainty structure) An uncertain polynomial (3) is said to have a polynomic uncertainty structure if each coefficient function $a_j(\mathbf{q})$, $j=0,\ldots,n$ is a multivariate polynomial in the components of $\mathbf{q}$.

DEFINITION 5 (Stability, Hurwitz stability) A fixed polynomial $p(s)$ is said to be stable if all its roots lie in the strict left half plane.

DEFINITION 6 (Robust stability) A given family of polynomials $P=\{p(\cdot,\mathbf{q}):\mathbf{q}\in Q\}$ is said to be robustly stable if, for all $\mathbf{q}\in Q$, $p(s,\mathbf{q})$ is stable; that is, for all $\mathbf{q}\in Q$, all roots of $p(s,\mathbf{q})$ lie in the strict left half plane.

THEOREM 1 (Zero exclusion principle)
The family of polynomials P mentioned above of invariant degree is robustly stable if and only if

a. there exists a stable polynomial $p(s,\mathbf{q})\in P$
b. $0\notin p(j\omega,\mathbf{q})$ for all $\omega\ge 0$ ♣

The set $p(j\omega,\mathbf{q})$ for any $\omega > 0$ is called the value set.

The Zero exclusion principle can be used to derive computational procedures for robust stability problems of interval polynomials and polynomials with affine linear, multilinear and polynomic uncertainty. Moreover, for more complicated uncertainty structures where no theoretical results are available the graphical test of zero exclusion can be applied. One can take many points of uncertainty set Q, plot the corresponding value sets and visually test if zero is excluded from all of them. The main problem consists in the choice of "sampling" density in some direction of an l-dimensional uncertain parameter $\mathbf{q}$ especially for high values of l.

4. Polynomials with quadratic parametric uncertainty

An efficient method analyzing robust stability of polynomials with uncertain coefficients being quadratic functions of interval parameters is presented in this section. A sufficient condition is derived by overbounding the (generally nonconvex) value set by a convex hull (polygon) for an arbitrary point in the complex plane lying on the boundary of chosen stability region and by determination whether zero is excluded from or included in this polygon. This test can be done either in computational or in graphical way. Profiting from appropriate properties of presented procedure the former is recommended especially for high number of parameters. This method can be used in principle for polynomials where the coefficients are arbitrary polynomic functions, which is shown in section 5.

4.1 Basic concept

Let us consider a polynomic interval family of polynomials

$$P(s,\mathbf{q}) = c_n(\mathbf{q})s^n + \cdots + c_1(\mathbf{q})s + c_0(\mathbf{q}),\ \mathbf{q} \in Q \subset \Re^l,\ \mathbf{q} = [q_1,\ldots,q_l]^T$$

$$Q = [q_1^-, q_1^+] \times \cdots \times [q_l^-, q_l^+],\ q_i \in [q_i^-, q_i^+],\ q_i^- < q_i^+,\ i = 1,\ldots,l\,. \tag{4}$$

Let us suppose that each coefficient $c_k(\mathbf{q})$, $k = 0,\ldots,n$ can be expressed as

$$c_k(\mathbf{q}) = \mathbf{q}^T \mathbf{B}^{(k)} \mathbf{q} + \left(\mathbf{d}^{(k)}\right)^T \mathbf{q} + v^{(k)},\ \mathbf{B}^{(k)} \in \Re^{l,l},\ \mathbf{d}^{(k)} \in \Re^l,\ v^{(k)} \in \Re,\ k = 0,\ldots,n\,. \tag{5}$$

Such a function is called a quadratic function and the polynomial $P(s,\mathbf{q})$ is referred to as a quadratic interval polynomial. To avoid dropping in degree, $c_n(\mathbf{q}) \neq 0$ for all $\mathbf{q} \in Q$ is assumed.

In the section if $\mathbf{B} \in \Re^{l,l}$ is a $(l \times l)$ matrix then b_{ij} denotes the element of $\mathbf{B}$ lying on the position (i, j), if $\mathbf{d} \in \Re^l$ is a vector then d_i denotes the element of $\mathbf{d}$ lying on the i-th position.

4.2 Determination of a convex polygon

Presented method deals with the value set of $P(s,\mathbf{q})$ evaluated at some complex point $s = s_0 = |s_0| e^{j\psi_0}$. The image $P(s_0,\mathbf{q})$ can be expressed as

$$P(s_0,\mathbf{q}) = \sum_{k=0}^{n} c_k(\mathbf{q}) s_0^k = c_{\mathrm{Re}}^{s_0}(\mathbf{q}) + j.c_{\mathrm{Im}}^{s_0}(\mathbf{q}) \tag{6}$$

where $c_{\mathrm{Re}}^{s_0}(\mathbf{q}), c_{\mathrm{Im}}^{s_0}(\mathbf{q})$ are real quadratic functions and are given by

$$c_{\mathrm{Re}}^{s_0}(\mathbf{q}) = \sum_{k=0}^{n} c_k(\mathbf{q})|s_0|^k \cos(k\psi_0), \quad c_{\mathrm{Im}}^{s_0}(\mathbf{q}) = \sum_{k=0}^{n} c_k(\mathbf{q})|s_0|^k \sin(k\psi_0) \cdot \tag{7}$$

The idea consists in determining the minimum and maximum differences $h_{\min}^{s_0}(\varphi), h_{\max}^{s_0}(\varphi)$ of the point [0, j0] from the set $P(s_0,\mathbf{q})$ in the complex plane in some direction φ, $\varphi \in [0,\pi]$, respectively (see Fig. 1).

Remark 1 It is worth noting that the difference is measured from the point [0, j0] in the direction φ, $\varphi \in [0,\pi]$. It means that the difference can be negative (in such a case the difference is measured from the point [0, j0] in the direction $\pi+\varphi$).

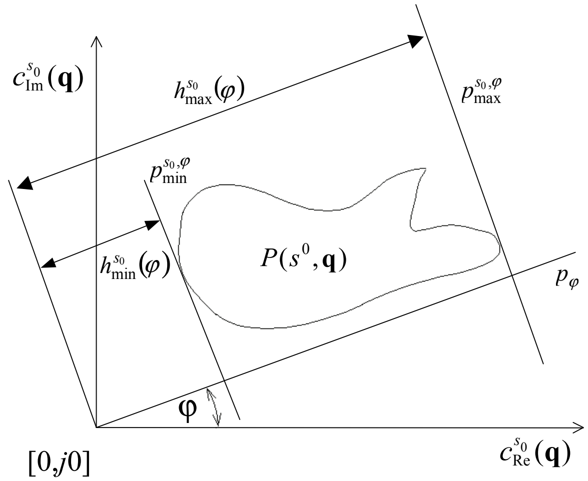

Figure 1. Minimum and maximum distance of $P(s_0,\mathbf{q})$ from [0, j0] in a direction φ

It can be easily shown that finding the minimum and maximum differences is equivalent to finding the minimum and maximum value of the function $c_{\varphi}^{s_0}(\mathbf{q})$,

$$c_{\phi}^{s_0}(\mathbf{q}) = c_{\mathrm{Re}}^{s_0}(\mathbf{q})\cos(\phi) + c_{\mathrm{Im}}^{s_0}(\mathbf{q})\sin(\phi) = \left[c_{\mathrm{Re}}^{s_0}(\mathbf{q}), c_{\mathrm{Im}}^{s_0}(\mathbf{q})\right] . \left[\cos(\phi), \sin(\phi)\right]^T \tag{8}$$

over the set Q.

From (8) it follows that $c_{\varphi}^{s_0}(\mathbf{q})$ is a real quadratic function of q. It means that $c_{\varphi}^{s_0}(\mathbf{q})$ is bounded and $h_{\min}^{s_0}(\varphi), h_{\max}^{s_0}(\varphi)$ are both finite.

The problem of finding extreme values of $c_{\varphi}^{s_0}(\mathbf{q})$ on a box Q is a task of mathematical programming. General formulation of a task of mathematical programming is as follows.

Let us consider the problem of minimization of a function $f_0(\mathbf{x})$, where the constraints are given in the form of inequalities

$$\min\left\{f_0(\mathbf{x}) \middle| f_j(\mathbf{x}) \le b_j, j = 1,\ldots,m\right\} \tag{9}$$

DEFINITION 7 Let a point ${}^0\mathbf{x}$ satisfy all constraints of (9). Let $J({}^0\mathbf{x})$ be the set of indices, for which the corresponding constraints are active (i.e., inequality changes to equality):

$$J\left({}^0\mathbf{x}\right)=\left\{j\middle|f_j\left({}^0\mathbf{x}\right)=b_j\right\} \tag{10}$$

The point ${}^0\mathbf{x}$ is said to be a regular point of the set X given by constraints in (9) if the gradients $\nabla f_j({}^0\mathbf{x})$ are linearly independent for all $j\in J({}^0\mathbf{x})$.

Necessary conditions for the extreme values can be formulated by the following theorem.

THEOREM 2 (Kuhn-Tucker conditions (Kuhn & Tucker, 1951))

Let ${}^*\mathbf{x}$ be a regular point of a set X and a function $f_0(\mathbf{x})$ has in some neighbourhood of ${}^*\mathbf{x}$ continuous first partial derivatives. If the function $f_0(\mathbf{x})$ has in the point ${}^*\mathbf{x}$ the local minimum on X, then there exists a (Lagrange) vector ${}^*\boldsymbol{\lambda}\in\Re^m$ such that

$$\begin{gathered}\nabla f_0\left({}^*\mathbf{x}\right)+\sum_{r=1}^{m}{}^*\lambda_r\nabla f_r\left({}^*\mathbf{x}\right)=0\\ {}^*\lambda_j\left(f_j\left({}^*\mathbf{x}\right)-b_j\right)=0\\ \lambda_j^*\geq 0\end{gathered} \tag{11}$$

hold for all $j = 1,...,m$.

REMARK 2 For maximization of a function $f_0(\mathbf{x})$ the last inequality of (11) is replaced by ${}^*\lambda_j\leq 0$.

To apply Theorem 2 for solving the problem it is necessary to check whether the preconditions of this theorem are satisfied. As $c_\varphi^{s_0}(\mathbf{q})$ is a quadratic function, its first partial derivatives are continuous $\forall\mathbf{q}\in Q$ and the second assumption is satisfied. In our case

$$\begin{aligned}&f_0(\mathbf{q})=c_\varphi^{s_0}(\mathbf{q})\\ &f_j(\mathbf{q})=(-1)^{j+1}q_i,\quad i=1,\ldots,l,\ \ j=2i-1,2i\\ &b_j=-q_i^-\ \text{ for } j \text{ even}\\ &b_j=\ q_i^+\quad \text{for } j \text{ odd}\end{aligned} \tag{12}$$

Then

$$\begin{aligned}&\nabla f_j(\mathbf{q})=(-1)^{j+1}\mathbf{e}^{(i)},\ \ \mathbf{q}\in Q,\ \ j=1,\ldots,2l,\\ &i=\frac{j+1}{2}\ \text{ for } j \text{ odd},\ \ i=\frac{j}{2}\ \text{ for } j\ \text{ even}\end{aligned} \tag{13}$$

where $\mathbf{e}^{(i)} = [0,...,0,1,0,...,0]^T$ with 1 being on the i-th position. Because for any $\mathbf{q}\in Q$ only even or only odd constraints (or none of them) can be active $(q_i^- < q_i^+)\ \forall i=1,\ldots,l$, the gradients $\nabla f_j(\mathbf{q})$ are linearly independent $\forall\mathbf{q}\in Q$, $j\in J(\mathbf{q})$. It means that all points $\mathbf{q}\in Q$ are regular.

Due to Theorem 2 it is necessary to determine the gradient $\nabla c_\varphi^{s_0}(\mathbf{q})$. From (8)

$$\nabla c_\varphi^{s_0}(\mathbf{q})=\left[\nabla c_{\mathrm{Re}}^{s_0}(\mathbf{q})\ ,\nabla c_{\mathrm{Im}}^{s_0}(\mathbf{q})\right]\ .\left[\cos(\phi),\sin(\phi)\right]^T \tag{14}$$

The components of $\nabla c_k(\mathbf{q})$,

$$\nabla c_k(\mathbf{q}) = \left[\frac{\partial c_k(\mathbf{q})}{\partial q_1}, \ldots, \frac{\partial c_k(\mathbf{q})}{\partial q_l}\right]^T \tag{15}$$

follow from (5):

$$\frac{\partial c_k(\mathbf{q})}{\partial q_i} = 2b_{ii}^{(k)} q_i + \sum_{\substack{r=1 \\ r\neq i}}^{l} \left(b_{ir}^{(k)} + b_{ri}^{(k)}\right) q_r, \; k = 0,\ldots,n \quad i = 1,\ldots,l \tag{16}$$

From (7)

$$\begin{aligned} \nabla c_{\mathrm{Re}}^{s_0}(\mathbf{q}) &= \sum_{k=0}^{n} \nabla c_k(\mathbf{q}) |s_0|^k \cos(k\psi_0) \\ \nabla c_{\mathrm{Im}}^{s_0}(\mathbf{q}) &= \sum_{k=0}^{n} \nabla c_k(\mathbf{q}) |s_0|^k \sin(k\psi_0) \end{aligned} \tag{17}$$

After substituting (12), (13), (14), (15), (16) and (17) to (11) the following system of equations and inequalities is obtained:

$$\left[\begin{array}{ccc|ccccc} W_{11} & \cdots & W_{1l} & 1 & -1 & 0 & \cdots & \cdots \\ \vdots & \ddots & \vdots & 0 & 0 & 1 & -1 & \cdots \\ & \ddots & & \vdots & \ddots & & \ddots & \ddots \\ W_{l1} & \cdots & W_{ll} & 0 & \cdots & 0 & 1 & -1 \end{array}\right] \cdot \begin{bmatrix} q_1 \\ \vdots \\ q_l \\ \lambda_1 \\ \vdots \\ \lambda_{2l} \end{bmatrix} = \begin{bmatrix} w_1 \\ \vdots \\ \vdots \\ w_l \end{bmatrix} \tag{18}$$

$$\begin{aligned} \lambda_1\left(q_1 - q_1^+\right) &= 0 \\ \lambda_2\left(-q_1 - q_1^-\right) &= 0 \\ \lambda_3\left(q_2 - q_2^+\right) &= 0 \\ \lambda_4\left(-q_2 - q_2^-\right) &= 0 \\ &\vdots \\ \lambda_{2l-1}\left(q_l - q_l^+\right) &= 0 \\ \lambda_{2l}\left(-q_l - q_l^-\right) &= 0 \end{aligned} \tag{19}$$

$$\begin{aligned} &\lambda_1, \ldots, \lambda_{2l} \geq 0 \;\text{ for minimization} \\ &\lambda_1, \ldots, \lambda_{2l} \leq 0 \;\text{ for maximization} \end{aligned} \tag{6.1}$$

where

$$W_{uv}=\left[\sum_{k=0}^{n}\left(b_{uv}^{(k)}+b_{vu}^{(k)}\right).|s_0|^k\cos(k\psi_0)\right].\cos(\varphi)+\left[\sum_{k=0}^{n}\left(b_{uv}^{(k)}+b_{vu}^{(k)}\right).|s_0|^k\sin(k\psi_0)\right].\sin(\varphi)$$

$$w_u=\left[\sum_{k=0}^{n}d_u^{(k)}.|s_0|^k\cos(k\psi_0)\right].\cos(\varphi)+\left[\sum_{k=0}^{n}d_u^{(k)}.|s_0|^k\sin(k\psi_0)\right].\sin(\varphi)$$

$$u,v=1,\ldots,l.$$

The important fact is that the equation (18) is linear. The computational way of solving the system (18-19) runs as follows. First all the solutions of (19) are determined. This corresponds to determining of all the parts of the box Q – interior and all the parts of the boundary of Q (all manifolds with the dimension i, i = 0,..., l-1 containing only points on the boundary of Q). Each solution of (19) corresponds to $2l$ linear equations (from (19) it follows that at least one of λ_{2i-1}, λ_{2i}, i = 1,..., l has to equal zero; if $\lambda_{2i-1}=0$ then either $\lambda_{2i}=0$ or $q_i=-q_i^-$, if $\lambda_{2i}=0$ then either $\lambda_{2i-1}=0$ or $q_i=q_i^+$ i = 1,..., l). These $2l$ equations together with l equations of (18) form $3l$ linearly independent linear equations for $3l$ unknown variables. It means that there exists a unique solution ($^*\boldsymbol{\lambda}$,$^*\mathbf{q}$) (for each solution of (19)) of system (18-19). Denote by $T_{\min}$ ($T_{\max}$) the set of t for which these conditions are satisfied,

$$\begin{aligned}T_{\min}&=\left\{t:{}^*\mathbf{q}^{(t)}\in Q,{}^*\lambda_j^{(t)}\geq 0\ \forall j=1,\ldots,2l\right\}\\ T_{\max}&=\left\{t:{}^*\mathbf{q}^{(t)}\in Q,{}^*\lambda_j^{(t)}\leq 0\ \forall j=1,\ldots,2l\right\}\end{aligned}\tag{20}$$

Then

$$\begin{aligned}h_{\min}^{s_0}(\varphi)&=\min_{t\in T_{\min}}\left[c_{\varphi}^{s_0}\left({}^*\mathbf{q}^{(t)}\right)\right]\\ h_{\max}^{s_0}(\varphi)&=\max_{t\in T_{\max}}\left[c_{\varphi}^{s_0}\left({}^*\mathbf{q}^{(t)}\right)\right]\end{aligned}\tag{21}$$

The minimum and maximum differences indicate that the set $P(s_0,\mathbf{q})$ lies in the complex plane in the space between the lines $p_{\min}^{s_0,\varphi}$ and $p_{\max}^{s_0,\varphi}$:

$$\begin{aligned}p_{\min}^{s_0,\varphi}&:\ c_{\mathrm{Im}}^{s_0}(\mathbf{q})=-\frac{1}{\tan(\varphi)}c_{\mathrm{Re}}^{s_0}(\mathbf{q})+\frac{h_{\min}^{s_0}(\varphi)}{\sin(\varphi)}\\ p_{\max}^{s_0,\varphi}&:\ c_{\mathrm{Im}}^{s_0}(\mathbf{q})=-\frac{1}{\tan(\varphi)}c_{\mathrm{Re}}^{s_0}(\mathbf{q})+\frac{h_{\max}^{s_0}(\varphi)}{\sin(\varphi)}\end{aligned}\tag{22}$$

In order to determine a convex hull overbounding the set $P(s_0,\mathbf{q})$, $\mathbf{q}\in Q$, the procedure described above is performed for a set of $\varphi_r\in\Phi$,

$$\Phi=\left\{\begin{array}{l}\varphi_r:0\leq\varphi_1\leq\cdots\leq\varphi_{R-1}\leq\varphi_R\leq\pi,\\ r=1,\ldots,R\end{array}\right\}\tag{23}$$

It means that the system (18-19) is solved for a set of φ. The higher the number R is, the "more tight" convex hull is obtained.

If one wants to determine the convex polygon computationally the set $V_{\Phi}(s_0)$ of the intersections of the following lines has to be determined:

$$
\begin{aligned}
V_{\Phi}(s_0) &= \left\{ S_m^{s_0} : m = 1,\ldots,2R \right\} \\
V_r^{s_0} &= \mathrm{insec}\left(p_{\min}^{s_0,\varphi_r}, p_{\min}^{s_0,\varphi_{r+1}}\right) \\
V_R^{s_0} &= \mathrm{insec}\left(p_{\min}^{s_0,\varphi_R}, p_{\max}^{s_0,\varphi_1}\right) \\
V_{r+R}^{s_0} &= \mathrm{insec}\left(p_{\max}^{s_0,\varphi_r}, p_{\max}^{s_0,\varphi_{r+1}}\right) \\
V_{2R}^{s_0} &= \mathrm{insec}\left(p_{\max}^{s_0,\varphi_R}, p_{\min}^{s_0,\varphi_1}\right) \\
r &= 1,\ldots,R-1
\end{aligned}
\tag{24}
$$

where insec(p_x, p_y) denotes the intersection of the lines p_x and p_y (see Fig. 2).

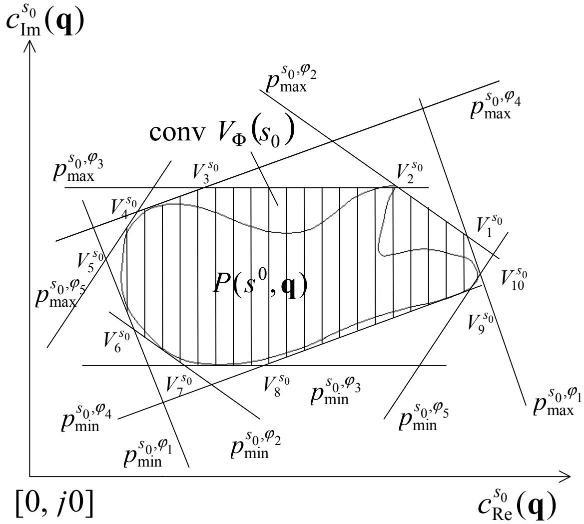

Figure 1. Convex hull $V_{\Phi}(s_0)$ for R = 5

The coordinates of intersections are given by

$$
\mathrm{insec}\left(p_{\mathrm{term}}^{s_0,\varphi_m}, p_{\mathrm{term}}^{s_0,\varphi_{m+1}}\right) = \begin{bmatrix} \dfrac{h_{\mathrm{term}}^{s_0}(\varphi_2)\sin(\varphi_1) - h_{\mathrm{term}}^{s_0}(\varphi_1)\sin(\varphi_2)}{\sin(\varphi_1 - \varphi_2)} \\ \dfrac{h_{\mathrm{term}}^{s_0}(\varphi_2)\cos(\varphi_1) - h_{\mathrm{term}}^{s_0}(\varphi_1)\cos(\varphi_2)}{\sin(\varphi_1 - \varphi_2)} \end{bmatrix}^T
\tag{25}
$$

where term stands for min or max.
Now the key theorems can be stated.

THEOREM 3 (Convex polygons overbounding the value set)
Denote by conv A the convex hull of a set A. Then

$$
P(s_0, \mathbf{q}) \subseteq \mathrm{conv}\ V_{\Phi}(s_0) \forall s_0 \in C
\tag{26}
$$

Using Theorem 1 the Zero exclusion principle gives a necessary condition for stability of a family of polynomials (4).

THEOREM 4 (Sufficient robust stability condition)
The family of polynomials (4) of constant degree containing at least one stable polynomial is robustly stable with respect to S if

$$0 \notin \text{conv } V_\Phi(s_0) \text{ for all } s_0 \in \partial S \tag{27}$$

where ∂S denotes the boundary of S.

The zero exclusion test can be performed in both graphical and computational way. The latter is recommended as described below because of saving a lot of time.

THEOREM 5
$0 \notin \text{conv } V_\Phi(s_0)$ if and only if there exists at least one $\varphi \in \Phi$, such that

$$h_{\min}^{s_0}(\varphi) \geq 0 \wedge h_{\max}^{s_0}(\varphi) \geq 0 \text{ or } h_{\min}^{s_0}(\varphi) \leq 0 \wedge h_{\max}^{s_0}(\varphi) \leq 0 \tag{28}$$

Theorem 5 makes it possible to decide about zero exclusion or inclusion without computing the set of intersections $V_\Phi(s_0)$. Proofs of all three theorems are evident from the construction of convex polygons and Zero exclusion theorem.

Let us illustrate the described procedure of checking robust stability of quadratic interval polynomials on two examples. As arbitrary stability region can be chosen a discrete-time uncertain polynomial will be considered at first.

EXAMPLE 1 Let a family of discrete-time polynomials be given by

$$P(z,\mathbf{q}) = c_2(\mathbf{q})z^2 + c_1(\mathbf{q})z + c_0(\mathbf{q})$$

where

$$\mathbf{q} = [q_1, q_2]^T, \; q_i \in [0,1]$$

and

$$\begin{aligned} c_2(\mathbf{q}) &= 1 \\ c_1(\mathbf{q}) &= 0.2 \cdot q_2 - 0.5 \cdot q_2^2 + 0.1 \cdot q_1 \cdot q_2 \\ c_0(\mathbf{q}) &= -0.3 \cdot q_1 + 0.2 \cdot q_1^2 - 0.5 \cdot q_2^2 + q_1 \cdot q_2 \end{aligned}$$

The question is whether this family of polynomials is Schur stable.

In this case the stability region S is the unit circle, therefore its boundary $\partial S = e^{j\omega}$, $\omega \in [0, 2\pi]$. The Zero exclusion principle will be tested graphically. Due to symmetry it is sufficient to plot the value set only for the points $s_0 = e^{j\omega}$, $\omega \in [0, \pi]$. The corresponding plot of the value sets and their convex hulls is shown in Fig. 3 and Fig. 4 (R = 6) respectively. As $0 \notin V_\Phi(s_0)$ for all $s_0 \in \partial S$, the polynomial $P(z,\mathbf{q})$ is robustly Schur stable. In Fig. 5 and Fig. 6 the value set and the convex hull for $s_0 = e^{j\pi/3}$ and different number of angles φ_r is plotted (R = 4 and R = 14 respectively).

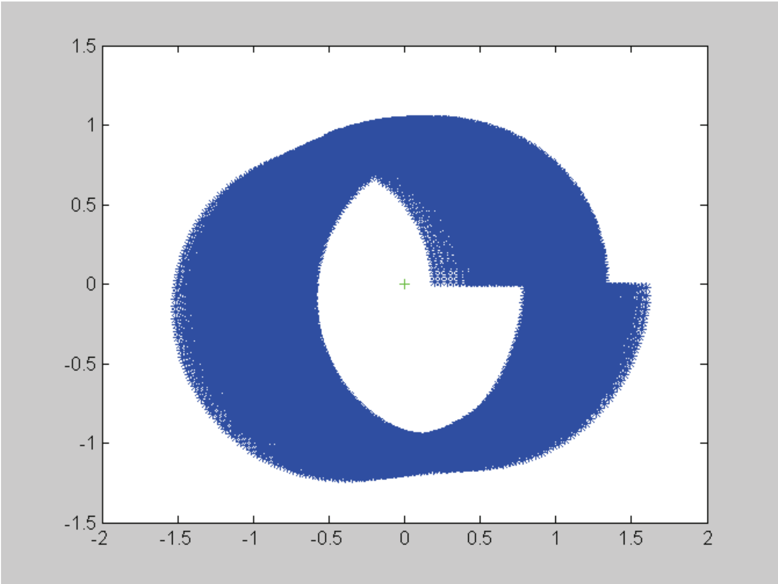

Figure 2. Plot of the value set for $s_0 = e^{j\omega}, \omega \in [0, \pi]$

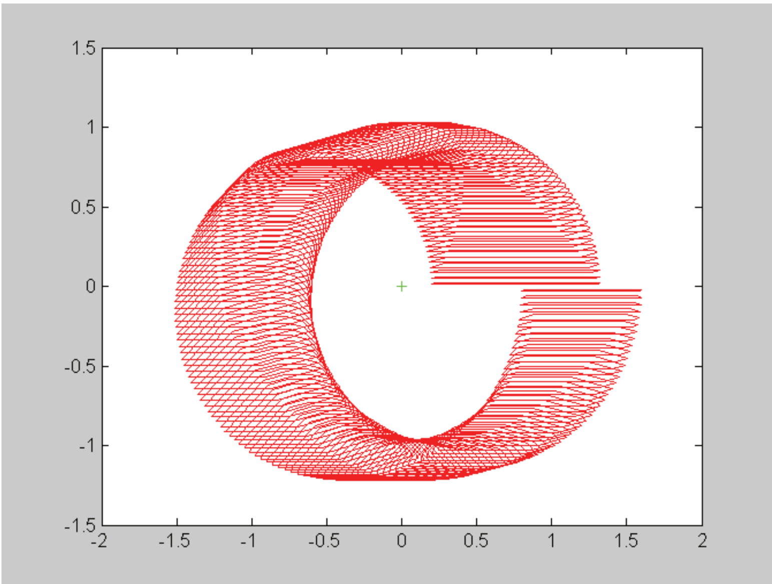

Figure 3. Plot of the convex hulls of the value set

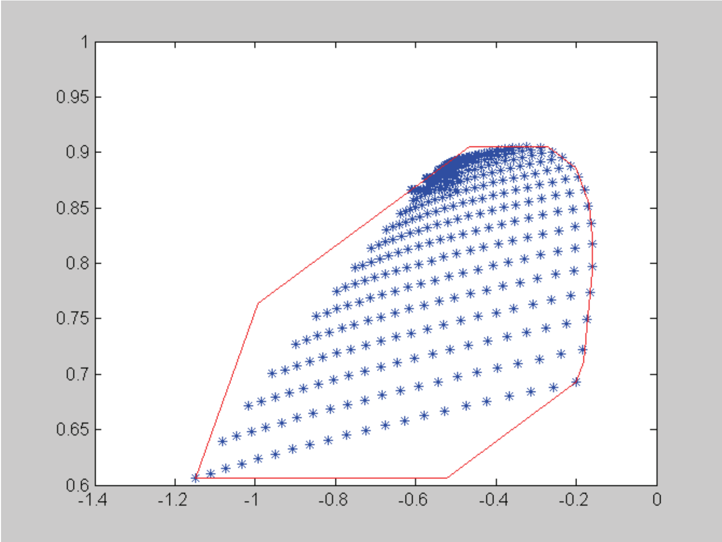

Figure 4. The value set and the convex hull for $s_0 = e^{j\pi/3}$ and $R = 4$

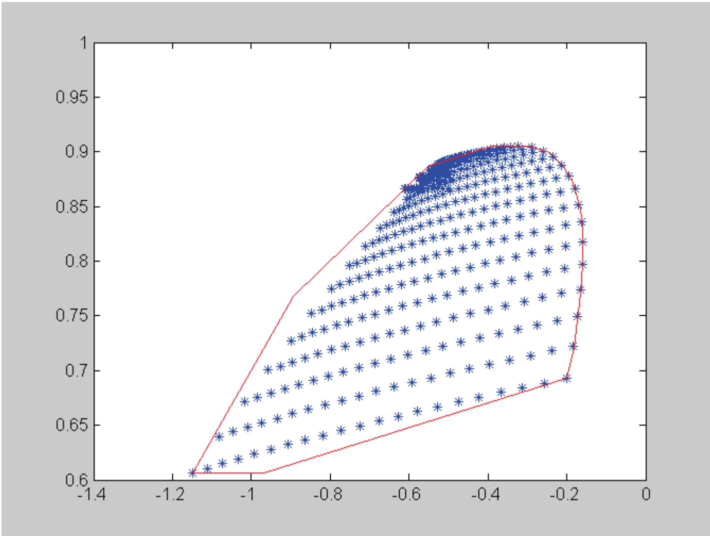

Figure 5. The value set and the convex hull for $s_0 = e^{j\pi/3}$ and $R = 14$

EXAMPLE 2 Let a family of continuous-time polynomials be given by

$$P(s, \mathbf{q}) = c_3(\mathbf{q})s^3 + c_2(\mathbf{q})s^2 + c_1(\mathbf{q})s + c_0(\mathbf{q})$$

where

$$\mathbf{q} = [q_1, q_2]^T, \; q_i \in [0,1]$$

and

$$c_3(\mathbf{q}) = 1$$
$$c_2(\mathbf{q}) = 7.7640 + 6.6486q_1 + 7.0064q_2 + 9.9945q_1^2 + 7.0357q_2^2 + 5.6677q_1 \cdot q_2$$
$$c_1(\mathbf{q}) = 4.8935 + 3.6537q_1 + 9.8271q_2 + 9.6164q_1^2 + 4.8496q_2^2 + 8.2301q_1 \cdot q_2$$
$$c_0(\mathbf{q}) = 1.8590 + 1.4004q_1 + 8.0664q_2 + 0.5886q_1^2 + 1.1461q_2^2 + 6.7395q_1 \cdot q_2$$

The question is whether this family of polynomials is Hurwitz stable.

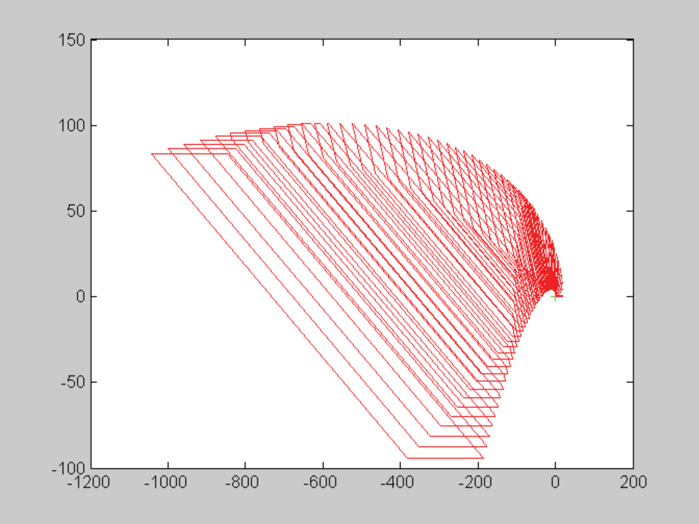

Figure 7. Plot of the convex hulls of the value sets for $s_0 = j\omega$, $\omega \in [0,5]$

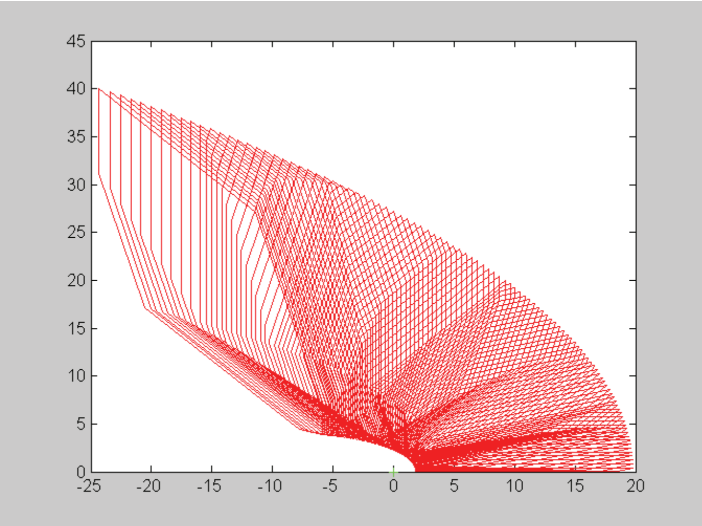

Figure 8. Plot of the convex hulls of the value sets for $s_0 = j\omega$, $\omega \in [0,1]$

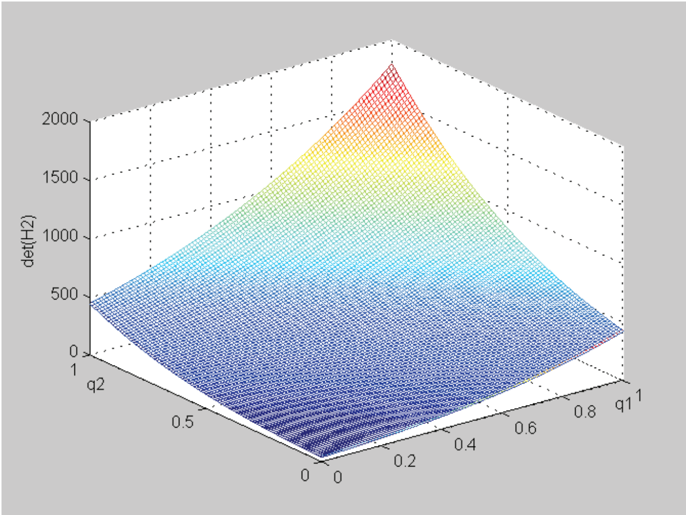

Figure 9. Plot of the determinant of the matrix $\mathbf{H}_2(\mathbf{q})$

Here the stability region S is the imaginary axis, therefore the boundary $\partial S = j\omega$, $\omega \in [-\infty, \infty]$. Due to symmetry it is sufficient to plot the value set only for $s_0 = j\omega$, $\omega \in [0, \infty]$. The corresponding plot of the convex hulls for $\omega \in [0,5]$ is shown in Fig. 7. As from this figure it is not apparent, whether zero is included or not, the same plot for $\omega \in [0,1]$ is shown in Fig. 8. From that it is clear that $0 \notin V_\Phi(s_0)$ for all $s_0 \in \partial S$. The polynomial $P(s,\mathbf{q})$ is robustly Hurwitz stable.

The obtained result can be confirmed by plotting the determinant of the $(n$-1)-th order Hurwitz matrix $\mathbf{H}_2(\mathbf{q})$ and checking its positivity as $c_0(\mathbf{q})$ is positive for admissible $\mathbf{q}$ evidently. Fig. 9 confirms the obtained result.

4. Polynomials of general polynomic parameter uncertainty

The result obtained in Theorem 5 is applicable for uncertain polynomials with arbitrary polynomic parameter dependency as well. In such case it is necessary to determine if the function $c_\varphi^{s_0}(\mathbf{q})$ is positive or negative on the set Q or it allows both positive and negative values on this set, i.e., if there exists a $\mathbf{q}^1 \in Q$ such that $c_\varphi^{s_0}(\mathbf{q}^1) > 0$ and $\mathbf{q}^2 \in Q$ such that $c_\varphi^{s_0}(\mathbf{q}^2) < 0$. Since $c_\varphi^{s_0}(\mathbf{q})$ is a polynomic function its positivity can be tested by effective algorithm of Bernstein expansion (Garloff, 1993).

The algorithm gives only sufficient stability condition. If for all $s_0 \in \partial S$ at least one φ_r is determined, such that the function $c_\varphi^{s_0}(\mathbf{q})$ is only positive or only negative on the set Q, then the origin is excluded from the convex hulls of value sets for all $s_0 \in \partial S$ and therefore also from the value set itself and the family of polynomials is stable. If not, it is not possible to decide about robust stability of the family.

The main advantage of this algorithm is that the number of coefficients of multivariate polynomic function $c_{\varphi}^{s_0}(\mathbf{q})$ is considerably smaller than the of Hurwitz determinant $\det(\mathbf{H}_{n-1}(\mathbf{q}))$ especially for higher number of uncertain parameters (however still moderate) because using the value set algorithm only the coefficients of tested polynomial are needed to store. For example, a polynomial of degree n = 5 with l = 4 uncertain parameters with highest degree equal to 4 appearing in each variable in each original coefficient contains generally 120 coefficients. The determinant of (n-1)-th order Hurwitz matrix, which has to be tested for positivity, contains generally 83521 coefficients. If the number of parameters is doubled (l = 8), the uncertain polynomial contains 240 coefficients, but the determinant of (n-1)-th order Hurwitz matrix contains huge $6.98 \cdot 10^9$ coefficients which is out of memory for standard computers. Therefore this algorithm can deal with much larger problems. This is demonstrated on the benchmark example of Fiat Dedra engine.

The proposed algorithm will be demonstrated on some examples and its efficiency compared with the of original application of algorithm of Bernstein expansion.

EXAMPLE 3 Let a family of continuous-time polynomials be given by

$$p(s,\mathbf{q}) = c_3(\mathbf{q})s^3 + c_2(\mathbf{q})s^2 + c_1(\mathbf{q})s + c_0(\mathbf{q})$$

where

$$\mathbf{q} = [q_1, q_2, q_3]^T, \quad q_i \in [0,1], \; i = 1,2,3$$

and

$$\begin{aligned}
c_3(\mathbf{q}) = {} & q_1 + q_1^2 + 3q_2 + 1q_1q_2 + 5q_1^2q_2 + 2q_1q_2^2 + q_1^2q_2^2 + 3q_3 + 4q_1q_3 + q_1^2q_3 + 3q_2q_3 \\
& + 2q_1q_2q_3 + q_1^2q_2q_3 + 4q_2^2q_3 + 4q_1q_2^2q_3 + 4q_1^2q_2^2q_3 + 3q_1q_3^2 + 2q_1^2q_3^2 + 3q_2q_3^2 \\
& + 5q_1q_2q_3^2 + 3q_1^2q_2q_3^2 + 2q_2^2q_3^2 + 4q_1q_2^2q_3^2 + 4q_1^2q_2^2q_3^2; \\
c_2(\mathbf{q}) = {} & 8 + 3q_1 + 3q_1^2 + 3q_2 + 5q_1q_2 + 2q_1^2q_2 + 10q_2^2 + 3q_1q_2^2 + 8q_1^2q_2^2 + 9q_3 + 3q_1q_3 \\
& + q_1^2q_3 + 3q_2q_3 + 7q_1q_2q_3 + 5q_2^2q_3 + 6q_1q_2^2q_3 + 7q_1^2q_2^2q_3 + 6q_3^2 + 7q_1q_3^2 \\
& + 8q_1^2q_3^2 + 9q_2q_3^2 + 10q_1q_2q_3^2 + 9q_1^2q_2q_3^2 + 2q_2^2q_3^2 + 10q_1q_2^2q_3^2 + 9q_1^2q_2^2q_3^2; \\
c_1(\mathbf{q}) = {} & 6 + 7q_1 + q_1^2 + 8q_2 + 5q_1q_2 + 9q_1^2q_2 + q_1q_2^2 + 7q_1^2q_2^2 + 6q_3 + 9q_1q_3 + 5q_1^2q_3 \\
& + 5q_2q_3 + 4q_1q_2q_3 + 4q_1^2q_2q_3 + 4q_2^2q_3 + 9q_1q_2^2q_3 + 8q_1^2q_2^2q_3 + 9q_3^2 + 8q_1q_3^2 \\
& + 9q_1^2q_3^2 + 8q_2q_3^2 + 4q_1q_2q_3^2 + 4q_1^2q_2q_3^2 + 2q_2^2q_3^2 + 4q_1^2q_2^2q_3^2; \\
c_0(\mathbf{q}) = {} & 6 + q_1 + q_1^2 + 6q_2 + 9q_1q_2 + 4q_1^2q_2 + 7q_2^2 + q_1q_2^2 + 5q_3 + 9q_1q_3 + 8q_1^2q_3 \\
& + 8q_2q_3 + 2q_1q_2q_3 + 7q_1^2q_2q_3 + 2q_2^2q_3 + 8q_3 + q_1q_2^2q_3 + 2q_1^2q_2^2q_3 + 2q_3^2 \\
& + 5q_1q_3^2 + q_1^2q_3^2 + 6q_2q_3^2 + 2q_1q_2q_3^2 + 9q_1^2q_2q_3^2 + 3q_2^2q_3^2 + 5q_1q_2^2q_3^2 + 8q_1^2q_2^2q_3^2
\end{aligned}$$

The dependency of polynomial coefficients $c_j(\mathbf{q}), j = 0,\ldots,3$ is no longer quadratic and Bernstein algorithm will be used to check positivity or negativity of all the distances. The algorithm checks in 0.34 seconds that for $\omega \in [0,2]$ with step 0.01 (R=10) the origin is excluded from all the convex hulls of value sets and therefore also from the value set itself and the family of polynomials is stable. This result is also confirmed by plotting the value set (Fig. 10). The Bernstein algorithm (Zettler & Garloff, 1998) applied on value sets gives the same result in 0.94s. The algorithm of Bernstein expansion can be also employed on positivity test of Hurwitz determinant. Using symbolic computations for determination of determinant of Hurwitz matrix the Bernstein algorithm reports the same result after 3.54s.

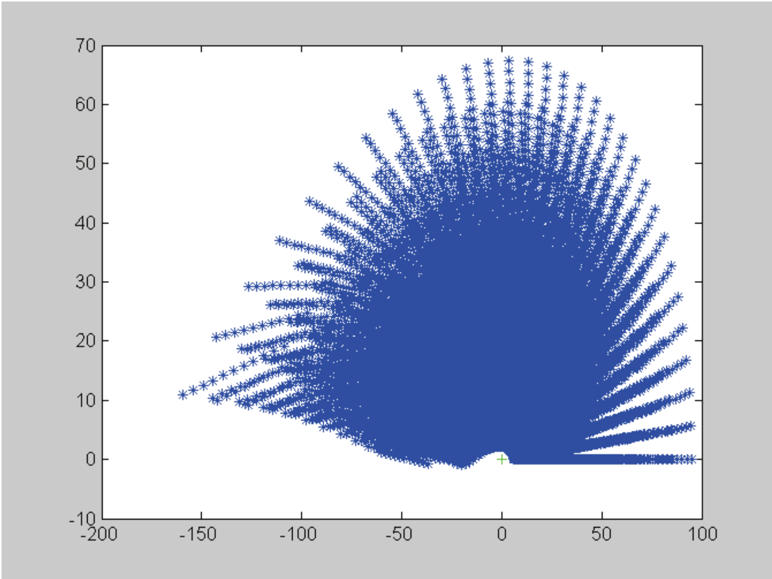

Figure 10. Plot of the value sets of $P(s,\mathbf{q})$ for $\omega \in [0,1.5]$

5. Fiat-Dedra engine

Let us consider a model of the Fiat Dedra engine given in (Barmish, 1994). The focal point is the idle speed control problem, which is particularly important for city driving; that is, fuel economy depends strongly on engine performance when idling.
The model has 7 uncertain parameters and a design of a fixed output controller leads to characteristic polynomial of 7-th order,

$$p(s,\mathbf{q}) = \sum_{j=0}^{7} a_j(\mathbf{q})\, s^j \tag{29}$$

The coefficients $a_j(\mathbf{q})$, j = 0,…,7 being polynomic functions of the parameters q_i, i = 1,...,7 are listed in (Barmish, 1994).
The parameters and the frequency are supposed to vary inside the following intervals:

$$\begin{aligned} &q_1 \in [2.1608,\ 3.4329];\ q_2 \in [0.1027,\ 0.1627];\ q_3 \in [0.0357,\ 0.1139]; \\ &q_4 \in [0.2539,\ 0.5607];\ q_5 \in [0.0100,\ 0.0208];\ q_6 \in [2.0247,\ 4.4962]; \\ &q_7 \in [1.0000,\ 10.000];\ \omega \in [0.0000,\ 2.3410] \end{aligned} \tag{30}$$

The question is whether the uncertain polynomial (29) is robustly stable for the parameters and frequency given in (30).
Firstly it has to be noted that this problem is relatively large and it is not possible to compute the determinant of the 6-th order Hurwitz matrix because storage capacity of a standard computer is too low to store all its coefficients.
The frequency step was chosen 0.01, the sufficient number of direction angles was 10. The described algorithm reports in 5.53s that the characteristic polynomial (29) is stable that corresponds to the result obtained by the Bernstein expansion (Zettler and Garloff, 1998) in 7.48s. All the computations were performed on a Pentium 4 CPU 3GHz 504MB RAM.

7. Conclusion

The algorithm checking robust stability of polynomials with polynomic dependency of its coefficients on vector interval parameter was presented. The method is based on testing the value set in frequency domain. The value set evaluated in a point lying on the boundary of stability region is overbounded by a convex polygon. The zero exclusion test is performed by positivity checking of multivariate polynomic functions using the Bernstein algorithm. The procedure results in sufficient stability condition. The main advantage of the presented algorithm over those based on computation of Hurwitz determinant consists in its capability of treating relatively large problems because of the low requirements on computer storage capacity. Moreover, arbitrary stability region can be chosen. Efficiency of the algorithm was verified on the benchmark example of the Fiat Dedra engine control by comparison with the Bernstein expansion algorithm.

8. Acknowledgements

This work has been supported by the project INGO 1P2007LA297, Research Program MSM6840770038 (sponsored by the Ministry of Education of the Czech Republic) and the project 1H-PK/22 (sponsored by Ministry of Industry and Trade of the Czech Republic).

9. References

Ackermann, J. (1993). *Robust Control, Systems with Uncertain Physical Parameters*, Springer, ISBN 0-387-19843-1, London

Barmish, B.R. (1994). *New Tools for Robustness of Linear Systems*. Macmillan Publishing Company, ISBN 0-02-306005-7, New York

Bartlett, A.C., Hollot, C.V. & Lin, H. (1988). Root Location of an Entire Polytope of Polynomials: It suffices to check the edges, *Mathematics of Controls, Signals and Systems*, Vol. 1, No. 1, pp. 61-71, ISSN 0932-4194

Bhattacharyya, S. P., Chapellat, H. & Keel, L. H. (1995). *Robust Control: the Parametric Approach*, Prentice-Hall Inc, ISBN 978-0137815760, New York

Garloff, J. (1985). Convergent Bounds for the Range of Multivariate Polynomials. *Interval Mathematics, Lecture Notes in Computer Science*, K. Nickel (Ed.), pp. 37-56, Springer Verlag, ISBN:3-387-16437-5, Berlin

Garloff, J. (1993). The Bernstein algorithm. *Interval Computations*, Vol. 2, No. 6, pp. 154-168, ISSN 0135-4868

Garloff, J., Graf, B. & Zettler, M. (1997). Speeding Up an Algorithm for Checking Robust Stability of Polynomials. *Fachhochschule Konstanz, Internal Report*

Gaston de, R.R. & Safonov, M.G. (1988). Exact Calculation of the Multiloop Stability Margin. *IEEE Transactions on Automatic Control,* Vol. 33, No. 2, pp. 156-171, ISSN 0018-9286

Chen, X. & Zhou, K. (2003). Fast parallel-frequency-sweeping algorithms for robust D-stability, *IEEE Transactions on Circuits and Systems,* Vol. 50, No. 3, pp. 418-428, ISSN 057-7122

Kaesbauer, D. (1993). On Robust Stability of Polynomials with Polynomial Parameter Dependency: Two/three parameter cases, *Automatica,* Vol. 29., No. 1, pp. 215-217, ISSN 0005-1098

Kharitonov, V. L. (1978). Asymptotic stability of an equilibrium position of a family of systems of linear differential equations. *Differencialnyje Uravnenija*, Vol. 14, No. 11, pp. 2086-2088, ISSN 0374 0641

Kuhn, H. W. & Tucker, A. (1951). Nonlinear Programming, *Proceedings of the 2nd Berkeley Symposium on Mathematical Statistics and Probability*, University of California Press, Berkeley

Malan, S., Milanese M. & Taragna, M. (1997). Robust Analysis and Design of Control Systems Using Interval Arithmetics, *Automatica,* Vol. 33, No. 7, pp. 1363-1372, ISSN 0005-1098

Murdock, T.M., Schmitendorf, W.E. & Forrest, S. (1991). Use of a Genetic Algorithm to Analyze Robust Stability Problems, *Proceedings of American Control Conference*, pp. 886-889, Boston, MA

Neimark,Y. I. (1949). Stability of Linearized Systems, *Aeronautical Engineering Academy*, Leningrad, USSR

Sideris, A. & de Gaston, R.R. (1986). Multivariable Stability Margin Calculation with Uncertain Correlated Parameters, *Proceedings of IEEE Conference on. Decision and Control*, Athens, Greece

Sideris, A. & Sánchez Peňa, R.S. (1989). Fast Computation of the Multivariate Stability Margin for Real Interrelated Uncertain Parameters, *IEEE Transactions on Automatic Control,* Vol. 34., No. 12, pp. 1272-1276, ISSN 0018-9286

Siljak, D. D. (1969). *Nonlinear Systems*, Wiley, New York

Siljak, D. D. and Stipanovic, D. M. (1999). Robust D-stability via positivity, *Automatica*, Vol. 35, No. 8, pp. 1477-1484, ISSN 0005-1098

Vicino, A., Tesi, A. & Milanese, M. (1990). Computation of Nonconservative Stability Perturbation Bounds for Systems with Nonlinearly Correlated Uncertainties, *IEEE Transactions on Automatic Control,* Vol. 35., No. 7, pp. 835-841, ISSN 0018-9286

Walter, E. and Jaulin, L. (1994). Guaranteed Characterization of Stability Domains Via Set Inversion, *IEEE Transactions on Automatic Control,* Vol. 39, No. 4, pp. 886-889, ISSN 0018-9286

Zadeh, L. A. and Desoer, C. A. (1963). *Linear Systems Theory,* McGraw Hill Book Co., New York

Zettler, M. and Garloff, J. (1998). Robustness Analysis of Polynomials with Polynomial Parameter Dependency Using Bernstein Expansion, *IEEE Transactions on Automatic Control*, Vol. 43, No. 3, pp. 425-431, ISSN 0018-9286

6

Fouling Detection Based on Parameter Estimation

Jaidilson Jó da Silva, Antonio Marcus Nogueira Lima
and José Sérgio da Rocha Neto
Federal University of Campina Grande
Brazil

1. Introduction

A severe problem that may occur when fluids are transported in duct systems and pipelines is the slow accumulation of organic or inorganic substances along the inner surface over time. Such accumulation of unwanted material is denoted fouling, and occasionally appears simultaneously with tube corrosion. Both, fouling and corrosion are major concerns for plant operation and lifetime in chemical, petroleum, food and pharmaceutical industries, due to the detrimental impact of such phenomenon on the reliability and security (Rose, 1995), (Cam et al., 2002), (Hay & Rose, 2003), (Siqueira et al., 2004). Tube corrosion is related to the presence of chemically aggressive trace elements and compounds in the transported materials, usually attributed to presence of sulfur or halogens. A sketch of the two occasionally simultaneously appearing processes is illustrated in Fig. 1, where the corrosion related shrinking of wall thickness is related to the growing fouling layer.

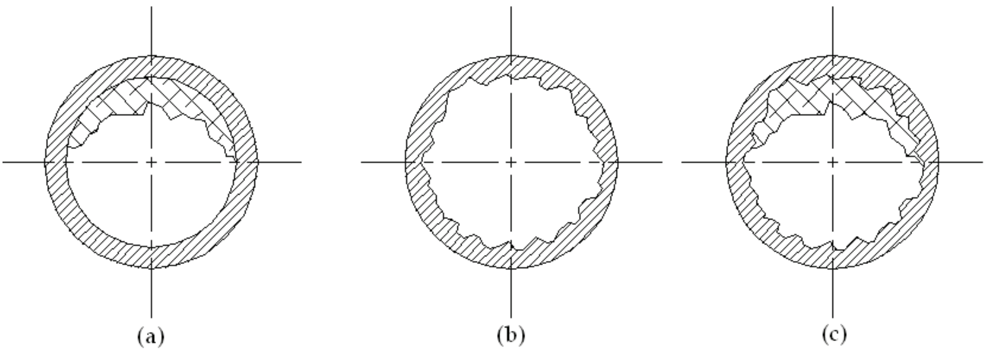

Figure 1. Cross-section view of tube aging processes: inhomogeneous fouling layer (a), corrosion (b), corrosion and fouling (c)

An example of tube fouling, observed in a selected duct section of an oil refining plant, is presented in Fig. 2. This duct is under test at the LIEC (Electronic Instrumentation and Control Laboratory) of Federal University of Campina Grande (UFCG).

The deposition rate commonly is very low, and it may take several months until critical thickness values are reached. Fouling in chemical plant duct systems and pipelines accounts for severe problems in plant operation as: reduction of the internal diameter of the tube; reduction of mechanical integrity and strength, reduction of plant operation lifetime, increase of the applied pressure to maintain flow through-put, crack formation and possibly catastrophic break-up. The associated increase of the energy consumption also comes along with higher operation and maintenance costs.

Figure 2. Photography showing the fouling layer formed in a duct section that transports crude oil (Petrobras-BR)

Duct systems and pipelines thus require regular and periodic inspection. Several methods have been proposed for early fouling detection in ducts, based on mass flow reduction (Krisher, 2003), electric resistance (Panchal, 1997) and ultrasonic techniques (Silva et al., 2005), (Lohr & Rose, 2002).

The key idea of the mass flow reduction technique is to monitor the corrosion process of a plate, made of the same material as the ducts. Such plate is put inside the pipe to obtain information regarding the fouling process (Krisher, 2003). The second group of methods, named electric resistance sensor techniques, is based on the analysis of the sensor resistance value to identify modifications in the pipe inner surface (Panchal, 1997). These two methods are intrusive, i.e. the elements for monitoring must be put inside the pipeline. This is a disadvantage, since plant operation should be interrupted for installation and analysis of the elements. On the other hand, the methods based on ultrasound are advantageous over those aforementioned methods, since those methods are not intrusive (Silva et al., 2005).

Guided acoustic waves are generated by the interference of Longitudinal (L) and Transverse (T) wave types: The longitudinal wave is generated when the movement of the particles is parallel to the wave propagation direction. The transverse wave is generated when the movement of the particles is perpendicular to the wave propagation direction. Guided waves are generated by the interference of these two wave types, when the thickness of the wall under test is smaller or equal than the wavelength of wave (Rose, 1995), (Lohr & Rose, 2002). Fig. 3 shows the formation of guided waves in a plate, when the thickness (d) of the plate is smaller or equal to the wavelength of wave (λ) (Silva et al., 2007).

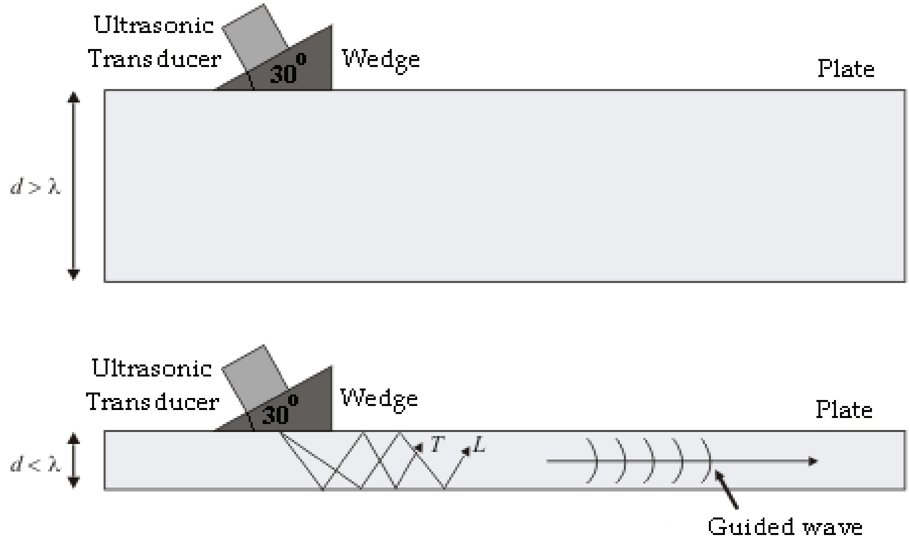

Figure 3. Representation of guided acoustic waves

Thus, to generate guided waves, two basic conditions are necessary: First, the pipe wall thickness under test should be smaller or equal than the wavelength of the spread signal, and this is possible adjusting the excitation frequency of the pulser; second, the angles of the used transducers must be chosen adequately. The angles of the transducers are determined by the shape of the wedge couplers that are made of acrylic. In the present case, it was observed that for angles larger than 40 deg the guided waves were not generated and the receiver didn't detect the transmitted signal (Silva, 2005). The transmitted waves were detected for wedge angles of 30 deg and 40 deg (commercial angular transducers are usually provided for 30 deg, 40 deg and 45 deg angles) (Silva, 2005).

Guided waves can travel up to 200 *m*, but there is a reduction in the amplitude of the signal due the attenuation in the medium and the distance (Rose, 1995). For the studied pipe, tests were accomplished with a distance variation among the transducers from 5 to 70 *cm* (size of the removable part of the pipe) and no amplitude reduction was observed, without fouling.

The ultrasonic transducers are typically excited with pulses and amplitudes that vary between 100 and 1000 *V*. The received signal can vary from microvolts to some volts. The received signal may exhibit frequency characteristics very different from the pulses used to excite the transmitter transducer, due the characteristics of the propagation media (Fortunko, 1991).

After recording at the receiver, the signals are amplified and filtered. The parameters like gain and bandwidth of the receiver are adjusted in agreement with the characteristics of the system under test. Choice of gain and bandwidth are also influenced by the used transducer, discontinuities and characteristics of the frequency response of the pulser. When the ultrasonic signal encounters a new interface (different material), the signal spreads also into this interface, and modifies the characteristics of the transmitted signal.
This chapter presents the use of a model for ultrasonic pulses, which spread through guided waves in a pipe, for fouling detection. The main goal is to estimate the parameters of the model and to observe the variations of these parameters with the presence of the fouling.
This chapter is organized in six sections: the first part is the introduction; section 2, the models and estimation method for ultrasonic pulses, in section 3 the proposed system, in section 4 the simulation results, experimental results in section 5 and concluding remarks are outlined in section 6.

2. Models and estimation for ultrasonic pulses

Some models of ultrasonic pulses are based on the diffraction scalar theory, while piezo-electric transducers were employed (Calmon et al, 2000).
When an ultrasonic pulse spreads through a layer of a medium of different material, the waveform of the pulse is modified, due to the attenuation and dispersion. In many media, a characteristic attenuation, which increases with frequency, has been observed. As result, the high frequency components of the pulse are more attenuated than the low frequency components. After crossing the layer, the transmitted pulse differs from the incident pulse, and it presents a different form (amplitude, frequency, phase) (He, 1998).
The patterns of ultrasonic pulses present important information regarding form, size and orientation of the reflections, as well as, the micro-structure of the propagation media of the pulses (Dermile & Saniie, 2001a), (Dermile & Saniie, 2001b).
Models of parametric signals are used to analyze ultrasonic pulses. These models are sensitive to the characteristics of the signal as bandwidth factor, return time, central frequency, amplitude and phase of the ultrasonic pulse. Some advantages have been discovered using signal modeling. First, estimates of parameters with high resolution can be found; second, the accuracy of the estimation can be evaluated; third, the analytical relationships between the parameters of the model and physical parameters of the system can be established. The ultrasonic pulses can be modeled in terms of Gaussian pulses, affected by noise. Each Gaussian pulse in the model is a non-linear function of the following parameters: bandwidth (α), return time (τ), central frequency (f_c), amplitude (β) and phase (φ). The estimation of these parameters can be obtained by non-linear parameter estimation techniques (Dermile & Saniie, 2001*a*), (Dermile & Saniie, 2001*b*).
Equation (1) is used by Dermile & Saniie (Dermile & Saniie, 2001*a*), (Dermile & Saniie, 2001*b*) to model the ultrasonic pulses.

$$S(\theta,t) = \beta e^{-\alpha(t-\tau)^2}\cos(2\pi fc(t-\tau)+\varphi) \tag{1}$$

Where $\theta = [\alpha\ \tau\ f_c\ \beta\ \varphi]$ represents the parameters to be estimated. The bandwidth determines the pulse time duration in the time domain, the return time is related with the location of the reflecting surface, the central frequency is governed by the frequency of the displacements in the material. The pulse displays an amplitude and a phase, according to the impedance, size and orientation of the reflecting surface. This model is used for parameter estimation, in combination with tests that use the pulse-echo method, and a transducer that operates as both, a pulser and receiver.

Considering the effect of the noise in the estimation, a noise process can be included to the model (Dermile & Saniie, 2001*a*), (Dermile & Saniie, 2001*b*). Thus, the ultrasonic pulse can be modeled by equation (2):

$$x(t) = S(\theta, t) + e(t) \tag{2}$$

Where $S(\theta,t)$ denotes the model of the ultrasonic pulse and $e(t)$ denotes the additive white Gaussian noise.

This model can be extended to consider multiple ultrasonic pulses by equation (3):

$$y(t) = \sum_{m=1}^{M} S(\theta_m, t) + e(t) \tag{3}$$

Each parametric vector θ_m defines the form and location of the corresponding pulse completely. For computer programming purposes, the observation model expressed by equation (2) for an ultrasonic pulse can be written in the discrete form (Dermile & Saniie, 2001*a*), (Dermile & Saniie, 2001*b*), (Silva et al., 2007).

The Gaussian pulse model has been chosen as the algorithm for parameter estimation, since this model is more accurate and the parameters resemble the ultrasonic pulse in a more complete approach. The Gaussian pulse model is thus appropriate to determine the parameters of the guided waves method and the analysis of the fouling process is achieved by observing the variation of the estimated parameters.

The estimation problem relies on the determination of the parameters of the model, and modifications of these parameters in presence of fouling. Here, the non-linear estimation approach is employed, using programs developed with the MATLAB code (Hansenlman & Littlefield, 1996).

3. Proposed system

The proposed system for fouling monitoring using ultrasonic transducers is illustrated by the block diagram presented in Fig. 4. This system is composed by the ultrasonic pulser and receiver which are connected to the transducers and coupled to the pipe, in order to generate longitudinal guided waves.

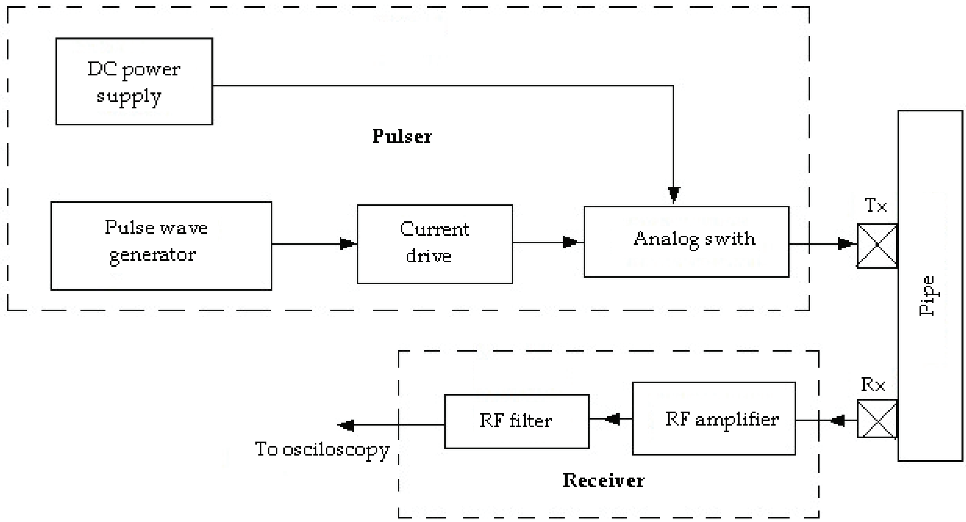

Figure 4. Block diagram of the proposed system with the pulser and receiver

The block diagram of the pulser circuit is shown in Fig. 5. The diagram comprises basically a DC power supply and a pulse wave generator, used to activate an analog switch, to obtain the pulses with the amplitude and frequency necessary to excite the ultrasonic transducer. A current drive is used to supply the current required by the analog switch.

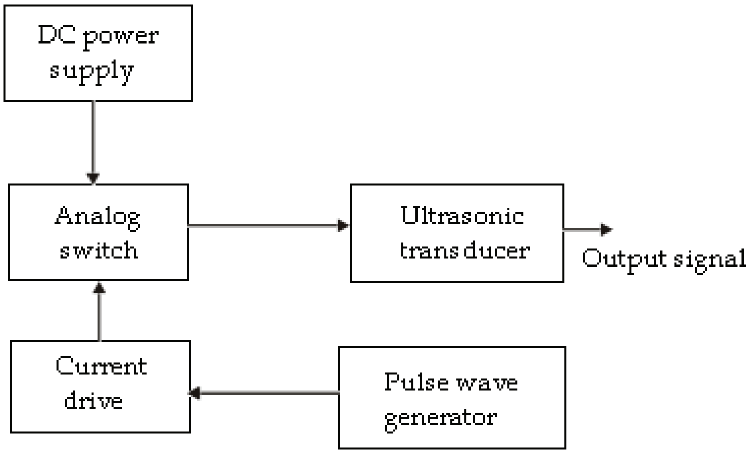

Figure 5. Block diagram of the pulser circuit

The waveform of the pulser output signal is shown in Fig. 6. This signal has 80 *V* maximum amplitude and 500 *kHz* frequency. These values are necessary for generation of the guided waves and monitoring at the receiver.

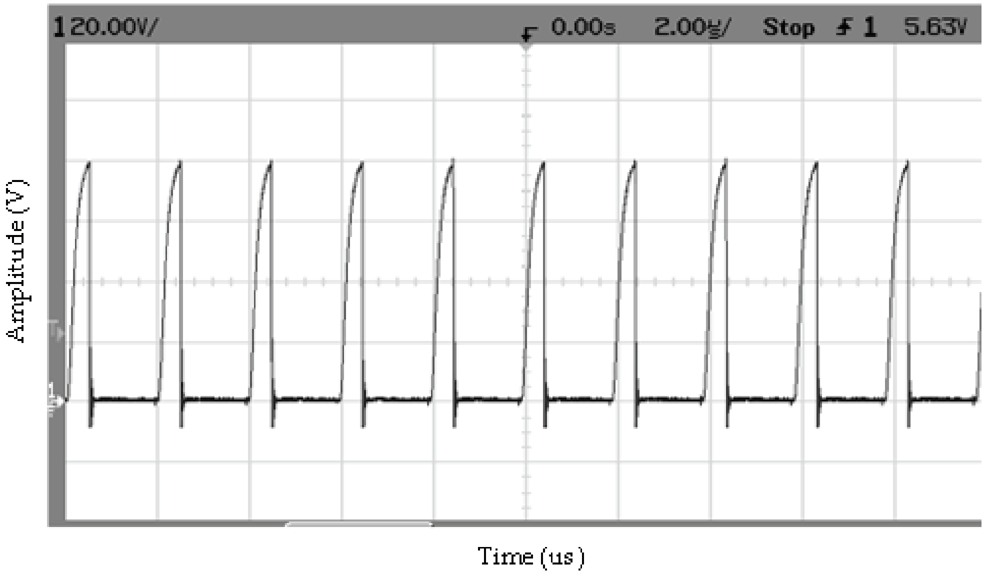

Figure 6. Waveform of the pulser output signal

The excitement signal of the pulser is a train of pulses with 80 *V* amplitude and 500 *kHz* frequency. This amplitude guarantees a minimum level of received signal (in the mV range), for smaller amplitude the received signal is too low to excite the receiver transducer. This frequency is necessary to guarantee the generation of the guided waves, once the propagation speed in the galvanized iron is known (4600 m/s) and the wavelength should be larger or equal than the pipe wall thickness (2.0 *mm*) (Silva et al., 2005).
A simplified block diagram of the receiver is presented in Fig. 7. In this diagram an initial amplification stage is used to increase the amplitude of the received signal, and a narrow band RF-filter to select the monitored signals.

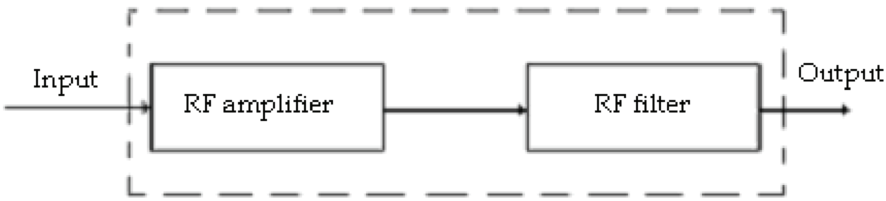

Figure 7. Simplified block diagram of the receiver

The receiver is designed, using amplification and filtering stages to detect the signals from the receiving transducer. The receiver circuit utilizes the integrated circuit AD8307, which is a logarithmic amplifier. Its output is a voltage value, proportional to the logarithm of the input signal amplitude, and its input impedance is equal to 50 Ω.

The waveform of the receiver output signal is presented in Fig. 8. This signal has 100 mV maximum amplitude and frequency in the MHz range, representing the typical feature of ultrasonic signals.

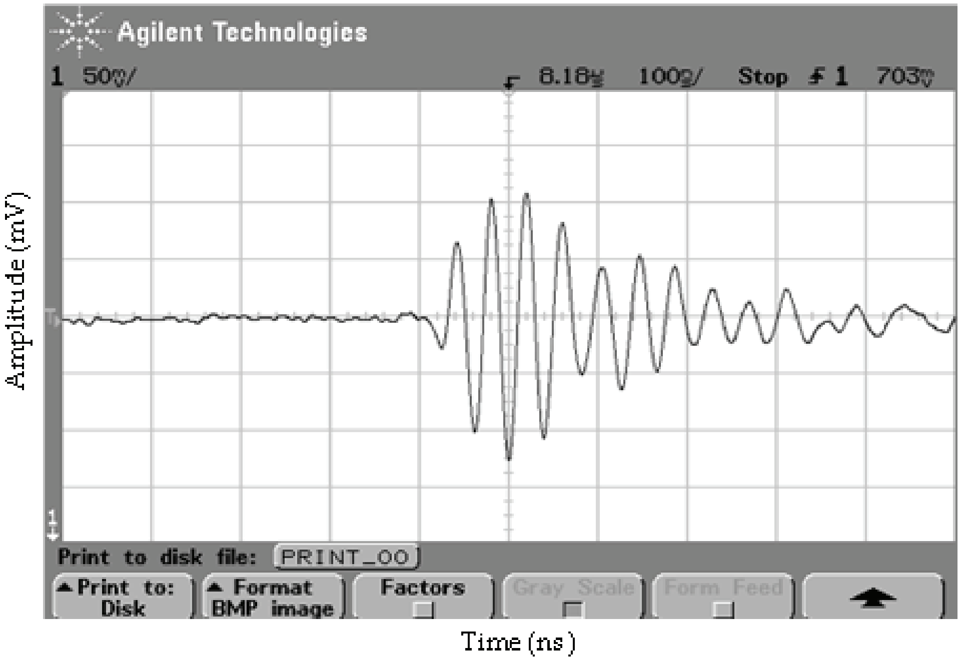

Figure 8. Waveform of the receiver output signal

The signals are monitored, using a digital oscilloscope. To detect the fouling layer, initially the amplitude reduction of the signals has been considered. However, towards an accurate analysis, other relevant features of the received signals are required as: frequency variations and phase. As mentioned before, the goal is to determine the parameters of a model for ultrasonic pulses and to analyze the variations of these parameters, under the effect of the fouling in the system. The fouling process was emulated by means of an experimental platform, in which the temperature, pressure and flow are monitored and controlled. Before each experiment, the tube was taken out of the experimental platform and the accelerated fouling layer deposition process inside the tube initiated. To speed up the fouling process, the same substances related to actual petroleum exploration were mixed with water and put into the pipe. The proportions of the substances deposited in the tube were subsequently increased. For 100 l of water, the following concentrations were used: 24.05 g of $Ca(OH)_2$; 9.9 g of $MgSO_4$; 2.472 kg of NaCl; and 16.99 g of $BaSO_4$. These proportions are the same, as found in the petroleum treatment factory of Petrobras in Guamare-RN-Brazil.
As outlined before, the model is used to determine the parameters using the method of the guided waves and the variation of the estimated parameters in the model of Gaussian pulses.
A diagram of the experimental platform for data acquisition is shown in Fig. 9. This platform was developed, in which the temperature, pressure and flow are monitored and

controlled (Silva, 2005). The tubes were used as a medium to guide ultrasonic waves and periodically over several weeks measurements were performed to monitor the fouling process (Silva et al., 2007).

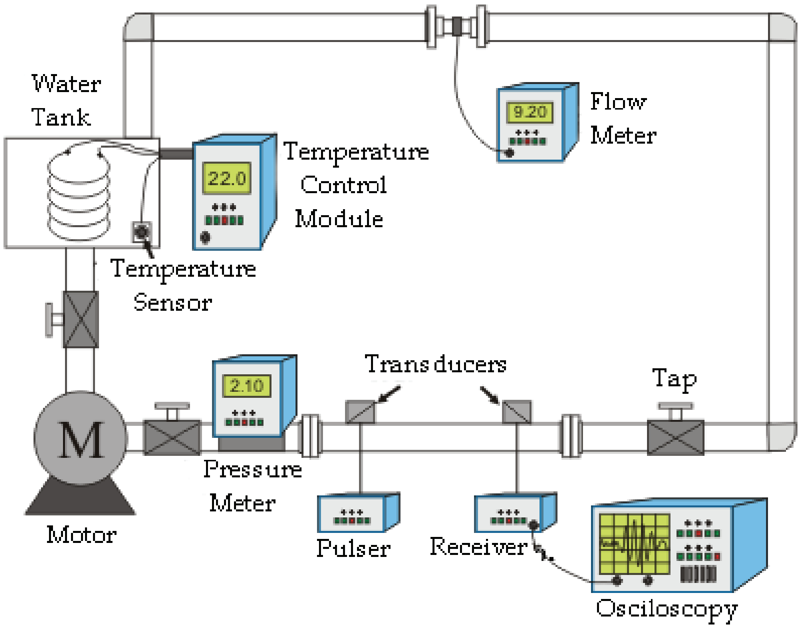

Figure 9. Diagram of the experimental platform

With the acquired data and using the models, the estimated parameters of the system have been used to analyze the behavior of the ultrasound signal and to observe the influence of the fouling. The non-linear estimation methods (least square non-linear) were used, with the software MATLAB, to determine the model parameters (Hansenlman & Littlefield, 1996).

4. Simulation results

A preliminary simulation study was accomplished by using the model for ultrasonic pulses provided in (1). The single pulse case was simulated and the parameter vector θ was estimated, using a program developed with MATLAB. In Table 1, the values obtained with the simulation for a single pulse are shown. The choice of θ_0, the initial parameter vector, is quite critical to obtain good results with relatively few iteration steps. The selection of the initial parameter relies on the characteristics of the observed signal.

	Real Parameters	Estimated Parameters
α	38.00	36.00
τ	0.70	0.50
f_c	18.00	16.00
β	0.80	0.70
φ	0.90	0.80

Table 1. Simulation results with single pulses

A signal with multiple pulses was also simulated with a program using MATLAB. In Table 2 are presented the values obtained with the simulation for multiple pulses.

	Real Parameters	Estimated Parameters
α_0	38.00	36.00
τ_0	0.70	0.50
f_{c0}	18.00	16.00
β_0	0.80	0.70
φ_0	0.90	0.80
α_1	38.00	36.00
τ_1	1.50	1.40
fc_1	16.00	14.00
β_1	0.60	0.50
φ_1	0.85	0.80

Table 2. Simulation results with multiple pulses

The results of simulation for the parameter estimation of a single pulse are presented in Fig. 10. The estimated parameters curve is quite similar with the real parameters curve. For this simulation the processing time is 4.42 *s*, the measurement error is 0.0099 (quadratic medium error) and the number of iterations is 20. The results of simulation for the parameter estimation of the signal with multiple pulses are presented in Fig. 11; this simulation also provides an excellent result in relation to the estimated parameters. For this simulation the processing time is 215.37 *s*, the measurement error is 0.0331 and the number of iterations is 40 (Silva et al., 2007).

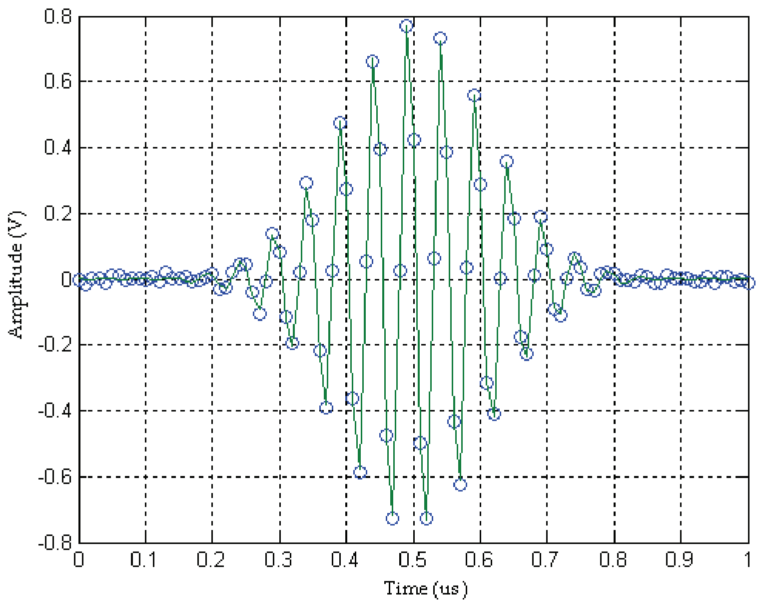

Figure 10. Results of the simulation for a single pulse: The points represent the real signal and the full line represents the estimated signal

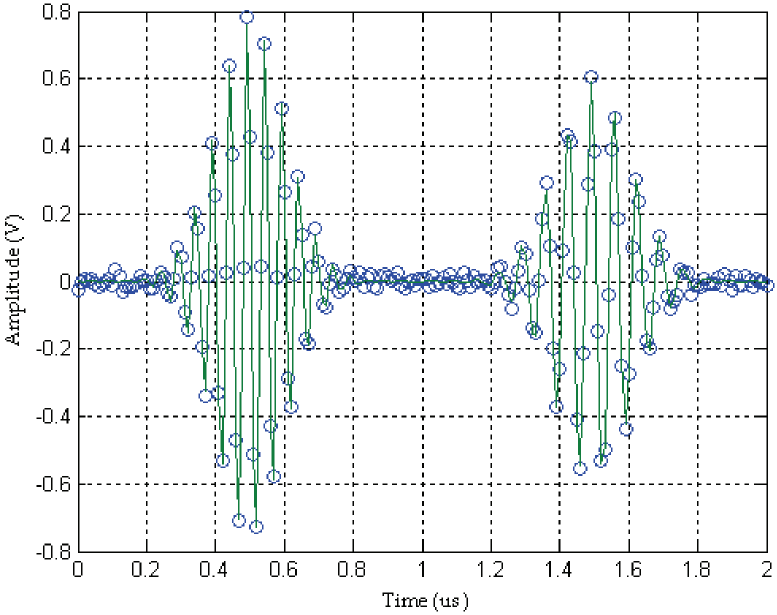

Figure 11. Results of the simulation for a multiple pulse: The points represent the real signal and the full line represents the estimated signal

As the number of ultrasonic pulses increases, the dimension of the parameter vector increases and, consequently the number of iteration steps also increases. To reduce the number of parameters to be estimated, we have employed spectral analysis (FFT) to determine what frequencies are present in the signal detected with multiple pulses, using MATLAB. The results of the simulation of a signal with multiple pulses and the FFT of this signal are presented in the Figs. 12 and 13 respectively. It was considered as parameters for the real signal: $\alpha_0 = 38$, $\tau_0 = 0.5$, $f_{c0} = 20$, $\beta_0 = 0.8$, $\varphi_0 = 1$; and $\alpha_1 = 28$, $\tau_1 = 1.0$, $f_{c1} = 15$, $\beta_1 = 0.6$, $\varphi_1 = 0.80$; and $\alpha_2 = 14$, $\tau_2 = 1.5$, $f_{c2} = 10$, $\beta_2 = 0.9$, $\varphi_2 = 0.90$. Using the FFT, the present frequencies in the signal can be determined accurately, thus reducing the number of parameters to be estimated. Fig. 13 shows the three present frequencies in the signal of the Fig. 12 (Silva et al., 2007).

With these simulations, it is possible to observe the behavior of the Gaussian pulses and to analyze the estimated parameters for these pulses, as well as to test the quality of the developed programs and to evaluate its performance. An important result in relation to the estimation procedure is the choice of the initial parameters, which is obtained from an observation of the measured signals. A bad choice increases the processing time substantially, and the estimation error.

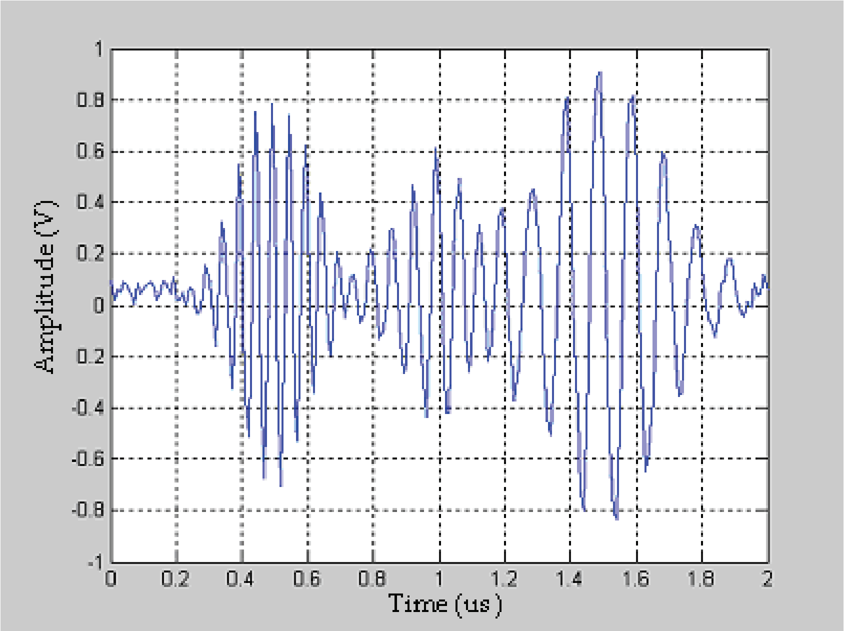

Figure 12. Representation of a signal with multiple pulses

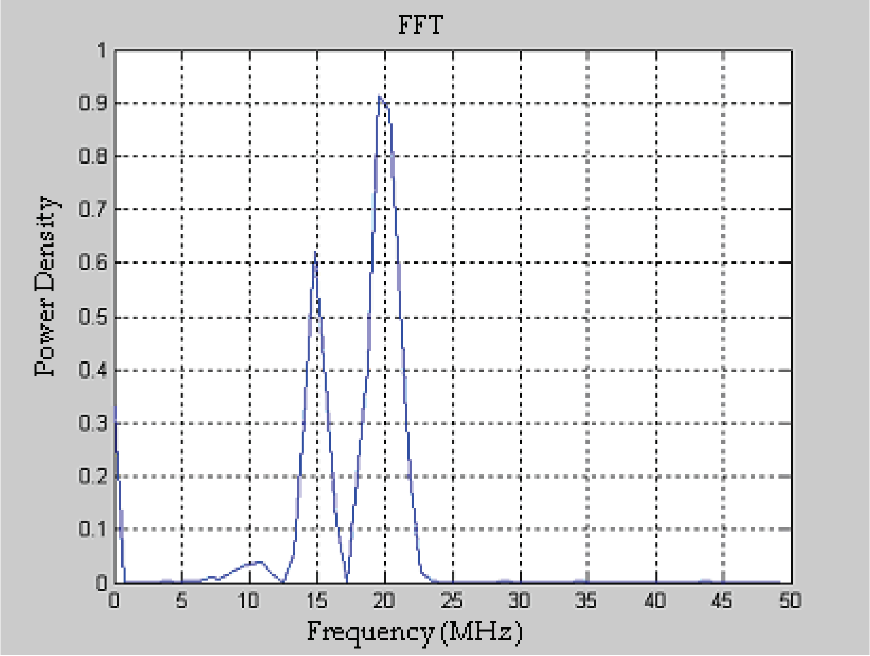

Figure 13. Representation of FFT for the signal of the Fig. 12.

5. Experimental results

A calibration step to define the pipeline signature is initially carried out and the pipe is completely cleaned, ensuring absence of a fouling layer. The inclination angle of the used transducers is 30^0. The maximum frequency of operation is 2 *MHz*, the transmitter is excited with pulses of 80 *V* and the sampling frequency is 100 *MHz*. The received signal is monitored, and the characteristics of these signals (amplitude, frequency, etc) are taken as reference for fouling detection.
The new results presented in this section were obtained with the same methodology presented in Silva (Silva et al., 2007).
In the experimental platform, it was possible to acquire the data in the receiver output by means of a digital oscilloscope. The obtained ultrasonic signals are illustrated in Figs. 14, 15 and 16, respectively. The signal shown in Fig. 14 represents the pipe signature, i.e., the pipe without fouling. The signal shown in Fig. 15 presents the pipe with 1 *mm* of fouling and Fig. 16 depicts an ultrasonic signal related to a pipe exhibiting a 3 *mm* fouling layer.
For the signal of Fig. 14, the processing time is 145.35 *s*, the measurement error is 2.65 (quadratic medium error) and the number of iterations is 8. For the signal of the Fig. 15 the processing time is 38.30 *s*, the measurement error is 1.25 and the number of iterations is 6. And for the signal of the Fig. 16 the processing time is 34.25 *s*, the measurement error is 1.15 and the number of iterations is 4.

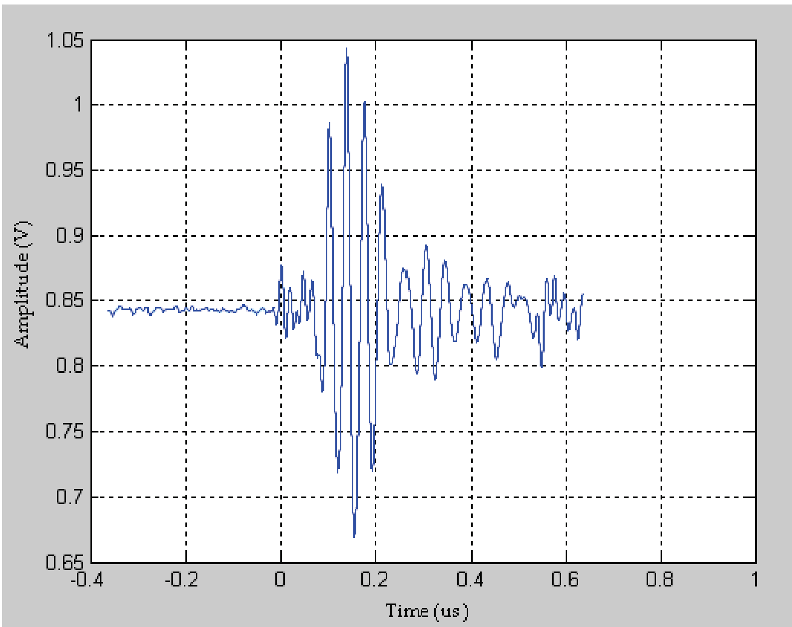

Figure 14. Representation of the receiver output signal without fouling using MATLAB

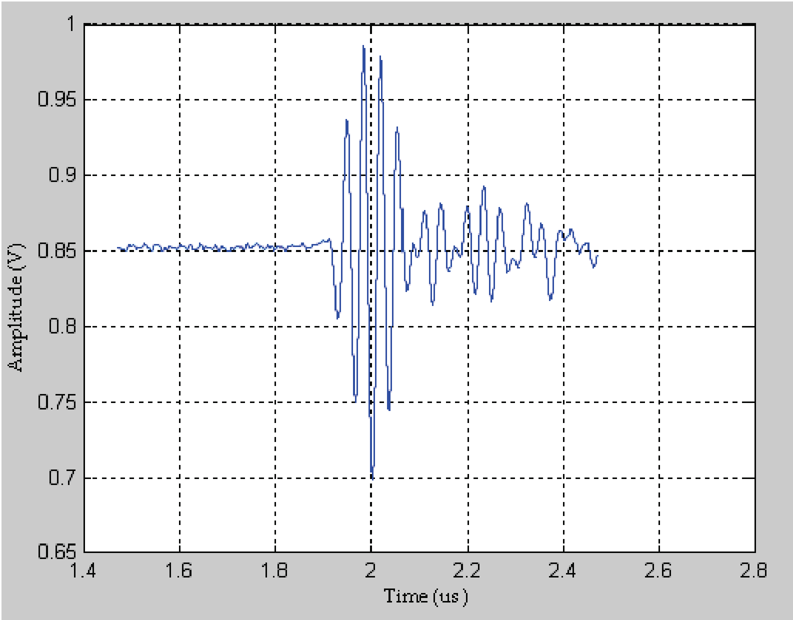

Figure 15. Representation of the receiver output signal with 1 *mm* of fouling using MATLAB

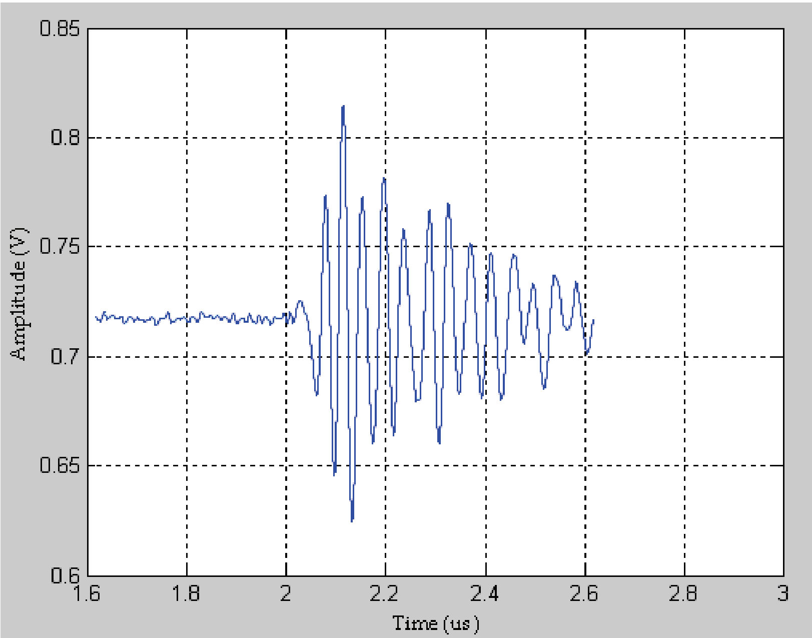

Figure 16. Representation of the receiver output signal with 3 *mm* of fouling using MATLAB

From the analysis of the ultrasonic signal, it was found that the amplitude reduction provides important information regarding the fouling process. This effect occurs, since the fouling layer modifies the propagation medium of the ultrasonic signals, thus providing a second leakage path in the received signal.

A further program, developed with MATLAB was used to determine the spectral features and frequencies in the measured signals in the time domain from Figs. 14, 15 and 16 respectively. The signals obtained with the FFT are represented in Figs. 17, 18 and 19 respectively. For the first signal, the determined frequency is 29 *MHz*, for the second signal (with 1 *mm* of fouling) the determined frequency is 27 *MHz* and for the third signal (with 3 *mm* of fouling) the determined frequency is 24 *MHz*. The estimated parameters for the frequency of the three signals represent a good approximation in relation to the measured real signal.

With the use of FFT, it was possible to determine the frequencies that are present in the ultrasonic signals. Since the frequencies of the pulses are not needed of being estimated and the number of parameters is reduced, the estimation times and the iteration numbers are also reduced.

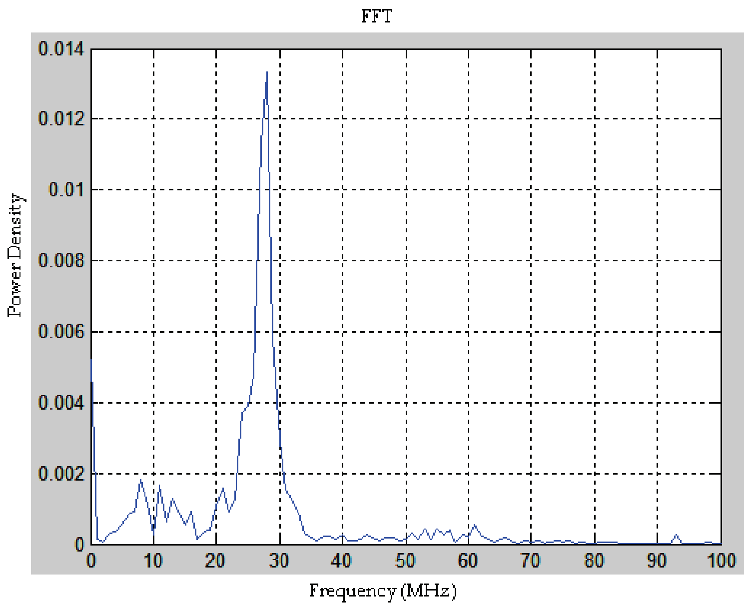

Figure 17. Representation of FFT for the measured signal without fouling

With the model for Gaussian pulses and using a program developed in MATLAB, it was possible to identify the parameters for the measured signal that are represented in Figs. 14, 15 and 16. The results with the parameter estimation for these signals are illustrated in Figs. 20, 21 and 22 respectively, and we can observe that the parameter modifications are due the fouling process in tubes.

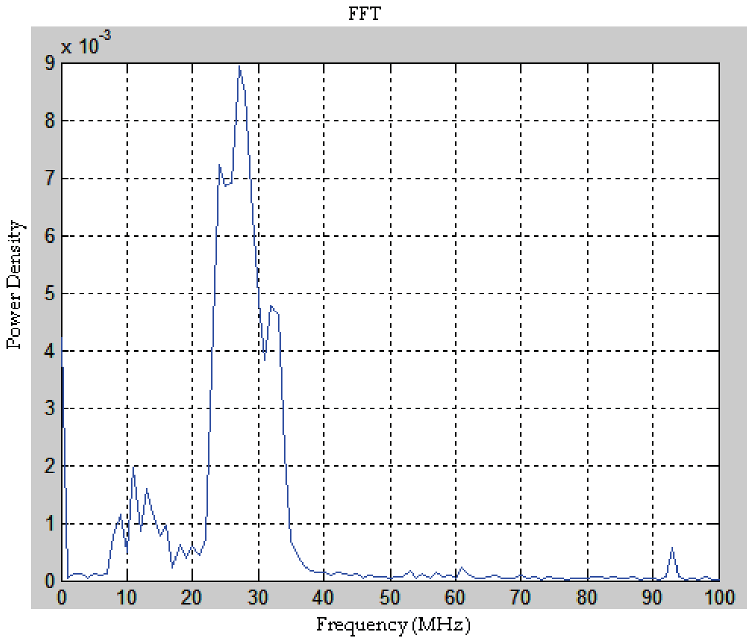

Figure 18. Representation of FFT for the measured signal with 1 *mm* of fouling

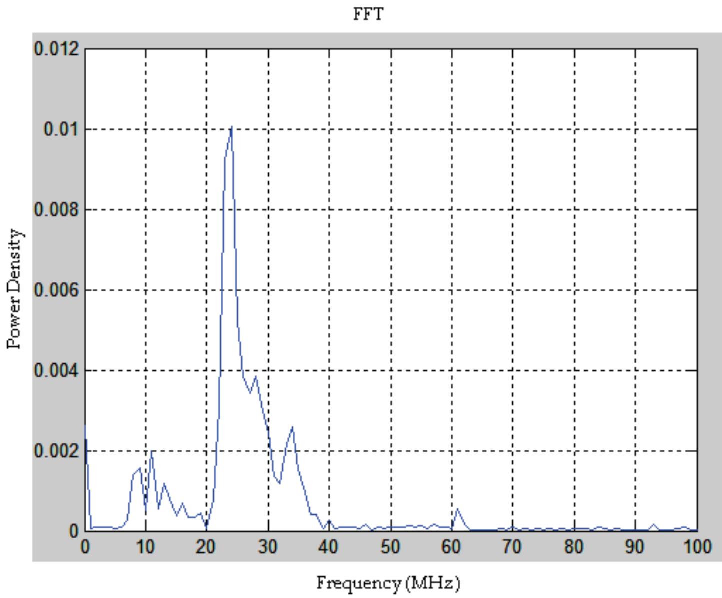

Figure 19. Representation of FFT for the measured signal with 3 *mm* of fouling

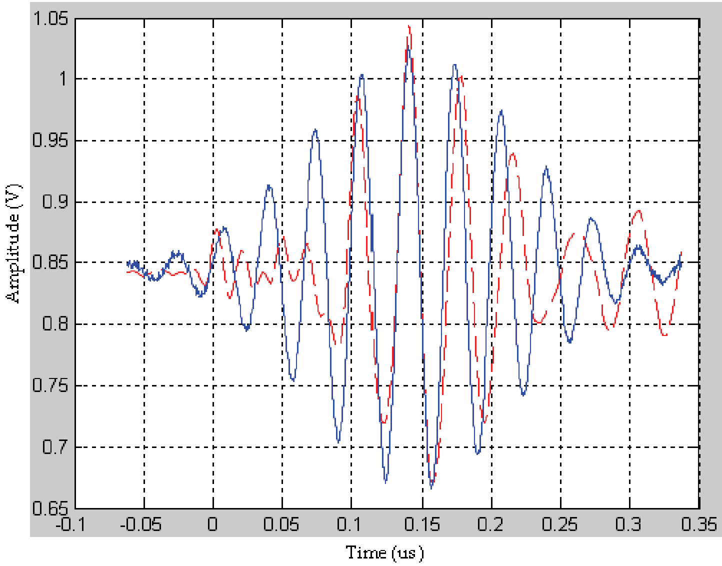

Figure 20. Representation of the measured signal (dashed signal) and of the estimated (continuous signal) without fouling

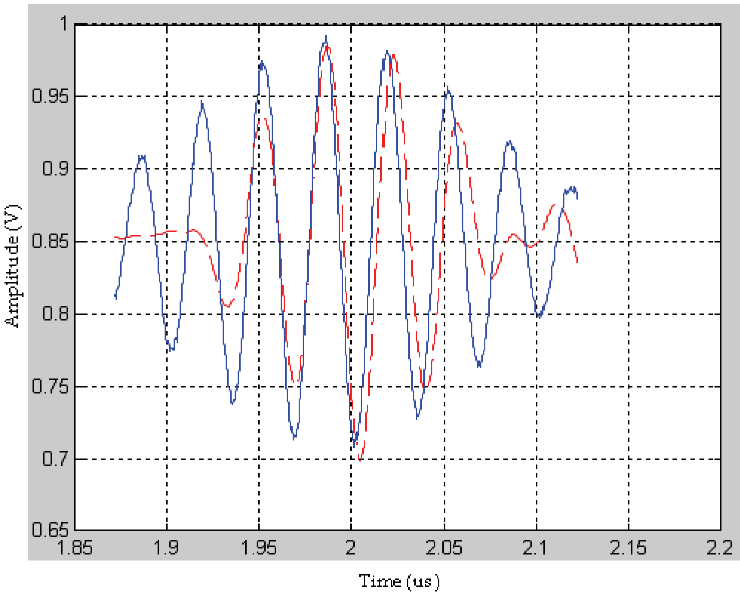

Figure 21. Representation of the measured signal (dashed signal) and of the estimated (continuous signal) with 1 *mm* of fouling

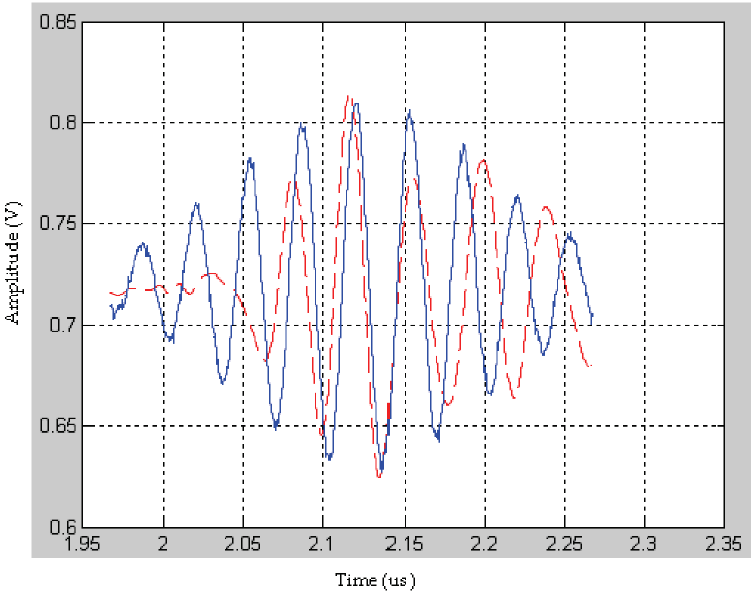

Figure 22. Representation of the measured signal (dashed signal) and of the estimated (continuous signal) with 3 *mm* of fouling

The estimated parameters for the signals are presented in the Table 3.

	Signal without fouling	**Signal with 1 *mm* of fouling**	**Signal with 3 *mm* of fouling**
α	85.0	80.0	75.0
τ	0.16	1.95	2.10
f_c	30.0	27.0	24.0
β	0.18	0.14	0.09
φ	0.80	0.85	0.90

Table 3. Estimated parameter values for the measured signal

Analyzing the data in Table 3, we observe that the parameters bandwidth (α), central frequency (f_c) and amplitude (β) decrease with the increase of the fouling layer, while the parameters return time (τ) and phase (φ) increase.

The presented models are considered as a good approach to resemble recorded real signals. Parameter variations resulting from the presence of tube fouling are well resolved. The absolute values of the signals are compared and modifications, as increase or reduction, of the absolute parameter values are easily observable.

6. Concluding remarks

In this chapter, a signal analysis method of ultrasonic signals has been presented and this method utilizes a parameter estimation algorithm for fouling detection. The model is based on Gaussian pulses, therefore this model is more complete and the parameter estimation provides higher accuracy. Results were obtained with simulations and with acquired experimental data. For treating of a non-linear system, this problem cannot be solved using optimization algorithms as efficient as the least square method.

Thus, programs were developed with MATLAB for estimation of non-linear systems. With the use of the Fast Fourier Transform (FFT) algorithm the spectral features i.e. frequencies present in the ultrasonic signals were resolved. Since the number of parameters is lowered, also the estimation time and number of required iterations are reduced.

With this approach presence of fouling layers can be easily detected, taking as reference the estimated parameters of the clean, fouling free tube section. Systematic variations of these parameters originate from inner tube fouling deposits. Different points of the pipe have been evaluated to identify their exact positions.

It is anticipated in future investigations to extend the analysis and include the attenuation rate of the received signal amplitude, in accordance with the amount of substance deposited onto the inner tube surface, and to verify the variation of the oscillations as a function of the substance type deposited inside the pipeline. In addition, it is also desired to evaluate other methods with ultrasonic waves, such as the circumferential guided wave method.

7. References

Calmon, P.; Roy, O. & Benoist, P. (2000). Simulation of Ultrasonic Examination. *IEEE Ultrasonic Symposium*. Pp.1265-1269, 2000.

Cam, E.; Lei, M.; Kocaarslan, I. & Taplamacioglu, C. (2002). Defect detection in a cantilever beam from vibration data. *Kirikkale University*. Faculty of Engineering, Department of Electrical and Electronics. Kirikkale, 2002.

Dermile, R. & Saniie, J. (2001*a*). Model-based estimation of ultrasonics echoes part I: Analysis and algorithms. *IEEE Transactions on ultrasonics, ferroeletrics and frequency control*. 2001.

Dermile, R. & Saniie, J. (2001*b*). Model-based estimation of ultrasonics echoes part II: Non-destructive evaluation applications. *IEEE Transactions on ultrasonics, ferroeletrics and frequency control*. 2001.

Fortunko, C. M. (1991). Generation and reception of ultrasonic signal. Ultrasonic Testing Equipment. *Nondestructive Testing Handbook*. 2 ed. Ultrasonic Testing. Vol. 7. USA. 1991.

Hansenlman, D. & Littlefield, B. (1996). *Mastering MATLAB - A comprehensive tutorial and reference*. Prentice Hall. USA, 1996.

Hay, T. R. & Rose, J. L. (2003). Fouling detection in the food industry using ultrasonic guided waves. *Food Control*. Elsevier. 2003.

He, P. (1998). Simulation of Ultrasound Pulse Propagation in Loss Media Obeying a Frequency Power Law. *IEEE Trans. on Ultrasonics, Ferroelectrics and Frequency Control*. Vol. 45, No.1, 1998.

Krisher, A. S. (2003). Technical information regarding coupon testing. *ASK Associates*. St. Louis, Missouri. November 2003.

Lohr, K. R. & Rose, J .L. (2002). Ultrasonic guided wave and acoustic impact methods for pipe fouling detection. *Journal of food engineering*. Elsevier Science, March 2002.

Panchal, C. B. (1997). Fouling mitigation of industrial heat exchange equipment. *Bengell House*. New York. 1997.

Rose, J. L. (1995). Recent advances in guided wave NDE. *IEEE Ultrasonic Symposium*. Pp.761-770. 1995.

Silva, J. J. (2005). *Development of a platform for fouling detection in pipelines*. Master's degree dissertation (in Portuguese). UFCG, Campina Grande, Brazil. 2005.

Silva, J. J.; Wanzeller, M. G.; Rocha Neto, J. S. & Farias, P. A. (2005). Development of circuits for excitement and reception in ultrasonic transducers for generation of guided waves in hollow cylinders for fouling detection. *IEEE Instrumentation and Measurement Technology Conference*. Ottawa, Ontario, Canada. 17-19 May 2005.

Silva, J. J.; Lima, A. M. N. & Rocha Neto, J. S. (2007). Fouling detection based on ultrasonic guided waves and parameter estimation. 3rd *IFAC Symposium on System, Structure and Control - SSSC 2007*. Foz do Iguaçu, Brazil, October, 2007.

Siqueira, M. H. S.; Gatts, C. E. N.; Silva, R. R. & Rebello, J. M. A. (2004). The use of ultrasonic guided waves and wavelets analysis in pipe inspection. *Ultrasonic*. Elsevier. Vol. 41, pp. 785-797. 2004.

7

Enhanced Fuzzy Controller for Nonlinear Systems: Membership-Function-Dependent Stability Analysis Approach

H.K. Lam and Mohammad Narimani
Division of Engineering, The King's College London, Strand, London
United Kingdom

1. Introduction

Fuzzy-model-based (FMB) control approach provides a systematic and effective way to control nonlinear systems. It has been shown by various applications (Lam et al., 1998; Lian et al., 2006; (b)Tanaka et al., 1998) that FMB control approach performs superior to some traditional control approaches. Based on the T-S fuzzy model (Sugeno & Kang, 1988; Takagi & Sugeno, 1985) the system dynamics of the nonlinear can be represented by some local linear models in the form of linear state-space equations. With the fuzzy logic technique, the overall system dynamics of the nonlinear plant is a fuzzy combination of the local linear models. Consequently, the fuzzy model offers a systematic way and general framework to represent the nonlinear plants in the form of averaged weighted sum of local linear systems. This particular structure exhibits favourable property to facilitate the system analysis and control synthesis.

In general, the stability analysis for FMB control systems can be classified into two categories, i.e., membership function (MF)-independent (Chen et al.,1993; Tanaka & Sugeno, 1992) and MF-dependent (Fang et al., 2006; Feng, 2006; Kim & Lee 2000; Liu & Zhang, 2003a; Liu & Zhang, 2003b; Tanaka et al., 1998a; Teixeira et al.,2003) stability analysis approaches. Under the MF-independent stability analysis, the membership functions of both fuzzy model and fuzzy controller are not considered during stability analysis. The system stability is guaranteed to be asymptotically stable if there exists a common positive definite matrix to a set of stability conditions in the form of Lyapunov inequalities (Chen et al.,1993; Tanaka & Sugeno, 1992). The main advantages under the MF-independent analysis approach are 1). The membership functions of the fuzzy controller can be designed freely. Some simple and easy-to-implement membership functions can be employed to realize the fuzzy controller to lower the implementation cost. 2). The grades of membership functions of the fuzzy model are not necessarily known which implies parameter uncertainties of the nonlinear plant are allowed. Consequently, the fuzzy controller exhibits an inherent robustness property for nonlinear plant subject to parameter uncertainties. However, the membership function mismatch (both fuzzy model and fuzzy controller do not share the same membership functions) leads to very conservative stability analysis results. Furthermore, it can be shown that the fuzzy controller designed based on the stability conditions in (Chen et al.,1993; Tanaka & Sugeno, 1992) can be replaced by a liner controller.

Under the MF-dependent stability analysis approach, the membership functions of both fuzzy model and fuzzy controller are considered. In (Wang et al., 1996), the importance of the membership functions to the stability analysis was shown. By sharing the same premise membership functions between fuzzy model and fuzzy controller which leads to perfect match of membership functions, relaxed stability conditions were achieved. Further relaxed MF-independent stability conditions were reported (Fang et al., 2006; Feng, 2006; Kim & Lee 2000; Liu & Zhang, 2003a; Liu & Zhang, 2003b; Tanaka et al., 1998a; Teixeira et al.,2003). As to achieve perfect match of membership functions between fuzzy model and fuzzy controller which implies the membership functions of the fuzzy model must be known, the design flexibility and inherent robustness property of the fuzzy controller are lost. In both MF-independent and dependent stability analysis approaches, the stability conditions can be represented in the form of linear matrix inequalities (Boyd et al., 1994), some convex programming techniques (e.g., MATLAB LMI toolbox) can be employed to solve the solution to the stability conditions numerically and effectively.

It can be seen that fuzzy controller designed based on stability conditions under MF-dependent or -independent stability analysis approaches offers different favourable and undesired properties. It is a good idea to get the most out of these two analysis approaches by combining the advantages and alleviate the disadvantages of them, thus, to widen the applicability of the FMB control approach. This idea motivates the investigation in this chapter. In this chapter, MF-dependent stability analysis approach is employed to investigate the stability of the FMB control systems under the condition of imperfect match of membership functions. As a result, the design flexibility and inherent robustness of the fuzzy controller can be retained (due to the imperfect match of the membership functions) and the stability conditions can be relaxed (due to the MF-dependent stability analysis approach). In order to strengthen the stabilization ability of the fuzzy controller, fuzzy feedback gains, which enhance the nonlinearity compensation ability, are introduced. In order to carry out stability analysis under MF-dependent Lyapunov-based approach, membership function conditions are proposed to guide the design of the membership functions. Based on membership function conditions, some free matrices can be introduced to the stability analysis and relax the stability conditions.

This chapter is organized as follows. In section II, the fuzzy model and the proposed fuzzy controller are introduced. In section III, system stability of FMB control system is investigated using Lyapunov's stability theory under MF-dependent stability analysis approach. LMI-based stability conditions are derived to aid the design of the fuzzy controller for the nonlinear plant. In section IV, simulation examples are given to illustrate the effectiveness of the proposed approach. In section V, a conclusion is drawn.

2. Fuzzy Model and Enhanced Fuzzy Controller

A fuzzy-model-based control system comprising a nonlinear plant represented by a fuzzy model and an enhanced fuzzy controller connected in a closed loop is considered.

2.1 Fuzzy Model

Let p be the number of fuzzy rules describing the nonlinear plant. The i-th rule is of the following format:

Rule i: IF $f_1(\mathbf{x}(t))$ is M_1^i AND … AND $f_\Psi(\mathbf{x}(t))$ is M_Ψ^i

$$\text{THEN } \dot{\mathbf{x}}(t) = \mathbf{A}_i\mathbf{x}(t) + \mathbf{B}_i\mathbf{u}(t) \tag{1}$$

where M_α^i is a fuzzy term of rule i corresponding to the known function $f_\alpha(\mathbf{x}(t))$, $\alpha = 1, 2, \ldots, \Psi$; $i = 1, 2, \ldots, p$; Ψ is a positive integer; $\mathbf{A}_i \in \Re^{n\times n}$ and $\mathbf{B}_i \in \Re^{n\times m}$ are known constant system and input matrices respectively; $\mathbf{x}(t) \in \Re^{n\times 1}$ is the system state vector and $\mathbf{u}(t) \in \Re^{m\times 1}$ is the input vector. The system dynamics are described by,

$$\dot{\mathbf{x}}(t) = \sum_{i=1}^{p} w_i(\mathbf{x}(t))\big(\mathbf{A}_i\mathbf{x}(t) + \mathbf{B}_i\mathbf{u}(t)\big) \tag{2}$$

where,

$$\sum_{i=1}^{p} w_i(\mathbf{x}(t)) = 1,\ w_i(\mathbf{x}(t)) \in [0 \quad 1] \text{ for all } i \tag{3}$$

$$w_i(\mathbf{x}(t)) = \frac{\mu_{\mathrm{M}_1^i}(f_1(\mathbf{x}(t))) \times \mu_{\mathrm{M}_2^i}(f_2(\mathbf{x}(t))) \times \cdots \times \mu_{\mathrm{M}_\Psi^i}(f_\Psi(\mathbf{x}(t)))}{\sum_{k=1}^{p}\Big(\mu_{\mathrm{M}_1^k}(f_1(\mathbf{x}(t))) \times \mu_{\mathrm{M}_2^k}(f_2(\mathbf{x}(t))) \times \cdots \times \mu_{\mathrm{M}_\Psi^k}(f_\Psi(\mathbf{x}(t)))\Big)} \tag{4}$$

is a nonlinear function of $\mathbf{x}(t)$ and $\mu_{\mathrm{M}_\alpha^i}(f_\alpha(\mathbf{x}(t)))$, $\alpha = 1, 2, \ldots, \Psi$, is the grade of membership corresponding to the fuzzy term of M_α^i.

2.2. Enhanced Fuzzy Controller

A fuzzy controller with p rules is considered. The j-th rule of the fuzzy controller is defined as follows.

Rule j: IF $g_1(\mathbf{x}(t))$ is N_1^j AND … AND $g_\Omega(\mathbf{x}(t))$ is N_Ω^j

$$\text{THEN } \mathbf{u}(t) = \mathbf{G}_j\big(\mathbf{x}(t)\big)\mathbf{x}(t),\ j = 1, 2, \ldots, p \tag{5}$$

where N_β^j is a fuzzy term of rule j corresponding to the function $g_\beta(\mathbf{x}(t))$, $\beta = 1, 2, \ldots, \Omega$; $j = 1, 2, \ldots, p$; Ω is a positive integer; $\mathbf{G}_j\big(\mathbf{x}(t)\big) \in \Re^{m\times n}$ is the constant and time-varying feedback gains of rule j. The time-varying feedback gain is defined as,

$$\mathbf{G}_j\big(\mathbf{x}(t)\big) = \sum_{k=1}^{p} m_k(\mathbf{x}(t))\mathbf{G}_{jk} \tag{6}$$

where $\mathbf{G}_{jk} \in \Re^{m\times n}$ are constant feedback gains. The inferred enhanced fuzzy controller is defined as,

$$\mathbf{u}(t) = \sum_{j=1}^{p}\sum_{k=1}^{p} m_j(\mathbf{x}(t))m_k(\mathbf{x}(t))\mathbf{G}_{jk}\mathbf{x}(t) \tag{7}$$

where

$$\sum_{j=1}^{p} m_j(\mathbf{x}(t)) = 1, \; m_j(\mathbf{x}(t)) \in [0 \quad 1], \; j = 1, 2, \ldots, p \tag{8}$$

$$m_j(\mathbf{x}(t)) = \frac{\mu_{\mathrm{N}_1^j}(g_1(\mathbf{x}(t))) \times \mu_{\mathrm{N}_2^j}(g_2(\mathbf{x}(t))) \times \cdots \times \mu_{\mathrm{N}_\Omega^j}(g_\Omega(\mathbf{x}(t)))}{\sum_{k=1}^{p}\left(\mu_{\mathrm{N}_1^k}(g_1(\mathbf{x}(t))) \times \mu_{\mathrm{N}_2^k}(g_2(\mathbf{x}(t))) \times \cdots \times \mu_{\mathrm{N}_\Omega^k}(g_\Omega(\mathbf{x}(t)))\right)} \tag{9}$$

is the normalized grade of membership which is a nonlinear function of $\mathbf{x}(t)$. $\mu_{\mathrm{N}_\beta^j}(g_\beta(\mathbf{x}(t)))$, $j = 1, 2, \ldots, p$, is the grade of membership corresponding to the fuzzy term N_β^j.

Remark 1: It should be noted that the proposed enhanced fuzzy controller of (7) is reduced to the traditional fuzzy controller (Chen et al., 1993; Fang et al., 2006; Feng, 2006; Liu & Zhang, 2003a; Liu & Zhang, 2003b; Tanaka et al., 1998a; Teixeira et al., 2003; Wang et al., 1996) when $\mathbf{G}_{jk} = \mathbf{F}_j$ for all j where $\mathbf{F}_j \in \Re^{m \times n}$ are the constant feedback gains.

3. Stability Analysis

In this section, the system stability of fuzzy-model-based control system formed by a nonlinear plant in the form of (2) and the enhanced fuzzy controller of (7) connected in a closed loop, is considered. Based on the Lyapunov stability theory, LMI-based stability conditions are derived to guarantee the asymptotic stability of the fuzzy-model-based control systems. For brevity, $w_i(\mathbf{x}(t))$ and $m_j(\mathbf{x}(t))$ are denoted as w_i and m_j respectively. The property of the membership functions in (3) and (8), i.e. $\sum_{i=1}^{p} w_i = \sum_{i=1}^{p} m_i = \sum_{i=1}^{p}\sum_{j=1}^{p} w_i m_j = 1$ is utilized to facilitate the stability analysis. From (2) and (7), we have,

$$\begin{aligned}\dot{\mathbf{x}}(t) &= \sum_{i=1}^{p} w_i \left(\mathbf{A}_i \mathbf{x}(t) + \mathbf{B}_i \sum_{j=1}^{p}\sum_{k=1}^{p} m_j m_k \mathbf{G}_{jk} \mathbf{x}(t) \right) \\ &= \sum_{i=1}^{p}\sum_{j=1}^{p}\sum_{k=1}^{p} w_i m_j m_k \left(\mathbf{A}_i + \mathbf{B}_i \mathbf{G}_{jk} \right) \mathbf{x}(t) \end{aligned} \tag{10}$$

As the membership functions of w_i and m_j do not match, which is one of the sources of conservativeness, the MF-dependent stability analysis approach in (Fang et al., 2006; Feng, 2006; Liu & Zhang, 2003a; Liu & Zhang, 2003b; Tanaka et al., 1998a; Teixeira et al., 2003) cannot be applied. In the following, membership function conditions are proposed to alleviate the conservativeness of stability analysis due to the imperfect match of membership functions. To proceed with the stability analysis, the following Lyapunov function candidate is employed to investigate the fuzzy-model-based control system of (10).

$$V(t) = \mathbf{x}(t)^{\mathrm{T}} \mathbf{P} \mathbf{x}(t) \tag{11}$$

where $\mathbf{P} = \mathbf{P}^{\mathrm{T}} \in \Re^{n \times n} > 0$. From (10) and (11),

$$\begin{aligned}
\dot{V}(t) &= \dot{\mathbf{x}}(t)^{\mathrm{T}}\mathbf{P}\mathbf{x}(t) + \mathbf{x}(t)^{\mathrm{T}}\mathbf{P}\dot{\mathbf{x}}(t) \\
&= \left(\sum_{i=1}^{p}\sum_{j=1}^{p}\sum_{k=1}^{p} w_i m_j m_k \left(\mathbf{A}_i + \mathbf{B}_i\mathbf{G}_{jk}\right)\mathbf{x}(t)\right)^{\mathrm{T}}\mathbf{P}\mathbf{x}(t) \\
&\quad + \mathbf{x}(t)^{\mathrm{T}}\mathbf{P}\left(\sum_{i=1}^{p}\sum_{j=1}^{p}\sum_{k=1}^{p} w_i m_j m_k \left(\mathbf{A}_i + \mathbf{B}_i\mathbf{G}_{jk}\right)\mathbf{x}(t)\right) \\
&= \sum_{i=1}^{p}\sum_{j=1}^{p}\sum_{k=1}^{p} w_i m_j m_k \mathbf{x}(t)\left(\left(\mathbf{A}_i + \mathbf{B}_i\mathbf{G}_{jk}\right)^{\mathrm{T}}\mathbf{P} + \mathbf{P}\left(\mathbf{A}_i + \mathbf{B}_i\mathbf{G}_{jk}\right)\right)\mathbf{x}(t) \\
&= \sum_{i=1}^{p}\sum_{j=1}^{p}\sum_{k=1}^{p} w_i m_j m_k \mathbf{z}(t)^{\mathrm{T}}\left(\mathbf{X}\left(\mathbf{A}_i + \mathbf{B}_i\mathbf{G}_{jk}\right)^{\mathrm{T}} + \left(\mathbf{A}_i + \mathbf{B}_i\mathbf{G}_{jk}\right)\mathbf{X}\right)\mathbf{z}(t) \qquad (12)
\end{aligned}$$

where $\mathbf{z}(t) = \mathbf{X}^{-1}\mathbf{x}(t)$ and $\mathbf{X} = \mathbf{P}^{-1} \in \Re^{n \times n}$. Let $\mathbf{G}_{jk} = \mathbf{N}_{jk}\mathbf{X}^{-1}$ where $\mathbf{N}_{jk} \in \Re^{m \times n}$. From (12), we have,

$$\dot{V}(t) = \sum_{i=1}^{p}\sum_{j=1}^{p}\sum_{k=1}^{p} w_i m_j m_k \mathbf{z}(t)^{\mathrm{T}}\mathbf{\Theta}_{ijk}\mathbf{z}(t) \qquad (13)$$

where $\mathbf{\Theta}_{ijk} = \mathbf{A}_i\mathbf{X} + \mathbf{X}\mathbf{A}_i^{\mathrm{T}} + \mathbf{B}_i\mathbf{N}_{jk} + \mathbf{N}_{jk}^{\mathrm{T}}\mathbf{B}_i^{\mathrm{T}}$. To facilitate the stability analysis, the membership functions of the fuzzy controllers are designed as follows.

$$\overline{w}_i = w_i - \left(\rho_i m_i + \sigma_i\right) > 0,\ i = 1, 2, \ldots, p \qquad (14)$$

where ρ_i and σ_i are scalars to be determined. From (12), we have,

$$\begin{aligned}
\dot{V}(t) &= \sum_{i=1}^{p}\sum_{j=1}^{p}\sum_{k=1}^{p}\left(w_i + \left(\rho_i m_i + \sigma_i\right) - \left(\rho_i m_i + \sigma_i\right)\right) m_j m_k \mathbf{z}(t)^{\mathrm{T}}\mathbf{\Theta}_{ijk}\mathbf{z}(t) \\
&= \sum_{i=1}^{p}\sum_{j=1}^{p}\sum_{k=1}^{p} m_i m_j m_k \mathbf{z}(t)^{\mathrm{T}}\rho_i\mathbf{\Theta}_{ijk}\mathbf{z}(t) + \sum_{i=1}^{p}\sum_{j=1}^{p}\sum_{k=1}^{p} m_j m_k \mathbf{z}(t)^{\mathrm{T}}\sigma_i\mathbf{\Theta}_{ijk}\mathbf{z}(t) \\
&\quad + \sum_{i=1}^{p}\sum_{j=1}^{p}\sum_{k=1}^{p}\overline{w}_i m_j m_k \mathbf{z}(t)^{\mathrm{T}}\mathbf{\Theta}_{ijk}\mathbf{z}(t) \\
&= \sum_{i=1}^{p}\sum_{j=1}^{p}\sum_{k=1}^{p} m_i m_j m_k \mathbf{z}(t)^{\mathrm{T}}\left(\rho_i\mathbf{\Theta}_{ijk} + \sum_{l=1}^{p}\sigma_l\mathbf{\Theta}_{ljk}\right)\mathbf{z}(t) \\
&\quad + \sum_{i=1}^{p}\sum_{j=1}^{p}\sum_{k=1}^{p}\overline{w}_i m_j m_k \mathbf{z}(t)^{\mathrm{T}}\mathbf{\Theta}_{ijk}\mathbf{z}(t) \qquad (15)
\end{aligned}$$

To alleviate the conservativeness of the stability analysis, from (14), we consider the following conditions.

$$w_i - \left(\rho_i m_i + \sigma_i\right) - \left(\gamma_i m_i + \zeta_i\right) = \overline{w}_i - \left(\gamma_i m_i + \zeta_i\right) < 0,\ i = 1, 2, \ldots, p \qquad (16)$$

where γ_i and ζ_i are scalars to be determined. The membership function conditions of (14) and (16) offer the condition to guide the design of the membership functions of fuzzy controller. Under these conditions, some free matrices can be introduced to relax the conservativeness of stability analysis due to the imperfect match of membership functions. From (16), we consider the following condition to introduce some free matrices to (15).

$$-\sum_{i=1}^{p}\sum_{j=1}^{p}\sum_{k=1}^{p}\overline{w}_i\left(\overline{w}_j-\left(\gamma_j m_j+\zeta_j\right)\right)m_k\left(\mathbf{S}_{ijk}+\mathbf{S}_{ijk}{}^{\mathrm{T}}\right)\geq 0 \tag{17}$$

where $\mathbf{S}_{ijk}=\mathbf{S}_{jik}{}^{\mathrm{T}}\in\Re^{n\times n}$ and $\mathbf{S}_{ijk}+\mathbf{S}_{ijk}{}^{\mathrm{T}}\geq 0$, j, k = 1, 2, ..., p; $i<j$. Furthermore, considering the property of the membership functions in (3) and (8), we have $\sum_{i=1}^{p}\left(w_i-m_i\right)=0$ which leads to $\sum_{i=1}^{p}\sum_{j=1}^{p}\sum_{k=1}^{p}\left(w_i-m_i\right)m_j m_k\left(\mathbf{V}_{jk}+\mathbf{V}_{jk}{}^{\mathrm{T}}\right)=\mathbf{0}$ for arbitrary matrix of $\mathbf{V}_{jk}\in\Re^{n\times n}$. From (15) and (17), we have,

$$\begin{aligned}
\dot{V}(t)\leq{}&\sum_{i=1}^{p}\sum_{j=1}^{p}\sum_{k=1}^{p}m_i m_j m_k\mathbf{z}(t)^{\mathrm{T}}\left(\rho_i\mathbf{\Theta}_{ijk}+\sum_{l=1}^{p}\sigma_l\mathbf{\Theta}_{ljk}\right)\mathbf{z}(t)\\
&+\sum_{i=1}^{p}\sum_{j=1}^{p}\sum_{k=1}^{p}\overline{w}_i m_j m_k\mathbf{z}(t)^{\mathrm{T}}\mathbf{\Theta}_{ijk}\mathbf{z}(t)+\sum_{i=1}^{p}\sum_{j=1}^{p}\sum_{k=1}^{p}\left(w_i-m_i\right)m_j m_k\mathbf{z}(t)^{\mathrm{T}}\left(\mathbf{V}_{jk}+\mathbf{V}_{jk}{}^{\mathrm{T}}\right)\mathbf{z}(t)\\
&-\sum_{i=1}^{p}\sum_{j=1}^{p}\overline{w}_i\left(\overline{w}_j-\left(\gamma_j m_j+\zeta_j\right)\right)m_k\mathbf{z}(t)^{\mathrm{T}}\left(\mathbf{S}_{ijk}+\mathbf{S}_{ijk}{}^{\mathrm{T}}\right)\mathbf{z}(t)\\
={}&\sum_{i=1}^{p}\sum_{j=1}^{p}\sum_{k=1}^{p}m_i m_j m_k\mathbf{z}(t)^{\mathrm{T}}\left(\rho_i\mathbf{\Theta}_{ijk}+\sum_{l=1}^{p}\sigma_l\mathbf{\Theta}_{ljk}-\left(\mathbf{V}_{jk}+\mathbf{V}_{jk}{}^{\mathrm{T}}\right)\right)\mathbf{z}(t)\\
&+\sum_{i=1}^{p}\sum_{j=1}^{p}\sum_{k=1}^{p}\overline{w}_i m_j m_k\mathbf{z}(t)^{\mathrm{T}}\mathbf{\Theta}_{ijk}\mathbf{z}(t)+\sum_{i=1}^{p}\sum_{j=1}^{p}\sum_{k=1}^{p}w_i m_j m_k\mathbf{z}(t)^{\mathrm{T}}\left(\mathbf{V}_{jk}+\mathbf{V}_{jk}{}^{\mathrm{T}}\right)\mathbf{z}(t)\\
&-\sum_{i=1}^{p}\sum_{j=1}^{p}\sum_{k=1}^{p}\overline{w}_i\left(\overline{w}_j-\left(\gamma_j m_j+\zeta_j\right)\right)m_k\mathbf{z}(t)^{\mathrm{T}}\left(\mathbf{S}_{ijk}+\mathbf{S}_{ijk}{}^{\mathrm{T}}\right)\mathbf{z}(t)\\
={}&\sum_{i=1}^{p}\sum_{j=1}^{p}\sum_{k=1}^{p}m_i m_j m_k\mathbf{z}(t)^{\mathrm{T}}\left(\rho_i\mathbf{\Theta}_{ijk}+\sum_{l=1}^{p}\sigma_l\mathbf{\Theta}_{ljk}-\left(\mathbf{V}_{jk}+\mathbf{V}_{jk}{}^{\mathrm{T}}\right)\right)\mathbf{z}(t)\\
&+\sum_{i=1}^{p}\sum_{j=1}^{p}\sum_{k=1}^{p}\overline{w}_i m_j m_k\mathbf{z}(t)^{\mathrm{T}}\mathbf{\Theta}_{ijk}\mathbf{z}(t)\\
&+\sum_{i=1}^{p}\sum_{j=1}^{p}\sum_{k=1}^{p}\left(w_i+\left(\rho_i m_i+\sigma_i\right)-\left(\rho_i m_i+\sigma_i\right)\right)m_j m_k\mathbf{z}(t)^{\mathrm{T}}\left(\mathbf{V}_{jk}+\mathbf{V}_{jk}{}^{\mathrm{T}}\right)\mathbf{z}(t)\\
&-\sum_{i=1}^{p}\sum_{j=1}^{p}\sum_{k=1}^{p}\overline{w}_i\left(\overline{w}_j-\left(\gamma_j m_j+\zeta_j\right)\right)m_k\mathbf{z}(t)^{\mathrm{T}}\left(\mathbf{S}_{ijk}+\mathbf{S}_{ijk}{}^{\mathrm{T}}\right)\mathbf{z}(t)
\end{aligned}$$

$$
\begin{aligned}
&= \sum_{i=1}^{p}\sum_{j=1}^{p}\sum_{k=1}^{p} m_i m_j m_k \mathbf{z}(t)^{\mathrm{T}}\left(\rho_i \mathbf{\Theta}_{ijk} + \sum_{l=1}^{p}\sigma_l \mathbf{\Theta}_{ljk} - \left(\mathbf{V}_{jk} + \mathbf{V}_{jk}^{\mathrm{T}}\right)\right)\mathbf{z}(t) \\
&+ \sum_{i=1}^{p}\sum_{j=1}^{p}\sum_{k=1}^{p} \overline{w}_i m_j m_k \mathbf{z}(t)^{\mathrm{T}}\left(\mathbf{\Theta}_{ijk} + \mathbf{V}_{jk} + \mathbf{V}_{jk}^{\mathrm{T}}\right)\mathbf{z}(t) \\
&+ \sum_{i=1}^{p}\sum_{j=1}^{p}\sum_{k=1}^{p} m_i m_j m_k \mathbf{z}(t)^{\mathrm{T}}\left(\rho_i\left(\mathbf{V}_{jk} + \mathbf{V}_{jk}^{\mathrm{T}}\right) + \sum_{l=1}^{p}\sigma_l\left(\mathbf{V}_{jk} + \mathbf{V}_{jk}^{\mathrm{T}}\right)\right)\mathbf{z}(t) \\
&- \sum_{i=1}^{p}\sum_{j=1}^{p}\sum_{k=1}^{p} \overline{w}_i \left(\overline{w}_j - \left(\gamma_j m_j + \zeta_j\right)\right) m_k \mathbf{z}(t)^{\mathrm{T}}\left(\mathbf{S}_{ijk} + \mathbf{S}_{ijk}^{\mathrm{T}}\right)\mathbf{z}(t)
\end{aligned}
$$

$$
\begin{aligned}
&= \sum_{i=1}^{p}\sum_{j=1}^{p}\sum_{k=1}^{p} m_i m_j m_k \mathbf{z}(t)^{\mathrm{T}}\left(\rho_i \mathbf{\Theta}_{ijk} + \sum_{l=1}^{p}\sigma_l\left(\mathbf{\Theta}_{ljk} + \mathbf{V}_{jk} + \mathbf{V}_{jk}^{\mathrm{T}}\right) + \left(\rho_i - 1\right)\left(\mathbf{V}_{jk} + \mathbf{V}_{jk}^{\mathrm{T}}\right)\right)\mathbf{z}(t) \\
&+ \sum_{i=1}^{p}\sum_{j=1}^{p}\sum_{k=1}^{p} \overline{w}_i m_j m_k \mathbf{z}(t)^{\mathrm{T}}\left(\mathbf{\Theta}_{ijk} + \mathbf{V}_{jk} + \mathbf{V}_{jk}^{\mathrm{T}}\right)\mathbf{z}(t) \qquad (18) \\
&- \sum_{i=1}^{p}\sum_{j=1}^{p}\sum_{k=1}^{p} \left(\overline{w}_i \overline{w}_j - \gamma_j \overline{w}_i m_j - \overline{w}_i \zeta_j\right) m_k \mathbf{z}(t)^{\mathrm{T}}\left(\mathbf{S}_{ijk} + \mathbf{S}_{ijk}^{\mathrm{T}}\right)\mathbf{z}(t)
\end{aligned}
$$

We consider the first term of (18) shown as follows.

$$\mathbf{\Xi} = \sum_{i=1}^{p}\sum_{j=1}^{p}\sum_{k=1}^{p} m_i m_j m_k \mathbf{\Xi}_{ijk} \qquad (19)$$

where

$$\mathbf{\Xi}_{ijk} = \rho_i \mathbf{\Theta}_{ijk} + \sum_{l=1}^{p}\sigma_l\left(\mathbf{\Theta}_{ljk} + \mathbf{V}_{jk} + \mathbf{V}_{jk}^{\mathrm{T}}\right) + \left(\rho_i - 1\right)\left(\mathbf{V}_{jk} + \mathbf{V}_{jk}^{\mathrm{T}}\right) \qquad (20)$$

From (19), by employing similar analysis procedure in (Fang et al., 2006), we have,

$$
\begin{aligned}
\mathbf{\Xi} &= \sum_{i=1}^{p} m_i^{3}\mathbf{\Xi}_{iii} + \sum_{i=1}^{p}\sum_{\substack{j=1\\ j\neq i}}^{r} m_i^{2} m_j\left(\mathbf{\Xi}_{iij} + \mathbf{\Xi}_{iji} + \mathbf{\Xi}_{jii}\right) \\
&+ \sum_{i=1}^{p-2}\sum_{j=i+1}^{p-1}\sum_{k=j+1}^{p} m_i m_j m_k\left(\mathbf{\Xi}_{ijk} + \mathbf{\Xi}_{ikj} + \mathbf{\Xi}_{jik} + \mathbf{\Xi}_{jki} + \mathbf{\Xi}_{kij} + \mathbf{\Xi}_{kji}\right)
\end{aligned} \qquad (21)
$$

Define $\mathbf{Y}_{ijk} \in \Re^{n\times n}$, $\mathbf{Y}_{iii} = \mathbf{Y}_{iii}^{\mathrm{T}}$, i = 1, 2, ..., p, $\mathbf{Y}_{iij} = \mathbf{Y}_{jii}^{\mathrm{T}}$, i, j = 1, 2, ..., p; $i \neq j$, $\mathbf{Y}_{ijk} = \mathbf{Y}_{ikj}^{\mathrm{T}}$, $\mathbf{Y}_{jik} = \mathbf{Y}_{jki}^{\mathrm{T}}$ and $\mathbf{Y}_{kij} = \mathbf{Y}_{kji}^{\mathrm{T}}$, i = 1, 2, ..., p – 2; j = 1, 2, ..., p – 1; k = 1, 2, ..., p. Let

$$\mathbf{Y}_{iii} > \mathbf{\Xi}_{iii},\ i = 1, 2, \ldots, p \qquad (22)$$

$$\mathbf{Y}_{iij} + \mathbf{Y}_{iji} + \mathbf{Y}_{jii} \geq \mathbf{\Xi}_{iij} + \mathbf{\Xi}_{iji} + \mathbf{\Xi}_{jii},\ i, j = 1, 2, \ldots, p;\ i \neq j \qquad (23)$$

$$\mathbf{Y}_{ijk} + \mathbf{Y}_{ikj} + \mathbf{Y}_{jik} + \mathbf{Y}_{jki} + \mathbf{Y}_{kij} + \mathbf{Y}_{kji} \geq \mathbf{\Xi}_{ijk} + \mathbf{\Xi}_{ikj} + \mathbf{\Xi}_{jik} + \mathbf{\Xi}_{jki} + \mathbf{\Xi}_{kij} + \mathbf{\Xi}_{kji}$$

$$,\ i = 1, 2, \ldots, p-2;\ j = 1, 2, \ldots, p-1;\ k = 1, 2, \ldots, p \qquad (24)$$

From (21) to (24), we have,

$$\begin{aligned}\boldsymbol{\Xi} \le &\sum_{i=1}^{p} m_i^{\,3}\mathbf{Y}_{iii} + \sum_{i=1}^{p}\sum_{\substack{j=1\\ j\ne i}}^{r} m_i^{\,2} m_j\left(\mathbf{Y}_{iij}+\mathbf{Y}_{iji}+\mathbf{Y}_{jii}\right)\\ &+\sum_{i=1}^{p-2}\sum_{j=i+1}^{p-1}\sum_{k=j+1}^{p} m_i m_j m_k\left(\mathbf{Y}_{ijk}+\mathbf{Y}_{ikj}+\mathbf{Y}_{jik}+\mathbf{Y}_{jki}+\mathbf{Y}_{kij}+\mathbf{Y}_{kji}\right)\end{aligned} \tag{25}$$

From (18) and (25), we have,

$$\begin{aligned}\dot V(t) \le &\sum_{i=1}^{p} m_i^{\,3}\mathbf{Y}_{iii} + \sum_{i=1}^{p}\sum_{\substack{j=1\\ j\ne i}}^{r} m_i^{\,2} m_j\left(\mathbf{Y}_{iij}+\mathbf{Y}_{iji}+\mathbf{Y}_{jii}\right)\\ &+\sum_{i=1}^{p-2}\sum_{j=i+1}^{p-1}\sum_{k=j+1}^{p} m_i m_j m_k\left(\mathbf{Y}_{ijk}+\mathbf{Y}_{ikj}+\mathbf{Y}_{jik}+\mathbf{Y}_{jki}+\mathbf{Y}_{kij}+\mathbf{Y}_{kji}\right)\\ &+\frac{1}{2}\sum_{i=1}^{p}\sum_{j=1}^{p}\sum_{k=1}^{p}\overline{w}_i m_j m_k \mathbf{z}(t)^{\mathrm T}\left(\begin{array}{l}\boldsymbol{\Theta}_{ijk}+\mathbf{V}_{jk}+\mathbf{V}_{jk}^{\mathrm T}+\gamma_j\left(\mathbf{S}_{ijk}+\mathbf{S}_{ijk}^{\mathrm T}\right)+\sum_{l=1}^{p}\zeta_l\left(\mathbf{S}_{ilk}+\mathbf{S}_{ilk}^{\mathrm T}\right)\\ +\boldsymbol{\Theta}_{ikj}+\mathbf{V}_{kj}+\mathbf{V}_{kj}^{\mathrm T}+\gamma_k\left(\mathbf{S}_{ikj}+\mathbf{S}_{ikj}^{\mathrm T}\right)+\sum_{l=1}^{p}\zeta_l\left(\mathbf{S}_{ilj}+\mathbf{S}_{ilj}^{\mathrm T}\right)\end{array}\right)\mathbf{z}(t)\\ &-\sum_{i=1}^{p}\sum_{j=1}^{p}\overline{w}_i^{\,2} m_k \mathbf{z}(t)^{\mathrm T}\left(\mathbf{S}_{ijk}+\mathbf{S}_{ijk}^{\mathrm T}\right)\mathbf{z}(t)-\sum_{j=1}^{p}\sum_{i<j}\sum_{k=1}^{p}\overline{w}_i\overline{w}_j m_k\mathbf{z}(t)^{\mathrm T}\left(\mathbf{S}_{ijk}+\mathbf{S}_{ijk}^{\mathrm T}+\mathbf{S}_{jik}+\mathbf{S}_{jik}^{\mathrm T}\right)\mathbf{z}(t)\end{aligned} \tag{26}$$

Define $\mathbf{R}_{ijk}=\mathbf{R}_{jik}^{\mathrm T}\in\Re^{n\times n}$, $i, j, k = 1, 2, ..., p$. Let

$$\mathbf{R}_{ijk}+\mathbf{R}_{jik}^{\mathrm T} \ge \frac{1}{2}\left(\begin{array}{l}\boldsymbol{\Theta}_{ijk}+\mathbf{V}_{jk}+\mathbf{V}_{jk}^{\mathrm T}+\gamma_j\left(\mathbf{S}_{ijk}+\mathbf{S}_{ijk}^{\mathrm T}\right)+\sum_{l=1}^{p}\zeta_l\left(\mathbf{S}_{ilk}+\mathbf{S}_{ilk}^{\mathrm T}\right)\\ +\boldsymbol{\Theta}_{ikj}+\mathbf{V}_{kj}+\mathbf{V}_{kj}^{\mathrm T}+\gamma_k\left(\mathbf{S}_{ikj}+\mathbf{S}_{ikj}^{\mathrm T}\right)+\sum_{l=1}^{p}\zeta_l\left(\mathbf{S}_{ilj}+\mathbf{S}_{ilj}^{\mathrm T}\right)\end{array}\right) \tag{27}$$

From (26) and (27), we have,

$$\begin{aligned}\dot V(t) \le &\sum_{i=1}^{p} m_i^{\,3}\mathbf{Y}_{iii} + \sum_{i=1}^{p}\sum_{\substack{j=1\\ j\ne i}}^{r} m_i^{\,2} m_j\left(\mathbf{Y}_{iij}+\mathbf{Y}_{iji}+\mathbf{Y}_{jii}\right)\\ &+\sum_{i=1}^{p-2}\sum_{j=i+1}^{p-1}\sum_{k=j+1}^{p} m_i m_j m_k\left(\mathbf{Y}_{ijk}+\mathbf{Y}_{ikj}+\mathbf{Y}_{jik}+\mathbf{Y}_{jki}+\mathbf{Y}_{kij}+\mathbf{Y}_{kji}\right)\\ &+\sum_{i=1}^{p}\sum_{j=1}^{p}\sum_{k=1}^{p}\overline{w}_i m_j m_k \mathbf{z}(t)^{\mathrm T}\left(\mathbf{R}_{ijk}+\mathbf{R}_{jik}^{\mathrm T}\right)\mathbf{z}(t)\\ &-\sum_{i=1}^{p}\sum_{j=1}^{p}\overline{w}_i^{\,2} m_k \mathbf{z}(t)^{\mathrm T}\left(\mathbf{S}_{ijk}+\mathbf{S}_{ijk}^{\mathrm T}\right)\mathbf{z}(t)-\sum_{j=1}^{p}\sum_{i<j}\sum_{k=1}^{p}\overline{w}_i\overline{w}_j m_k\mathbf{z}(t)^{\mathrm T}\left(\mathbf{S}_{ijk}+\mathbf{S}_{ijk}^{\mathrm T}+\mathbf{S}_{jik}+\mathbf{S}_{jik}^{\mathrm T}\right)\mathbf{z}(t)\\ &\le \sum_{i=1}^{p} m_k\begin{bmatrix}\mathbf{r}(t)\\ \mathbf{s}(t)\end{bmatrix}^{\mathrm T}\begin{bmatrix}\mathbf{Y}_k & \mathbf{R}_k^{\mathrm T}\\ \mathbf{R}_k & \mathbf{S}_k\end{bmatrix}\begin{bmatrix}\mathbf{r}(t)\\ \mathbf{s}(t)\end{bmatrix}\end{aligned} \tag{28}$$

where $\mathbf{r}(t)=\begin{bmatrix} m_1\mathbf{z}(t) \\ m_2\mathbf{z}(t) \\ \vdots \\ m_p\mathbf{z}(t) \end{bmatrix}$, $\mathbf{s}(t)=\begin{bmatrix} \overline{w}_1\mathbf{z}(t) \\ \overline{w}_2\mathbf{z}(t) \\ \vdots \\ \overline{w}_p\mathbf{z}(t) \end{bmatrix}$, $\mathbf{Y}_k=\begin{bmatrix} \mathbf{Y}_{1k1} & \mathbf{Y}_{1k2} & \cdots & \mathbf{Y}_{1kp} \\ \mathbf{Y}_{2k1} & \mathbf{Y}_{2k2} & \cdots & \mathbf{Y}_{2kp} \\ \vdots & \vdots & \vdots & \vdots \\ \mathbf{Y}_{pk1} & \mathbf{Y}_{pk2} & \cdots & \mathbf{Y}_{pkp} \end{bmatrix}$,

$\mathbf{R}_k=\begin{bmatrix} \mathbf{R}_{11k} & \mathbf{R}_{12k} & \cdots & \mathbf{R}_{1pk} \\ \mathbf{R}_{21k} & \mathbf{R}_{22k} & \cdots & \mathbf{R}_{2pk} \\ \vdots & \vdots & \vdots & \vdots \\ \mathbf{R}_{p1k} & \mathbf{R}_{p2k} & \cdots & \mathbf{R}_{ppk} \end{bmatrix}$ and $\mathbf{S}_k=-2\begin{bmatrix} \mathbf{S}_{11k} & \mathbf{S}_{12k} & \cdots & \mathbf{S}_{1pk} \\ \mathbf{S}_{21k} & \mathbf{S}_{22k} & \cdots & \mathbf{S}_{2pk} \\ \vdots & \vdots & \vdots & \vdots \\ \mathbf{S}_{p1k} & \mathbf{S}_{p2k} & \cdots & \mathbf{S}_{ppk} \end{bmatrix}$, k = 1, 2, ..., p.

It can be seen from (28) that, if $\begin{bmatrix} \mathbf{Y}_k & \mathbf{R}_k^{\mathrm{T}} \\ \mathbf{R}_k & \mathbf{S}_k \end{bmatrix}<0$ for all k, $\dot{V}(t)\le 0$ (equality holds for $\begin{bmatrix} \mathbf{r}(t) \\ \mathbf{s}(t) \end{bmatrix}=\begin{bmatrix} \mathbf{0} \\ \mathbf{0} \end{bmatrix}$) which implies the asymptotic stability of the fuzzy-model-based control system of (10). The stability analysis results are summarized in the following theorem.

Theorem 1: *The fuzzy-model-based control system of* (10)*, formed by the nonlinear system in the form of (2) and the proposed enhanced fuzzy controller of (7) connected in closed loop, is guaranteed to be asymptotically stable if the membership functions are designed to satisfy the membership function conditions of* $\overline{w}_i(\mathbf{x}(t))=w_i(\mathbf{x}(t))-\left(\rho_i m_i(\mathbf{x}(t))+\sigma_i\right)>0$ *and* $\overline{w}_i(\mathbf{x}(t))-\left(\gamma_i m_i(\mathbf{x}(t))+\zeta_i\right)<0$ *for all i and* $\mathbf{x}(t)$ *where* $\rho_i>0$, σ_i, γ_i *and* ζ_i *are scalars, and there exist matrices of* $\mathbf{N}_{jk}\in\Re^{m\times n}$, *j, k = 1, 2, ..., p;* $\mathbf{R}_{ijk}=\mathbf{R}_{jik}^{\mathrm{T}}\in\Re^{n\times n}$, $\mathbf{S}_{ijk}=\mathbf{S}_{jik}^{\mathrm{T}}\in\Re^{n\times n}$, *j, k = 1, 2, ..., p; i < j;* $\mathbf{V}_{jk}\in\Re^{n\times n}$, *j, k = 1, 2, ..., p;* $\mathbf{X}=\mathbf{X}^{\mathrm{T}}\in\Re^{n\times n}$, $\mathbf{Y}_{iii}=\mathbf{Y}_{iii}^{\mathrm{T}}\in\Re^{n\times n}$, *i = 1, 2, ..., p,* $\mathbf{Y}_{iij}=\mathbf{Y}_{jii}^{\mathrm{T}}\in\Re^{n\times n}$, *i, j = 1, 2, ..., p; i ≠ j,* $\mathbf{Y}_{ijk}=\mathbf{Y}_{ikj}^{\mathrm{T}}\in\Re^{n\times n}$, $\mathbf{Y}_{jik}=\mathbf{Y}_{jki}^{\mathrm{T}}\in\Re^{n\times n}$ *and* $\mathbf{Y}_{kij}=\mathbf{Y}_{kji}^{\mathrm{T}}\in\Re^{n\times n}$, *i = 1, 2, ..., p – 2; j = 1, 2, ..., p – 1; k = 1, 2, ..., p such that the following LMIs hold.*

$$\mathbf{X}>0\text{; } \mathbf{S}_{ijk}+\mathbf{S}_{ijk}^{\mathrm{T}}\ge 0,\ j, k = 1, 2, ..., p;\ i<j;\ \mathbf{Y}_{iii}>\mathbf{\Xi}_{iii},\ i = 1, 2, ..., p;$$

$$\mathbf{Y}_{iij}+\mathbf{Y}_{iji}+\mathbf{Y}_{jii}\ge\mathbf{\Xi}_{iij}+\mathbf{\Xi}_{iji}+\mathbf{\Xi}_{jii},\ i, j = 1, 2, ..., p;\ i\ne j;$$

$$\mathbf{Y}_{ijk}+\mathbf{Y}_{ikj}+\mathbf{Y}_{jik}+\mathbf{Y}_{jki}+\mathbf{Y}_{kij}+\mathbf{Y}_{kji}\ge\mathbf{\Xi}_{ijk}+\mathbf{\Xi}_{ikj}+\mathbf{\Xi}_{jik}+\mathbf{\Xi}_{jki}+\mathbf{\Xi}_{kij}+\mathbf{\Xi}_{kji},$$

$$i = 1, 2, ..., p-2;\ j = 1, 2, ..., p-1;\ k = 1, 2, ..., p;$$

$$\mathbf{R}_{ijk}+\mathbf{R}_{jik}^{\mathrm{T}}\ge\frac{1}{2}\begin{pmatrix} \mathbf{\Theta}_{ijk}+\mathbf{V}_{jk}+\mathbf{V}_{jk}^{\mathrm{T}}+\gamma_j\left(\mathbf{S}_{ijk}+\mathbf{S}_{ijk}^{\mathrm{T}}\right)+\sum_{l=1}^{p}\zeta_l\left(\mathbf{S}_{ilk}+\mathbf{S}_{ilk}^{\mathrm{T}}\right) \\ +\mathbf{\Theta}_{ikj}+\mathbf{V}_{kj}+\mathbf{V}_{kj}^{\mathrm{T}}+\gamma_k\left(\mathbf{S}_{ikj}+\mathbf{S}_{ikj}^{\mathrm{T}}\right)+\sum_{l=1}^{p}\zeta_l\left(\mathbf{S}_{ilj}+\mathbf{S}_{ilj}^{\mathrm{T}}\right) \end{pmatrix},\ i, j, k = 1, 2, ..., p;$$

$$\begin{bmatrix} \mathbf{Y}_k & \mathbf{R}_k^{\mathrm{T}} \\ \mathbf{R}_k & \mathbf{S}_k \end{bmatrix}<0,\ k = 1, 2, ..., p \text{ where}$$

$$\mathbf{Y}_k = \begin{bmatrix} \mathbf{Y}_{1k1} & \mathbf{Y}_{1k2} & \cdots & \mathbf{Y}_{1kp} \\ \mathbf{Y}_{2k1} & \mathbf{Y}_{2k2} & \cdots & \mathbf{Y}_{2kp} \\ \vdots & \vdots & \vdots & \vdots \\ \mathbf{Y}_{pk1} & \mathbf{Y}_{pk2} & \cdots & \mathbf{Y}_{pkp} \end{bmatrix}, \mathbf{R}_k = \begin{bmatrix} \mathbf{R}_{11k} & \mathbf{R}_{12k} & \cdots & \mathbf{R}_{1pk} \\ \mathbf{R}_{21k} & \mathbf{R}_{22k} & \cdots & \mathbf{R}_{2pk} \\ \vdots & \vdots & \vdots & \vdots \\ \mathbf{R}_{p1k} & \mathbf{R}_{p2k} & \cdots & \mathbf{R}_{ppk} \end{bmatrix} \textit{and } \mathbf{S}_k = -2\begin{bmatrix} \mathbf{S}_{11k} & \mathbf{S}_{12k} & \cdots & \mathbf{S}_{1pk} \\ \mathbf{S}_{21k} & \mathbf{S}_{22k} & \cdots & \mathbf{S}_{2pk} \\ \vdots & \vdots & \vdots & \vdots \\ \mathbf{S}_{p1k} & \mathbf{S}_{p2k} & \cdots & \mathbf{S}_{ppk} \end{bmatrix}$$

and $\mathbf{\Xi}_{ijk} = \rho_i \mathbf{\Theta}_{ijk} + \sum_{i=1}^{p} \sigma_l \left(\mathbf{\Theta}_{ljk} + \mathbf{V}_{jk} + \mathbf{V}_{jk}^{\mathrm{T}}\right) + (\rho_i - 1)\left(\mathbf{V}_{jk} + \mathbf{V}_{jk}^{\mathrm{T}}\right)$, *i, j, k = 1, 2, ..., p and the feedback gains are designed as* $\mathbf{G}_{jk} = \mathbf{N}_{jk}\mathbf{X}^{-1}$, *j, k = 1, 2, ..., p.*

4. Simulation Examples

Two simulation examples are given in this section to illustrate the effectiveness of the proposed approach.

4.1 Simulation Example 1

A numerical example is given in this sub-section to investigate the stability region of the fuzzy-model-based control systems. Consider the following fuzzy model similar to that in (Fang et al., 2006).

$$\text{Rule } i\text{: IF } x_1(t) \text{ is } \mathrm{M}_1^i \text{ THEN } \dot{\mathbf{x}}(t) = \mathbf{A}_i\mathbf{x}(t) + \mathbf{B}_i u(t),\ i = 1, 2, 3 \tag{29}$$

where $\mathbf{A}_1 = \begin{bmatrix} 1.59 & -7.29 \\ 0.01 & 0 \end{bmatrix}$, $\mathbf{A}_2 = \begin{bmatrix} 0.02 & -4.64 \\ 0.35 & 0.21 \end{bmatrix}$ and $\mathbf{A}_3 = \begin{bmatrix} -a & -4.33 \\ 0 & 0.05 \end{bmatrix}$; $\mathbf{B}_1 = \begin{bmatrix} 1 \\ 0 \end{bmatrix}$, $\mathbf{B}_2 = \begin{bmatrix} 8 \\ 0 \end{bmatrix}$ and $\mathbf{B}_3 = \begin{bmatrix} -b+6 \\ -3 \end{bmatrix}$ where $\mathbf{x}(t) = [x_1(t) \quad x_2(t)]^{\mathrm{T}}$, $4 \le a \le 12$ and $4 \le b \le 12$. From (2), the inferred fuzzy model is given as follows.

$$\dot{\mathbf{x}}(t) = \sum_{i=1}^{3} w_i(x_1(t))\left(\mathbf{A}_i\mathbf{x}(t) + \mathbf{B}_i u(t)\right) \tag{30}$$

It is assumed that the fuzzy model works in the operating domain of $x_1(t) = [-\pi \quad \pi]$. The membership functions of the fuzzy model are chosen arbitrarily as

$$w_1(x_1(t)) = \mu_{\mathrm{M}_1^1}(x_1(t)) = 0.1e^{\frac{-(x_1(t)-\pi)^2}{5}} + 0.02\cos\left(x_1(t)^2\right)^2 + 0.25$$

$$w_2(x_1(t)) = \mu_{\mathrm{M}_1^2}(x_1(t)) = 0.1e^{\frac{-(x_1(t)+\pi)^2}{5}} - 0.02\sin\left(x_1(t)^2\right)^2 + 0.25$$

and

$$w_3(x_1(t)) = \mu_{\mathrm{M}_1^3}(x_1(t)) = 1 - w_1(x_1(t)) - w_2(x_1(t))$$

A three-rule fuzzy controller with the following rules is designed for the fuzzy model of (30).

$$\text{Rule } i\text{: IF } x_1(t) \text{ is } \mathrm{N}_1^i \text{ THEN } u(t) = \mathbf{G}_j(\mathbf{x}(t))\mathbf{x}(t),\ i = 1, 2, 3 \tag{31}$$

From (7), the inferred enhanced fuzzy controller is given as follows.

$$u(t) = \sum_{j=1}^{3}\sum_{k=1}^{3} m_j(x_1(t)) m_k(x_1(t)) \mathbf{G}_{jk}\mathbf{x}(t) \tag{32}$$

The membership functions of the enhanced fuzzy controller are chosen as

$$m_1(x_1(t)) = \mu_{\mathrm{N}_1^1}(x_1(t)) = \frac{3(x_1(t)+\pi)^2}{100\pi^2} + 0.255,$$

$$m_2(x_1(t)) = \mu_{\mathrm{N}_1^2}(x_1(t)) = \frac{3(x_1(t)-\pi)^2}{100\pi^2} + 0.255$$

and

$$m_3(x_1(t)) = \mu_{\mathrm{N}_1^3}(x_1(t)) = 1 - m_1(x_1(t)) - m_2(x_1(t))$$

It can be shown that the membership conditions of (14) and (16) are satisfied with $\rho_1 = \rho_2 = 0.945$, $\rho_3 = 0.915$; $\sigma_1 = \sigma_2 = 0.0005$, $\sigma_3 = 0.009$; $\gamma_1 = \gamma_2 = 0.11$, $\gamma_3 = 0.12$; $\zeta_1 = \zeta_2 = \zeta_3 = 0$.

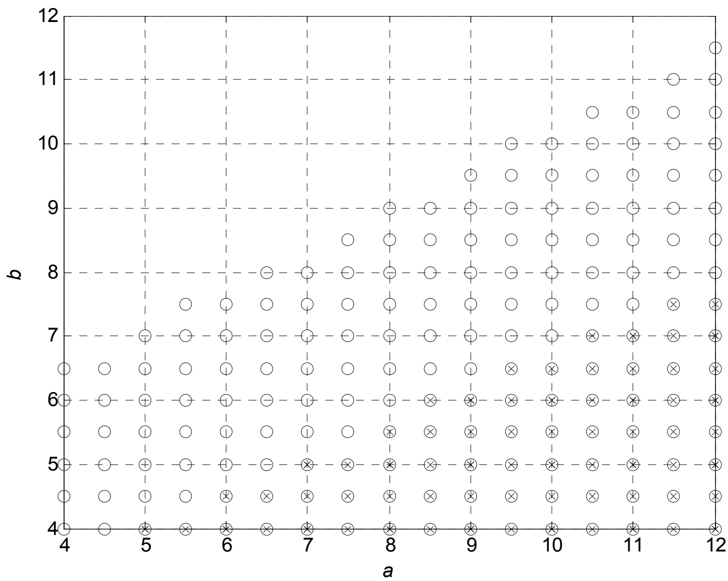

Figure 1. Stability regions for stability conditions in Theorem 1 indicated by “o” and in (Fang et al., 2006) indicated by indicated by “×”

Theorem 1 are employed to investigate the stability region of the fuzzy-model-based control system formed by (30) and (32). Fig. 1 shows the stability region indicated by “o”. For comparison purpose, the stability conditions in (Fang et al., 2006) is employed to investigate the stability region of the fuzzy-model-based control system. Fig. 1 shows the stability region given by the stability conditions in (Fang et al., 2006) indicated by “×”. It should be noted that the stability conditions in (Fang et al., 2006; Kim & Lee 2000; Liu & Zhang, 2003a; Liu &

Zhang, 2003b; Tanaka et al., 1998a; Teixeira et al.,2003; Wang et al., 1996) can be applied to fuzzy-model-based control systems with both fuzzy model and fuzzy controller sharing the same membership functions. It was reported in (Fang et al., 2006) that the stability conditions in (Fang et al., 2006; Kim & Lee 2000; Liu & Zhang, 2003a; Liu & Zhang, 2003b; Tanaka et al., 1998a; Teixeira et al.,2003) are subset of that in (Fang et al., 2006). In this example, in order to obtain the stability region for the stability conditions in (Fang et al., 2006), the fuzzy controller takes the membership functions of the fuzzy model. Referring to figure 1, it can be seen that the proposed enhanced fuzzy controller offers a larger stability region. Furthermore, as the proposed enhanced fuzzy controller does not need to share the same membership functions with the fuzzy model, simple membership functions can be employed to realize the fuzzy controller which can lower the implementation cost.

4.2. Simulation Example 2

In this example, the proposed enhanced fuzzy controller is designed based on Theorem 1 for an inverted pendulum which is described by the following dynamic equations (Ma & Sun, 2001).

$$\dot{x}_1(t) = x_2(t) \tag{33}$$

$$\dot{x}_2(t) = \frac{\begin{pmatrix} -F_1(M+m)x_2(t) - m^2l^2x_2(t)^2\sin x_1(t)\cos x_1(t) + F_0 mlx_4(t)\cos x_1(t) \\ +(M+m)mgl\sin x_1(t) - ml\cos x_1(t)u(t) \end{pmatrix}}{(M+m)(J+ml^2) - m^2l^2(\cos x_1(t))^2} \tag{34}$$

$$\dot{x}_3(t) = x_4(t) \tag{35}$$

$$\dot{x}_4(t) = \frac{\begin{pmatrix} F_1 mlx_2(t)\cos x_1(t) + (J+ml^2)mlx_2(t)^2\sin x_1(t) - F_0(J+ml^2)x_4(t) \\ -m^2gl^2\sin x_1(t)\cos x_1(t) + (J+ml^2)u(t) \end{pmatrix}}{(M+m)(J+ml^2) - m^2l^2(\cos x_1(t))^2} \tag{36}$$

where $x_1(t)$ and $x_2(t)$ denote the angular displacement (rad) and the angular velocity (rad/s) of the pendulum from vertical respectively, $x_3(t)$ and $x_4(t)$ denote the displacement (m) and the velocity (m/s) of the cart respectively, g = 9.8 m/s^2 is the acceleration due to gravity, m = 0.22 kg is the mass of the pendulum, M = 1.3282 kg is the mass of the cart, l = 0.304 m is the length from the center of mass of the pendulum to the shaft axis, $J = ml^2/3$ kgm^2 is the moment of inertia of the pendulum around the center of mass, F_0 = 22.915 $N/m/s$ and F_1 = 0.007056 N/rad/s are the friction factors of the cart and the pendulum respectively, and $u(t)$ is the force (N) applied to the cart.

In this example, the control objective is to balance the pole and drive the cart to the origin, i.e., $x_k(t) \to 0$, k = 1, 2, ,3, 4, as time tends to infinite. To facilitate the design of fuzzy controller, the following fuzzy model for the inverted pendulum of (33) to (36) is considered (Ma & Sun, 2001).

$$\text{Rule } i\text{: IF } x_1(t) \text{ is } \mathrm{M}_1^i \text{ THEN } \dot{\mathbf{x}}(t) = \mathbf{A}_i\mathbf{x}(t) + \mathbf{B}_i u(t),\ i = 1, 2 \tag{37}$$

The inferred system dynamics of the fuzzy model are described by,

$$\dot{\mathbf{x}}(t) = \sum_{i=1}^{2} w_i(x_1(t))\big(\mathbf{A}_i\mathbf{x}(t) + \mathbf{B}_i u(t)\big) \tag{38}$$

where $\mathbf{x}(t)=\begin{bmatrix}x_1(t) & x_2(t) & x_3(t) & x_4(t)\end{bmatrix}^{\mathrm{T}}$;

$$\mathbf{A}_1=\begin{bmatrix}0 & 1 & 0 & 0\\ (M+m)mgl/a_1 & -F_1(M+m)/a_1 & 0 & F_0ml/a_1\\ 0 & 0 & 1 & 0\\ -m^2gl^2/a_1 & F_1ml/a_1 & 0 & -F_0(J+ml^2)/a_1\end{bmatrix}$$

$$\mathbf{A}_2=\begin{bmatrix}0 & 1 & 0 & 0\\ \frac{3\sqrt{3}}{2\pi}(M+m)mgl/a_2 & -F_1(M+m)/a_2 & 0 & F_0ml\cos(\pi/3)/a_2\\ 0 & 0 & 1 & 0\\ -\frac{3\sqrt{3}}{2\pi}m^2gl^2\cos(\pi/3)/a_2 & F_1ml\cos(\pi/3)/a_2 & 0 & -F_0(J+ml^2)/a_1\end{bmatrix},$$

$$\mathbf{B}_1=\begin{bmatrix}0\\ -ml/a_1\\ 0\\ (J+ml^2)/a_1\end{bmatrix},\ \mathbf{B}_2=\begin{bmatrix}0\\ -ml\cos(\pi/3)/a_2\\ 0\\ (J+ml^2)/a_2\end{bmatrix};$$

$a_1=(M+m)(J+ml^2)-m^2l^2$, $a_2=(M+m)(J+ml^2)-m^2l^2\cos(\pi/3)^2$ and the membership functions are defined as

$$w_1(x_1(t)) = \mu_{\mathrm{M}_1^1}(x_1(t)) = \left(1-\frac{1}{1+e^{-7(x_1(t)-\pi/6)}}\right)\frac{1}{1+e^{-7(x_1(t)+\pi/6)}}$$

and

$$w_2(x_1(t)) = \mu_{\mathrm{M}_1^2}(x_1(t)) = 1-\mu_{\mathrm{M}_1^1}(x_1(t))$$

which are shown as the bell shape in Fig. 2.

Based on the fuzzy model of (38), a two-rule enhanced fuzzy controller is employed to realize stabilize the plant. The rule of the fuzzy controller is of the following format.

Rule j: IF $x_1(t)$ is N_1i THEN $u(t)=\mathbf{G}_j(\mathbf{x}(t))\mathbf{x}(t)$, j = 1, 2 (39)

From (7), the inferred enhanced fuzzy controller is given as follows.

$$u(t)=\sum_{j=1}^{2}\sum_{k=1}^{2}m_j(x_1(t))m_k(x_1(t))\mathbf{G}_{jk}\mathbf{x}(t) \tag{40}$$

The membership functions for the fuzzy model are chosen as $m_1(x_1(t))$ = $\mu_{\mathrm{N}_1^1}(x_1(t))$ =
$$\begin{cases}0 & \text{for } x_1(t)<-0.9\\ \frac{37}{28}(x+0.9) & \text{for } -0.9\le x_1(t)\le -0.2\\ 1 & \text{for } -0.2<x_1(t)<0.2\\ -\frac{37}{28}(x-0.9) & \text{for } 0.2\le x_1(t)\le 0.9\\ 0 & \text{for } x_1(t)>0.9\end{cases}$$
and $m_2(x_1(t))$ = $\mu_{\mathrm{N}_1^2}(x_1(t))$ = $1-\mu_{\mathrm{M}_1^1}(x_1(t))$ which are

shown as the trapezoids in Fig. 2. It can be shown that the membership conditions of (14) and (16) are satisfied with $\rho_1 = 0.99$, $\rho_2 = 0.95$; $\sigma_1 = 0.07$, $\sigma_2 = 0.02$; $\gamma_1 = \gamma_2 = 0.05$; $\zeta_1 = 0.1$, $\zeta_2 = 0.085$.

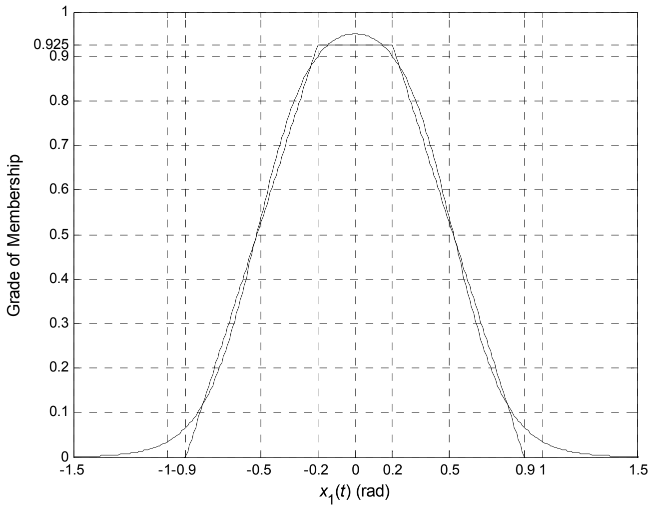

a) $\mu_{M_1^1}(x_1(t))$ (bell) and $\mu_{N_1^1}(x_1(t))$ (trapezoid)

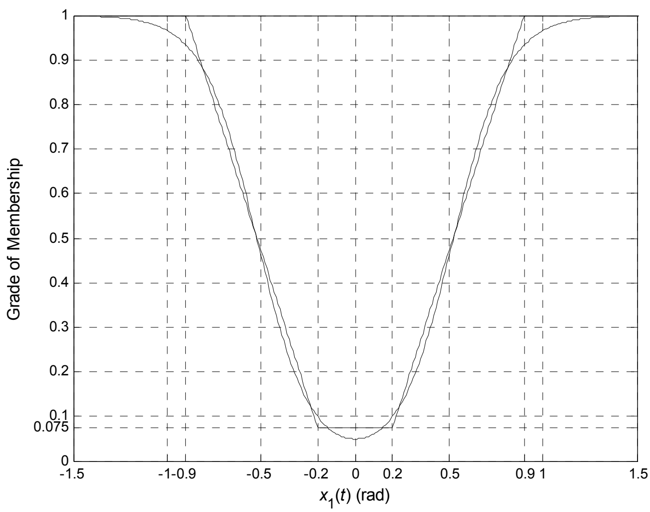

b) $\mu_{M_1^2}(x_1(t))$ (bell) and $\mu_{N_1^2}(x_1(t))$ (trapezoid)

Figure 2. Membership functions of fuzzy model and fuzzy controller in simulation example 2

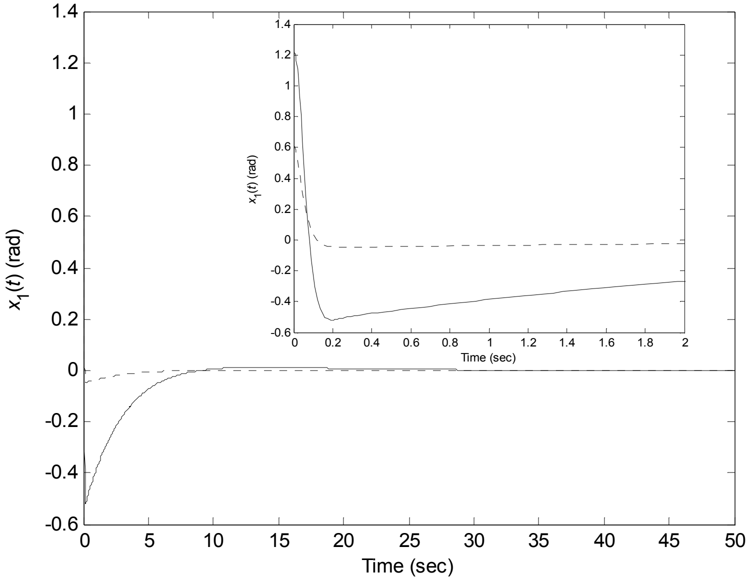
$x_1(t)$ (rad)
Time (sec)
$x_1(t)$ (rad)
Time (sec)

a) $x_1(t)$

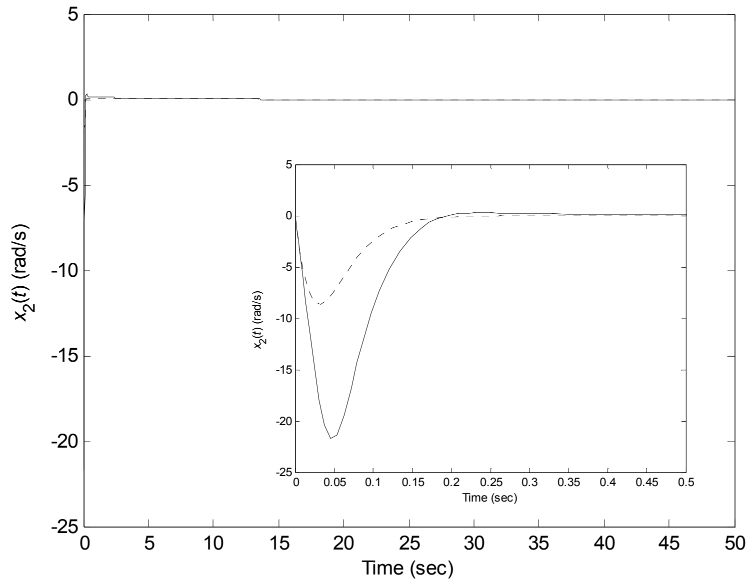
$x_2(t)$ (rad/s)
Time (sec)
$x_2(t)$ (rad/s)
Time (sec)

b) $x_2(t)$

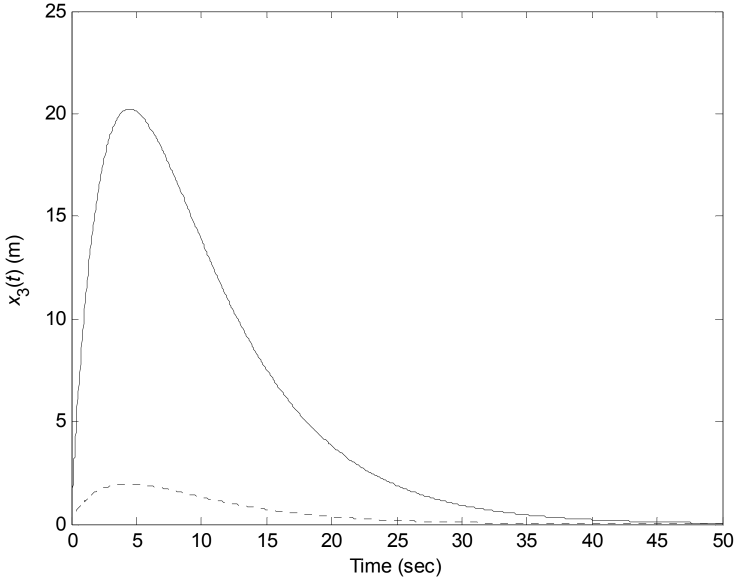

c) $x_3(t)$

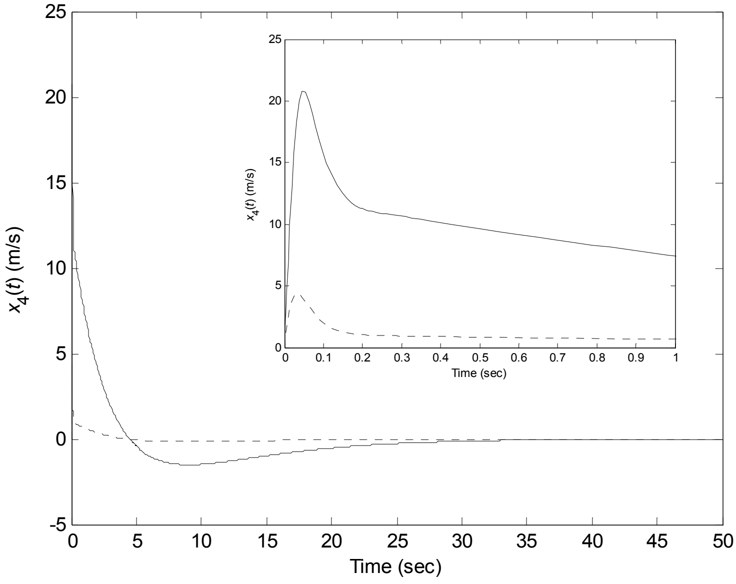

d) $x_4(t)$

Figure 3. System state responses for the fuzzy-model-based control system under different initial system state conditions in simulation example 2

To obtain the feedback gains for the enhanced fuzzy controller of (40), stability conditions in Theorem 1 are employed to achieve a stabilizing fuzzy controller of (40). With the help of Matlab LMI toolbox to solve the solution to the stability conditions in Theorem 1, we have $\mathbf{G}_{11}$ = [702.0204 51.4864 3.1163 54.5589], $\mathbf{G}_{12}$ = [707.8873 48.2611 3.0247 53.4503], $\mathbf{G}_{21}$ = [707.8873 48.2611 3.0247 53.4503] and $\mathbf{G}_{22}$ = [965.2063 63.0629 3.7704 60.9679]. Fig. 3 shows the system state responses for the fuzzy-model-based control system with $x(0) = [7\pi/18 \quad 0 \quad 0 \quad 0]^T$ and $[7\pi/36 \quad 0 \quad 0 \quad 0]^T$ respectively. It can be seen that the proposed enhanced fuzzy controller is able to stabilize the nonlinear plant. It is worth noting that the stability conditions in (Fang et al., 2006; Kim & Lee 2000; Liu & Zhang, 2003a; Liu Zhang, 2003b; Tanaka et al., 1998a; Teixeira et al., 2003; Wang et al., 1996) cannot apply to design the fuzzy controller as the members functions for both fuzzy model and fuzzy controllers are different in this example.

5. Conclusion

The system stability of fuzzy-model-based control systems has been investigated in this chapter. An enhanced fuzzy controller has been proposed for the control process. The stabilization ability of the proposed fuzzy controller is strengthened by the enhanced nonlinear feedback gains. Imperfect match of membership functions between fuzzy model and fuzzy controller has been considered. Compared to the existing approaches, greater design flexibility can be achieved due to the membership functions for the fuzzy controller can be designed freely. Under such a situation, most of the published stability conditions cannot be applied for the design of stable fuzzy-model-based control systems. To alleviate the conservativeness of stability analysis due to imperfect match of membership functions, membership function conditions have been proposed to govern the design of the membership functions of the fuzzy controller. With such membership function conditions, free matrices can be introduced to the Lyapunov-based stability analysis to relax the stability conditions. Simulation examples have been given to illustrate the effectiveness of the proposed approach.

6. Acknowledgement

The work described in this chapter was supported by King's College London.

7. References

Boyd,S.; Ghaoui,L. El; Feron, E. & Balakrishnan,V. (1994). *Linear Matrix Inequalities in Systems and Control Theory*, ser. SIAM studies in Applied Mathematics, Philadelphia, PA: SIAM, 1994.

Chen,,C.L.; Chen, P.C.; Chen, C.K. (1993). Analysis and design of fuzzy control system, *Fuzzy Sets and Systems*, vol. 57, no 2, 26, Jul. 1993, pp. 125-140.

Fang, C.H.; Liu, Y.S.; Kau, S.W.; Hong, L. & Lee, C.H. (2006) A new LMI-based approach to relaxed quadratic stabilization of T-S fuzzy control systems, *IEEE Trans. on Fuzzy Systems*, vol. 14, no. 3, Jun. 2006, pp. 386-397.

Feng, G. (2006). A Survey on Analysis and Design of Model-Based Fuzzy Control Systems, *IEEE Trans Fuzzy Systems*, vol. 14, no. 5, 2006, pp. 676- 697.

Kim, E. & Lee, H. (2000) New approaches to relaxed quadratic stability conditions of fuzzy control systems, *IEEE Trans. Fuzzy Syst.*, vol. 8, no. 5, 2000, pp. 523-534.

Lam, H.K.; Leung, F.H.F. & Tam, P.K.S. (1998). Fuzzy control of dc-dc switching converters based on TS-modeling approach,, *Proceeding of 24th Annual Conf. IEEE Ind. Electron. Society IECON'*98, pp. 1052-105498, Germany, 1998, Aachen, ,.

Lam, H.K.; Leung, F.H.F. & Tam, P.K.S. (2001). Fuzzy control of DC-DC switching converters: stability and robustness analysis, *Proceeding of 27th Annual Conf. IEEE Ind. Electron. Society IECON'*01, pp. 899-902, USA, 29 Nov.-2 Dec. 2001, Denver, Colorado.

Lian, K.Y.; Chiu C.S.; Chiang T.S. & Liu, P. (2001). LMI-based fuzzy chaotic synchronization and communication, *IEEE Trans. Fuzzy Systems*, vol. 9, no. 4, Feb. 2001, pp. 539-553.

Lian, K.Y.; Liou, J.J. & Huang, C.Y. (2006). LMI-based Integral fuzzy control of DC-DC converters, *IEEE Trans. Fuzzy Systems*, vol. 14, no. 1, Feb. 2006, , pp. 71-80.

Liu, X. & Zhang Q. (2003a). New approaches to H∞ controller designs based on fuzzy observers for T-S fuzzy systems via LMI, *Automatica*, vol. 39, no. 9, Sep. 2003, pp. 1571-1582.

Liu, X. & Zhang, Q. (2003b). Approaches to quadratic stability conditions and H∞ control designs for T-S fuzzy systems, *IEEE Trans. Fuzzy Syst.*, vol. 11, no. 6, 2003, pp. 830-839.

Ma, X.J. & Sun Z.Q. (2001). Analysis and design of fuzzy reduced-dimensional observer and fuzzy functional observer, *Fuzzy Sets and Systems*, vol. 120, 2001, pp. 35-63.

Sugeno, M. & Kang, G.T. (1988). Structure identification of fuzzy model, *Fuzzy sets and systems*, vol. 28, 1988, pp. 15-33.

Tanaka, K. & Sugeno M. (1992) Stability analysis and design of fuzzy control systems, *Fuzzy Sets and Systems*, vol. 45, 1992, pp.135-156.

Tanaka, K., Ikeda, T. & Wang, H.O. (1998a). Fuzzy regulator and fuzzy observer: Relaxed stability conditions and LMI-based designs, *IEEE Trans. Fuzzy Syst.*, vol. 6, no. 2, , 1998, pp. 250-265.

Tanaka, K.; Ikeda T. & Wang H.O. (1998b). A unified approach to controlling chaos via an LMI-based fuzzy control system design, *IEEE Trans. Circuits and Systems I: Fundamental Theory and Applications*, vol. 45, no. 10, Oct. 1998, pp. 1021-1040.

Takagi, T. & Sugeno, M. (1985). Fuzzy identification of systems and its applications to modeling and control, *IEEE Trans. Sys., Man., Cybern.*, vol. smc-15 no. 1, Jan., 1985, pp. 116-132.

Teixeira, M.C.M.; Assunção, E. & Avellar, R.G. (2003). On relaxed LMI-based designs for fuzzy regulators and fuzzy observers, *IEEE Trans. on Fuzzy Systems*, vol. 11, no. 5, Oct. 2003, pp. 613-623.

Wang, H.O.; Tanaka, K., & Griffin, M.F. (1996). An approach to fuzzy control of nonlinear systems: stability and the design issues, *IEEE Trans. Fuzzy Syst.*, vol. 4, no. 1, Feb., 1996, pp. 14-23.

8

Almost Global Synchronization of Symmetric Kuramoto Coupled Oscillators

Eduardo Canale and Pablo Monzón
Facultad de Ingeniería, Universidad de la República
Uruguay

1. Introduction

A few decades ago, Y. Kuramoto introduced a mathematical model of weakly coupled oscillators that gave a formal framework to some of the works of A.T. Winfree on biological clocks [Kuramoto (1975), Kuramoto (1984), Winfree (1980)]. The model proposes the idea that several oscillators can *interact* in a way such that the individual oscillation properties change in order to achieve a global behavior for the interconnected system. The Kuramoto model serves as a good representation of many systems in several contexts: biology, engineering, physics, mechanics, etc. [Ermentrout (1985), York (1993), Strogatz (1994), Dussopt et al. (1999), Strogatz (2000), Jadbabaie et a. (2003), Rogge et al. (2004), Marshall et al. (2004), Moshtagh et al. (2005)].
Recently, many works on the control community have focused on the analysis of the Kuramoto model, specially the one with sinusoidal coupling. The *consensus* or *collective synchronization* of the individuals is particularly important in many applications representing coordination, cooperation, emerging behavior, etc. Local stability properties of the consensus have been initially explored in [Jadbabaie et al. (2004)]. It must be noted that little attention has been devoted to the influence of the underlying interconnection graph on the stability properties of the system. The reason could be the fact that the local stability does not depend on the interconnection [van Hemmen et al. (1993)]. Global or *almost global* dynamical properties were studied in [Monzón et al. (2005), Monzón (2006), Monzón et al. (2006)]. In these works, the relevance of the interconnection graph of the system was hinted. In the present chapter, we go deeper on the analysis of the relationships between the dynamical properties of the system and the algebraic properties of the interconnection graph, exploiting the strong algebraic structure that every graph has. We step forward into a classification of the interconnection graphs that ensure almost global attraction of the set of synchronized states.
In Section 2 we present the Kuramoto model for sinusoidally coupled oscillators, its general properties and the notion of almost global synchronization; in Section 3 we review some basic facts on algebraic graph theory; the symmetric Kuramoto model and the block analysis are presented in Sections 4 and 5; Section 6 gives some examples and applications of the main results; Section 7 presents the problem of classification of almost global synchronizing topologies.

2. The Kuramoto model

In the 1970s, Kuramoto proposed a model to describe a population of weakly coupled oscillators. In this model, each individual oscillator is described by its phase and the coupling between two individuals is a function of the phase difference. The general Kuramoto model takes the following form [Strogatz (2000)]:

$$\dot{\theta}_i = \omega_i + \sum_{j=1}^{N} \Gamma_{ij}\left(\theta_i - \theta_j\right) \quad , \quad i = 1,\ldots,N$$

where Γ_{ij} are the *interaction* functions that represent the coupling and *N* is the total number of oscillators. Since each angle $\theta_i \in [0,2\pi)$, the corresponding state space is the *N*-dimensional torus T^N. We consider the particular case of sinusoidally coupled oscillators,

$$\dot{\theta}_i = \omega_i + \frac{K}{N} . \sum_{j \in N_i} \sin\left(\theta_i - \theta_j\right) \quad , \quad i = 1,\ldots,N \tag{1}$$

where N_i refers to the set of index of agents that affect the behavior of agent *i* -the *neighbors* of *i*- and *K* is the strength of the coupling. We will assume that all the agents have the same natural frequency. So, with a suitable shift, and simplifying the notation by eliminating the factor $\frac{K}{N}$ -this amount for to renormalizing time- we can write the previous model as

$$\dot{\theta}_i = \sum_{j \in N_i} \sin\left(\theta_i - \theta_j\right) \quad , \quad i = 1,\ldots,N \tag{2}$$

We want to emphasize the following aspects of system (2):

- The dynamic depends only on the phase difference of the oscillators. Then, there are several properties that are invariant under translations on the torus. For example, if $\overline{\theta}$ is an equilibrium point, so is[1] $\overline{\theta} + c.1_N$ for every $c \in [0,2\pi)$.
- As was done by Kuramoto [Kuramoto (1984)], we associate the individual oscillator phases to points running around the circle of radius 1 in the complex plane. Then, each oscillator can be described by the unitary phasor $V_i = e^{j\theta_i}$.

Equation (2) has always two kinds of *trivial* equilibria:

- We call **consensus** or **synchronization** the state where all the phase differences are zero, i.e. the diagonal of the state space. Every consensus state is of the form $\overline{\theta} = c.1_N$, with $c \in [0,2\pi)$. We have a closed curve of consensus points. Observe that at a consensus point, all the associated phasors coincide.

---

[1] $\mathbf{1}_p$ denotes the column vector in R^p with all the elements equal to one. Analogously, $\mathbf{0}_p$ denotes the column vector in R^p with all the elements equal to zero.

- We say we have *partial synchronization* when all the phasors are parallel but they are not synchronized; i.e. most of the phases takes the value 0 (taking a suitable reference), but there are *m* agents with phase $\pm\pi$, for some $0 < 2m \le N$.
- The other equilibrium points have non-parallel phasors and we refer to them as *non synchronized*.

Example 2.1: Consider the graph *G* shown at the left of Figure 1. A non synchronized equilibrium point of (2) with interconnection graph *G* is given by

$$\overline{\theta} = [-160.95, 90, -19.09, 160.91, -90, 19.09, 0, 180]^T$$

and it is shown at the right of Figure 1 (the angles are measured in degrees). ♦

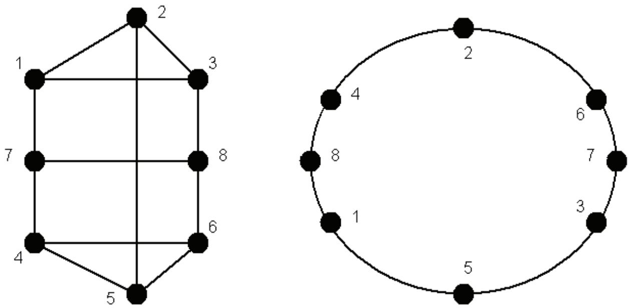

Figure 1. Phasor representation of the equilibrium point $\overline{\theta}$ of Example 2.1. The underlying graph is shown on the left

The key question we try to answer in this work is whether or not the system behavior of (2) reaches *consensus*, since this particular equilibrium may represent a desired behavior of the system. Recently, the Kuramoto model has received the attention of control theorists interested in the coordination and consensus of multi-agent systems (see [Jadbabaie et al (2004)] and references there in). We focus on the global properties of the consensus equilibrium. Since the system has many equilibria, we can not talk about global stability or global synchronization. But we may wonder if the system present the so called *almost global stability* property, that is, if the set of initial conditions that no lead to synchronization has zero Lebesgue measure. From an engineering point of view, this is a nice property [Rantzer (2001)], specially when it is combined with local stability. When the system has the almost global stability property, almost every initial condition leads to the synchronization of the system. So, we will use the expression *almost global synchronization* and the abbreviation a.g.s.

2.1 General properties

The following results are true for the general dynamic (2)

Proposition 2.1: At any equilibrium point $\overline{\theta}$ of (2), it must be true that the phasors $\sum_{h \in N_i} V_h$ and V_i are parallel in the complex plane, for every *i*.

Proof: For $i = 1,\ldots,N$, consider the number

$$\alpha_i = \sum_{h\in N_i} \frac{V_h}{V_i} = \sum_{h\in N_i} e^{j(\theta_h-\theta_i)} = \sum_{h\in N_i} \cos(\theta_h - \theta_i) + j.\sum_{h\in N_i} \sin(\theta_h - \theta_i)$$

Since $\bar{\theta}$ is an equilibrium point, α_i is a real number and $\sum_{h\in N_i} V_h = \alpha_i .V_i$. ♦

Important consequences of Proposition 2.1 will be presented in further sections. Nevertheless, we can write a direct corollary.

Corollary 2.1: Consider an agent i such that $N_i = \{k\}$, $i \neq k$. Then, at an equilibrium point $\bar{\theta}$, it must be true that $\bar{\theta}_i = \bar{\theta}_k$ or $\bar{\theta}_i = \bar{\theta}_k + \pi$. ♦

For example, if the underlying graph is a tree (see Section 3), an iterative application of Corollary 2.1 shows that the only equilibria are full or partial synchronized points.

To conclude this Section, we introduce the concept of *phase-locking solution*. We say that a solution $\theta(t)$ is *phase-locking* when the phase difference between any two agents remains constant in time. It follows that for $i = 1,..., N$, we have $\dot{\theta}_i = \Omega$ and $\theta_i(t) = \Omega t + \theta_{0i}$. For the particular case of $\Omega = 0$, we have the equilibrium points described above. Phase-locking solutions with $\Omega \neq 0$ correspond to closed periodic orbits in T^N and play important roles in many contexts, such pace generators or muscular contractions in biology [Ermentrout (1985)], cyclic pursuit problems [Marshall et al. (2004)] or circular polarization generation with antennas [Dussopt et al. (1999).

3. Brief review of algebraic graph theory

We will use a graph to naturally describe the interconnection topology between the agents in the Kuramoto model. In this Section we review the basic facts on algebraic graph theory that will be used along the article. A more detailed introduction to this theory can be found in [Biggs (1983); Cvetkovic et al. (1979)]. A graph G consists in a set of n *nodes* or *vertices* $VG = \{v_1,..., v_n\}$ and a set of m *links* or *edges* $EG = \{e_1,..., e_m\}$ that describes how the nodes are related to each other. If n=1 the graph is called *trivial*. We say that two nodes are neighbors or adjacent if there is a link in EG between them. If all the vertices are pairwise adjacent the graph is called *complete* or *all to all* and written K_n . A *walk* is a sequence $v_0, v_1,..., v_l$ of adjacent vertices. If the vertices are different except the first and the last which are equal ($v_i \neq v_j$, $0 < i < j$ and $v_0 = v_l$) the walk is called a *cycle*. A graph with no cycle is called *acyclic*. The graph is *connected* if there is a walk between any given pair of vertices. A *tree* is an acyclic connected graph and has m=n-1 edges. The graph is *oriented* if every link has a starting node and a final node. The topology of an oriented graph may be described by the *incidence* matrix B with n rows and m columns:

$$B_{ij} = \begin{cases} 1 & \text{if edge } j \text{ reaches node } i \\ -1 & \text{if edge } j \text{ leaves node } i \\ 0 & \text{otherwise} \end{cases}$$

Observe that $B^T 1_n = 0$. The semidefinite matrix $L = B^T B$ is called the Laplacian of *G* and contains the *spectral* information of the graph. The *vertex space* and the *edge space* of *G* are the sets of real functions with domain *VG* and *EG* respectively, which we sometimes will identify, respectively, with the vectors spaces R^n and R^m. Thus, the incidence matrix *B* can be seen as a linear transformation from the edge space to the vertex space. The kernel of *B* is called the *cycle space* of the graph *G* and its elements are called *flows*. Every *flow* can be thought as a vector of weights assigned to every link in a way that the total algebraic sum at each node is zero. The cycle space is spanned by the flows determined by the cycles: given a cycle $v_0,...,v_l = v_0$, its associated flow $f_C(e)$ is ± 1 if *e* leaves some v_i and reaches $v_{i\pm 1}$ and 0 otherwise.

If the graph *G* is the union of two nontrivial graphs G_1 and G_2 with one and only one node v_i in common, then v_i is called a *cut-vertex* of *G*. A connected graph with more than two vertices and no cut-vertex is called *2-connected* and it follows that for every pair of nodes, there are at least two different walks between them. A *bridge* is a link with the following particular property: if it is removed, the resulting graph is not connected. Given a subset $V_1 \subset VG$, its *induced subgraph* is $\langle V_1 \rangle$, with vertex set V_1 and edge set $\{e \in EG: \ e \text{ joins vertices of } V_1\}$. The maximal induced subgraphs of *G* with no cut-vertex, are called the *blocks* of *G*. Every graph has the form of Figure 2: a collection of blocks joined by cut-vertices. For a complete graph, there is only one block, the graph itself. A tree can be seen as a collection of K_2.

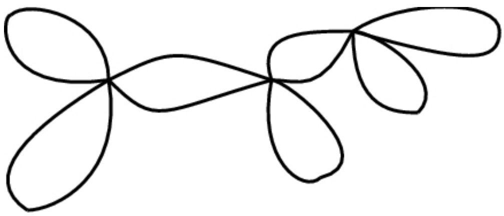

Figure 2. Representation of a graph as a union of blocks

The complement $\overline{G}$ of a graph *G* is another graph with the same nodes as *G* and such that two nodes are related in $\overline{G}$ if and only if they are not related in *G*. It follows that $G + \overline{G}$ is a complete graph, where the sum of two graphs with the same set of nodes is defined as a new graph which has all the edges of the original graphs.

We will use the following vector notation: given a *n*-dimensional vector $\overline{\theta} = [\theta_1,...,\theta_n]$, then $\overline{\theta}(i:j) = [\theta_i,...,\theta_j]$ and $\overline{\theta}(i) = \theta_i$.

4. Symmetric Kuramoto model

4.1. Dynamics

The dynamic of a given agent depends on the sine of its phase differences with its neighbors. Symmetry is characterized by $i \in N_k \Rightarrow k \in N_i$. As in [Jadbabaie et al. (2003)], we can build a directed graph G with the agents as nodes and the edges representing the relationships between agents. We only put one link between neighbors, with arbitrary orientation. Let M be the number of edges. We construct the incidence matrix $B_{N\times M}$ as in previous Section. In matrix notation, the dynamic (2) can be written as

$$\dot{\theta} = -B.\sin\left(B^T\theta\right) \tag{3}$$

We must emphasize that equation (3) does not depend on the particular orientation we have chosen for the links of the underlying graph. First of all, we show that the only phase-locking solutions of a symmetric system are the ones with $\Omega = 0$.

Lemma 4.1: The only phase-locking solutions of system (3) are equilibrium points.

Proof: Symmetry implies that the sum of all the phases is a constant magnitude of the system:

$$\frac{d}{dt}\sum_{i=1}^{N}\theta_i = \sum_{i=1}^{N}\dot{\theta}_i = 1^T.\dot{\theta} = -1^T.B.\sin\left(B^T\theta\right) = 0$$

since $B^T.1 = 0$. At a phase-locking solution, $\dot{\theta} = \Omega.1 = 0$. Then, $0 = 1^T.\dot{\theta} = \Omega.1^T.1 = N.\Omega$

So, $\Omega = 0$ and we have an equilibrium point. ♦

We remark that through this article, we deal with connected graph topologies.

4.1. Stability analysis

Local stability of the consensus point for system (3) was studied in [Jadbabaie et al. (2004)] using La Salle's invariance principle [Khalil (1996)]. The function

$$U(\theta) = M - 1_M^T.\cos\left(B^T\theta\right) \tag{4}$$

is non-negative, and such that the system can be written in the gradient form: $\dot{\theta} = -\nabla U(\theta)$.

In particular this implies that the derivative of U along the trajectories is $\dot{U}(\theta) = -\left\|\dot{\theta}\right\|^2$.

Hence, the function U is non-increasing along the trajectories. Since $U \equiv 0$ at the consensus set, it is a local Lyapunov function for the consensus set, meaning that if we start near enough to this set, we will converge to it. Since the state space is compact, every trajectory has a non-empty ω-limit set [Guckenheimer et al. (1983)]. La Salle's result ensures that every trajectory goes to the set

$$W = \left\{\theta : \quad \dot{U}(\theta) = -\left\|\dot{\theta}\right\|^2 = 0\right\}$$

which consists only of equilibrium points. In particular, this proves that the system admits no closed limit cycles and we recover the conclusion of Lemma 4.1. In order to establish almost global attraction of the consensus set (almost global synchronization, a.g.s.), it must be true that this set is the only attractor. Frequently, when we are dealing with an a.g.s. system, we will say that the underlying graph G is a.g.s.. The next Example shows a system without the a.g.s. property.

Example 4.1: Consider the case with N=6 in which the dynamics of the agents are as follows:

$$\dot{\theta}_i = \sin(\theta_{i-1} - \theta_i) + \sin(\theta_{i+1} - \theta_i) \qquad i = 1, \ldots, N$$

Here the configuration is circular; we identify θ_7 with θ_1 and θ_0 with θ_6. Consider the equilibrium point showed in Figure 3. Using an approach that will be presented later, it can be shown that this configuration is locally attractive. ♦

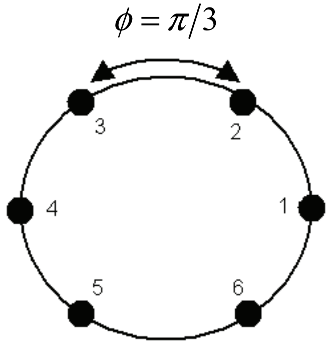

Figure 3. Stable non-consensus equilibrium for the Kuramoto model of Example 4.1

We thus see that guaranteeing almost global asymptotical consensus is more involved. We will analyze the stability of the equilibrium points using Jacobian linearization. A first order approximation of the system at an equilibrium point $\overline{\theta}$ takes the form $\dot{\delta\theta} = A.\delta\theta$, with $\delta\theta = \theta - \overline{\theta}$ and A the symmetric matrix $N \times N$ with entries

$$\begin{cases} a_{ii} = -\sum_{k \in N_i} \cos(\overline{\theta}_k - \overline{\theta}_i) = -\alpha_i \\ a_{hi} = \begin{cases} \cos(\overline{\theta}_k - \overline{\theta}_i) & , \quad h \in N_i \\ 0 & , \quad h \in N_i \end{cases} \end{cases}$$

with α_i defined as in Proposition 2.1. The matrix A can be written as

$$A = -B.diag(\cos(B^T\theta)).B^T \tag{5}$$

and can be seen as a *weighted* Laplacian, since $A = -L = -B.B^T$ at a consensus equilibrium. Two facts must be remarked. First of all, A is symmetric, reflecting the bidirectional influence of the agents. This implies that it is a diagonalizable matrix, with real eigenvalues. Note also that $A.1_N = 0$. Hence, A always has the zero eigenvalue, with associated eigenvector 1_N. We will analyze the transversal stability of the consensus set [Khalil (1996)], that is, the convergence to the consensus set.

The following results are true for general graph topologies. Their were originally introduced in [Monzón et al. (2005), Monzón (2006) and Monzón et al. (2006)].

Lemma 4.2: Let $\overline{\theta}$ be an equilibrium point of (3), such that at least one $\alpha_i < 0$. Then, $\overline{\theta}$ is unstable.

Proof: The numbers $-\alpha_i$ appear at the diagonal of the matrix symmetric *A*. So, a negative α_i implies that *A* has a positive eigenvalue. Then, $\overline{\theta}$ is unstable. ♦

Lemma 4.3: Let $\overline{\theta}$ be an equilibrium point of (3), such that $\cos\left(\overline{\theta}_k - \overline{\theta}_i\right) > 0$ for every $k \in N_i$, $i = 1,\ldots,N$. Then, $\overline{\theta}$ is stable.

Proof: Since the underlying graph *G* is connected, 0 is a simple eigenvalue of the Laplacian matrix $L = BB^T$ [Biggs, (1993)]. The linearization matrix *A* described in (5) is a *weighted* version of *L*. Since the weigths are all positive, i.e., the matrix $diag\left\lfloor\cos\left(B^T\theta\right)\right\rfloor$ is positive definite, $\overline{\theta}$ is stable. ♦

Example 4.2: Lemma 4.3 explains Example 4.1. In that case, the characteristic polynomial of the linear approximation has the roots 0 and -2 (simple), and $-\frac{1}{2}$ and $-\frac{3}{2}$ (double). Indeed, for large *N*, there can be equilibrium configurations with all neighboring angles lesser than $\frac{\pi}{2}$, and thus provide other attractors than the consensus set. ♦

Proposition 4.1: Let $\overline{\theta}$ be a partial consensus equilibrium point of (3). Then $\overline{\theta}$ is unstable.

Proof: At a partial equilibrium point, we have agents at phase 0 and agents at phase π. Define the vector $v = \cos\left(\overline{\theta}\right)$, which only contains 1 and -1. Then, an element of vector $B^T.v$ is null if the link related to the *l*-h row of B^T joins agents with distinct phases. Then, after some calculus, we have that $v.A^T.v = 4.c$, where *c* is the number of links that join agents of the two groups. Then, *A* has a positive eigenvalue and then, $\overline{\theta}$ is unstable. ♦

If for a given graph *G* we can prove that the only equilibrium points correspond to partial or total consensus, we can ensure the almost global stability of the synchronized state. This observation leads us to our first main result.

Lemma 4.4: Consider the system (3) with an associated graph *G* that is a tree. Then, the only equilibrium points are the trivial ones: partial or full consensus.

Proof: With an appropriate reference, a (partial or total) consensus state $\overline{\theta}$ is such that $\sin\left(B^T\theta\right) = 0$. In order to have only partial or total consensus equilibria, 0 must be the only solution of the equation: 0=*B.x*. That is, the cycle space must be trivial. Observe that for a connected graph, the matrix *B*, with *N* rows and *e* columns, has always rank *N*-1. Then, the previous equation has only the trivial solution when *e*=*N*-1, that is, it has full column rank. The only connected graphs with *N*-1 links are the trees. ♦

Theorem 4.1: Consider the system (3). If the associated graph *G* is a tree, it is almost globally stable.

Proof: The result is a direct consequence of Lemma 4.3 and Proposition 4.1. ♦

If we have several systems with underlying topology given by trees, we can interconnect them using single links, keeping the almost global synchronization property. The next Example illustrates that fact.

Example 4.3: A star graph is a connected tree graph that has a particular node, a *hub*, which is related with all of the rest of the nodes, while all the rest of the nodes are related to the hub only. The graph can be sketched as a star and it models several examples of centralized interactions between agents. It is a particular case of Theorem 4.1. The synchronized state is an almost global attractor. Moreover, if we have two star graphs and we couple them through their hubs, as in Figure 4, (or through any pair of agents), we obtain a new almost globally stable system (a kind of *synchronization preserving interconnection*). If we add one more link to a connected tree, we must have a cycle, and we may lose the almost global stability property, as in Example 4.1. ♦

To conclude this Section we present another important result. It states that complete graphs are always a.g.s. The result was originally hinted in several works [Jadbabaie et al. (2004); van Hemmen et al. (1993)]. The prove can be found in [Monzón et al. (2005)].

Theorem 4.2: Consider the system (3). If the underlying graph *G* is complete, the consensus set is almost globally stable. ♦

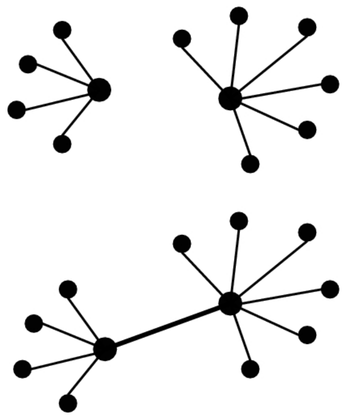

Figure 4. Two star graphs coupled through their hubs (Example 4.3)

5. Block analysis and synchronizing interconnection

In this Section we present some results that help to answer the question of whether or not a graph is a.g.s. They were originally presented in [Monzón et al. (2007); Canale et al. (2007)]. Here, we give a longer presentation.

From equation (3) we see that a phase angle vector θ is an equilibrium point if and only if $\sin\left(B^T\theta\right)$ is a flow on *G*. Thus, it should be possible that the equilibrium points of (3) could be obtained from the equilibrium points of the blocks of the graph *G*. In fact, this is exactly what happens. Furthermore, the stability of these equilibria depends only on the stability of the associated equilibrium points of the blocks. Firstly, we present some basic results. We include two different proofs for Lemma 5.1, in order to show two distinct interpretations of the same facts: one based on linear algebra, the other using graph theory elements. Then, we study the relationship between the equilibria of *G* and the equilibria of its blocks, which will follow directly from Lemma 5.1. After that we focus on the stability properties.

Lemma 5.1: Consider a graph *G*, with *v* a cut-vertex between G_1 and G_2. Then, an edge space element $f: EG \to R$ is a flow on *G*, if and only if $f\,|_{EG_1}$ and $f\,|_{EG_2}$ are a flows on G_1 and G_2 respectively.

Proof 1: Suppose that the i vertices of G_1 and its k edges come first in the chosen labelling. Suppose, also, that $v = v_i$, then B has the following form:

$$B = \left[\begin{array}{c|c} W_1 & 0_{(i-1)\times(m-k)} \\ \hline w_1^T & w_2^T \\ \hline 0_{(n-i)\times k} & W_2 \end{array}\right]$$

where w_1 and w_2 are column vectors with appropriate dimensions. With this notation, the incidence matrices of G_1 and G_2 are, respectively

$$B_1 = \left[\begin{array}{c} W_1 \\ \hline w_1^T \end{array}\right] \quad , \quad B_2 = \left[\begin{array}{c} w_2^T \\ \hline W_2 \end{array}\right]$$

Besides, B_1, as incidence matrix, verifies $1_i^T B_1 = 0$, thus $1_{(i-1)}^T W_1 + w_1^T = 0$, so

$$w_1^T = -1_{(i-1)}^T W_1 \tag{6}$$

Let f be a flow on G. In order to prove that $f_1 = f\,|_{EG_1}$ is a flow on G_1, we must show that $B_1.f_1 = 0$, i.e. $W_1.f_1 = 0_{(i-1)}$ and $w_1^T.f_1 = 0$. The former is true because since f is a flow on G, $B.f = 0$ and $W_1.f_1 = (B.f)(1:i-1)$. On the other hand, by (6), we have that, $w_1^T.f_1 = (-1_{(i-1)}^T.W_1)f_1 = -1_{(i-1)}^T.(W_1.f_1) = -1_{(i-1)}^T.0_{(i-1)} = 0$. With the same arguments, we obtain that $f_2 = f\,|_{EG_2}$ is a flow on G_2.

Conversely, if f_1 and f_2 are flows on G_1 and G_2 respectively, we have that $(Bf)(1:i-1) = B_1.f_1 = 0_i$ and $(Bf)(i+1:n) = B_2.f_2 = 0_{(n-i+1)}$. Finally, a direct calculation gives $(Bf)(i) = w_1^T.f_1 + w_2^T.f_2 = 0 + 0 = 0$. ♦

Proof 2: Following [Biggs (1993), Lemma 5.1, Theorem 5.2], given a spanning tree T of G, we obtain a basis of the cycle space in the following form: for each edge $e \in E' = EG \setminus ET$, we have a unique cycle $cyc(T,e)$ which determines a flow $f_{T,e}$. The set B of these flows is a basis of the cycle-space. However, since v is a cut-vertex, any cycle is included either in G_1 or in G_2, so its associated flow is null either in G_1 or in G_2. If we regard a flow on G which is null in EG_1 as a flow on G_2, we can split B into two sets B_1 and B_2, cycle-space basis of G_1 and G_2 respectively. Thus the cycle-space of G is the direct sum of the cycle-spaces of G_1 and G_2. ♦

Lemma 5.2: Let G be a graph, $V_1 \subset VG$ and $G_1 = \langle V_1 \rangle$ the subgraph of G induced by the vertices V_1 with incidence matrix B_1. Let $H : R \to R$ be any real function, $\overline{\theta} : VG \to R$ an element of the vertex-space of G and $f = H\left(B^T \overline{\theta}\right)$. Then, if

$$f_1 : f\,|_{EG_1} \qquad , \qquad \overline{\theta}_1 = \overline{\theta}\,|_{VG_1}$$

it is true that

$$f_1 = H\left(B_1^T \overline{\theta}_1\right)$$

Proof: Suppose that the *i* vertices and *k* edges of G_1 come first in the chosen labelling. Then, for some B', B'' and $\overline{\theta}_2$, we have that

$$B^T \overline{\theta} = \left[\begin{array}{c|c} B_1^T & 0_{i\times k} \\ \hline B' & B'' \end{array}\right]\begin{bmatrix} \overline{\theta}_1 \\ \overline{\theta}_2 \end{bmatrix} = \begin{bmatrix} B_1^T \overline{\theta}_1 \\ B'\overline{\theta}_1 + B''\overline{\theta}_2 \end{bmatrix}$$

Thus, $\left(B^T \overline{\theta}\right)(1:k) = B_1^T \overline{\theta}_1$, and $f_1 = f(1:k) = H\left(B^T \overline{\theta}\right)(1:k) = H\left[\left(B^T \overline{\theta}\right)(1:k)\right] = H\left(B_1^T \overline{\theta}_1\right)$. ♦

5.1 Equilibria

If $\theta_1 : VG_1 \to R$ is in the vector space of a subgraph G_1 of *G*, we will regard it also as its unique extension to the vector space of *G* which is null elsewhere of G_1. The same for an element of the edge space.

Proposition 5.1: Consider the graph *G* with a cut-vertex *v* between G_1 and G_2. If $\overline{\theta}$ is an equilibrium point of *G*, then $\overline{\theta}_1 = \overline{\theta}\,|_{VG_1}$ and $\overline{\theta}_2 = \overline{\theta}\,|_{VG_2}$ are equilibrium points of G_1 and G_2 respectively. Conversely, if $\overline{\theta}_1$ and $\overline{\theta}_2$ are equilibrium points of G_1 and G_2 respectively, there exists a real number α such that $\overline{\theta}'_2 = \overline{\theta}_2 + \alpha 1_{N-k}$ is an equilibrium point of G_2 and $\overline{\theta} = \overline{\theta}_1 + \overline{\theta}_2$ is an equilibrium point of *G*.

Proof: Let *B*, B_1, B_2, etc. like in Lemma 5.1. If $\overline{\theta}$ is an equilibrium point of *G*, then $f = \sin\left(B^T \overline{\theta}\right)$ is a flow on *G*, thus, by Lemma 5.1, $f_1 = f\,|_{EG_1}$ is a flow on G_1. Thus, it is enough to prove that $f_1 = \sin\left(B_1^T \overline{\theta}_1\right)$, which follows from Lemma 5.2, taking $H(x) = \sin(x)$ and noticing that G_1 is an induced subgraph of *G*. The case for G_2 follows by the same arguments.

Now, assume that $\overline{\theta}_1$ and $\overline{\theta}_2$ are equilibrium points of G_1 and G_2 respectively. Let $\alpha = \overline{\theta}_1(v) - \overline{\theta}_2(v)$, $\overline{\theta}'_2 = \overline{\theta}_2 + \alpha 1_{N-k}$, $\overline{\theta} = \overline{\theta}_1 + \overline{\theta}'_2$, and $f = \sin\left(B^T \overline{\theta}\right)$. Then, by Lemma 5.2, $f_1 = f\,|_{EG_1} = \sin\left(B_1^T \overline{\theta}_1\right)$ and $f_1 = f\,|_{EG_1} = \sin\left(B_1^T \overline{\theta}_1\right)$. On the other hand, due to the invariance of the system we have remarked on Section 2, the vector $\overline{\theta}'_2$ is also an equilibrium point of G_2, and then, f_1 and f_2 are flows in G_1 and G_2 respectively. Therefore, by Lemma 5.1, $f_1 + f_2$ is a flow on *G*. But $f = f_1 + f_2$, because $EG_1 \cap EG_2 = \Phi$. ♦

5.2 Stability analysis

We will relate the stability properties of the graph G with a cut-vertex with the stability properties of the subgraphs G_1 and G_2 joined by it. Since every equilibrium of G defines an equilibria for G_1 and G_2, we wonder whether or not the dynamical characteristics of these equilibria are or not the same. We will use Jacobian linearization. Recall that the zero eigenvalue is always present due to the invariance of the system by translations parallel to 1_n. If the multiplicity of the zero eigenvalue is more than one, Jacobian linearization may fail in classifying the equilibria. In this work, we assume that we always have a single null eigenvalue. We do not present here the study of this particular problem.

Theorem 5.1: Consider the graph G, with a cut-vertex v joining the subgraphs G_1 and G_2 of graph G. Let $\overline{\theta} \in R^n$ be an equilibrium point of G. Then, $\overline{\theta}$ is locally stable if and only if $\overline{\theta}_1 |_{VG_1}$ and $\overline{\theta}_2 |_{VG_2}$ are locally stable and coincide in $v = VG_1 \cap VG_2$.

Proof: Recall that the first order approximation of the system around an equilibrium point is given by

$$A_G = -B.diag\left(\cos\left(B^T \theta\right)\right)B^T$$

Suppose that G_1 has i vertices, that they come first in the chosen labelling and that v is the last of them $(v = v_i)$. Then, a direct calculation gives:

$$A_G = A_1 + A_2 \tag{7}$$

with

$$A_1 = \left[\begin{array}{c|c} A_{G_1} & 0_{i\times(n-i)} \\ \hline 0_{(n-i)\times i} & 0_{(n-i)\times(n-i)} \end{array}\right]$$

and

$$A_2 = \left[\begin{array}{c|c} 0_{(i-1)\times(i-1)} & 0_{(i-1)\times(n-i+1)} \\ \hline 0_{(n-i+1)\times(i-1)} & A_{G_2} \end{array}\right]$$

Observe that these matrices partially *overlap*, so the matrix A takes the form:

$A=$ 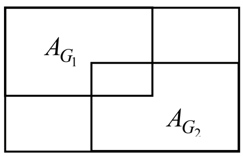

First of all, we consider the case with $\overline{\theta}_1$ and $\overline{\theta}_2$ stable and $\overline{\theta}_1(i) = \overline{\theta}_2(1)$. Then, A_{G_1} and A_{G_2} are stable and equation (7) holds for $\overline{\theta} = \left(\overline{\theta}_1, \overline{\theta}_2(2:n-i)\right)$. So, A_G is the sum of two semidefinite negative matrices which gives rise a semidefinite negative one. Besides, the kernel of A_G has dimension 1, since if $A_G w = 0$, then $w^T A_G w = 0$. Thus, $w^T A_1 w + w^T A_2 w = 0$. But, $w^T A_1 w = w_1^T A_{G_1} w_1$ and $w^T A_2 w = w_2^T A_{G_2} w_2$ for $w_1 = w|_{VG_1}$ and

$w_2 = w|_{VG_2}$. Then $w_1^T A_{G_1} w_1 + w_2^T A_{G_2} w_2 = 0$. That can happen if only if $w_1^T A_{G_1} w_1 = 0$ and $w_2^T A_{G_2} w_2 = 0$. But the kernels of A_{G_1} and A_{G_2} are spanned by 1_i and 1_{n-i+1} respectively. Thus $w_1 = \alpha.1_i$ and $w_1 = \beta.1_{n-i}$. Since $w_1(i) = w_2(1) = w(i)$, we have $\alpha = \beta$ and $w = \alpha.1_n$. This proves the stability of A_G.

Now, we focus on the case with $\overline{\theta}_1$ or $\overline{\theta}_2$ unstable. We analyze the first case, since the other is similar. Suppose that A_{G_1} has a positive eigenvalue with associated eigenvector w_1, thus

$$w_1^T A_{G_1} w_1 > 0$$

Define the column vector

$$w = \begin{bmatrix} w_1 \\ w_1(i).1_{n-i} \end{bmatrix} = \begin{bmatrix} w_1(1:i-1) \\ w_1(i).1_{n-i+1} \end{bmatrix}$$

Then,

$$w^T A_G w = w_1^T A_{G_1} w_1 + w_1^2(i).1_{n-i+1}^T A_{G_2} 1_{n-i+1}$$

which actually is $w_1^T A_{G_1} w_1 > 0$ since $w_1^2(i).1_{n-i+1}^T A_{G_2} 1_{n-i+1} = 0$. Then, $\overline{\theta}$ is unstable. ♦

We are now ready to state and prove one of the main results of this Chapter.

Theorem 5.2: Consider the graph *G*, with a cut-vertex v_i joining the subgraphs G_1 and G_2. Then, G_1 and G_2 have the almost global synchronization property if and only if *G* does.

Proof: First of all, let $\overline{\theta}$ be an equilibrium point of *G*. According to Theorem 5.1., $\overline{\theta}$ is stable only if $\overline{\theta}_1 = \overline{\theta}|_{VG_1}$ and $\overline{\theta}_2 = \overline{\theta}|_{VG_2}$ are too. If G_1 and G_2 are a.g.s., the only locally stable set is the consensus, and since they have a vertex in common, the only locally stable equilibria of *G* is also the consensus and *G* is a.g.s.

In the other direction, if $\overline{\theta}_1$ is a locally stable equilibrium of G_1, we chose $\overline{\theta} = \left(\overline{\theta}_1, \overline{\theta}_1(i).1_{n-1}\right)$ and we construct a stable equilibrium for *G* (as we have mentioned before, a consensus equilibrium is always locally stable [Jadbabaie et al. (2004)]. Since *G* is a.g.s., $\overline{\theta}$, and so $\overline{\theta}_1$, must be consensus equilibrium points. ♦

Theorem 5.2 has many direct consequences. We point out some of them, with a brief hint of the respective proofs.

Proposition 5.2: Consider a graph *G* with a bridge e_k between the nodes v_i and v_j and let G_1 and G_2 be the connected components of $G \setminus \{e_k\}$. Then, *G* is a.g.s. if and only if G_1 and G_2 are.

Proof: If a graph has a *bridge*, the behavior of the system depends only on the parts connected by the bridge. Indeed, the bridge together with its ends vertices form a block, which is in fact a complete graph and its vertices are cut-vertices of the graph, as is shown in

Figure 5. Since any complete graph is a.g.s., the a.g.s. character of the original graph depends on the other blocks. ♦

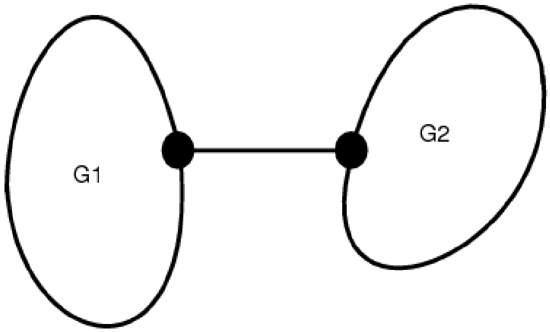

Figure 5. A graph with a bridge

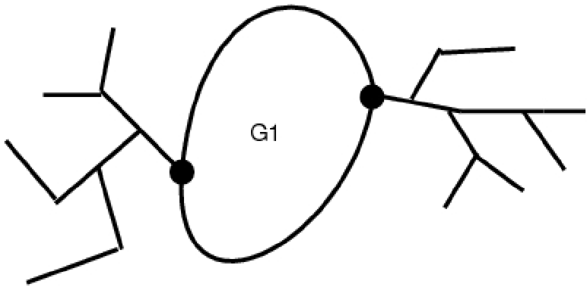

Figure 6. A graph with *arboricities*

We are now ready to present a different proof of Theorem 4.1:
Proof 2: We can iteratively apply Proposition 5.2, since in a tree, every link is a bridge.
If we have a graph with *arboricities*, like the one shown in Figure 6, we can neglect the trees in order to prove the a.g.s. property. ♦
*Corollary 5.1:*A graph with the structure shown in Figure 6 is a.g.s. if and only if the graph G_1 is.

Proof: The result is a straightforward application of Theorem 5.2. ♦
Now, we state an important result in order to classify a.g.s. graphs:
Theorem 5.3: A graph *G* is a.g.s. if and only if every block of *G* is a.g.s.
Proof: The graph *G* can be partitioned into its blocks. Then, *G* can be thought as a collection of subgraphs connected by cut-vertices. An iterative use of Theorem 5.2 leads us to the result. ♦
Theorem 5.3 reduces the characterization of the family of a.g.s. graphs to the analysis of 2-connected graphs. As an application, consider the case where we connect two a.g.s. graphs through another a.g.s. graph. In this way, we construct a new a.g.s. graph. Figures 7 and 8 illustrate the situation. Using the known fact that every complete graph is a.g.s., we derive the following result.
Theorem 5.4: If *G* is a graph such that all its blocks are complete graphs, then *G* is a.g.s.
Proof: As we have seen in Theorem 4.2, complete graphs are always a.g.s. So, the conclusion follows from Theorem 5.3. ♦

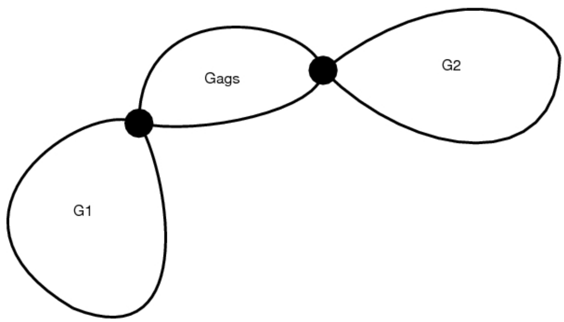

Figure 7. Two graphs connected by an a.g.s. graph

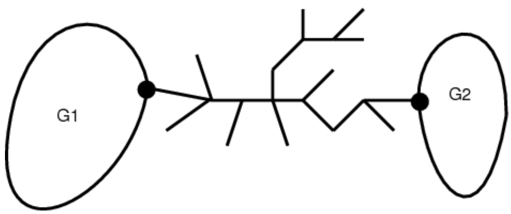

Figure 8. Two graphs connected by a tree

Finally, we present two direct consequences of Theorem 5.3. They are illustrated in Figure 9.

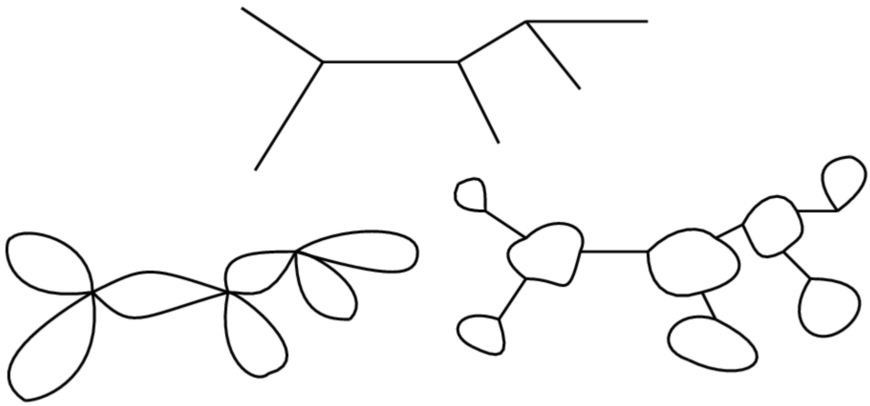

Figure 9. Situation of Propositions 5.3 and 5.4

Proposition 5.4: If G is a tree and we build a new graph K replacing some (or every) edges of G by an a.g.s. graph, then K is a.g.s. ♦

Proposition 5.5: If G is a tree and we build a new graph K replacing some (or every) nodes of G by an a.g.s. graph, then K is a.g.s. ♦

Previous results, specially Theorem 5.3, imply that in order to establish that a graph is a.g.s., we only need to deal with its blocks. So, we must focus in the general analysis of 2-connected graphs, as s*tructural pieces* of every connected graph. We know that complete graphs are a.g.s. 2-connected graphs. As long as we are able to find new a.g.s. 2-connected graphs, we are moving forward on the classification of all a.g.s. graphs.

6. Examples

In this Section we present some examples that illustrate applications of the theoretical results we have presented.

Example 6.1: Consider two Kuramoto systems with complete underlying interconnection graphs $G_1 = K_3$ and $G_1 = K_5$ (both a.g.s.). Starting from arbitrary initial conditions, each system quickly reaches a consensus state. At time T=3 seconds, we connect the two systems through a bridge between an arbitrary pair of agents. Then, the whole systems reaches a new consensus state. Observe that this convergency is slower than the previous (for the rate of local convergency, see [Jadbabaie et al. (2004)). Figure 10-left shows the results obtained from the simulation. They perfectly agree with Proposition 5.2. ♦

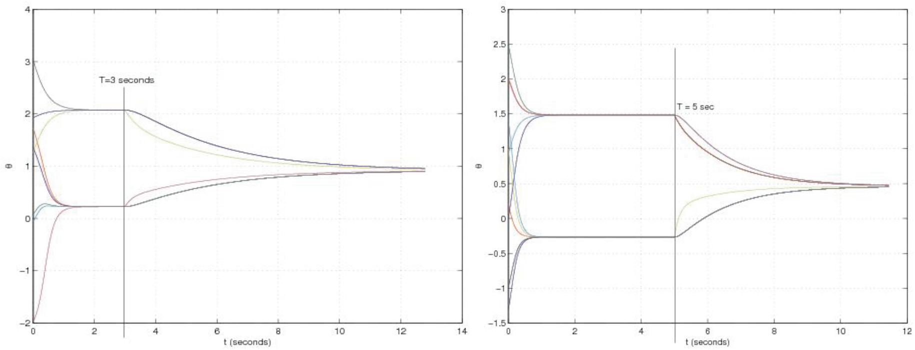

Figure 10. Left: two a.g.s. systems connected by a bridge; the connection takes place at time T=3 seconds. Right: two a.g.s. systems that become connected by a vertex; the connection takes place at time T=5 seconds

Example 6.2: Consider two a.g.s. systems, with underlying graphs $G_1 = K_5$ and $G_1 = K_7$. They run independently and at time T=5 seconds, an agent of the first system gets connected with some agents of the second one. Then, the new system has a new underlying graph G which has a vertex at this agent. Figure 11-right shows the evolution of the system. ♦

7. On the classification of A.G.S. graphs

In this Section, we introduce two operations on graphs. The first one transforms any connected graph into an a.g.s. graph. The second one destroy the a.g.s. property. Firstly, we introduce the idea of *twin vertices*.

Definition 7.1: We said that two vertices u and v are *twins* if their have the same common neighbors:

$$N_u \setminus \{v\} = N_v \setminus \{u\}$$

Previous definition does no assume that u and v are adjacent vertices. So, we will distinguish between two cases.

7.1 Adjacent twin vertices

The following Lemma generalizes previous results for complete graphs.

Lemma 7.1: Let $\overline{\theta}$ be a stable equilibrium point of (5), then any set of adjacent twin vertices should be synchronized.

Proof: Let $S = \{v_1,\ldots,v_k\}$ a set of twin vertices with the set SN of adjacent twins and their common neighbors. Let α be the sum of all the phasors of SN. Then

$$\alpha = \sum_{j\in SN} V_j = V_i.\left(1 + \sum_{\substack{j\in SN \\ j\neq i}} \frac{V_j}{V_i}\right) = V_i.(1+\alpha_i)$$

with α_i as in Proposition 2.1. First, notice that all the V_i should be parallel. Otherwise, let V_i and V_j be linearly independent. Since $V_i.(1+\alpha_i) = \alpha = V_j.(1+\alpha_j)$, we should have $(1+\alpha_i) = 0$, thus $\alpha_i = -1$ and, by Lemma 4.2, the equilibrium can not be stable. So, we have a group of say *a* vertices of SN in phase θ_0 and another group of *b*=*k*-*a* ones in phase $\theta_0 + \pi$. We claim that *b* should be zero. Indeed, let v_i and v_j vertices of *SN* in the first and second group respectively, then:

$$\alpha_i = (a-1) - b + \sum_{l\in SN\setminus S} \cos(\theta_0 - \theta_l)$$

and

$$\alpha_j = (b-1) - a + \sum_{l\in SN\setminus S} \cos(\theta_0 + \pi - \theta_l)$$

But, $\cos(\theta_0 + \pi - \theta_l) = -\cos(\theta_0 - \theta_l)$, thus $\alpha_i + \alpha_j = -2$ and at least one of them should be negative. This means that $\overline{\theta}$ is unstable. ♦

As a consequence of this Lemma, we have a new way to prove that any complete graph is a.g.s. since all its vertices are adjacent twins. But, as we will prove, we have even more, if the identification of adjacent twin vertices give rise a tree, then the graph is a.g.s. Since being adjacent (or itself) and twin is an equivalence relation we can make the *quotient graph* by this relation. In the quotient graph, the vertices are the classes of the equivalence and two vertices are adjacent in the quotient if the classes have adjacent vertices. We will say that a graph is a *twin cover* of its quotient graph.

Theorem 7.1: Consider a given graph *G* and its quotient graph G_Q by the adjacent-twin relation. If G_Q is a tree, *G* is a.g.s.

Proof: Let $\overline{\theta}$ be a stable equilibrium point of *G*. Then, $\sin\left(B^T\overline{\theta}\right)$ is a flow on it. This flow gives rise the following flow in the quotient graph. Consider two adjacent vertices *u* and *v* in *G* which are not twins. Then, the classes $[u]$ and $[v]$ are adjacent in G_Q. Since $\overline{\theta}$ is stable, by Lemma 7.1, all the neighbors of u have the phase $\overline{\theta}_u$. In the same way, we define $\overline{\theta}_v$. Assign the number

$$\left|[u]\right|.\left|[v]\right|.\sin\left(\overline{\theta}_v - \overline{\theta}_u\right)$$

to the edge in G_Q joining the node classes $[u]$ and $[v]$ ($\left|[u]\right|$ denotes the number of elements of the class $[u]$). We affirm that this assignment is a flow in G_Q. Indeed,

$$\sum_{[v]\in N_{[u]}}\left|[u]\right|.\left|[v]\right|.\sin\left(\overline{\theta}_v - \overline{\theta}_u\right) = \left|[u]\right|.\sum_{[v]\in N_{[u]}}\left|[v]\right|.\sin\left(\overline{\theta}_v - \overline{\theta}_u\right)$$

Observe that if $v \in N_u \setminus [\mathbf{u}]$ in G, then, the term $\sin\left(\overline{\theta}_u - \overline{\theta}_v\right)$ appears $\left|[v]\right|$ times in the expression of $\dot{\theta}_u$. Then,

$$\sum_{[v]\in N_{[u]}}\left|[v]\right|.\sin\left(\overline{\theta}_v - \overline{\theta}_u\right) = \sum_{v\in N_u\setminus[\mathbf{u}]}\sin\left(\overline{\theta}_v - \overline{\theta}_u\right) = \dot{\theta}_u\Big|_{\overline{\theta}} = 0$$

So, the stable equilibrium point $\overline{\theta}$ of G induces another equilibrium point $\overline{\theta}_Q$ in G_Q. If G_Q is a tree, $\overline{\theta}_Q$ is a partial or full synchronized point. If it is a partial synchronization state, the phase value of each class in G_Q is 0 or π (taking a suitable reference) and $\overline{\theta}$ is also a partial synchronization state and so is unstable, which contradicts the hypothesis. Then, $\overline{\theta}_Q$ and $\overline{\theta}$ are consensus equilibrium and G is a.g.s. ♦

The opposite result is obviously not true. We present several corollaries that recover some known results and introduce tools for building a.g.s. graphs.

Corollary 7.1: Any complete graph is a.g.s.

Proof: Its quotient graph is the trivial one. ♦

Corollary 7.2: Any complete graph minus an edge is a.g.s.

Proof: Its quotient graph is a tree: the only one with three vertices. ♦

Corollary 7.3: Any complete graph minus any proper subset of the edges adjacent to a given vertex is a.g.s.

Proof: Its quotient graph is again the only tree with three vertices. The three groups of twins are: first the vertex that lost more edges, those who lost only one edge and those who did not lose any edge. ♦

The following Theorem shows that a connected graph G can be *enlarged*, adding twin vertices, in order to obtain a new a.g.s. graph.

Lemma 7.2: In a connected graph, no equilibrium but the synchronized one is possible with all phasors in a half of the unit circle.

Proof: Indeed, by absurd, suppose that there are unsynchronized vertices and without loss of generality that $\overline{\theta}_i \in [0,\pi]$ for all i, then $\overline{\theta}_{i_m} = \min\overline{\theta}_i < \max\overline{\theta}_i = \overline{\theta}_{i_M}$. We claim that there should exists an agent j achieving the minimum but unsynchronized with at least one of its neighbors. Indeed, it suffices to consider a walk from vertex i_m to vertex i_M and the first moment when the angle grows. Thus, for some j, for all $i \in N_j$ we have $\overline{\theta}_i - \overline{\theta}_j \geq 0$, and $\overline{\theta}_k - \overline{\theta}_j \geq 0$ for someb $k \in N_j$. But since the angles are in $[0,\pi]$, we hace such $\sin\left(\overline{\theta}_k - \overline{\theta}_j\right) > 0$. Therefore,

$$\sum_{i \in N_j} \sin\left(\overline{\theta}_i - \overline{\theta}_j\right) > 0$$

contradicting the equilibrium hypothesis. ♦

Theorem 7.2: Any connected graph G admits an a.g.s. twin cover.

Proof: Remember that by Lemma 7.1, twin vertices in a stable equilibrium should be synchronized. Thus, we can restrict our study to a set $V = \{v_1,...,v_n\}$ of representants of the twins. We will identify V with the vertices of G. Furthermore, we will prove that given $\varepsilon > 0$, there is a twin cover such that for any stable equilibrium $\overline{\theta}$, the angle differences $\left|\overline{\theta}_i - \overline{\theta}_j\right|$ are less than ε for all pairs (v_i, v_j) of adjacent vertices. Thus, if the graph is connected with diameter D, the result will follow by taking $\varepsilon = \pi/D$ and applying Lemma 7.2. Notice that we can restrict our self to pairs (v_i, v_j) in a spanning tree.

Let us suppose that we have constructed the cover by splitting each vertex v_i of G in a number a_i of twins vertices. Then, the flow equation for (any twin of) vertex v_i in the new graph becomes:

$$\sum_{j \in N_i} a_j.\sin\left(\overline{\theta}_j - \overline{\theta}_i\right) = 0$$

Then, for any $k \in N_i$

$$a_k.\sin\left(\overline{\theta}_k - \overline{\theta}_i\right) = -\sum_{\substack{j \in N_i \\ j \neq k}} a_j.\sin\left(\overline{\theta}_j - \overline{\theta}_i\right)$$

and

$$\left|\sin\left(\overline{\theta}_k - \overline{\theta}_i\right)\right| \leq \frac{\sum_{j \in N_i, j \neq k} a_j}{a_k}$$

So, in order to find an upper bound for the difference $\left|\overline{\theta}_k - \overline{\theta}_i\right|$ it is enough to find an upper bound for the last term together with a lower one for $\cos\left(\overline{\theta}_k - \overline{\theta}_i\right)$. Now, we will construct the spanning tree *T*. Let S_i be the vertices at distance *i* from vertex v_1 (i.e. the sphere in the graph of center v_1 and ratio *i*). Then, sort each set S_i with an order $<_i$. We consider the following lexicographical order: given two vertices $v \in S_i$ and $w \in S_j$, we say that $v < w$ if $i < j$ or if $i = j$ and $v <_i w$. The order defined in this way is total, so we can relabel the vertices following this order, having $v_1 < v_2 < \ldots < v_n$. Next, set $a_i = (\Delta/\varepsilon)^{n-i}$ (rounded up) where Δ is the maximum degree of a vertex in *G*. Then *T* will be the spanning subgraph of *G* that joins vertices v_i and v_j if $a_i = \max_{l \in N_j}\{a_l\}$. We claim that *T* is a tree. Indeed, it is acyclic, because for each *i*>1, any vertex in S_i is adjacent to exactly one vertex in S_{i-1}. Besides any vertex reaches vertex v_1, thus *T* is connected as well.

Let us now find an upper bound for the sine of the difference between adjacent vertices of *T*. Let v_i and v_k be adjacent vertices of *T* with $i > k$. Then

$$\left|\sin\left(\overline{\theta}_k - \overline{\theta}_i\right)\right| \le \frac{\sum_{j \in N_i, j \ne k} a_j}{a_k} \le \frac{(\Delta - 1).\left[(\Delta/\varepsilon)^{n-k-1} + 1\right]}{(\Delta/\varepsilon)^{n-k}} < \varepsilon$$

for any $\varepsilon < \Delta$. On the other hand, since the equilibrium is stable we have that

$$a_i - 1 + \sum_{j \in N_i} a_j.\cos\left(\overline{\theta}_j - \overline{\theta}_i\right) \ge 0$$

Thus, by the same argument

$$\cos\left(\overline{\theta}_i - \overline{\theta}_k\right) \ge -\frac{a_i + \sum_{j \in N_i, j \ne k} a_j.\cos\left(\overline{\theta}_j - \overline{\theta}_i\right)}{a_k} > -\varepsilon.\left(1 + \Delta^{-1}\right)$$

Thus, choosing ε small enough we will have that the angles differ in less than any prescribed ε'. ♦

We can prove a *dual* version of this theorem which says that if we add an enough amount of vertices to an edge which is not a bridge we will obtain a non a.g.s. graph.

Theorem 7.3 Let *e* be an edge of a graph *G*. Then, if *e* is not a bridge, there is an integer n_0 such that the graph obtained from *G* by making $n > n_0$ subdivisions of *e* is not a.g.s.

Proof: The idea is the following. Consider the cycle C_n, with $n \ge 6$. As was mentioned in Example 4.1 and Lemma 4.3, C_n is not a.g.s. because $\overline{\theta}_i = \frac{2\pi}{n}$ is an *equally distributed* stable equilibrium point. Consider also the graph $G \setminus \{e\}$, obtained from *G* by removing the edge *e*. Take a edge of C_n, say *uv* and replace it by $G \setminus \{e\}$, joining the vertices of *e* with *u* and *v*.

The new graph we have obtained is the original G with the edge e split into several edges (see the sketch of Figure 11).

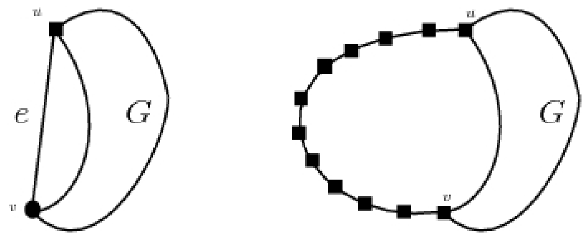

Figure 11. Situation of Theorem 7.3

The idea is the following: if n is large enough, the *force* induced by C_n will be weak enough to change the trivial equilibrium point of G to another still stable one.

Let $v_1,\ldots,v_m$ be the vertices of G and let $e = v_1v_2$. Since e is not a bridge, $G' = G\setminus\{e\}$ is connected and 0_m is an stable equilibrium point of G'. Now, connect the vertices v_1 and v_2 of G' through a path $P_n : v_1 = w_1,\ldots,w_n = v_2$ to obtain a graph $\widetilde{G}$ with vertices $\widetilde{V} = \{w_1,\ldots,w_n,v_3,\ldots,v_m\}$. We want to prove that for n large enough, there exist an $\varepsilon > 0$ and angles θ_i^ε, $1 \le i \le m$, such that the point $\theta_i^\varepsilon : \widetilde{V} \to R$ defined by:

$$\theta^\varepsilon \,/\, \theta_x^\varepsilon = \begin{cases} i\varepsilon, \textbf{ if } x = w_i \\ \theta_i^\varepsilon, \textbf{ if } x = v_i \end{cases}$$

is a stable equilibrium point of $\widetilde{G}$. In order for θ^ε to be an equilibrium it must satisfies:

$$\sum_{y\in N_x} \sin\left(\theta_y^\varepsilon - \theta_x^\varepsilon\right) = 0 \qquad , \qquad x \in \widetilde{V}$$

where N_x is the set of neighbors of vertex x in graph $\widetilde{G}$. These equations are trivially fulfilled for $x = w_2,\ldots,w_{n-1}$. Thus, it remains the following set of equations:

$$\begin{cases} \sum\limits_{y\in N'_{v_1}} \sin\left(\theta_y^\varepsilon - \theta_{v_1}^\varepsilon\right) + \sin(\varepsilon) = 0 \\ \sum\limits_{y\in N'_{v_2}} \sin\left(\theta_y^\varepsilon - \theta_{v_2}^\varepsilon\right) - \sin(\varepsilon) = 0 \\ \sum\limits_{y\in N_x} \sin\left(\theta_y^\varepsilon - \theta_x^\varepsilon\right) = 0 \qquad x \in \widetilde{V}\setminus\{v_1, v_2\} \end{cases}$$

where N and N' denote neighbors in G and G' respectively. This system can be thought as an ε--perturbation of the system that defines the equilibrium of G'. Moreover, if we add an adequate equation, e.g. $\theta_{v_1} = 0$, the system verifies the hypothesis of the implicit function theorem for $\theta = 0_m$ and $\varepsilon = 0$. Thus, it implicitly defines the angles θ_x^ε as a function of ε, for each $x \in V_G$, in a neighborhood $\left(-\varepsilon_0, \varepsilon_0\right)$ of 0. Moreover, we will have that θ^{ε} is a C^{∞} curve in R^n passing through 0_m for $\varepsilon = 0$.

Finally, in order to prove stability, we notice that when $\varepsilon = 0$, all the cosines $\cos\left(\theta_i^{\varepsilon} - \theta_j^{\varepsilon}\right)$ are positive, thus, the eigenvalues of the Jacobian linearization are negative, by Lemma 4.3. Thus, by the continuous dependence of the eigenvalues, ε_0 could be taken in such a way to assure the stability of equilibrium points θ^{ε} for each $\varepsilon \in \left(-\varepsilon_0, \varepsilon_0\right)$. Therefore it suffices to take $n_0 > 2\pi/\varepsilon_0$, and for each $n > n_0$, to set $\varepsilon = 2\pi/n$. ♦

7.2 Non adjacent twins

When the vertices are twins but not adjacent, previous arguments does not work, but something interesting can however be said. Indeed, let $S = \{v_1, \ldots, v_t\}$ a set of non adjacent twin vertices with the set SN of common neighbors. As in Proposition 2.1, let α be the sum of the phasors of *SN*. Then

$$\alpha = \sum_{j \in SN} V_j = V_i \cdot \sum_{j \in SN} \frac{V_j}{V_i} = \alpha_i . V_i \qquad , \quad i = 1, \ldots, t$$

So if two of them, say V_i and V_j are linearly independent, then, one of them is linearly independent to any of the others. So, α_k should be zero for any $k = 1, \ldots, t$.

Otherwise, if all of them are parallel, but non synchronized, we have a group of say *a* vertices of *SN* in a phase θ_0 and another group of $b = t - a$ ones in phase $\theta_0 + \pi$. Let v_i and v_j be in each group. Then:

$$\alpha_i = \sum_{l \in SN} \cos(\theta - \theta_l) \quad \text{and} \quad \alpha_j = \sum_{l \in SN} \cos(\theta + \pi - \theta_l)$$

But, $\cos\left(\theta + \pi - \theta_l\right) = -\cos\left(\theta - \theta_l\right)$, thus $\alpha_i + \alpha_j = 0$. As this argument could be repeated for any of the others pair of not synchronized vertices, if $a, b > 1$, we have a consistent homogeneous system of equations which has the null solution as the only one. Then, each α_i should be zero. If *a* or *b* is 1, either both α_i and α_j are null or some of them is negative. Summing all this up we have the following result.

Lemma 7.3: Let $\overline{\theta}$ be an equilibrium point of (3), then any set of *t* twin vertices should have their α_i equal to 0 if the equilibrium is stable or the synchronized twins are more than one. ♦

In that case, the matriz *A* of (5) will have a block of zeros (the one corresponding to the set of twins), thus either *A* has a kernel of dimension greater than one or it has positive eigenvalues and so is unstable. Thus we have the following result.

Proposition 7.1: Let $\overline{\theta}$ be a non degenerated stable equilibrium point of (3), then any set of non adjacent twin vertices should be synchronized. ♦

8. Conclusions

In this work we have introduced the idea of almost global synchronization (a.g.s.) of Kuramoto coupled oscillators. Local stability properties of the synchronization were recently stated and the are independent of the underlying interconnection graph. We have shown that the algebraic properties of this graph play a fundamental role when we look for global properties. Algebraic and dynamical properties are extremely related for these kind of systems. So, we presented the idea of a.g.s. graphs and started a characterization of this family of graphs. We have shown that the trees, the simplest graphs, are a.g.s. We have proved that complete graphs, the most complex, are also a.g.s. Several counterexamples illustrates that there are non a.g.s. graphs. We have proved that the characterization of a.g.s graphs can be reduced to the analysis of 2-connected graphs, since a graph is a.g.s. if and only if its block are. Typical techniques for graphs classification, like the use of homeomorphisms, can not be applied here, since we have shown that the a.g.s. property is not preserved by this way. Then, a different approach must be considered to go on with the classification.

9. References

Biggs, N. (1993). *Algebraic Graph Theory*, Cambridge University Press.

Canale, E. & Monzón, P. (2007). Gluing Kuramoto coupled oscillators networks, *46th IEEE Conference on Decisión and Control*, pp. 4596-4601, New Orleans, USA.

Cvetkovic, D; Doob, M. & Sachs, H. (1979) *Spectra of Graphs: theory and applications*. Ney York Academic Press.

Dussopt, L. & Laheurte, J. (1999). Coupled oscillator array generating circular polarization, *IEEE Microwave Guided Wave Letters*, vol. 9, Nº4, pp.160-162.

Ermentrout, G. (1985). The behavior of ring coupled oscillators, *Journal of Mathematical Biology*, vol. 23, pp.55-74.

Guckenheimer, J. & Holmes, P. (1983). *Nonlinear oscillations, dynamical systems and bifurcations of vector fields*, Applied Mathematical Sciences 42, Springer-Verlag.

Jadbabaie, A.; Lin, J. & Morse, S. (2003). Coordination of groups of mobile autonomous agents using nearest neighbor rules, *IEEE Trans. on Automatic Control*, vol. 48, Nº6, pp.988-1000.

Jadbabaie, A.; Barahona, M. & Motee, N. (2004). On the stability of the Kuramoto model of coupled nonlinear oscillators, in *Proc. of the Amerincan Control Conference.*

Khalil, H. (1996). *Nonlinear Systems*, Prentice-Hall.

Kuramoto, Y. (1975). In International Symposium on Mathematical problems in Theoretical Physics, *Lecture Notes on Physic*, vol. 39, pp.420.

Kuramoto, Y. (1984) Cooperative dynamics of oscillator community, *Progress of Theoretical Physics Suppl.*, Nº 79, pp.223-240.

Marshall, J.; Broucke, M. & Francis, B. (2004). Formations of vehicles in cyclic pursuit, *IEEE Trans. on Automatic Control*, vol. 49, Nº11, pp.1963-1974.

Moshtagh, N.; Jadbabaie, A. & Daniilidis, K. (2005). Distributed geodesic control laws for flocking of nonholonomic agents, in *Proc. of the Joint 44th IEEE Conference on Decision and Control and European Control Conference*, pp. 2835-2838, Seville.

Monzón, P & Paganini, F. (2005). Global considerations on the Kuramoto model of sinusoidally coupled oscillators, in *Proc. of the Joint 44th IEEE Conference on Decision and Control and European Control Conference*, pp.3923-3928, Seville.

Monzón, P. (2006). Almost global stability of dynamical systems, Ph.D. Dissertation, Universidad de la República, Uruguay.

Monzón, P & Paganini, F. (2006). Global properties of symmetric coupled oscillators with non complete associated interconnection graph, in *Congresso Brasileiro de Automática*, pp.470-475, Bahia, Brazil.

Monzón, P. & Canale, E. (2007). Single interconnection of Kuramoto coupled oscillators, *3rd IFAC Symposium on System, Structure and Control*, WM2-5, Foz de Iguaçu, Brasil.

Rantzer, A. (2001). A dual to Lyapunov' stability Theorem, *Systems & Control Letters*, 42(3), pp.161-168.

Rogge, J.A. & Aeyels, R.D. (2004). Stability of phase-locking solutions in a ring of unidirectionally coupled oscillators, *Journal of Physics A: Mathematical and General*, vol. 37, pp.11135-11148.

Strogatz, S. (1994). *Nonlinear Dynamics and Chaos: with applications to Physics, Biology, Chemistry and Engineering*. Perseus.

Strogatz, S. (2000).From Kuramoto to Crawford: exploring the onset of synchronization in populations of coupled nonlinear oscillators", Physica D, Nº143, pp.1-20.

van Hemmen, J.L. & Wreszinski, W.F. (1993). Lyapunov function for the Kuramoto model of nonlinearly coupled oscillators, *Journal of Statistical Physics*, 72(1/2), pp.145-166.

Winfree, A. (1980). *The Geometry of Biological Time*, Springer.

York, R. (1993). Nonlinear analysis of phase relationships in quasi-optical oscillator arrays, *IEEE Trans. on Microwave Theory and Applications*, vol. 41, Nº 10, pp.1799-1808.

9

On Stability of Multivariate Polynomials

E. Rodriguez-Angeles
Mexico State Autonomous University, Engineering Faculty
Mexico

1. Introduction

In the univariate polynomial case there are only two notions of stability: Hurwitz stability for continuous polynomials, and Schur stability for discrete polynomials. However, in the multivariate polynomial case there exists a more complex situation since there are more classes of stability: Wide Sense Stable (*WSS*), Scattering Hurwitz Stable (*SHS*) and Strict Sense Stable (*SSS*) for continuous polynomials (Fettweis & Basu, 1987), and Wide Sense Schur Stable (*WSSS*), Scattering Schur (*SS*) and Strict Sense Schur Stable (*SSSS*) for discrete polynomials (Basu & Fettweis, 1987). These classes have different properties, for example some classes reduce to the Hurwitz or antiSchur univariate notion and some polynomials from some classes may lose their stability property in the presence of arbitrary small coefficient variations. Besides, between these classes has not been possible to establish a similar relationship as it does for Hurwitz and Schur univariate polynomials by the Moebius transformation (Bose, 1982).

For a long time, *SSS* and *SSSS* polynomials have been employed to obtain key properties of stability and robust stability in their own domain because they have more coincident characteristics with Hurwitz and Schur univariate notions than the other multivariate classes have (Basu & Fettweis, 1987; Fettweis & Basu, 1987). Despite of this, in this work the interest is focused in two different notions of stability: Stable class for the continuous case (Kharitonov & Torres-Muñoz, 1999), and Schur Stable class for the discrete case (Torres-Muñoz et al., 2006). The reason is twofold: firstly, both classes have the property of being the largest classes preserving stability when faced to arbitrary small coefficient variations, and secondly, it has been recently shown that any member of the Stable class is associated, by a bilinear transformation, to one member of the Schur Stable class in the same way that Hurwitz and Schur univariate polynomials are related by the Moebius transformation (Torres-Muñoz et al., 2006). Besides, both classes are the natural extension of their univariate counterpart: Hurwitz and Schur univariate classes.

In general, in the analysis and control of any system is important to have efficient, from the computational point of view, criteria to test the stability of its characteristic polynomial. For the univariate case, there is a big variety of well-known efficient algorithms to deal with the Hurwitz and Schur stabilities (Barnett, 1983; Parks & Hahn, 1992; Bhattacharyya, 1995). However, in the multivariate case this problem is more complex: in the m-variate ($m > 2$) case there are few algorithms reported and they have the problem of their efficiency (Bose, 1982). Despite of this, in the bivariate ($m = 2$) case there are a lot of algorithms to deal with the Schur Stable bivariate issue and some of them are efficient (Anderson & Jury, 1973;

Maria & Fahmy, 1973; Siljak, 1975; Bose, 1977; Jury, 1988; Yang & Unbehauen, 1998; Bistritz, 2002; Xu et al., 2004; Dumitrescu, 2006). In contrast, in the continuous bivariate case the reported algorithms are devoted to the *SSS* class (Zeheb & Walach, 1981; Bose, 1982), i.e. there are no reported algorithms dealing with the Stable bivariate class. In this work an attempt is made to give a simple and efficient criterion to the Stable bivariate class.

In the univariate case, the fact that the Moebius transformation of any Hurwitz polynomial gives a Schur polynomial and viceversa has allowed extending stability and robust stability results from one domain to the other (Parks & Hahn, 1992). In this work it is used a similar fact between the Stable and Schur Stable bivariate classes in the following way: firstly it is obtain the discrete counterpart of a given continuous bivariate polynomial, next its Schur stability is proved, and finally the Schur stability of this polynomial implies the stability of the continuous polynomial. For this, a new Schur Stable bivariate test is developed by constructing a reduced order polynomial array for univariate Schur polynomials with literal coefficients in such a way that the Schur stability of these polynomials together with specific coefficient conditions implies the stability of the original polynomial.

This work begins with the introduction of some preliminaries notions and notation of multivariate polynomials and a summary of some key properties of the Stable and Schur Stable classes. Next the problem is clearly defined, following with the presentation of the Schur Stable and Stable tests. Finally, some examples and conclusions remarks are given.

2. Preliminaries of multivariate polynomials

(Bose, 1982) A multivariate polynomial in the variable vector $\mathbf{s}=(s_1, s_2, \ldots, s_m)$ is a finite sum of the form

$$p(\mathbf{s})=\sum_{i_1=0}^{n_1}\sum_{i_2=0}^{n_2}\cdots\sum_{i_m=0}^{n_m} a_{i_1 i_2\cdots i_m} s_1^{i_1} s_2^{i_2}\cdots s_m^{i_m} \tag{1}$$

where s_k, $k=1,2,\ldots,m$ are the independent variables of partial degree $n_k=\deg_k\{p(\mathbf{s})\}$, $k=1,2,\ldots,m$. The coefficients $a_{i_1 i_2\cdots i_m}$ are given real (or complex numbers). One may define, following the lexicographic order of the indices, the coefficient vector

$$\mathbf{a}=\left(a_{00\cdots 0}, a_{10\cdots 0}, a_{20\cdots 0}, \ldots, a_{n_1 n_2\cdots n_m}\right).$$

In the analysis of multivariate polynomials is very useful to write the polynomial $p(\mathbf{s})$ as an univariate polynomial with polynomial coefficients, i.e.

$$p(\mathbf{s})=\sum_{k=0}^{n_i} a_k^{(i)}(s_1, s_2, \ldots, s_{i-1}, s_{i+1}, \ldots, s_m)\, s_i^k \tag{2}$$

for $i=1,2,\ldots,m$, and where the coefficients

$$a_k^{(i)}(s_1, s_2, \ldots, s_{i-1}, s_{i+1}, \ldots, s_m)=\sum_{i_1=0}^{n_1}\sum_{i_2=0}^{n_2}\cdots\sum_{i_{i-1}=0}^{n_{i-1}}\sum_{i_{i+1}=0}^{n_{i+1}}\cdots\sum_{i_m=0}^{n_m} a_{i_1 i_2\cdots i_{i-1} k i_{i+1}\cdots i_m} s_1^{i_1} s_2^{i_2}\cdots s_{i-1}^{i_{i-1}} s_{i+1}^{i_{i+1}}\cdots s_m^{i_m}$$

are $(m-1)$-variate polynomials. In this case, the free and the main polynomial coefficients with respect to the variable s_i correspond to $k=0$ and $k=n_i$ respectively.

A root of $p(\mathbf{s})$ is a vector $\mathbf{s_0} = (s_{10}, s_{20}, \dots, s_{m0})$ such that $p(\mathbf{s_0}) = 0$. If $(s_2, s_3, \dots, s_m) = (s_{20}, s_{30,\dots}, s_{m0})$ are fixed to some arbitrary value, then $p(s_1, s_{20}, \dots, s_{m0})$ is an univariate polynomial in the variable s_1 of degree n_1. In conclusion, and in contrast with the univariate case, a multivariate $p(\mathbf{s})$ has a finite number of root manifolds in a n-dimensional complex space.
Besides, in contrast with the univariate case, two multivariate polynomials may be coprime but possessing common roots (Kharitonov & Torres-Muñoz, 1999).
Let us denote the set of constant degree m-variate polynomials by

$$P_{\mathbf{n}} = \{p(\mathbf{s}) \mid \deg\{p(\mathbf{s})\} = \mathbf{n}\}$$

where $\mathbf{n} = (n_1, n_2, \dots, n_m)$, $n_i \in \mathcal{N}$, is the vector of constant partial degrees. Similar definitions will hold for univariate polynomials.
In the analysis of the continuous multivariate polynomials is often used the notion of the conjugate polynomial. The conjugate polynomial of $p(\mathbf{s})$ with respect to the variable s_1, using $p(\mathbf{s})$ as in the decomposition (2) with respect to the variable s_1, is given by

$$p^*(\mathbf{s}) = \overline{p}(-s_1, s_2, \dots, s_m) = \sum_{k=0}^{n_1} \overline{a_k^{(1)}}(s_2, s_3, \dots, s_m)\,(-s_1)^k \tag{3}$$

where $\overline{a_k^{(1)}}(s_2, s_3, \dots, s_m)$ means that all coefficients and variables $s_2, s_3, \dots, s_m$ are changed by their complex conjugates. Clearly, the conjugate polynomial can be taken from one until m variables. Hereafter it will be considered, unless otherwise stated, the conjugate $p^*(\mathbf{s})$ with respect to the variable s_1.
To distinguish the discrete polynomials from the continuous case, and for tradition, a discrete multivariate polynomial is notated as $q(\mathbf{z})$, the variable vector and the coefficient vector used are $\mathbf{z} = (z_1, z_2, \dots, z_m)$ and $\mathbf{b} = (b_{00\cdots0}, b_{10\cdots0}, b_{20\cdots0}, \dots, b_{n_1n_2\cdots n_m})$ respectively. Besides, the structure of a discrete polynomial is the same as (1) and it is also possible to write it as in the decomposition (2).
In the analysis of the discrete multivariate polynomials is often used the notion of the reciprocal conjugate polynomial. The reciprocal conjugate polynomial of $q(\mathbf{z})$ with respect to the variable z_1, using $q(\mathbf{z})$ as in the decomposition (2) with respect to the variable z_1, is given by

$$q^{\otimes}(\mathbf{z}) = z_1^{n_1}\overline{q}\left(z_1^{-1}, z_2, \dots, z_m\right) = z_1^{n_1}\sum_{k=0}^{n_1} \overline{b_k^{(1)}}(z_2, z_3, \dots, z_m)\, z_1^{-k} \tag{4}$$

where $\overline{b_k^{(1)}}(z_2, z_3, \dots, z_m)$ means that all coefficients and variables $z_2, z_3, \dots, z_m$ are changed by their complex conjugates. Clearly, the reciprocal conjugate polynomial can be taken from one until m variables. Hereafter it will be considered, unless otherwise stated, the conjugate $q^{\otimes}(\mathbf{z})$ with respect to the variable z_1.

2.1 Stable multivariate polynomials

In the continuous case consider the following polydomain

$$\Gamma_m^{(0)} = \{(s_1, s_2, \ldots, s_m) \mid \mathrm{Re}(s_i) \geq 0\ ,\ i = 1,2,\ldots,m\}$$

together with its essential boundary

$$\Omega^{(m)} = \{(s_1, s_2, \ldots, s_m) \mid \mathrm{Re}(s_i) = 0\ ,\ i = 1,2,\ldots,m\}.$$

Definition 1: *A multivariate polynomial $p(\mathbf{s}) \in P_\mathbf{n}$ is called Stable if it satisfies the following conditions*

1) $p(\mathbf{s}) \neq 0 \quad \forall \mathbf{s} \in \Gamma_m^{(0)}$.

2) Main $(m-1)$-variate polynomials $a_{n_i}^{(i)}(s_1, s_2, \ldots, s_{i-1}, s_{i+1}, \ldots, s_m)$, for $i = 1,2,\ldots,m$, are Stable polynomials, according to this definition, with degree $(n_1, n_2, \ldots, n_{i-1}, n_{i+1}, \ldots, n_m)$.

A polynomial satisfying just condition 1 is called Strict Sense Stable (*SSS*). Such class of polynomials has played an important role in stability and robust stability analysis (Feetweis & Basu, 1987). This class reduces to the standard notion of Hurwitz stability in the univariate case, but may lose its stability property in the presence of small arbitrary coefficients perturbations (Kharitonov & Torres-Muñoz, 1999). This fragility is very undesirable when one studies the robustness issue.

Note that the stable class is a proper subclass of the *SSS* class, as it is the largest multivariate class preserving stability under small coefficient variations (Kharitonov & Torres-Muñoz, 1999). Besides, the stable class reduces to the traditional Hurwitz class in the univariate case, so the stable class also preserves several useful properties of univariate Hurwitz polynomials too (Kharitonov & Torres-Muñoz, 1999; Kharitonov & Torres-Muñoz, 2002). A summary of some of properties of the stable multivariate class is the following.

Lemma 1: *Let $p(\mathbf{s}) \in P_\mathbf{n}$ be a stable multivariate polynomial. Let s_1 be fixed at some value s_{10} such that $\mathrm{Re}(s_{10}) \geq 0$. Then the $(m-1)$-variate polynomial $p(s_{10}, s_2, \ldots, s_m)$ is a stable polynomial of degree $(n_2, n_3, \ldots, n_m)$.*

Lemma 2: *Let $p(\mathbf{s}) \in P_\mathbf{n}$ be a stable multivariate polynomial. Assume that $n_1 > 0$, then the polynomial $\hat{p}(\mathbf{s}) = s_1^{n_1} p(s_1^{-1}, s_2, \ldots, s_m)$ is a stable multivariate polynomial of the same degree as $p(\mathbf{s})$.*

Notice that, by successive aplication, in Lemma 1 and Lemma 2 can be taken from one until m variables.

Next result is the extension of the Lucas' Theorem for the Hurwitz univariate polynomials (Marden, 1949), i.e. it shows the invariance of the stability property under differentiation that can be taken, by successive application, from one until m variables.

Theorem 3: *Let $p(\mathbf{s}) \in P_\mathbf{n}$ be a stable multivariate polynomial. Assume that $n_1 > 0$, then the polynomial $\tilde{p}(\mathbf{s}) = \dfrac{\partial p(s_1, s_2, \ldots, s_m)}{\partial s_1}$ is a stable multivariate polynomial of degree $(n_1 - 1, n_2, \ldots, n_m)$.*

Lemma 4: *Let $p(\mathbf{s}) \in P_\mathbf{n}$ be a stable multivariate polynomial. Then all $(m-1)$-variate polynomial coefficients $a_k^{(i)}(s_1, s_2, \ldots, s_{i-1}, s_{i+1}, \ldots, s_m)$ for $k = 0,1,\ldots,n_i$, in the decomposition (2) with respect to the variable s_i for $i = 1,2,\ldots,m$, are stable polynomials of degree $(n_1, n_2, \ldots, n_{i-1}, n_{i+1}, \ldots, n_m)$.*

Next property is the extension of the classical Stodola's Condition for Hurwitz univariate polynomials (Gantmacher, 1959).

Theorem 5: *Let $p(\mathbf{s}) \in P_{\mathbf{n}}$ be a stable multivariate polynomial with real coefficients. Then all coefficients $a_{i_1 i_2 \cdots i_m}$ of the polynomial have the same sign: either all of them are positive, or all of them are negative.*

Lemma 6: *Let $p(\mathbf{s}) \in P_{\mathbf{n}}$ be a stable multivariate polynomial. Then the main coefficient $a_{n_1 n_2 \cdots n_m}$ is not zero.*

Proof: *For the case $m = 1$ the statement is obvious.*

For $m = 2$, consider a stable bivariate polynomial $p(s_1, s_2)$ of degree (n_1, n_2). By Definition 1, its main univariate polynomial coefficient $a_{n_1}^{(1)}(s_2)$, in the decomposition (2) with respect to the variable s_1, is a Hurwitz stable polynomial of degree n_2, i.e. coefficient $a_{n_1 n_2} \neq 0$.

Assume that the statement is true for $(m-1)$-variate polynomials and consider the m-variate case. Given a stable multivariate polynomial $p(\mathbf{s})$ of degree $(n_1, n_2, \ldots, n_m)$, from Definition 1 follows that its main $(m-1)$-variate polynomial coefficient $a_{n_1}^{(1)}(s_2, s_3, \ldots, s_m)$, in the decomposition (2) with respect to the variable s_1, is a stable $(m-1)$-variate polynomial of degree $(n_2, n_3, \ldots, n_m)$, then, by the induction hypothesis, coefficient $a_{n_1 n_2 \cdots n_m} \neq 0$.

Next results show that for stable multivariate polynomials the robust stability can be considered without structural restrictions on uncertain parameters, and that a stable multivariate polynomial has no roots close to the essential boundary.

Theorem 7: *Let $p(\mathbf{s}) \in P_{\mathbf{n}}$ be a stable multivariate polynomial. Then there always exists $\varepsilon>0$ such that every multivariate polynomial with a coefficient vector lying in the ε-neighbourhood of the coefficient vector of $p(\mathbf{s})$ is stable too.*

Theorem 8: *Let $p(\mathbf{s}) \in P_{\mathbf{n}}$ be a stable multivariate polynomial. Then there always exists $\varepsilon>0$ such that it has no roots in the ε-neighbourhood of the essential boundary $\Omega^{(m)}$.*

2.2 Schur Stable multivariate polynomials

In the discrete domain consider the polydisc given by

$$U_m^{(0)} = \{(z_1, z_2, \ldots, z_m) \mid |z_i| \geq 1,\ i = 1,2,\ldots,m\}$$

and its essential boundary given by

$$T^{(m)} = \{(z_1, z_2, \ldots, z_m) \mid |z_i| = 1,\ i = 1,2,\ldots,m\}.$$

Definition 2: *A multivariate polynomial $q(\mathbf{z}) \in P_{\mathbf{n}}$ is called Schur Stable if $q(\mathbf{z}) \neq 0 \quad \forall \mathbf{z} \in U_m^{(0)}$.*

The so-called Strict Sense Schur Stable (*SSSS*) class is often employed in the literature and it considers a $q(\mathbf{z}) \in P_{\mathbf{n}}$ *SSSS* if $q(\mathbf{z}) \neq 0$ for all $\mathbf{z} \in \{(z_1, z_2, \ldots, z_m) \mid |z_i| \leq 1,\ i = 1,2,\ldots,m\}$, (Basu & Feetweis, 1987). Despite of *SSSS* class preserves stability under small coefficient variations, it reduces to the standard antiSchur polynomials notion in the univariate case, so some key properties of Schur univariate polynomials can not be extended to the multivariate case as the invariance of the Schur stability property under differentiation (Torres-Muñoz et al., 2006).

The Schur stable class, in the sense of Definition 2, is also used in the literature (Huang, 1972; Kaczorek, 1985). Actually, it is the reciprocal class of the *SSSS* class and also preserves stability under small coefficient variations. Besides, the Schur stable class reduces to the standard Schur class in the univariate case, so several useful properties may be extended from the univariate Schur polynomials to the multivariate case (Torres-Muñoz et al., 2006). A summary of some of the properties of the Schur stable multivariate class is the following.

Lemma 9: *Let* $q(\mathbf{z}) \in P_{\mathbf{n}}$ *be a Schur stable multivariate polynomial. Let* z_1 *be fixed at some value* z_{10} *such that* $|z_{10}| \geq 1$. *Then the* $(m-1)$*-variate polynomial* $q(z_{10}, z_2, \ldots, z_m)$ *is a Schur stable polynomial of degree* $(n_2, n_3, \ldots, n_m)$.

Lemma 10: *Let* $q(\mathbf{z}) \in P_{\mathbf{n}}$ *be a Schur stable multivariate polynomial. Assume that* $n_1 > 0$, *then the polynomial* $\tilde{q}(\mathbf{z}) = q(-z_1, z_2, \ldots, z_m)$ *is a Schur stable multivariate polynomial of the same degree as* $q(\mathbf{z})$.

Theorem 11: *Let* $q(\mathbf{z}) \in P_{\mathbf{n}}$ *be a Schur stable multivariate polynomial. Assume that* $n_1 > 0$, *then the polynomial* $\tilde{q}(\mathbf{z}) = \dfrac{\partial q(z_1, z_2, \ldots, z_m)}{\partial z_1}$ *is a Schur stable multivariate polynomial of degree* $(n_1 - 1, n_2, \ldots, n_m)$.

Notice that Lemma 9, Lemma 10 and Theorem 11 are the discrete version of Lemma 1, Lemma 2 and Theorem 3 respectively, then it can be also taken from one until m variables.

Lemma 12: *Let* $q(\mathbf{z}) \in P_{\mathbf{n}}$ *be a Schur stable multivariate polynomial. Then the main* $(m-1)$*-variate polynomial coefficients* $b_{n_i}^{(i)}(z_1, z_2, \ldots, z_{i-1}, z_{i+1}, \ldots, z_m)$, *for* $i = 1, 2, \ldots, m$, *in the decomposition (2) with respect to the variable* z_i, *are Schur stable polynomials of degree* $(n_1, n_2, \ldots, n_{i-1}, n_{i+1}, \ldots, n_m)$.

It is worth to mention that other polynomial coefficients, different from the main polynomial coefficients, in the decomposition (2), are not necessarily Schur stable (Torres-Muñoz et al., 2006).

Next property is the extension of the classical coefficient condition for Schur univariate polynomials (Bhattacharyya, 1995).

Lemma 13: *Let* $q(\mathbf{z}) \in P_{\mathbf{n}}$ *be a Schur stable multivariate polynomial. Then the coefficient condition* $|b_{00\cdots 0}| < |b_{n_1 n_2 \cdots n_m}|$ *is hold.*

Corollary 14: *Let* $q(\mathbf{z}) \in P_{\mathbf{n}}$ *be a Schur stable multivariate polynomial. Then the main coefficient* $b_{n_1 n_2 \cdots n_m}$ *is not zero.*

Proof*: It directly follows from Lemma 13 and the fact that* $0 \leq |b_{00\cdots 0}|$.

Next results show that the Schur stable multivariate class is suitable to study the robustness issue.

Theorem 15: *Let* $q(\mathbf{z}) \in P_{\mathbf{n}}$ *be a Schur stable multivariate polynomial. Then there always exists* ε>0 *such that every multivariate polynomial with a coefficient vector lying in the* ε*-neighbourhood of the coefficient vector of* $q(\mathbf{z})$ *is Schur stable too.*

Theorem 16: *Let* $q(\mathbf{z}) \in P_{\mathbf{n}}$ *be a Schur stable multivariate polynomial. Then there always exists* ε>0 *such that it has no roots in the* ε*-neighbourhood of the essential boundary* $T^{(m)}$.

3. Problem statement

From a practical point of view is essential to dispose of computationally feasible polynomial stability criteria. For the univariate case, there are some very well-known efficient stability criteria (Barnett, 1983; Parks & Hahn, 1992; Bhattacharyya, 1995), but for the m-variate case there aren't. However, there are some criteria for the bivariate case (Jury, 1988; Bistritz, 2002; Xu et al., 2004; Dumitrescu, 2006), but their implementation in the multivariate case is not easy. In this work the main goal is to tackle the following.

Problem: *Given a continuous bivariate polynomial $p(s_1, s_2)$, find an efficient polynomial coefficients dependent criterion allowing to conclude whether or not it belongs to the stable class, in the sense of Definition 1. This criterion must be also potentially suitable for its extension to the multivariate case.*

At first glance, by nature of the continuous stable class, trying to obtain non-recursive criteria might be a hard task. This contrasts with the discrete Schur case where research efforts leaded to reliable algorithms allowing to analyze stability depending on the polynomial coefficients in a finite number of steps.

In the univariate polynomial case, Hurwitz stability implies Schur stability and viceversa. This correspondence has allowed to translate stability results between continuous and discrete domains. For instance, translation of Routh-Hurwitz stability criterion inspired the development of coefficient-based algorithms for Schur stability (Parks & Hahn, 1992).

In such a vein, the belief that *SSS* bivariate polynomials are in strict equivalence with Schur stable bivariate polynomials was in the center of earlier attempts to develope a bivariate stability theory. In these attempts were used a different transformation of transformation (5). Unfortunately, the early conclusion was only *SSS* stability is implied by Schur stability and not in the reverse sense (Bose, 1982). The same conclusion is obtained using transformation (5): consider the *SSS* polynomial $p(\mathbf{s}) = s_1 s_2 + s_2 + 1$, it turns out that the transformed discrete polynomial, using transformation (5), $q(\mathbf{z}) = 3z_1 z_2 - z_1 + z_2 + 1$ is not Schur stable as it has the root $(-1,1) \in U_2^{(0)}$, (Torres-Muñoz et al., 2006) . Therefore, there is no way to infer stability results between *SSS* and Schur stable classes.

However, recently was shown that the multivariate stable class in the sense of Definition 1 is the counterpart of the multivariate Schur stable class in the sense of Definition 2.

Theorem 17: *(Torres-Muñoz et al., 2006) The polynomial $p(\mathbf{s})$ of degree $(n_1, n_2, \ldots, n_m)$ is stable if and only if the polynomial*

$$q(\mathbf{z}) = (z_1 - 1)^{n_1} (z_2 - 1)^{n_2} \cdots (z_m - 1)^{n_m}\, p\left(\frac{z_1 + 1}{z_1 - 1}, \frac{z_2 + 1}{z_2 - 1}, \ldots, \frac{z_m + 1}{z_m - 1}\right) \tag{5}$$

is a Schur stable polynomial of degree $(n_1, n_2, \ldots, n_m)$.

Observe that this transformation is the natural extension of the Moebius univariate transformation. This result was used as a bridge to translate properties and stability results from the continuous domain to the discrete one and viceversa (Torres-Muñoz et al., 2006).

4. An indirect criterion for continuous bivariate polynomial stability

On the basis of Theorem 17, an indirect bivariate continuous stability algorithm can be stated as follows:

Given a continuous bivariate polynomial

$$p(\mathbf{s}) = \sum_{i_1=0}^{n_1} \sum_{i_2=0}^{n_2} a_{i_1 i_2} s_1^{i_1} s_2^{i_2}$$

1. Construct the discrete polynomial $q(\mathbf{z})$ using the transformation (5). If $q(\mathbf{z})$ has the same degree as $p(\mathbf{s})$, then continue. If it is not the case, then the polynomial $p(\mathbf{s})$ is not stable.
2. Apply any Schur bivariate stability test to $q(\mathbf{z})$.
3. If $q(\mathbf{z})$ is Schur stable, then the polynomial $p(\mathbf{s})$ is stable. If it is not the case, then the polynomial $p(\mathbf{s})$ is not stable.

It is worth noticing that there exists a variety of criteria for the Schur bivariate stability case (Jury, 1988; Bistritz 2002) that might be potentially adapted to the case of continuous bivariate stable polynomials in the step 2. However, a new simple Schur stability test was introduced recently as one alternative way to tackle the problem of giving a reliable criterion for the continuous stable class (Rodriguez-Angeles et al., 2007). The underlying philosophy is, inspired on the univariate case, to try to find an array of reduced degree polynomials whose stability will imply stability of the original polynomial (Bhattacharyya et al., 1995).

Theorem 18: *(Rodriguez-Angeles et al., 2007) The polynomial $q(z_1, z_2) \in P_{\mathbf{n}}$ is Schur stable if and only if*

i) $q(z_{10}, z_2) \neq 0$ for all $|z_2| \geq 1$ and for a fixed $z_1 = z_{10}$ such that $|z_{10}| \geq 1$.

ii) Given the following polynomial sequence

$$q^{(j+1)}(z_1, z_{20}) = \frac{1}{z_1}\left\{\overline{b_{n_1-j}^{(1,j)}}(z_{20})\, q^{(j)}(z_1, z_{20}) - b_0^{(1,j)}(z_{20})\left[q^{(j)}(z_1, z_{20})\right]^{\otimes}\right\} \tag{6}$$

the following inequality holds

$$\left|b_{n_1-j}^{(1,j)}(z_{20})\right| > \left|b_0^{(1,j)}(z_{20})\right| \tag{7}$$

for all $z_2 = z_{20}$ such that $|z_{20}| = 1$, where $q^{(0)}(z_1, z_{20}) = q(z_1, z_{20})$ and $b_k^{(1,j)}(z_{20})$ is the k-th coefficient of the j–th polynomial $q^{(j)}(z_1, z_{20})$ for $j = 0,1,\ldots,n_1 - 1$.

The Schur bivariate stability algorithm, based on Theorem 18, can be stated as follows:

Given a discrete bivariate polynomial in the decomposition (2) with respect to the variable z_1

$$q(\mathbf{z}) = \sum_{i_1=0}^{n_1}\sum_{i_2=0}^{n_2} b_{i_1 i_2} z_1^{i_1} z_2^{i_2} = \sum_{k=0}^{n_1} b_k^{(1)}(z_2)\, z_1^k$$

1. Verify if the univariate polynomial $q(1, z_2)$ is Schur stable. If it is Schur stable, then continue. If it is not the case, then the bivariate polynomial $q(\mathbf{z})$ is not Schur stable.
2. Verify step by step if the inequality

$$\left|b_{n_1-j}^{(1,j)}\left(e^{j\theta}\right)\right| > \left|b_0^{(1,j)}\left(e^{j\theta}\right)\right|$$

holds for all $\theta \in [0, 2\pi]$ and for $j = 0,1,\ldots,n_1 - 1$, and where coefficients $b_{n_1-j}^{(1,j)}\left(e^{j\theta}\right)$ and $b_0^{(1,j)}\left(e^{j\theta}\right)$ are obtained from sequence (6) with $z_2 = e^{j\theta}$. If all inequalities hold, then the bivariate polynomial $q(\mathbf{z})$ is Schur stable. If one of the coefficient conditions fails, then stop and the bivariate polynomial $q(\mathbf{z})$ is not Schur stable.

Actually, the step 2 can be implemented in a numerical and graphical way providing a simple test for Schur bivariate stability. Besides, notice that the graphical testing is just needed in a bounded interval independently of the polynomial vector degree.

Example 1: *Determine the stability of the continuous bivariate polynomial*

$$p(\mathbf{s}) = \left(0.75 + s_2 + 1.25 s_2^2\right) + \left(1 + 2s_2 + 3s_2^2\right)s_1 + \left(1.25 + 3s_2 + 2.75 s_2^2\right)s_1^2 .$$

According to Theorem 17 the stability of $p(\mathbf{s})$ is equivalent to the Schur stability of the transformed polynomial $q(\mathbf{z})$ given by

$$q(\mathbf{z}) = \left(0.25 z_2^2\right) + \left(0.25 z_2 + 0.5 z_2^2\right)z_1 + \left(0.25 + 0.5 z_2 + z_2^2\right)z_1^2 .$$

Hence $q(\mathbf{z})$ has the same degree as $p(\mathbf{s})$, one has to check the Schur stability of $q(\mathbf{z})$. Following the algorithm for Schur bivariate stability, one may verify the step 1. Then let us tackle the step 2.

The first polynomial of the sequence (6) is

$$q^{(0)}\left(z_1, e^{j\theta}\right) = \left(0.25 e^{j2\theta}\right) + \left(0.25 e^{j\theta} + 0.5 e^{j2\theta}\right)z_1 + \left(0.25 + 0.5 e^{j\theta} + e^{j2\theta}\right)z_1^2 .$$

From Figure 1 one can see that the inequality $\left|b_2^{(1,0)}\left(e^{j\theta}\right)\right| > \left|b_0^{(1,0)}\left(e^{j\theta}\right)\right|$ holds for all $\theta \in [0, 2\pi]$. Then, let us continue with the test.

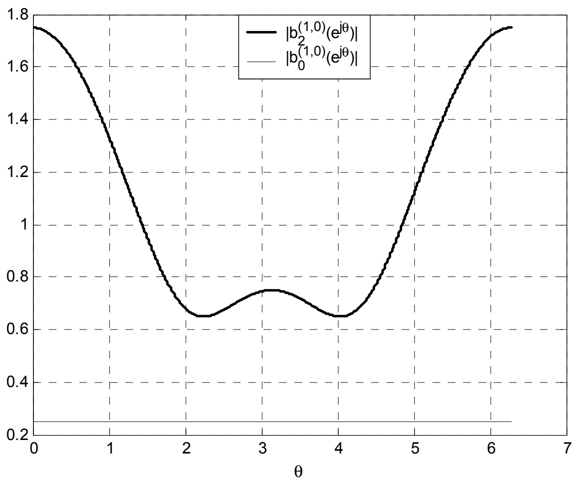

Figure 1. Coefficient condition for the 1st polynomial $q^{(0)}\left(z_1, e^{j\theta}\right)$ of the polynomial sequence

The second polynomial of the sequence (6) is

$$q^{(1)}\left(z_1, e^{j\theta}\right) = \left(0.5 + 0.25 e^{-j\theta} + 0.25 e^{j\theta} + 0.125 e^{j2\theta}\right) + \left(1.25 + 0.625 e^{-j\theta} + 0.625 e^{j\theta} + 0.25 e^{-j2\theta} + 0.25 e^{j2\theta}\right)z_1 .$$

From Figure 2 one can see that the inequality $\left|b_1^{(1,1)}\left(e^{j\theta}\right)\right| > \left|b_0^{(1,1)}\left(e^{j\theta}\right)\right|$ holds for all $\theta \in [0, 2\pi]$. Then the discrete bivariate polynomial $q(\mathbf{z})$ is Schur stable as it is reported in several papers

(Huang, 1972; Jury, 1988; Bistritz, 2002). Therefore, the continuous bivariate polynomial $p(\mathbf{s})$ is stable.

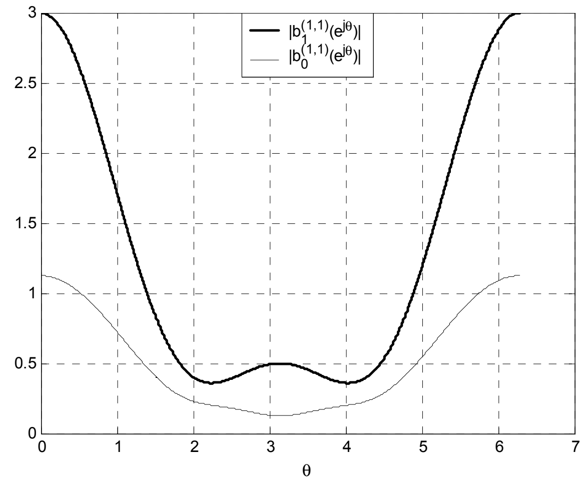

Figure 2. Coefficient condition for the 2nd polynomial $q^{(1)}(z_1, e^{j\theta})$ of the polynomial sequence

5. Numerical examples

The aim is to show the potential applicability of the indirect algorithm presented in the previous section when dealing with bivariate polynomials of relatively high degree. From a computational point of view, it is instrumental to take into account the relationship between the coefficients of a continuous multivariate polynomial $p(\mathbf{s})$ and those of its discrete counterpart $q(\mathbf{z})$. Actually, the coefficients of the bivariate polynomials $p(s_1, s_2)$ and $q(z_1, z_2)$ are related by a linear transformation as it is expressed in the following.

Theorem 19: *Let* $p(\mathbf{s}) = \sum_{i_1=0}^{n_1} \sum_{i_2=0}^{n_2} a_{i_1 i_2} s_1^{i_1} s_2^{i_2}$ *be a given bivariate polynomial of degree* (n_1, n_2). *Consider its transformed discrete bivariate polynomial*

$$q(\mathbf{z}) = (z_1 - 1)^{n_1} (z_2 - 1)^{n_2} p\left(\frac{z_1 + 1}{z_1 - 1}, \frac{z_2 + 1}{z_2 - 1}\right) \tag{8}$$

then $q(\mathbf{z})$ *can be expressed as*

$$q(\mathbf{z}) = \sum_{i_1=0}^{n_1} \sum_{i_2=0}^{n_2} b_{i_1 i_2} z_1^{i_1} z_2^{i_2}$$

where the coefficients $a_{i_1 i_2}$ *and* $b_{i_1 i_2}$ *are related as follows*

$$b_{i_1 i_2} = \sum_{j_1=0}^{n_1} \sum_{j_2=0}^{n_2} a_{k_1 k_2} \left[\sum_{l_1=m_1}^{r_1} \sum_{l_2=m_2}^{r_2} \binom{n_1 - j_1}{l_1} \binom{n_2 - j_2}{l_2} \binom{j_1}{i_1 - l_1} \binom{j_2}{i_2 - l_2} (-1)^{\phi} \right]$$

where

$$\begin{aligned}
k_1 &= n_1 - j_1, \\
k_2 &= n_2 - j_2, \\
m_1 &= i_1 - \min(i_1, j_1), \\
m_2 &= i_2 - \min(i_2, j_2), \\
r_1 &= \min(i_1, n_1 - j_1), \\
r_2 &= \min(i_2, n_2 - j_2), \\
\phi &= j_1 + j_2 + l_1 + l_2 - i_1 - i_2.
\end{aligned}$$

Corollary 20: *Let $p(\mathbf{s})$ and $q(\mathbf{z})$ two bivariate polynomials related as in (8) with coefficient vectors $\mathbf{a}$ and $\mathbf{b}$ respectively. The coefficient vectors are related through the matrix equation $\mathbf{b} = \mathbf{T}\mathbf{a}$. This relationship can be expressed as*

$$\begin{bmatrix} \mathbf{b}_{n_1} \\ \mathbf{b}_{n_1-1} \\ \vdots \\ \mathbf{b}_0 \end{bmatrix} = \mathbf{T} \begin{bmatrix} \mathbf{a}_{n_1} \\ \mathbf{a}_{n_1-1} \\ \vdots \\ \mathbf{a}_0 \end{bmatrix}$$

where $\mathbf{a}_i = [a_{in_2}, a_{in_2-1}, \ldots, a_{i0}]^T$, $\mathbf{b}_i = [b_{in_2}, b_{in_2-1}, \ldots, b_{i0}]^T$ *and* $\mathbf{T}$ *is a constant nonsingular matrix given by*

$$\mathbf{T} = \begin{bmatrix} T_{1,1} & T_{2,1} & \cdots & T_{n_1+1,1} \\ T_{1,2} & T_{2,2} & \cdots & T_{n_1+1,2} \\ \vdots & \vdots & \ddots & \vdots \\ T_{1,n_1+1} & T_{2,n_1+1} & \cdots & T_{n_1+1,n_1+1} \end{bmatrix}$$

where

$$T_{i,j} = \begin{bmatrix} t_{1,1}^{(i,j)} & t_{1,2}^{(i,j)} & \cdots & t_{1,n_2+1}^{(i,j)} \\ t_{2,1}^{(i,j)} & t_{2,2}^{(i,j)} & \cdots & t_{2,n_2+1}^{(i,j)} \\ \vdots & \vdots & \ddots & \vdots \\ t_{n_2+1,1}^{(i,j)} & t_{n_2+1,2}^{(i,j)} & \cdots & t_{n_2+1,n_2+1}^{(i,j)} \end{bmatrix}$$

with

$$t_{k,l}^{(i,j)} = \sum_{p=m_1}^{r_1} \sum_{q=m_2}^{r_2} \binom{n_1 - i + 1}{p} \binom{n_2 - l + 1}{q} \binom{i-1}{n_1 - j - p + 1} \binom{l-1}{n_2 - k - q + 1} (-1)^{\phi}$$

where

$$\begin{aligned}
m_1 &= n_1 - j - \min(n_1 - j + 1, i - 1) + 1, \\
m_2 &= n_2 - k - \min(n_2 - k + 1, l - 1) + 1, \\
r_1 &= \min(n_1 - j + 1, n_1 - i + 1), \\
r_2 &= \min(n_2 - k + 1, n_2 - l + 1), \\
\phi &= i + j + k + l + p + q - n_1 - n_2.
\end{aligned}$$

Notice that previous statements may be deduced by straightforward matrix calculations from the transformation (8).

Besides, for the computational implementation it is useful to write a polynomial $p(\mathbf{s}) = \sum_{i_1=0}^{n_1} \sum_{i_2=0}^{n_2} a_{i_1 i_2} s_1^{i_1} s_2^{i_2}$ in a matrix form, i.e.

$$p(\mathbf{s}) = \mathbf{s}_1^T \mathbf{A} \mathbf{s}_2 \tag{9}$$

where $\mathbf{s}_i = \left[1, s_i, \ldots, s_i^{n_i}\right]^T$ for $i = 1,2$ and

$$\mathbf{A} = \begin{bmatrix} a_{00} & a_{01} & \cdots & a_{0n_2} \\ a_{10} & a_{11} & \cdots & a_{1n_2} \\ \vdots & \vdots & \ddots & \vdots \\ a_{n_1 0} & a_{n_1 1} & \cdots & a_{n_1 n_2} \end{bmatrix}.$$

Example 2: *Check the stability of the* $(11,6)$*-degree continuous polynomial* $p(\mathbf{s})$ *expressed in the form (9) with*

$$\mathbf{A} = \begin{bmatrix} 31.48 & 204.27 & 208.83 & 539.64 & 303.39 & 195.02 & 25.37 \\ 309.64 & 1627.41 & 4783.46 & 6549.36 & 6401.40 & 2713.10 & 573.71 \\ 1262.99 & 6618.74 & 19317.08 & 20982.39 & 18707.68 & 6668.39 & 1126.03 \\ 4709.04 & 27049.89 & 80827.85 & 97595.24 & 93651.45 & 34208.89 & 7844.98 \\ 7542.04 & 39201.83 & 108598.78 & 120303.72 & 99540.80 & 34799.89 & 6280.04 \\ 15449.72 & 84868.56 & 250832.28 & 295166.17 & 271691.44 & 94090.95 & 23230.21 \\ 10114.02 & 49422.82 & 146547.85 & 155032.07 & 128235.49 & 42495.42 & 8600.23 \\ 11403.69 & 61815.44 & 192019.44 & 223116.98 & 214378.74 & 71019.48 & 20629.75 \\ 3268.07 & 16771.33 & 45043.39 & 52752.20 & 41378.44 & 14103.27 & 3229.63 \\ 1869.30 & 9736.73 & 34143.05 & 39425.71 & 41892.57 & 13418.74 & 4809.57 \\ 170.10 & 771.73 & 2855.26 & 2569.22 & 2729.21 & 610.5541 & 268.0381 \\ 59.20 & 131.84 & 942.98 & 482.68 & 1371.35 & 260.29 & 229.77 \end{bmatrix}.$$

Applying Theorem 19 or Corollary 20 it is possible to find its discrete counterpart $q(\mathbf{z}) = \mathbf{z}_1^T \mathbf{B} \mathbf{z}_2$ with

$$\mathbf{B} = \begin{bmatrix} 1.0104 & 1.2885 & 1.0728 & 1.1404 & 1.3005 & 4.0107 & 8.6281 \\ 1.3895 & 1.1343 & 1.6465 & 2.1553 & 1.1160 & 1.6695 & 5.6868 \\ 1.5998 & 1.0654 & 2.1054 & 1.6767 & 2.9511 & 6.8432 & 1.6960 \\ 1.2380 & 1.3298 & 1.3324 & 1.1543 & 2.8162 & 1.9281 & 1.0090 \\ 1.6711 & 1.1183 & 2.1497 & 1.4480 & 5.0204 & 1.0897 & 2.8963 \\ 1.1488 & 4.7785 & 2.1156 & 1.0795 & 9.2660 & 2.7439 & 1.6748 \\ 7.7516 & 1.8247 & 1.0305 & 5.4882 & 2.4008 & 3.3660 & 0.64643 \\ 3.0988 & 1.5180 & 3.0174 & 1.3338 & 6.1266 & 1.2426 & 1.9972 \\ 3.1737 & 1.9988 & 1.3906 & 3.7818 & 1.4017 & 1.1261 & 0.083623 \\ 1.4275 & 2.4748 & 2.0228 & 1.4274 & 4.4073 & 10.103 & 1.4442 \\ 1.1867 & 1.8995 & 4.3172 & 3.6410 & 1.1026 & 1.3655 & 1.4409 \\ 2.3584 & 1.0134 & 1.3097 & 2.0179 & 1.6222 & 2.0122 & 27.189 \end{bmatrix}.$$

Hence $q(\mathbf{z})$ has the same degree as $p(\mathbf{s})$, one has to check the Schur stability of $q(\mathbf{z})$. Following the Schur bivariate stability algorithm, it is easy to check that step 1 holds. Then let us proceed to check step 2 of the algorithm.

Actually, the sequence of polynomials (6) and the coefficient conditions (7) of the Schur bivariate stability algorithm may be easily implemented in a numerical way. Indeed one may generate step by step a sequence of graphics allowing to decide if such conditions are satisfied. In this example we have the following graphics.

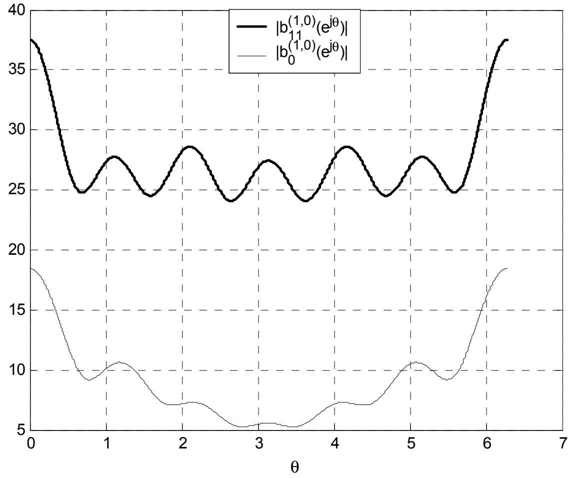

Figure 3. Coefficient condition for the 1st polynomial $q^{(0)}(z_1, e^{j\theta})$ of the polynomial sequence

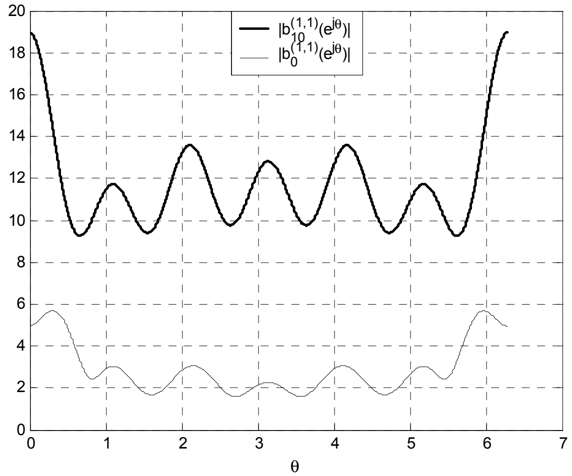

Figure 4. Coefficient condition for the 2nd polynomial $q^{(1)}(z_1, e^{j\theta})$ of the polynomial sequence

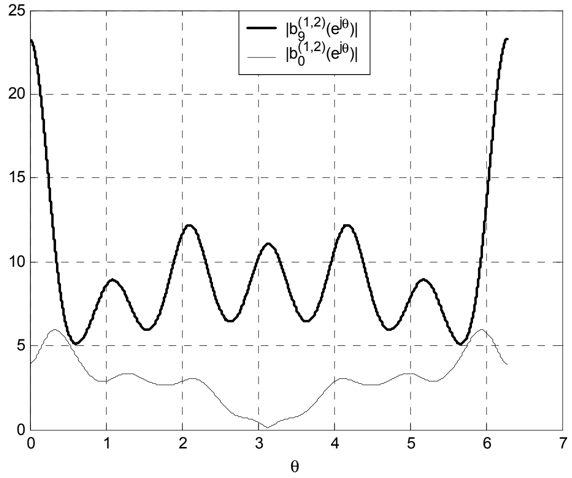

Figure 5. Coefficient condition for the 3rd polynomial $q^{(2)}\left(z_1, e^{j\theta}\right)$ of the polynomial sequence

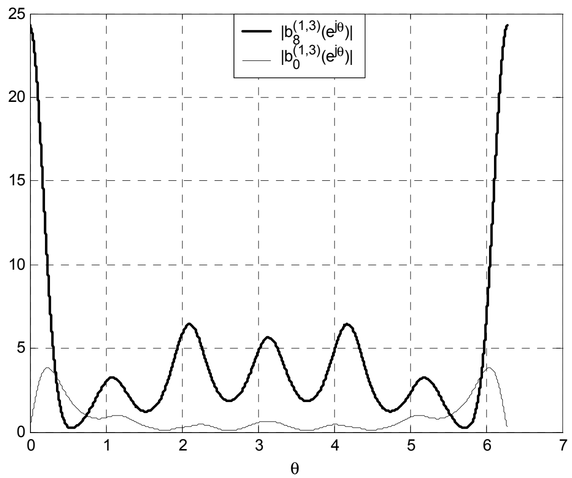

Figure 6. Coefficient condition for the 4th polynomial $q^{(3)}\left(z_1, e^{j\theta}\right)$ of the polynomial sequence

The first graphics, Figure 3, Figure 4 and Figure 5, show that condition (7) is hold. However, the last graphic, Figure 6, shows that condition (7) is not respected. Certainly, polynomial $q(\mathbf{z})$ is not Schur stable and by consequence polynomial $p(\mathbf{s})$ is not stable.

7. Conclusions

In this work, an unified multivariate polynomial stability theory was considered and it is based on the Stable and the Schur stable multivariate classes, for continuous and discrete domains respectively. The main focus was to give feasible criteria to determine whether or not a continuous bivariate polynomial belongs to the Stable class.

In a direct approach, the recursive nature of the continuous Stable class imposes the needing of checking Hurwitz stability of the two main univariate polynomial coefficients, where partial degree preservation is required as well, and the *SSS* stability of the original polynomial. To check the first items one can use every of the well-known univariate criteria, and to check the *SSS* stability there are some criteria that can be used, but them have some efficient problems.

In an indirect approach, the stability of a continuous bivariate polynomial is deduced by analyzing the Schur stability of its discrete bivariate polynomial counterpart. Firstly, the method presented in this work requires of checking Schur stability of a constant coefficients univariate polynomial, and secondly checking Schur stability of an univariate polynomial with literal coefficients. To check the first item there are no problem. To check the last item it is necessary the fulfilment of a sequence of coefficient conditions, of the form (7), in the finite frequency interval $\theta \in [0,2\pi]$. If these two items are satisfied, then the continuous polynomial belongs to the Stable class. Because of its simplicity, coefficient conditions are feasible in a graphical manner and, by construction, the complexity of the algorithm is independent of the polynomial degree.

In a future work, the extension of the proposed indirect bivariate algorithm to the multivariate case can be analyzed, and there are another way to use the relationship between Stable and Schur stable multivariate polynomials: obtain a direct continuous stability criterion by translating, through the relation (5), an existing Schur stable test.

8. References

Anderson, B.D.O. & Jury, E.I. (1973). Stability Test for Two-Dimensional Recursive Filters. *IEEE Transactions on Audio and Electroacoustics,* Vol.21, No.4, August 1973, pp.366-372, ISSN 0018-9278.

Barnett, S. (1983). *Polynomials and Linear Control Systems,* Marcel Dekker Inc., ISBN 0824718984, New York.

Basu, S. & Fettweis, A. (1987). New Results on Stable Multidimensional Polynomials Part II: Discrete Case. *IEEE Transactions on Circuits and Systems,* Vol.34, No.11, November 1987, pp.1264-1274, ISSN 0098-4094.

Bhattacharyya, S.P.; Chapellat, H. & Keel, L.H. (1995). *Robust Control: The Parametric Approach.,* Prentice Hall, ISBN 013781576X, Upper Saddle River.

Bistritz, Y. (2002). On Testing Stability of 2-D Discrete Systems by a Finite Collection of 1-D Stability Tests. *IEEE Transactions on Circuits and Systems-I,* Vol.49, No.11, November 2002, pp.1634-1638, ISSN 1057-7122.

Bose, N.K. (1977). Implementation of a New Stability Test for Two-Dimensional Filters. *IEEE Transactions on Acoustics, Speech and Signal Processing,* Vol.25, No.2, April 1977, pp.117-120, ISSN 0096-3518.

Bose, N.K. (1982). *Applied Multidimensional Systems Theory,* Van Nostrand Reinhold Company, ISBN 0442272146, New York.

Dumitrescu, B. (2006). Stability Test of Multidimensional Discrete-Time Systems via Sum-of-Squares Decomposition. *IEEE Transactions on Circuits and Systems-I,* Vol.53, No.4, April 2006, pp.928-936, ISSN 1057-7122.

Fettweis, A. & Basu, S. (1987). New Results on Stable Multidimensional Polynomials Part I: Continuous Case. *IEEE Transactions on Circuits and Systems,* Vol. 34, No.10, October 1987, pp.1221-1232, ISSN 0098-4094.

Gantmacher, F.R. (1959). *The Theory of Matrices Vol. II*, Chelsea Publishing Company, ISBN 0828401314, New York.

Huang, T.S. (1972). Stability of Two-Dimensional Recursive Digital Filters. *IEEE Transactions on Audio and Electroacoustics,* Vol.20, No.2, June 1972, pp.158-163, ISSN 0018-9278.

Jury, E.I. (1988). Modified Stability Table for 2-D Digital Filters. *IEEE Transactions on Circuits and Systems,* Vol.35, No.1, January 1988, pp.116-119, ISSN 0098-4094.

Kaczorek, T. (1985). *Two-Dimensional Linear Systems*, in Lecture Notes in Control and Information Sciences No.68, Springer-Verlag, ISBN 0387150862.

Kharitonov, V.L. & Torres-Muñoz, J.A. (1999). Robust Stability of Multivariate Polynomials Part I: Small Coefficient Perturbations. *Multidimensional Systems and Signal Processing,* Vol.10, No.1, January 1999, pp.7-20, ISSN 0923-6082.

Kharitonov, V.L. & Torres-Muñoz, J.A. (2002). Recent Results on the Robust Stability of Multivariate Polynomials. *IEEE Transactions on Circuits and Systems-I,* Vol.49, No.6, June 2002, pp.715-724, ISSN 1057-7122.

Marden, M. (1949). *The Geometry of Zeros of a Polynomial in a Complex Variable,* American Mathematical Society, ISBN 0821815032, New York.

Maria, G.A. & Fahmy, M.M. (1973). On the Stability of Two-Dimensional Digital Filters. *IEEE Transactions on Audio and Electroacoustics,* Vol.21, No.5, October 1973, pp.470-472, ISSN 0018-9278.

Parks P.C. & Hahn, V. (1992). *Stability Theory,* Prentice Hall, ISBN 0138340455.

Rodriguez-Angeles, E.; Torres-Muñoz, J.A. & Mendez-Barrios, C.F. (2007). A Simple Test for Stability of Continuous Bivariate Polynomials. *3rd IFAC Symposium on System, Structure and Control,* Foz do Iguassu (Brazil), October 2007.

Siljak, D.D. (1975). Stability Criteria for Two-Variable Polynomials. *IEEE Transactions on Circuits and Systems,* Vol.22, No.3, March 1975, pp.185-189, ISSN 0098-4094.

Torres-Muñoz, J.A.; Rodriguez-Angeles, E. & Kharitonov, V.L. (2006). On Schur Stable Multivariate Polynomials. *IEEE Transactions on Circuits and Systems-I,* Vol.53, No.5, May 2006, pp.1166-1173, ISSN 1057-7122.

Xu, L.; Yamada, M.; Lin, Z.; Saito, O. & Anazawa, Y. (2004). Further Improvements on Bose's 2D Stability Test. *International Journal of Control, Automation and Systems,* Vol.2, No.3, September 2004, pp.319-332, ISSN 15986446.

Yang, X. & Unbehauen, R. (1998). New Stability Test Algorithm for Two-Dimensional Digital Filters. *IEEE Transactions on Circuits and Systems-I,* Vol.45, No.7, July 1998, pp.739-741, ISSN 1057-7122.

Zeheb, E. & Walach, E. (1981). Zero Sets of Multiparameter Functions and Stability of Multidimensional Systems. *IEEE Transactions on Acoustics, Speech and Signal Processing,* Vol.29, No.2, April 1981, pp.197-206, ISSN 0096-3518.

10

LQ and H_2 Tuning of Fixed-Structure Controller for Continuous Time Invariant System with H_∞ Constraints

Igor Yadykin and Michael Tchaikovsky
Institute of Control Sciences of Russian Academy of Sciences
Russia

1. Introduction

The problem of fixed-order and fixed-structure controller tuning has been known for more than half a century and is a one of the classic problems of the control theory. Great number of papers and several monographs are devoted to this problem (e.g., Rotach et al., 1984; Datta, 1998; Datta et al., 2000; Astrom & Hagglund, 2006). Analytic methods based on information on structure and form of plant mathematical model play the main role among the methods for solving this problem. These include:

- tuning methods based on single-stage solution of controller parameters synthesis problem (Rotach et al., 1984; Astrom & Hagglund, 2006);
- automatic tuning methods based on application of relay feedback (Rotach et al., 1984; Datta, 1998; Datta et al., 2000; Hjalmarsson, 2002; Astrom & Hagglund, 2006);
- methods based on indirect adaptive control, or implicit reference model (internal model control) (Petrov & Rutkovskiy, 1965; Datta, 1998; Datta et al., 2000; Astrom & Hagglund, 2006).

For recent two decades, many papers devoted to application of powerful $\mathcal{H}_2$ and $\mathcal{H}_\infty$ optimization tools to design and tuning problems for fixed-structure controllers have been presented (McFarlane & Glover, 1992; Zhou et al., 1996; Balandin & Kogan, 2007). Moreover, the concepts of robust design have brought to a new view of known controller tuning methods.

In (McFarlane & Glover, 1992), a practically effective solution for fixed-order controller tuning problem was obtained. It is based on shaping frequency responses of open control loop by means of pre- and post-filters (loop shaping) in conjunction with minimizing $\mathcal{H}_\infty$ norm of closed-loop system. The main advantage of this approach consists in that the resulting controller is not only stabilizing, but possesses assured performance characteristics in conditions of uncertainty. The method has been successfully applied for synthesis of PID (Proportional-Intagrating-Derivative) controller for SISO (Single-Input Single-Output) plant, as well as multiloop PID controller for MIMO (Multi-Input Multi-Output) plant. The controller tuning problem is close to the plant identification problem that implies using of constrained and unconstrained optimization technique for finding optimal controller tuning algorithms in model matching problem (Poznyak, 1991) and, in particular, in internal model control. In (Tan et al., 2002), for solving the problem of PID controller design for MIMO plant the authors use BMI (bilinear matrix inequality) technique and minimization of $\mathcal{H}_\infty$ norm of adjusted system transfer function introduced in (McFarlane & Glover, 1992). In (Balandin & Kogan, 2007), the authors present the synthesis method for adjusted system with fixed-order controller based on LMI (linear matrix inequality) technique guaranteeing boundedness of $\mathcal{H}_2$ norm of the adjusted system transfer matrix together with its stability.

In (Bao et al., 1999), the authors introduce a technique for multiloop PID controller tuning based on Bounded Real Lemma (BRL) allowing to obtain the numerical solution via semi-definite programming. This method of controller tuning based on direct synthesis algorithms with application of LMI technique has certain advantages, namely:

- This is the first LMI-based controller tuning method that has shown its validity and effectiveness in solving a number of applied problems.
- There is standard software tools (e.g., Matlab) for implementation of this method.

But this tuning method also has a number of drawbacks:

- This approach poorly fits for synthesis from viewpoint of required control performance.
- The synthesis problem solution results in controller of general full-order observer form. It requires solving additional approximation problem in frequency domain for PID controller tuning.
- For fixed-structure controller, the method requires use of pre- and post-filters and, in general case, results in solving BMIs.
- The solution depends on choosen initial conditions.

The problem of fixed-order and fixed-structure controller tuning formulated in terms of quadratic optimization was solved in (Yadykin, 1985). It results in classic least-squares method of controller tuning algorithm synthesis. This approach is based on application of indirect adaptive control with implicit reference model of linear plant (also called internal model control). The principal distinction between this approach and other methods mentioned before consists in that the adjusted system performance is given directly by fixed parameters of the implicit reference model. Criterion of proximity for dynamic characteristics of the adjusted control system and its reference model can be expressed in terms of Frobenius norm for coefficients of polynomials generated by transfer functions of the control system and its reference model. The main idea of new approach introduced in this Chapter consists in replacement of the aforementioned tuning functional by $\mathcal{H}_2$ norm of difference between transfer functions of closed-loop adjusted and reference systems and switching from unconstrained optimization to optimization under constraints in form of LMIs guaranteeing bounded $\mathcal{H}_\infty$ norm of transfer function of closed-loop system. By virtue of Parseval's Theorem, it is the $\mathcal{H}_2$ norm of difference between transfer functions of closed-loop adjusted and reference systems gives direct estimation of difference between transients in the closed-loop adjusted and reference systems. Thus, the tuning objective consists in providing the adjusted system with transient performance of the reference model.

2. Problem Statement

Consider linear continuous time invariant control system consisting of the dynamic plant and fixed-structure controller

$$P(s): \quad \left[\frac{\dot{x}_p(t)}{y(t)}\right] = \left[\begin{array}{c|c} A_p & B_p \\ \hline C_p & 0 \end{array}\right] \left[\frac{x_p(t)}{u(t)}\right], \quad x_p(0) = x_{p0}, \tag{1}$$

$$K(s): \quad \left[\frac{\dot{x}_c(t)}{u(t)}\right] = \left[\begin{array}{c|c} A_{cm} & B_c \\ \hline C_{cm} & D_c \end{array}\right] \left[\frac{x_c(t)}{g(t)-y(t)}\right], \quad x_c(0) = x_{c0}, \tag{2}$$

where $x_p(t) \in \mathbb{R}^{n_p}$ is the plant state, $y(t) \in \mathbb{R}^1$ is the plant output, $u(t) \in \mathbb{R}^1$ is the control, $x_c(t) \in \mathbb{R}^{n_c}$ is the controller state, $g(t) \in \mathbb{R}^1$ is the reference signal, and the matrices A_p, B_p, C_p, A_{cm}, B_p, C_{cm}, and D_c have compatible dimensions. Assume that plant (1) is completely controllable and observable, the state-space realizations (A_p, B_p, C_p) and $(A_{cm}, B_c, C_{cm}, D_c)$ are minimal, and the matrices A_p, B_p, and C_p are known or can be defined at the earlier stage of parametric identification. Also assume $g(t) \in \mathcal{L}_2[0, +\infty)$. We are interested in tracking the reference input $g(t)$ for an arbitrary set of plant parameters inside of some bounded region Σ. It is assumed that controller (2) has fixed structure. The feature of this controller tuning problem is in that the controller structure does not change in tuning process, i.e. the matrices A_{cm} and C_{cm} are fixed, and only elements of the vector B_c and scalar value D_c are to be adjusted. Such situation appears, for instance, when controller (2) is a PID controller. Denote the generalized tuning vector

$$G = \begin{bmatrix} B_c^{\mathrm{T}} & D_c \end{bmatrix}^{\mathrm{T}}. \tag{3}$$

The goal of controller tuning on the base of principle of internal model of control loop consists in reaching the identity

$$y(t) \equiv y_m(t), \tag{4}$$

where $y_m(t) \in \mathbb{R}^1$ is the output of implicit (virtual) reference model of system (1)–(2) under assumption that the plant input is fed by the test signal $g(t)$ and the plant parameters belong to some admissible and bounded set

$$\Sigma = \left\{ A_p, B_p, C_p : \underline{a}_{pij} \leqslant a_{pij} \leqslant \overline{a}_{pij}, \underline{b}_{pij} \leqslant b_{pij} \leqslant \overline{b}_{pij}, \underline{c}_{pij} \leqslant c_{pij} \leqslant \overline{c}_{pij} \right\}.$$

The implicit reference model can be described by the following state-space equation system

$$P_m(s): \quad \left[\frac{\dot{x}_{pm}(t)}{y_m(t)}\right] = \left[\begin{array}{c|c} A_{pm} & B_{pm} \\ \hline C_{pm} & 0 \end{array}\right] \left[\frac{x_{pm}(t)}{u_m(t)}\right], \quad x_{pm}(0) = x_{pm0}, \tag{5}$$

$$K_m(s): \quad \left[\frac{\dot{x}_{cm}(t)}{u_m(t)}\right] = \left[\begin{array}{c|c} A_{cm} & B_{cm} \\ \hline C_{cm} & D_{cm} \end{array}\right] \left[\frac{x_{cm}(t)}{g(t)-y_m(t)}\right], \quad x_{cm}(0) = x_{cm0}, \tag{6}$$

where the state vectors of reference plant and controller, as well as the reference plant output and control have the same dimensions as their counterparts in system (1)–(2). Naturally, reference closed-loop system (5), (6) is assumed to be stable. The standard controller tuning procedure after plant identification consists of two stages (Astrom & Hagglund, 2006):

- synthesis of the controller parameters in nominal mode;
- optimal controller tuning according to given tuning criterion.

At that, it is assumed that the plant parameters at zero time take on any constant values from the admissible set Σ.

Tuning objective (4) in frequency domain under assumption of zero initial conditions is equivalent to the identities

$$\Phi(j\omega) \equiv \Phi_m(j\omega) \quad \forall\omega \in (-\infty, +\infty), \tag{7}$$

$$W(j\omega) \equiv W_m(j\omega) \quad \forall\omega \in (-\infty, +\infty), \tag{8}$$

where $W(s)$ and $\Phi(s) = W(s)/(1+W(s))$ are the transfer functions of open- and closed-loop systems, respectively. Denote in advance that identities (7) and (8) are equivalent if some conditions, namely, full adaptability conditions hold true. The conditions (criteria) of weak, full, and partial adaptability of a control system (Yadykin, 1981) are some generalizations of controllability and observability criteria. Similar to the latter criteria, adaptability of a system can be determined in terms of ranks of some special adaptability matrices. The notion of system adaptability will be considered in the next section.

Condition (8) expresses the requirement of proximity of the dynamic operators of the adjusted and reference open-loop systems along the whole set of admissible plant parameters Σ. This is equivalent to proximity of transient responses of these systems when their inputs are fed with the unit step. Condition (7) expresses the same requirement for the closed-loop systems. In nominal mode we obviously have $W(j\omega) = W_m(j\omega)$.

Let us pass from the identity of transfer functions to the identity of polynomials generated by these transfer functions. The transfer functions of plant (1) and controller (2), as well as transfer functions of reference plant (5) and controller (6) are given by

$$P(s) = C_p(sI - A_p)^{-1} B_p, \tag{9}$$

$$K(s) = C_{cm}(sI - A_{cm})^{-1} B_c + D_c, \tag{10}$$

$$P_m(s) = C_{pm}(sI - A_{pm})^{-1} B_{pm}, \tag{11}$$

$$K_m(s) = C_{cm}(sI - A_{cm})^{-1} B_{cm} + D_{cm}, \tag{12}$$

respectively. Substituting expressions (9)–(12) into identity (8), we obtain the following polynomial controller tuning equation:

$$\begin{aligned} &C_p(sI - A_p)^{-1} B_p C_{cm}(sI - A_{cm})^{-1} B_c + C_p(sI - A_p)^{-1} B_p D_c \\ &\quad = C_{pm}(sI - A_{pm})^{-1} B_{pm} C_{cm}(sI - A_{cm})^{-1} B_{cm} + C_{pm}(sI - A_{pm})^{-1} B_{pm} D_{cm}. \end{aligned} \tag{13}$$

Applying series expansion of resolvents in left-hand and right-hand parts of the last equality and multiplying its both parts to the product of characteristic polynomials of the plant, controller, and implicit reference plant and controller models, we obtain the following equation for the controller tuning polynomial (Datta, 1998):

$$(P_1 - N_1)s^{2n_c+n_p-1} + \cdots + (P_{2n_c+n_p-1} - N_{2n_c+n_p-1})s + (P_{2n_c+n_p} - N_{2n_c+n_p}) = 0.$$

Define the adaptability matrices

$$L = \begin{bmatrix} L_{\mu 1} & L_{\mu 2} \end{bmatrix}, \quad N^{\mathrm{T}} = \begin{bmatrix} N_{\mu 1}^{\mathrm{T}} & N_{\mu 2}^{\mathrm{T}} \end{bmatrix} \tag{14}$$

and the linear-quadratic (LQ) tuning functional J_1 as follows

$$J_1 = \sum_{\mu=0}^{2n_c+n_p-1} \mathrm{tr}(P_\mu - N_\mu)^{\mathrm{T}}(P_\mu - N_\mu), \quad P_\mu = L_{\mu 1}B_c + L_{\mu 2}D_c, \quad N_\mu = N_{\mu 1} + N_{\mu 2}, \tag{15}$$

$$L_{\mu 1} = \sum_{\sigma=0}^{n_c}\sum_{i=j}^{n_c-1}\sum_{\eta=\nu}^{n_p-1} a_{m\sigma}a_{cm\eta+1}a_{j+1}C_pA_p^{i-j}B_pC_{cm}A_{cm}, \quad L_{\mu 2} = \sum_{\sigma=0}^{n_c}\sum_{i=j}^{n_c-1}\sum_{\nu=0}^{n_p} a_{m\sigma}a_{cm\nu}a_{i+1}C_pA_p^{i-j}B_p,$$

$$N_{\mu 1} = \sum_{\sigma=0}^{n_c}\sum_{i=j}^{n_c-1}\sum_{\eta=\nu}^{n_p-1} a_\sigma a_{cm\eta+1}a_{i+1}C_{pm}A_{pm}^{i-j}B_{pm}C_{cm}A_{cm}^{\eta-\nu}B_{cm}, \; N_{\mu 2} = \sum_{\sigma=0}^{n_c}\sum_{i=j}^{n_c-1}\sum_{\nu=0}^{n_p} a_\sigma a_{cm\nu}a_{i+1}C_{pm}A_{pm}^{i-j}B_{pm}D_{cm},$$

$$\forall \sigma, \nu, j : \sigma + \nu + j = \mu,$$

where a_i, a_{mi}, a_{cmi} are the coefficients of the characteristic polynomials of the plant, as well as implicit reference model of plant and controller, correspondingly.
Identity (8) can be rewritten as

$$\frac{M_c(j\omega)M_p(j\omega)}{Q_c(j\omega)Q_p(j\omega)} = \frac{M_o(j\omega)}{Q_o(j\omega)} \equiv \frac{M_{om}(j\omega)}{Q_{om}(j\omega)} = \frac{M_{cm}(j\omega)M_{pm}(j\omega)}{Q_{cm}(j\omega)Q_{pm}(j\omega)} \quad \forall \omega \in (-\infty, +\infty),$$

where $M_o(s)$, $M_c(s)$, $M_p(s)$ are the numerator polynomials of transfer functions of the open-loop system, controller, and plant, $Q_o(s)$, $Q_c(s)$, $Q_p(s)$ are the respective denominator polynomials of these transfer functions. Let us denote

$$P_o(s) = M_o(s)Q_{cm}(s), \quad N_o(s) = M_{om}(s)Q_o(s), \quad F_o(s) = P_o(s) - N_o(s).$$

Then

$$F_o(s) = \sum_{i=0}^{2n_c+n_p-1} (P_i - N_i)s^i.$$

Let us also consider another one tuning functional

$$J_2 = \|\Phi(s) - \Phi_m(s)\|_2^2 = \frac{1}{2\pi}\int_{-\infty}^{+\infty} (\Phi(-j\omega) - \Phi_m(-j\omega))(\Phi(j\omega) - \Phi_m(j\omega))d\omega \tag{16}$$

as a criterion of proximity of the adjusted and reference closed-loop systems.
Having introduced the tuning functionals J_1 and J_2, let us formulate the following two tuning problems for given plant (1), the controller matrices A_{cm}, C_{cm}, and reference model (5), (6).

Problem 1 (LQ Optimal Controller Tuning): Find $G = \begin{bmatrix} B_c^{\mathrm{T}} & D_c \end{bmatrix}^{\mathrm{T}}$ such that

$$J_1 \to \min_G. \tag{17}$$

Problem 2 ($\mathcal{H}_2$ Optimal Controller Tuning): Find G such that

$$J_2 \to \min_G . \tag{18}$$

Before giving solutions to the established problems, we need consider the notice of control system adaptability and properties of the adaptability matrices in some more details.

3. Adaptability of Control System and Properties of Adaptability Matrices

Adaptability is a structural property of a control system. It characterizes the potential ability of the control system to retain its dynamic characteristics when adjusting the parameters of the system toward its given reference model in the situation where the parameter set of the plant scatters around the parameter set of the nominal (reference) operating conditions of the control system (Yadykin, 1999).

Let us consider a control system consisting of plant (1) and controller (2) given stable closed-loop reference model (5), (6). It is assumed that plant (1) is completely controllable and observable, and the state-space realizations $(A_p, B_p, C_p) \in \Sigma$ and $(A_{cm}, B_c, C_{cm}, D_c)$ are minimal. Define the output error of system (1), (2) with respect to reference model (5), (6) as

$$e(t) = y(t) - y_m(t). \tag{19}$$

Definition 1 (Complete Adaptability): Control system (1), (2) is said to be completely adaptable with respect to the output $y(t)$ if for any triple of matrices $(A_p, B_p, C_p) \in \Sigma$ there exists a unique vector $G^* = \begin{bmatrix} B_c^{\mathrm{T}*} & D_c^* \end{bmatrix}^{\mathrm{T}}$ such that

$$\inf_{(A_p, B_p, C_p) \in \Sigma} \left\| e(t, g, x_{p0}, x_{c0}, x_{pm0}, x_{cm0}, A_p, B_p, C_p, G^*) \right\|_2 = 0$$

$$\forall t \in [0, +\infty),\ g(t) \in \mathcal{L}_2[0, +\infty),\ x_{p0},\ x_{c0},\ x_{pm0},\ x_{cm0}.$$

Definition 2 (Partial Adaptability): Control system (1), (2) is said to be partially adaptable with respect to the output $y(t)$ if for any triple of matrices $(A_p, B_p, C_p) \in \Sigma$ and any vectors G there exists a unique vector G^* such that

$$\inf_{(A_p, B_p, C_p) \in \Sigma} \left\| e(t, g, x_{p0}, x_{c0}, x_{pm0}, x_{cm0}, A_p, B_p, C_p, G) \right\|_2 = \left\| e(t, g, x_{p0}, x_{c0}, x_{pm0}, x_{cm0}, A_p, B_p, C_p, G^*) \right\|_2$$

$$\forall t \in [0, +\infty),\ g(t) \in \mathcal{L}_2[0, +\infty),\ x_{p0},\ x_{c0},\ x_{pm0},\ x_{cm0}.$$

Definition 3 (Weak Adaptability): Control system (1), (2) is said to be weakly adaptable with respect to the output $y(t)$ if for any triple of matrices $(A_p, B_p, C_p) \in \Sigma$ and any vectors G there exists a set of vectors G^* such that

$$\inf_{(A_p, B_p, C_p) \in \Sigma} \left\| e(t, g, x_{p0}, x_{c0}, x_{pm0}, x_{cm0}, A_p, B_p, C_p, G) \right\|_2 = \left\| e(t, g, x_{p0}, x_{c0}, x_{pm0}, x_{cm0}, A_p, B_p, C_p, G^*) \right\|_2$$

$$\forall t \in [0, +\infty),\ g(t) \in \mathcal{L}_2[0, +\infty),\ x_{p0},\ x_{c0},\ x_{pm0},\ x_{cm0}.$$

Notice that all three kinds of adaptability characterize structural properties of the control system but not of the plant characterized by the invariant properties called controllability, observability, stabilizability, and detectability. Also denote that the adaptability property can be verified experimentally.

The above adaptability definitions can be extended onto linear discrete time invariant systems, dynamic systems with static nonlinearities, bilinear control systems, as well as onto MIMO linear and bilinear control systems (Yadykin, 1981, 1983, 1985, 1999; Morozov & Yadykin, 2004; Yadykin & Tchaikovsky, 2007).

Adaptability matrices (14) possess the following properties (Yadykin, 1999):

1. The adaptability matrix L is the block Toeplitz matrix for MIMO systems. For SISO systems L is the Toeplitz matrix.
2. The adaptability matrix L has maximal column rank if and only if
$$\det(C_p B_p) \neq 0. \tag{20}$$
Condition (20) is the necessary and sufficient condition of partial adaptability of control system (1), (2), as well as the necessary condition of its complete adaptability.
3. Each block N_μ of the block adaptability matrix N equals to (block) scalar product of the (block) row of the matrix L and column vector G where all variables subscripts are added with subscript m in the cases when it is absent, and vice versa.
4. Each block of the matrix L is a linear combination of block products of the plant matrices $C_p A_p^{i-j} B_p$, controller matrices $C_{cm} A_{cm}^{\eta-\nu}$, B_c, D_c, and products of the coefficients of the characteristic equations of the plant, controller, and their reference models.
5. Upper and lower square blocks of the adaptability matrix L have upper and lower triangle form, respectively.

4. Solutions to *LQ* and H_2 Tuning Problems

In this section we consider the solutions of LQ and $\mathcal{H}_2$ optimal tuning problems (17) and (18) for fixed-structure controllers formulated in Section 2 and briefly outline an approach to LQ optimal multiloop PID controller tuning for bilinear MIMO control system.

4.1 *LQ* Optimal Tuning of Fixed-Structure Controller

Let us determine the gradient of the tuning functional J_1 given by (15) with respect to vector argument using formula
$$\frac{\partial\, \mathrm{tr}(Ax)}{\partial x} = A^{\mathrm{T}}.$$

Applying this formula to expression (15), we obtain
$$\frac{\partial J_1}{\partial G} = 2\sum_{\mu=0}^{2n_p+n_c-1} (P_\mu - N_\mu)\frac{\partial P_\mu}{\partial G}, \quad \frac{\partial P_\mu}{\partial G} = L_\mu^{\mathrm{T}}, \quad \frac{\partial L_\mu}{\partial G} = L_\mu^{\mathrm{T}}, \quad \mu = \overline{0, 2n_p + n_c - 1}.$$

Thus, the necessary minimum condition for the tuning functional J_1 is

$$\frac{\partial J_1}{\partial G} = L^{\mathrm{T}}(LG - N) = 0. \tag{21}$$

In paper (Yadykin, 2008) it has been shown that necessary minimum condition (21) holds true in the following two cases:

1. If $LG - N = 0$ then system (1), (2) is completely adaptable.
2. If $LG - N \neq 0$ but $L^{\mathrm{T}}(LG - N) = 0$ then system (1), (2) is partially or weakly adaptable.

In the first case (complete adapatability), the equation

$$LG - N = 0 \tag{22}$$

has a unique exact solution. In this case, necessary minimum condition (21) is also sufficient.
In the second case (partial or weak adaptability), equation (22) does not have an exact solution, but the equation

$$L^{\mathrm{T}}(LG - N) = 0 \tag{23}$$

has a unique approximate solution or a set of approximate solutions. Thus, if the matrix L has maximal column rank, then the vector (matrix)

$$G^* = (L^{\mathrm{T}}L)^{-1}L^{\mathrm{T}}N = L^+N \tag{24}$$

is the solution to equation (23). In expression (24), L^+ denotes Moore-Penrose generalized inverse of the matrix L (Bernstein, 2005).
The following Theorem establishing the necessary and sufficient conditions of complete and partial adaptability of system (1), (2) follows from the theory of matrix algebraic equations (Gantmacher, 1959).
Theorem 1: Let plant (1) be completely controllable and observable, and the state-space realizations (A_p, B_p, C_p) and $(A_{cm}, B_c, C_{cm}, D_c)$ be minimal. Control system (1), (2) is completely adaptable with respect to the output $y(t)$ if and only if

$$\operatorname{Im} N \subseteq \operatorname{Im} L, \tag{25}$$

$$\operatorname{Ker} L = 0, \tag{26}$$

where Im denotes the matrix image and Ker denotes the matrix kernel. Control system (1), (2) is partially adaptable with respect to the output $y(t)$ if and only if condition (26) holds.
To illustrate LQ optimal tuning algorithm (24), let us consider a simple example.
Example 1: Let control system (1), (2) consists of a linear oscillator and PI (Proportional-Intagrating) controller in forward loop closed by the negative unitary feedback. The state-space realizations of the plant and controller are given by

$$\left[\begin{array}{c|c} A_p & B_p \\ \hline C_p & 0 \end{array}\right] = \left[\begin{array}{cc|c} 0 & 1 & 0 \\ -1 & -1/(2\varsigma_p T_p) & b \\ \hline 1 & 0 & 0 \end{array}\right], \quad \left[\begin{array}{c|c} A_{cm} & B_c \\ \hline C_{cm} & D_c \end{array}\right] = \left[\begin{array}{c|c} 0 & k_P k_I \\ \hline 1 & k_P \end{array}\right].$$

We suppose that $\Sigma=\{b: \underline{b}\leqslant b\leqslant \overline{b},\, b\neq 0\}$. The transfer functions of the plant and controller, as well as the reference plant and controller are as follows:

$$P(s)=\frac{b}{T_p^2 s^2+2T_p\varsigma_p s+1},\quad K(s)=k_P+\frac{k_P k_I}{s}=k_P k_{Im}\frac{k_{Im}^{-1}s+1}{s},$$

$$P_m(s)=\frac{b_m}{T_{pm}^2 s^2+2T_{pm}\varsigma_{pm} s+1},\quad K_m(s)=k_{Pm}k_{Im}\frac{k_{Im}^{-1}s+1}{s}.$$

Substituting these expressions into identity (8) and eliminating equal factors, we obtain

$$bk_P=b_m k_{Pm}$$

from which it follows that *LQ* optimal tuning of the controller parameters is given by

$$k_P^*=b^{-1}b_m k_{Pm}. \tag{27}$$

Thus, for any values of the plant coefficient b from the admissible set Σ tuning algorithm (27) provides identical coincidence of the transfer functions of the open-loop adjusted system and its reference model. This means that the considered system is completely adaptable with respect to the output in terms of Definition 1 in the class of the linear oscillators with a single variable parameter (coefficient b).
Let as now assume that the plant is characterized by three variable parameters:

$$\Sigma=\{b,T_p,\varsigma_p : \underline{b}\leqslant b\leqslant \overline{b},\, \underline{T}_p\leqslant T_p\leqslant \overline{T}_p,\, \underline{\varsigma}_p\leqslant \varsigma_p\leqslant \overline{\varsigma}_p,\, b\neq 0\}.$$

We are interested in tuning of two parameters of PI controller, k_P and k_I, or, equivalently, the scalars B_c and D_c. Applying formulas (15), one can easily obtain the following expressions for the adaptability matrices:

$$L=\begin{bmatrix} b & 0\\ 2bT_{pm}\varsigma_{pm} & b\\ bT_p^2 & 2bT_{pm}\varsigma_{pm}\\ 0 & bT_p^2\end{bmatrix},\quad N=\begin{bmatrix} b_m B_{cm}\\ 2b_m B_{cm}\varsigma_p T_p+b_m D_{cm}\\ b_m B_{cm}T_p^2+2b_m D_{cm}\varsigma_p T_p\\ b_m D_{cm}T_p^3\end{bmatrix},$$

where $B_{cm}=k_{Pm}k_{Im}$, $D_{cm}=k_{Pm}$. Denote that the elements of the matrix L are periodic:

$$l_{11}=l_{22},\; l_{21}=l_{32},\; l_{31}=l_{42},\; l_{41}=l_{12}.$$

According to *LQ* tuning algorithm (24), the optimal controller parameters are defined as

$$\begin{bmatrix} B_c^*\\ D_c^*\end{bmatrix}=\frac{b_m}{b}\begin{bmatrix} 1+4T_{pm}^2\varsigma_{pm}^2+T_p^4 & 2T_{pm}\varsigma_{pm}(1+T_p^2)\\ 2T_{pm}\varsigma_{pm}(1+T_p^2) & 1+4T_{pm}^2\varsigma_{pm}^2+T_p^4\end{bmatrix}^{-1}\begin{bmatrix} 1 & 0\\ 2T_{pm}\varsigma_{pm} & 1\\ T_p^2 & 2T_{pm}\varsigma_{pm}\\ 0 & T_p^2\end{bmatrix}^{\mathrm{T}}\begin{bmatrix} B_{cm}\\ 2B_{cm}\varsigma_p T_p+D_{cm}\\ B_{cm}T_p^2+2D_{cm}\varsigma_p T_p\\ D_{cm}T_p^3\end{bmatrix}.$$

4.2 *LQ* Optimal PID Controller Tuning for Bilinear MIMO System

Let us outline an approach to extension of *LQ* optimal fixed-structure (PID) controller tuning algorithm presented in Subsection 4.1 onto the class of bilinear continuous time invariant MIMO systems with piecewise constant input signals. This approach can be found in more details in papers (Morozov & Yadykin, 2004; Yadykin & Tchaikovsky, 2007).
Let us consider the bilinear continuous time-invariant plant described by the equations

$$\left.\begin{aligned} &\dot{x}(t) = A_p x(t) + B_p u(t) + \sum_{i=1}^{r} N_{pi} x(t) u_i(t), \\ &y(t) = C_p x(t), \end{aligned}\right\} \tag{28}$$

where $x_p(t) \in \mathbb{R}^n$ is the plant state, $u(t) = \begin{bmatrix} u_1(t) & \cdots & u_r(t) \end{bmatrix}^{\mathrm{T}} \in \mathbb{R}^r$ is the control, $y(t) \in \mathbb{R}^r$ is the plant output, and the matrices A_p, B_p, C_p, N_{pi}, $i = \overline{1,r}$, have compatible dimensions. Also consider the fixed-structure controller, namely, multiloop PID controller for plant (28) with transfer matrix

$$K(s) = \mathrm{diag}\{K_1(s), \ldots, K_r(s)\}, \tag{29}$$

where

$$K_i(s) = k_i\left(1 + \frac{1}{TS_i s} + TD_i s\right)\frac{1}{TL_i s + 1}.$$

The state-space equations for PID controller (29) are given by (2) with

$$\begin{gathered} A_c = \mathrm{diag}\{A_{c1}, \ldots, A_{cr}\}, \quad A_{ci} = \begin{bmatrix} -k_{1i} & 0 \\ 0 & 0 \end{bmatrix}, \quad B_c = \mathrm{diag}\left\{\begin{bmatrix} k_{21} \\ k_1 \end{bmatrix}, \ldots, \begin{bmatrix} k_{2r} \\ k_r \end{bmatrix}\right\}, \\ C_c = \mathrm{diag}\{[1 \quad 1], \ldots, [1 \quad 1]\}, \quad D_c = \mathrm{diag}\{k_{31}, \ldots, k_{3r}\}, \\ k_{1i} = (TL_i)^{-1}, \quad k_{3i} = k_i TD_i / L_i, \quad k_{2i} = k_i / TL_i - (k_i / TS_i + k_i TD_i / TL_i^2). \end{gathered}$$

The reference plant model is given by

$$\left.\begin{aligned} &\dot{x}_m(t) = A_{pm} x_m(t) + B_{pm} u_m(t) + \sum_{i=1}^{r} N_{pmi} x_m(t) u_{mi}(t), \\ &y_m(t) = C_{pm} x_m(t), \end{aligned}\right\} \tag{30}$$

where all vectors and matrices have the same dimensions as their counterparts in actual plant (28). The reference controller has the same structure as controller (29):

$$K_m(s) = \mathrm{diag}\{K_{m1}(s), \ldots, K_{mr}(s)\}, \tag{31}$$

where

$$K_{mi}(s) = k_{mi}\left(1 + \frac{1}{T_m S_{mi} s} + T_m D_{mi} s\right)\frac{1}{T_m L_{mi} s + 1},$$

and its state-space equations are given by (6) with corresponding structure of the realization matrices.

We are interested in tuning the parameters k_i, TD_i, TS_i, TL_i, $i=\overline{1,r}$, of controller (29) such that to ensure the identity

$$y(t) \equiv y_m(t)$$

in steady-state mode provided that the parameters of plant (28) and control signal vary as step functions of time within some bounded regions Σ, Ω.

The main idea of applying approach described in Subsection 4.1 for solving this problem consists in linearization of bilinear plant (28) and reference plant (30) with respect to the deviations from the steady-state values. In this case we obtain the linearized model of the actual plant

$$\left[\begin{array}{c} \Delta\dot{x}_p(t) \\ \hline \Delta y(t) \end{array}\right] = \left[\begin{array}{c|c} \bar{A}_p & \bar{B}_p \\ \hline \bar{C}_p & 0 \end{array}\right] \left[\begin{array}{c} \Delta x_p(t) \\ \hline \Delta u(t) \end{array}\right], \tag{32}$$

$$\bar{A}_p = A_p + \sum_{i=1}^{r} N_{pi}(u_i^{\mathrm{o}} + \Delta u_i^{\mathrm{o}}), \quad \bar{B}_p = B_p, \quad \bar{C}_p = C_p,$$

and the reference plant

$$\left[\begin{array}{c} \Delta\dot{x}_{pm}(t) \\ \hline \Delta y_m(t) \end{array}\right] = \left[\begin{array}{c|c} \bar{A}_{pm} & \bar{B}_{pm} \\ \hline \bar{C}_{pm} & 0 \end{array}\right] \left[\begin{array}{c} \Delta x_{pm}(t) \\ \hline \Delta u_m(t) \end{array}\right], \tag{33}$$

$$\bar{A}_{pm} = A_{pm} + \sum_{i=1}^{r} N_{pmi}(u_i^{\mathrm{o}} + \Delta u_i^{\mathrm{o}}), \quad \bar{B}_{pm} = B_{pm}, \quad \bar{C}_{pm} = C_{pm}.$$

Then, the problem of PID controller tuning for bilinear plant (28) reduces to Problem 1, and we can apply *LQ* optimal controller tuning algorithm described in Subsection 4.1 to solve it.

4.3 *H*2 Optimal Tuning of Fixed-Structure Controller

To evaluate the squared $\mathcal{H}_2$ norm of difference between the transfer functions of the adjusted and reference closed-loop systems, we need the following result.

Lemma 1: Let $W(s) = (A,B,C)$ be the strictly proper transfer function of a stable dynamic system of order n without multiple poles. Let (A,B,C)-realization of the transfer function $W(s)$ be the minimal realization. Then the following relations hold

$$\|W(s)\|_2^2 = \sum_{i=1}^{n} W^{+}(s_{i-}) \mathfrak{Res}\, W^{-}(s_{i-}) = \sum_{i=1}^{n} \left. \frac{M^{+}(s)M^{-}(s)}{Q^{+}(s)\frac{d}{ds}Q^{-}(s)} \right|_{s_i = s_{i-}}, \tag{34}$$

$$\|W(s)\|_2^2 = \sum_{i=0}^{n} \frac{\sum_{\lambda=0}^{n}\left\{ s_{i-}^{\lambda} \sum_{j=\lambda+1}^{n} a_j C A^{j-\lambda-1} B \right\} \sum_{\lambda=0}^{n}\left\{ (-1^{\lambda}) s_{i-}^{\lambda} \sum_{j=\lambda+1}^{n} a_j C A^{j-\lambda-1} B \right\}}{\sum_{j=0}^{n}\left\{ a_j s_{i-}^{j} \sum_{j=0}^{n}\left\{ j a_j s_{i-}^{j} \sum_{j=0}^{n} (-1)^j a_j s_{i-}^{j} \right\}\right\}}, \tag{35}$$

where s_{i+} are the poles of the main system, s_{i-} are the poles of the adjoint system, that is, $s_{i+} = (-1)\cdot s_{i-}$, a_j are the coefficients of the characteristic polynomial of the matrix A,

$$W^+(s) = \frac{M^+(s)}{Q^+(s)}, \qquad W^-(s) = \frac{M^-(s)}{Q^-(s)},$$
$$M^+(s) = M(s),\ Q^+(s) = Q(s), \qquad M^-(s) = M(s)\big|_{s=-s},\ Q^-(s) = Q(s)\big|_{s=-s},$$
$$Q^+(s_{i+}) = 0, \qquad Q^-(s_{i-}) = 0.$$

Proof: When the Lemma 1 assumptions hold true, we have for the main and adjoint systems

$$W^+(s) = C(sI-A)^{-1}B = \frac{M^+(s)}{Q^+(s)},\quad W^-(s) = C(-sI-A)^{-1}B = \frac{M^-(s)}{Q^-(s)}. \tag{36}$$

As is well known, the resolvent of the matrix A has the following series expansion (Strejc, 1981):

$$(sI-A)^{-1} = \frac{1}{\sum_{i=0}^{n} a_i s^i} \sum_{j=0}^{n-1} s^j \sum_{i=j+1}^{n} a_i A^{i-j-1}. \tag{37}$$

Substitution of (37) into (36) gives

$$M^+(s) = \sum_{j=0}^{n-1} s^j \sum_{i=j+1}^{n} a_i C A^{i-j-1} B,\quad Q^+(s) = \sum_{i=0}^{n} a_i s^i, \tag{38}$$

$$M^-(s) = \sum_{j=0}^{n-1} (-1)^j s^j \sum_{i=j+1}^{n} a_i C A^{i-j-1} B,\quad Q^-(s) = \sum_{i=0}^{n} (-1)^i a_i s^i. \tag{39}$$

By definition of $\mathcal{H}_2$ norm,

$$\|W(s)\|_2^2 = \frac{1}{2\pi}\int_{-\infty}^{+\infty} W(-j\omega)W(j\omega)d\omega.$$

Since by assumption the integration element in the last integral is strictly proper rational function, let us apply the Theorem of Residues forming closed contour $\mathfrak{C}$ consisting of the imaginary axis and semicircle with infinitely big radius and center at the origin at the right half of the complex plain. Inside of this contour, there are only isolated singularities defined by the roots of the characteristic equation $Q^-(s) = 0$ of the adjoint system. It follows that

$$\frac{1}{2\pi}\int_{-\infty}^{+\infty} W(-j\omega)W(j\omega)d\omega = \sum_{i=1}^{n} \frac{M^+(s)M^-(s)}{Q^-(s)\frac{d}{ds}Q^+(s) + Q^+(s)\frac{d}{ds}Q^-(s)}\Bigg|_{s_i = s_{i-}}$$
$$= \sum_{i=1}^{n} \frac{M^+(s)M^-(s)}{Q^+(s)\frac{d}{ds}Q^-(s)}\Bigg|_{s_i = s_{i-}} = \sum_{i=1}^{n} W^+(s_{i-})\mathfrak{Res}\,W^-(s_{i-}).$$

Applying (38), (39), we obtain expression (35).

Correctness of the following equalities in notation of Section 2 can be proved by direct substitution:

$$W(s)-W_m(s)=\frac{M_o(s)Q_{om}(s)-M_{om}(s)Q_o(s)}{Q_o(s)Q_{om}(s)}=\frac{F_o(s)}{Q_o(s)Q_{om}(s)}, \tag{40}$$

$$\Phi(s)-\Phi_m(s)=\frac{F_o(s)}{(Q_o(s)+M_o(s))(Q_{om}(s)+M_{om}(s))}. \tag{41}$$

It is obvious that if the adjusted system is completely adaptable then $F_o(s)\equiv 0$ and

$$\operatorname{Arg}\min_G J_1=\operatorname{Arg}\min_G J_2.$$

The following Theorem answer the question: Whether this equality retains when the system is not completely adaptable?

Theorem 2: Let plant (1) be completely controllable and observable, the transfer functions $P(s)=(A_p,B_p,C_p)$ and $K(s)=(A_c,B_c,C_c,D_c)$ be strictly proper rational functions with no multiple and right poles. Then the following statements hold true:

1. The necessary minimum conditions for functionals J_1 and J_2 coincides and are given by either

$$LG-N=0 \tag{42}$$

   or $LG-N\neq 0$, but

$$L^{\mathrm{T}}(LG-N)=0. \tag{43}$$

2. If equation (42) has a unique solution, then the necessary minimum condition is also sufficient.
3. The optimal controller tuning algorithms for functionals J_1 and J_2 coincide and are given by

$$G^*=L^+N. \tag{44}$$

Proof: Applying Lemma 1 and equality (41), we obtain

$$J_2=\sum_{i=1}^{n_p+n_c}\frac{F_o^+(s)}{R_o^+(s)R_{om}^+(s)}\frac{F_o^-(s)}{R_{om}^-(s)\frac{d}{ds}R_o^-(s)}\Bigg|_{s=s_{i-}^c}+\sum_{i=1}^{n_p+n_c}\frac{F_o^+(s)}{R_o^+(s)R_{om}^+(s)}\frac{F_o^-(s)}{R_{om}^-(s)\frac{d}{ds}R_o^-(s)}\Bigg|_{s=s_{mi-}^c}, \tag{45}$$

where $R_o(s)=Q_o(s)+M_o(s)$ and $R_{om}(s)=Q_{om}(s)+M_{om}(s)$ are the characteristic polynomials of closed-loop system and its implicit reference model (superscripts " + " and " − " are used for the main and adjoint systems, respectively), s_{i-}^c and s_{mi-}^c are the poles of the adjoint system and its reference model. Denoting

$$S^+(s)=\begin{bmatrix}1 & s & s^2 & \cdots & s^{2n_c+n_p-1}\end{bmatrix},\ S^-(s)=\begin{bmatrix}1 & -s & s^2 & \cdots & (-1)^{2n_c+n_p-1}s^{2n_c+n_p-1}\end{bmatrix},$$

one can put down

$$\frac{\partial}{\partial G}(W(s)-W_m(s))=\frac{1}{N_o(s)N_{om}(s)}\frac{\partial}{\partial G}F_o(s)=\frac{1}{N_o(s)N_{om}(s)}\frac{\partial\operatorname{tr}\{S(s)(LG-N)\}}{\partial G}=\frac{L^{\mathrm{T}}S^{\mathrm{T}}(s)}{N_o(s)N_{om}(s)}. \tag{46}$$

Applying expressions (40), (45), and (46) to the transfer functions and characteristic polynomials of the main and adjoint systems, we have

$$\frac{\partial J_2}{\partial G} = \left(\frac{\partial J_2}{\partial G}\right)_I + \left(\frac{\partial J_2}{\partial G}\right)_{II}, \tag{47}$$

where

$$\begin{aligned}\left(\frac{\partial J_2}{\partial G}\right)_I &= \sum_{i=1}^{n_p+n_c} \left\{ \frac{\frac{\partial}{\partial G} F_o^+(s)}{R_o^+(s) R_{om}^+(s)} \frac{F_o^-(s)}{R_{om}^-(s) \frac{d}{ds} R_o^-(s)} + \frac{F_o^+(s)}{R_o^+(s) R_{om}^+(s)} \frac{\frac{\partial}{\partial G} F_o^-(s)}{R_{om}^-(s) \frac{d}{ds} R_o^-(s)} \right\} \Bigg|_{s=s_{i-}^c} \\ &+ \sum_{i=1}^{n_p+n_c} \left\{ \frac{\frac{\partial}{\partial G} F_o^+(s)}{R_o^+(s) R_{om}^+(s)} \frac{F_o^-(s)}{R_o^-(s) \frac{d}{ds} R_{om}^-(s)} + \frac{F_o^+(s)}{R_o^+(s) R_{om}^+(s)} \frac{\frac{\partial}{\partial G} F_o^-(s)}{R_o^-(s) \frac{d}{ds} R_{om}^-(s)} \right\} \Bigg|_{s=s_{mi-}^c},\end{aligned} \tag{48}$$

$$\begin{aligned}\left(\frac{\partial J_2}{\partial G}\right)_{II} &= \sum_{i=1}^{n_p+n_c} \left\{ \frac{F_o^+(s) F_o^-(s)}{(R_o^+(s))^2 R_{om}^+(s)} \frac{\frac{\partial}{\partial G} R_o^+(s)}{R_{om}^-(s) \frac{d}{ds} R_o^-(s)} - \frac{F_o^+(s) F_o^-(s)}{R_o^+(s) R_{om}^+(s)} \frac{\frac{\partial}{\partial G} \frac{d}{ds} R_o^-(s)}{R_{om}^-(s) (\frac{d}{ds} R_o^-(s))^2} \right\} \Bigg|_{s=s_{i-}^c} \\ &- \sum_{i=1}^{n_p+n_c} \left\{ \frac{\frac{\partial}{\partial G} R_o^+(s)}{(R_o^+(s))^2 R_{om}^+(s)} \frac{F_o^+(s) F_o^-(s)}{R_o^-(s) \frac{d}{ds} R_{om}^-(s)} - \frac{F_o^+(s) F_o^-(s)}{R_o^+(s) R_{om}^+(s)} \frac{\frac{\partial}{\partial G} \frac{d}{ds} R_o^-(s)}{R_o^-(s) (\frac{d}{ds} R_{om}^-(s))^2} \right\} \Bigg|_{s=s_{mi-}^c}.\end{aligned} \tag{49}$$

With (45) and (46) in mind, denoting

$$H(s) = \operatorname{diag}\left\{(-1)^{j-1} s^{2(j-1)}\right\},$$

let us transform expressions (48), (49) into

$$\begin{aligned}\left(\frac{\partial J_2}{\partial G}\right)_I = &\left\{ \sum_{i=1}^{n_p+n_c} \left\{ \frac{1}{R_o^+(s) R_{om}^+(s)} \frac{H(s)}{R_{om}^-(s) \frac{d}{ds} R_o^-(s)} + \frac{1}{R_o^+(s) R_{om}^+(s)} \frac{H(s)}{R_{om}^-(s) \frac{d}{ds} R_o^-(s)} \right\} \Bigg|_{s=s_{i-}^c} \right. \\ &\left. + \sum_{i=1}^{n_p+n_c} \left\{ \frac{1}{R_o^+(s) R_{om}^+(s)} \frac{H(s)}{R_o^-(s) \frac{d}{ds} R_{om}^-(s)} + \frac{1}{R_o^+(s) R_{om}^+(s)} \frac{H(s)}{R_o^-(s) \frac{d}{ds} R_{om}^-(s)} \right\} \Bigg|_{s=s_{mi-}^c} \right\} \cdot 2L^{\mathrm{T}}(LG - N),\end{aligned} \tag{50}$$

$$\begin{aligned}\left(\frac{\partial J_2}{\partial G}\right)_{II} &= \sum_{i=1}^{n_p+n_c} \left\{ \frac{(LG-N)^{\mathrm{T}}}{(R_o^+(s))^2 R_{om}^+(s)} \frac{H(s) \frac{\partial}{\partial G} R_o^+(s)(LG-N)}{R_{om}^-(s) \frac{d}{ds} R_o^-(s)} \right\} \Bigg|_{s=s_{i-}^c} \\ &- \sum_{i=1}^{n_p+n_c} \left\{ \frac{(LG-N)^{\mathrm{T}}}{R_o^+(s) R_{om}^+(s)} \frac{H(s) \frac{\partial}{\partial G} \frac{d}{ds} R_o^-(s)(LG-N)}{R_{om}^-(s) (\frac{d}{ds} R_o^-(s))^2} \right\} \Bigg|_{s=s_{i-}^c} \\ &- \sum_{i=1}^{n_p+n_c} \left\{ \frac{(LG-N)^{\mathrm{T}}}{(R_o^+(s))^2 R_{om}^+(s)} \frac{H(s) \frac{\partial}{\partial G} R_o^+(s)(LG-N)}{R_o^-(s) \frac{d}{ds} R_{om}^-(s)} \right\} \Bigg|_{s=s_{mi-}^c} \\ &- \sum_{i=1}^{n_p+n_c} \left\{ \frac{(LG-N)^{\mathrm{T}}}{R_o^+(s) R_{om}^+(s)} \frac{H(s) \frac{\partial}{\partial G} \frac{d}{ds} R_o^-(s)(LG-N)}{R_o^-(s) (\frac{d}{ds} R_{om}^-(s))^2} \right\} \Bigg|_{s=s_{mi-}^c}.\end{aligned} \tag{51}$$

For the numerator polynomial of the open-loop system we have

$$M_o(s) = \frac{LG}{\sum_{i=0}^{n_c} a_{mi} s^i}.$$

Differentiating the last expression, we obtain

$$\frac{\partial}{\partial G} M_o^+(s) = S_1^+(s) L^{\mathrm{T}},\ \frac{\partial}{\partial G} M_o^-(s) = S_1^-(s) L^{\mathrm{T}},\ \frac{\partial}{\partial G}\frac{d}{ds} M_o^+(s) = T^+(s) L^{\mathrm{T}},\ \frac{\partial}{\partial G}\frac{d}{ds} M_o^-(s) = T^-(s) L^{\mathrm{T}},$$

where

$$S_1^+(s) = \mathrm{diag}\left\{\frac{s^{j-1}}{\sum_{i=0}^{n_c} a_{mi} s^i}\right\},\quad S_1^-(s) = \mathrm{diag}\left\{\frac{(-1)^{j-1} s^{j-1}}{\sum_{i=0}^{n_c} a_{mi} s^i}\right\},$$

$$T^+(s) = \frac{d}{ds} S_1^+(s) = \mathrm{diag}\left\{(j-1)s^{j-2} - \frac{s^{j-1}\sum_{i=0}^{n_c} i a_{mi} s^{i-1}}{\left\{\sum_{i=0}^{n_c} a_{mi} s^i\right\}^2}\right\},$$

$$T^-(s) = \frac{d}{ds} S_1^-(s) = \mathrm{diag}\left\{(-1)^{j-1}(j-1)s^{j-2} - \frac{(-1)^{j-1} s^{j-1}\sum_{i=0}^{n_c} i a_{mi} s^{i-1}}{\left\{\sum_{i=0}^{n_c} a_{mi} s^i\right\}^2}\right\}.$$

Using these formulas, it is not hard to obtain

$$\begin{aligned}\left(\frac{\partial J_2}{\partial G}\right)_{II} = & \sum_{i=1}^{n_p+n_c}\left\{\frac{(LG-N)^{\mathrm{T}}}{(R_o^+(s))^2 R_{om}^+(s)}\frac{H(s)S(s)L^{\mathrm{T}}(LG-N)}{R_{om}^-(s)\frac{d}{ds}R_o^-(s)}\right\}\Bigg|_{s=s_{i-}^c} \\ & -\sum_{i=1}^{n_p+n_c}\left\{\frac{(LG-N)^{\mathrm{T}}}{R_o^+(s)R_{om}^+(s)}\frac{H(s)T^-(s)L^{\mathrm{T}}(LG-N)}{R_{om}^-(s)(\frac{d}{ds}R_o^-(s))^2}\right\}\Bigg|_{s=s_{i-}^c} \\ & -\sum_{i=1}^{n_p+n_c}\left\{\frac{(LG-N)^{\mathrm{T}}}{(R_o^+(s))^2 R_{om}^+(s)}\frac{H(s)S(s)L^{\mathrm{T}}(LG-N)}{R_o^-(s)\frac{d}{ds}R_{om}^-(s)}\right\}\Bigg|_{s=s_{mi-}^c} \\ & -\sum_{i=1}^{n_p+n_c}\left\{\frac{(LG-N)^{\mathrm{T}}}{R_o^+(s)R_{om}^+(s)}\frac{H(s)S_1^-(s)L^{\mathrm{T}}(LG-N)}{R_o^-(s)(\frac{d}{ds}R_{om}^-(s))^2}\right\}\Bigg|_{s=s_{mi-}^c}.\end{aligned} \tag{52}$$

From (50) and (52) it follows that all terms of sum (47) are the products of the complex matrices being the values of the complex-valued diagonal matrices with compatible dimensions in the poles of the adjoint closed-loop system and its reference model and the matrix factors of the form $L^{\mathrm{T}}(LG-N)$ and $(LG-N)^{\mathrm{T}}$. Since the complex-valued matrix factors cannot be identically zero on the set Σ, the necessary conditions for minimum of the functional J_2 are given by (42) or (43) and coincide with the necessary minimum conditions for the functional J_1. Thus, the first statement of the Theorem is proved.

Let equation (43) have a unique solution for any given point of the plant parameter set Σ. Then this solution is given by (44) and determines one of the local minimums of the functionals J_1 and J_2. The analytic expressions for the functionals J_1 and J_2 include as factors the polynomials $F_o^+(s)$ and $F_o^-(s)$ that equal to zero according to (7). Since equality (42) holds true, conditions (21) hold and, consequently, the mentioned minimums must be global and coinciding. This proves the second and third statements of the Theorem.
The tuning procedure determined by (44) gives the solution to unconstrained minimization problem for the criteria J_1 and J_2. But it does not guarantee stability of the adjusted system for the whole set Σ.
The main drawback of this tuning algorithm consists in that the direct control of stability margin of the adjusted system is impossible. This drawback can be partially weakened by evaluating the characteristic polynomial of the closed-loop system or its roots. Let us consider another approach to managing the mentioned drawback.

5. H_2 Tuning of Fixed-Structure Controller with H_∞ Constraints

The most well-known and, perhaps, the most efficient approach to solving this problem is the direct minimization of $\mathcal{H}_\infty$ norm of transfer function of the adjusted system on the base of loop-shaping (McFarlane & Glover, 1992; Tan et al., 2002). The main advantages of this approach consist in the direct solution to the controller tuning problem via synthesis, simplicity of the design procedure subject to internally contradictory criteria of stability and performance, as well as good interpretation of engineering design methods.
Drawbacks consist in need for design of pre- and post-filters complicating the controller structure, as well as in optimization result dependence on chosen initial approach. Bounded Real Lemma allows expressing boundedness condition for $\mathcal{H}_\infty$ norm of transfer function of the adjusted system in terms of linear matrix inequality for rather common assumptions on the control system properties (Scherer, 1990). Consider application of Bounded Real Lemma to forming linear constraint for the constrained optimization problem.
The feature of mixed tuning problem statement is that the linear constraints guarantee some stability margin, but not performance, since it is assumed that performance can be provided by proper choice of matrices of the implicit reference model, and then performance can only be maintained by means of adaptive controller tuning.
The problem statement is as follows. Let us consider the closed-loop system consisting of plant (1) and fixed-structure controller (2)

$$\Phi(s): \quad \left[\begin{array}{c} \dot{x}_{\text{cl}}(t) \\ \hline y(t) \end{array}\right] = \left[\begin{array}{c|c} A_{\text{cl}} & B_{\text{cl}} \\ \hline C_{\text{cl}} & 0 \end{array}\right] \left[\begin{array}{c} x_{\text{cl}}(t) \\ \hline g(t) \end{array}\right] \tag{53}$$

with

$$\left[\begin{array}{c|c} A_{\text{cl}} & B_{\text{cl}} \\ \hline C_{\text{cl}} & 0 \end{array}\right] = \left[\begin{array}{cc|c} A_p - B_p D_c C_p & B_p C_{cm} & B_p D_c \\ -B_c C_p & A_{cm} & B_c \\ \hline C_p & 0 & 0 \end{array}\right],$$

and the closed-loop reference model

$$\Phi_m(s): \quad \left[\begin{array}{c}\dot{x}_{\mathrm{cl}m}(t) \\ \hline y_m(t)\end{array}\right] = \left[\begin{array}{c|c} A_{\mathrm{cl}m} & B_{\mathrm{cl}m} \\ \hline C_{\mathrm{cl}m} & 0 \end{array}\right] \left[\begin{array}{c} x_{\mathrm{cl}m}(t) \\ \hline g(t)\end{array}\right], \tag{54}$$

$$\|\Phi_m(s)\|_\infty < \gamma_m. \tag{55}$$

We are interested in finding the controller parameters B_c and D_c such that

$$J_2 = \|\Phi(s) - \Phi_m(s)\|_2 \to \min_{B_c, D_c}, \tag{56}$$

$$\|\Phi(s)\|_\infty < \gamma \tag{57}$$

$\forall A_p, B_p, C_p \in \Sigma$ and the matrix A_{cl} be Hurwitz.
By virtue of Theorem 2, the necessary condition for minimum of functional (56) is

$$L^{\mathrm{T}} L \begin{bmatrix} B_c^{\mathrm{T}} & D_c \end{bmatrix}^{\mathrm{T}} - L^{\mathrm{T}} N = 0 \tag{58}$$

$\forall A_p, B_p, C_p \in \Sigma.$ According to Bounded Real Lemma (Scherer, 1990), condition (57) holds true if and only if there exists a solution $X = X^{\mathrm{T}} > 0$ to matrix inequality

$$\begin{bmatrix} XA_{\mathrm{cl}} + A_{\mathrm{cl}}^{\mathrm{T}} X & XB_{\mathrm{cl}} & C_{\mathrm{cl}}^{\mathrm{T}} \\ B_{\mathrm{cl}}^{\mathrm{T}} X & -\gamma I & 0 \\ C_{\mathrm{cl}} & 0 & -\gamma I \end{bmatrix} < 0. \tag{59}$$

Matrix inequality (59) is not linear and jointly convex in variables X, B_c, and D_c. In order to pass from inequality (59) to LMI constraints, let us use a technique similar to (Gahinet & Apkarian, 1994; Balandin & Kogan, 2007). Define the matrix of the controller parameters

$$\Theta = \begin{bmatrix} A_{cm} & B_c \\ C_{cm} & D_c \end{bmatrix}$$

and represent the closed-loop system matrices as

$$A_{\mathrm{cl}} = A_0 + B\Theta C, \quad B_{\mathrm{cl}} = B_0 + B\Theta D_1, \quad C_{\mathrm{cl}} = C_0 + D_2 \Theta C,$$

$$A_0 = \begin{bmatrix} A_p & 0 \\ 0 & 0 \end{bmatrix}, \quad B_0 = 0, \quad C_0 = \begin{bmatrix} C_p & 0 \end{bmatrix}, \quad B = \begin{bmatrix} 0 & B_p \\ I & 0 \end{bmatrix}, \quad C = \begin{bmatrix} 0 & I \\ -C_p & 0 \end{bmatrix}, \quad D_1 = \begin{bmatrix} 0 \\ I \end{bmatrix}, \quad D_2 = 0.$$

Substitute these expressions into (59) and represent the resulting inequality as linear matrix inequality with respect to Θ:

$$\Psi + P^{\mathrm{T}} \Theta^{\mathrm{T}} Q + Q^{\mathrm{T}} \Theta P < 0, \tag{60}$$

$$\Psi = \begin{bmatrix} A_0^{\mathrm{T}} X + XA_0 & 0 & C_0^{\mathrm{T}} \\ 0 & -\gamma I & 0 \\ C_0 & 0 & -\gamma I \end{bmatrix}, \quad P = \begin{bmatrix} C & D_1 & 0 \end{bmatrix}, \quad Q = \begin{bmatrix} B^{\mathrm{T}} X & 0 & 0 \end{bmatrix}.$$

According to Projection Lemma (Gahinet & Apkarian, 1994), inequality (60) is solvable with respect to the matrix Θ if and only if

$$W_P^{\mathrm{T}}\begin{bmatrix} A_0^{\mathrm{T}}X+XA_0 & 0 & C_0^{\mathrm{T}} \\ 0 & -\gamma I & 0 \\ C_0 & 0 & -\gamma I \end{bmatrix}W_P<0,\ \ W_Q^{\mathrm{T}}\begin{bmatrix} A_0^{\mathrm{T}}X+XA_0 & 0 & C_0^{\mathrm{T}} \\ 0 & -\gamma I & 0 \\ C_0 & 0 & -\gamma I \end{bmatrix}W_Q<0, \tag{61}$$

where the columns of the matrices W_P and W_Q form the respective bases of $\operatorname{Ker}P$ and $\operatorname{Ker}Q$. To eliminate the unknown matrix X from the matrix Q, let us represent

$$Q=R\begin{bmatrix} X & 0 & 0 \\ 0 & I & 0 \\ 0 & 0 & I \end{bmatrix},\ \ R=\begin{bmatrix} B^{\mathrm{T}} & 0 & 0 \end{bmatrix},$$

from which it follows that

$$W_Q=\begin{bmatrix} X^{-1} & 0 & 0 \\ 0 & I & 0 \\ 0 & 0 & I \end{bmatrix}W_R.$$

Substituting this expression into (61) and denoting $Y=X^{-1}$, we obtain the following result.

Theorem 3: Given $\gamma>0$, fixed-structure controller (2) providing minimum for the tuning functional J_2 and ensuring condition (57) exists if and only if there exist the inverse matrices $X=X^{\mathrm{T}}>0$ and $Y=Y^{\mathrm{T}}>0$ such that

$$W_P^{\mathrm{T}}\begin{bmatrix} A_0^{\mathrm{T}}X+XA_0 & 0 & C_0^{\mathrm{T}} \\ 0 & -\gamma I & 0 \\ C_0 & 0 & -\gamma I \end{bmatrix}W_P<0,\ \ W_R^{\mathrm{T}}\begin{bmatrix} A_0Y+YA_0^{\mathrm{T}} & 0 & YC_0^{\mathrm{T}} \\ 0 & -\gamma I & 0 \\ C_0Y & 0 & -\gamma I \end{bmatrix}W_R<0,\ \ XY=I. \tag{62}$$

If conditions (62) hold true, and the matrices X and Y are found, the controller parameters B_c and D_c are defined from solution of linear matrix inequality (60) subject to equality constraint (58).

Denote that further simplification of (62) via respective choice of the matrices W_P and W_R is possible (see, e.g., Gahinet & Apkarian, 1994), but this is not required by the numerical algorithm for solving linear matrix inequalities with respect to inverse matrices presented in (Balandin & Kogan, 2005).

Taking into account the block structure of the controller matrix Θ that includes constant and variable blocks, let us consider some aspects of solving inequality (60). Let the matrix X satisfying (62) be found. Partition it into the blocks

$$X=\begin{bmatrix} X_{11} & X_{12} \\ X_{12}^{\mathrm{T}} & X_{22} \end{bmatrix}$$

in accordance with the orders of plant and controller. Then

$$\Psi = \begin{bmatrix} A_p^{\mathrm{T}} X_{11} + X_{11} A_p & A_p^{\mathrm{T}} X_{12} & 0 & C_p^{\mathrm{T}} \\ X_{12}^{\mathrm{T}} A_p & 0 & 0 & 0 \\ 0 & 0 & -\gamma I & 0 \\ C_p & 0 & 0 & -\gamma I \end{bmatrix}, \tag{63}$$

$$P = \begin{bmatrix} 0 & I & 0 & 0 \\ -C_p & 0 & I & 0 \end{bmatrix}, \quad Q = \begin{bmatrix} X_{12}^{\mathrm{T}} & X_{22} & 0 & 0 \\ B_p^{\mathrm{T}} X_{11} & B_p^{\mathrm{T}} X_{12} & 0 & 0 \end{bmatrix},$$

$$Q^{\mathrm{T}} \Theta P = \begin{bmatrix} -(X_{12} B_c + X_{11} B_p D_c) C_p & X_{12} A_{cm} + X_{11} B_p C_{cm} & X_{12} B_c + X_{11} B_p D_c & 0 \\ -(X_{22} B_c + X_{12}^{\mathrm{T}} B_p D_c) C_p & X_{22} A_{cm} + X_{12}^{\mathrm{T}} B_p C_{cm} & X_{22} B_c + X_{12}^{\mathrm{T}} B_p D_c & 0 \\ 0 & 0 & 0 & 0 \\ 0 & 0 & 0 & 0 \end{bmatrix}. \tag{64}$$

Substituting (63) and (64) into (60), one can obtain linear matrix inequality with respect to the unknown controller parameters B_c and D_c.

Thus, the procedure of $\mathcal{H}_2$ optimal controller tuning with $\mathcal{H}_\infty$ constraints consists of two stages. At the first stage, one need find two inverse positive-definite matrices X and Y satisfying (62) with $\gamma = \gamma_m$. At the second stage, when the matrices X and Y are obtained, the controller parameters B_c and D_c can be found from linear matrix inequality (60), (63), (64) subject to equality constraint (58). Numerical solution to linear matrix inequality subject to linear equality constraints can be obtained using Matlab software toolbox SeDuMi Interface (Peaucelle, 2002).

For the purpose of numerical illustration, let us give a simple numerical example.

Example 2: Consider the problem of a first-order controller tuning for a second-order unstable linear oscillator. The reference model is given by (5), (6) with

$$\left[\begin{array}{c|c} A_{pm} & B_{pm} \\ \hline C_{pm} & 0 \end{array}\right] = \left[\begin{array}{cc|c} 0 & 1 & 1 \\ -100 & 0.3 & 0 \\ \hline 1 & 0 & 0 \end{array}\right], \quad \left[\begin{array}{c|c} A_{cm} & B_{cm} \\ \hline C_{cm} & D_{cm} \end{array}\right] = \left[\begin{array}{c|c} -23.33604 & -2.54 \cdot 10^{-5} \\ \hline -9.09 \cdot 10^{-7} & 31.62046 \end{array}\right], \tag{65}$$

at that $\lambda_{1,2}(A_{pm}) = 0.15 \pm 9.9989 j$. The reference model controller $K_m(s)$ is a solution to the following $\mathcal{H}_\infty$ suboptimal problem: find fixed-order controller (6) for plant (5) guaranteeing internal stability of reference closed-loop system (54) and fulfilment of condition (55) with $\gamma_m = 1.02$ (Balandin & Kogan, 2007). In this example, we consider the actual plant given by (1) with two sets of parameters:

$$\left[\begin{array}{c|c} A_p & B_p \\ \hline C_p & 0 \end{array}\right] = \left[\begin{array}{cc|c} 0 & 1 & 0.6 \\ -140 & 0.5 & 0 \\ \hline 1.4 & 0 & 0 \end{array}\right], \quad \lambda_{1,2}(A_p) = 0.25 \pm 11.8295 j, \tag{66}$$

and

$$\left[\begin{array}{c|c} A_p & B_p \\ \hline C_p & 0 \end{array}\right] = \left[\begin{array}{cc|c} 0 & 1 & 1.4 \\ -60 & 0.1 & 0 \\ \hline 0.6 & 0 & 0 \end{array}\right], \quad \lambda_{1,2}(A_p) = 0.05 \pm 7.7458j. \tag{67}$$

Given controller structure and order ($A_c = A_{cm}$, $C_c = C_{cm}$), we are interested in finding the matrices B_c and D_c such that conditions (56), (57) hold with $\gamma = \gamma_m$.
At the first stage of tuning process described above we have obtained the following numerical solutions to dual LMI (56) with $\gamma = \gamma_m = 1.02$:

$$X = \begin{bmatrix} 0.0754 & -0.0003 & -0.0304 \\ -0.0003 & 0.0005 & -0.0001 \\ -0.0304 & -0.0001 & 1.0646 \end{bmatrix}, \quad Y = \begin{bmatrix} 13.4456 & 6.9922 & 0.3846 \\ 6.9922 & 1836.7693 & 0.3456 \\ 0.3846 & 0.3456 & 0.9503 \end{bmatrix}$$

for plant (1) with realization (65) and

$$X = \begin{bmatrix} 0.0687 & -0.0001 & 0.0000 \\ -0.0001 & 0.0011 & 0.0000 \\ 0.0000 & 0.0000 & 1.0000 \end{bmatrix}, \quad Y = \begin{bmatrix} 14.5580 & 1.4755 & 0.0000 \\ 1.4755 & 873.4150 & 0.0000 \\ 0.0000 & 0.0000 & 1.0000 \end{bmatrix}$$

for plant (1) with realization (66).
At the second stage, solving LMI (60), (63), (64) subject to equality constraint (58) we have obtained the controller

$$\left[\begin{array}{c|c} A_{cm} & B_c^* \\ \hline C_{cm} & D_c^* \end{array}\right] = \left[\begin{array}{c|c} -23.33604 & -104.30004 \\ \hline -9.09 \cdot 10^{-7} & 52.71044 \end{array}\right] \tag{68}$$

for realization (66) and

$$\left[\begin{array}{c|c} A_{cm} & B_c^* \\ \hline C_{cm} & D_c^* \end{array}\right] = \left[\begin{array}{c|c} -23.33604 & -1.44589 \cdot 10^{-7} \\ \hline -9.09 \cdot 10^{-7} & 17.71328 \end{array}\right] \tag{69}$$

for realization (67). Denote that controller (68) results in $\|\Phi(s)\|_\infty = 1.0125 < \gamma = 1.02,$ and controller (69) results in $\|\Phi(s)\|_\infty = 1.0069 < \gamma = 1.02.$
Simulation results for reference system (65), as well as for actual plants (66), (67) with controllers (68), (69), respectively, are presented in Fig. 1. The left red-coloured diagrams correspond to plant (66) and controller (68), whereas the right blue-coloured diagrams show transients and control for plant (67) and controller (69). The diagrams for the reference system are shown in black colour. At the top diagrams, the step responces of reference and actual plants are presented. The middle plots show the step responces of closed-loop reference and actual systems. The control signals generated by reference and adjusted controllers are given at the bottom diagrams. One can denote good visual proximity of step responces of the reference and adjusted closed-loop systems at the middle diagrams.

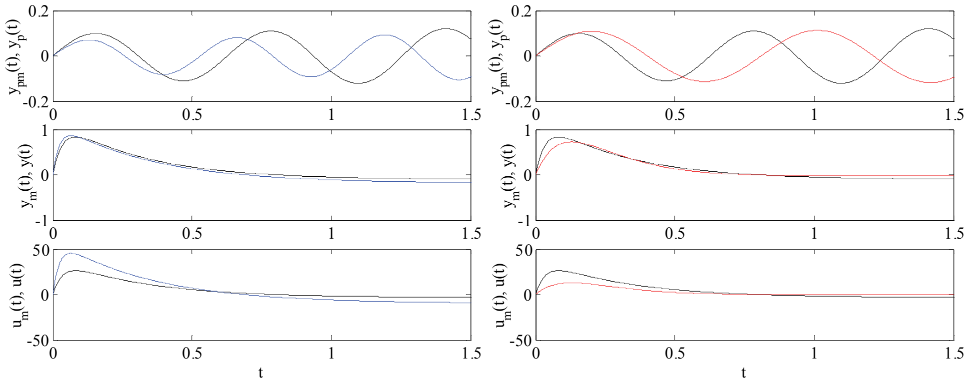

Figure 1. Step responces and control for reference and actual systems

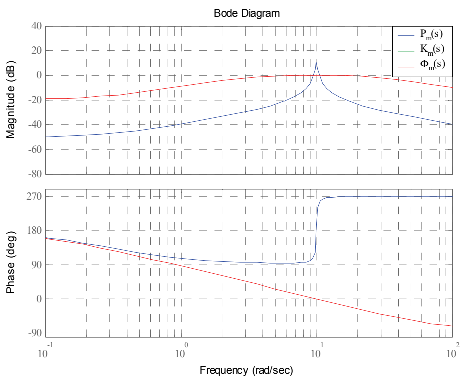

Figure 2. Bode diagram for reference system

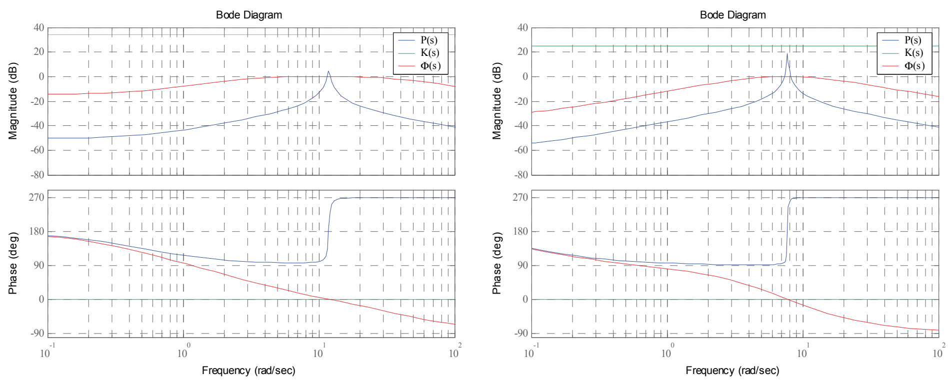

Figure 3. Bode diagrams for actual systems

The Bode diagrams for the reference and actual systems are shown in Fig. 2 and Fig. 3, correspondingly, including diagrams for plants (blue lines), controllers (green lines), and closed-loop systems (red lines). At Fig. 3, the left plots correspond to plant (66) and controller (68), the right plots represent plant (67) and controller (69).

6. Conclusion

One of the main results of this Chapter consists in that the necessary minimum conditions for the functional given by $\mathcal{H}_2$ norm of the difference between the transfer functions of the closed-loop adjusted and reference systems coincide with the necessary minimum conditions for Frobenius norm of the controller tuning polynomial generated by these transfer functions that have been obtained earlier.

Theorem 2 shows that in spite of complexity of analytic expressions for the "direct" tuning functionals J_1 and J_2, optimal values of the adjusted parameters can be found via comparatively simple pseudosolution of linear matrix algebraic equation. This approach ensures proximity of transient responses of the adjusted and reference systems and, consequently, the best (in sense of $\mathcal{H}_2$ norm) stability of performance indicies of the adjusted system.

The properties of complete, partial, and weak adaptability of a system with respect to its output belongs to the system invariants. The adaptability criteria, just as Kalman's criteria of controllability and observability, are formulated in terms of rank properties of the adaptability matrices. One of the main properties of the adaptabilty matrices is Toeplitz property.

Although $\mathcal{H}_2$ norm in functional J_2 is defined for the closed-loop systems, the elements of the adaptability matrices depend only on the coefficients of the characteristic polynomials, matrices and matrix coefficients of the resolvent series expansions of the plant, controller, and their reference models. An advantage of finding optimal controller parameters via the mentioned pseudosolution consists in that individual plant poles can be unstable on condition that all poles of adjusted closed-loop system are stable.

The main drawback of LQ and $\mathcal{H}_2$ optimal tuning algorithms consists in that the direct control of stability margin of the adjusted system is impossible. This drawback can be partially weakened by evaluating the characteristic polynomial of the closed-loop system or its roots. This drawback can be eliminated by use of $\mathcal{H}_2$ optimal tuning algorithm together with $\mathcal{H}_\infty$ constraint.

Another one important result of this Chapter consists in the presented $\mathcal{H}_2$ optimal fixed-structure controller tuning algorithm with $\mathcal{H}_\infty$ constraint for SISO systems represented by minimal state-space realization that can be easily extended onto MIMO systems. This approach is based on minimization of $\mathcal{H}_2$ criterion of proximity of transient responses of the closed-loop system and its implicit reference model subject to constraint onto $\mathcal{H}_\infty$ norm of the transfer function of the closed-loop system formulated in terms of LMIs.

The obtained algorithms of optimal tuning of multiloop PID controller for bilinear MIMO plant have the same structure as the similar algorithms for linear MIMO plant (Morozov & Yadykin, 2004; Yadykin & Tchaikovsky, 2007). However, the optimal tuning procedures for the bilinear plant are more complex than similar procedures for the linear plant:

- Identification procedures for bilinear plants depend on operating point of the process, increment of piecewise-constant control, and its sign in various combinations. This gives rise to need in considering many modes of identification and tuning.

- The models of bilinear plant and reference system, as well as tuning criteria and algorithms have to be matched.
- Dynamics of transients in the adjusted system depends on the sign and magnitude of the test control increment. For positive increments, the transients, in general, accelerate and their decrement decrease, whereas for negative increments the transient decrement increase and it decelerate.

The obtained results can be also considered as a solution to the controller design problem for linear time invariant SISO and MIMO systems on the base of the constrained minimization of $\mathcal{H}_2$ norm of the difference between the transfer functions of the closed-loop designed and reference systems subject to constraint onto $\mathcal{H}_\infty$ norm of the transfer function of the designed system established in terms of LMIs.

7. References

Astrom, K.J. & Hagglund, T. (2006). *Advanced PID Control*, ISA — The Instrumentation, Systems, and Automation Society

Balandin, D.V. & Kogan, M.M. (2005). An optimization algorithm for checking feasibility of robust $\mathcal{H}_\infty$ control problem for linear time-varying uncertain systems. *Int. J. of Control*, Vol. 77, No. 5, 498-503

Balandin, D.V. & Kogan, M.M. (2007). *Synthesis of Control Laws on the Base of Linear Matrix Inequalities*. Nauka, Moscow (in Russian)

Bao, J., Forbse, J.F. & McLennan, P. (1999). Robust multiloop PID controller design: a successive semidefinite programming approach. *Ind. & Eng. Chem. Res.*, Vol. 38, 3407-3413

Bernstein, D.S. (2005). *Matrix Mathematics: theory, Facts, and Formulas with Application to Linear Systems Theory*. Princeton University Press, New Jersey

Datta, A. (1998). *Adaptive Internal Model Control*, Springer-Verlag, Berlin

Datta, A., Ho., M.T. & Bhattacharrya, S.P. (2000). *Structure and Synthesis of PID Controller*, Springer-Verlag, Berlin

Gahinet, P. & Apkarian, P. (1994). A linear matrix inequality approach to $\mathcal{H}_\infty$ control. *Int. J. on Robust and Nonlinear Control*, Vol. 4, 421-448

Gantmacher, F.R. (1959). *The Theory of Matrices*, Vol. I and Vol. II, Chelsea, New York.

Hjalmarsson, H. (2002). Iterative feedback tuning — overview. *Int. J. of Adaptive Control and Signal Processing*, Vol. 16, No. 5, 373-395

McFarlane, D. & Glover, K. (1992). A loop shaping design procedure using $\mathcal{H}_\infty$ synthesis. *IEEE Trans. AC*, Vol. 37, No. 6, 759-769

Morozov, M.V. & Yadykin, I.B. (2004). Adaptability analysis and controller optimal tuning method for MIMO bilinear systems. *Proceedings of 2nd IFAC Symposium on System, Structure, and Control*, pp. 561-566, Oaxaca, Mexico, December 2004

Peaucelle, D., Henrion, D. & Labit, Y. (2002) *User's Guide for SeDuMi Interface 1.01: Solving LMI Problems with SeDuMi*. LAAS-CNRS, Toulouse, France

Petrov, B.N. & Rutkovskiy, V.Yu. (1965). Double invariance of automatic regulation systems. *Doklady Akademii Nauk SSSR*, Vol. 24, No. 6, 789-790 (in Russian)

Poznyak, A.S. (1991). *Basics of Robust Control ($\mathcal{H}_\infty$ Theory)*. MPTI Publishing, Moscow (in Russian)

Rotach, V.Ya., Kuzischin, V.F. & Klyuev, A.S., et al. (1984). *Automation of Control System Tuning*, Energoatomizdat, Moscow (in Russian)

Scherer, C. (1990). *The Riccati Inequality and State-Space* $\mathcal{H}_\infty$*-optimal Control*. Ph.D. Dissertation. University Wursburg, Germany

Strejc, V. (1981). *State-Space Theory of Discrete Linear Control*. Academia, Prague

Tan, W., Chen, T. & Marques, H.J. (2002). Robust controller design and PID tuning for multivariable processes. *Asian J. of Control*, Vol. 4, 439-451

Yadykin, I.B. (1981). Regulator adptability in adaptive control systems. *Soviet Physics Doklady*, Vol. 26, No. 7, 641

Yadykin, I.B. (1983). Controller adaptability and two-level algorithms of adjustment of adaptive control system parameters. *Automation and Remote Control*, Vol. 44, No. 5, 617-686

Yadykin, I.B. (1985). Optimal tuning of linear controllers. *Soviet Physics Doklady*, Vol. 20, No. 11, 914

Yadykin, I.B. (1999). On the Toeplitz properties of adaptability matrices. *Automation and Remote Control*, Vol. 60, No. 12, 1782-1790

Yadykin, I.B. & Tchaikovsky, M.M. (2007). PID controller tuning for bilinear continuous time invariant MIMO system. *Proceedings of 3rd IFAC Symposium on System, Structure, and Control*, Foz do Iguassu, Brazil, October 2007

Yadykin, I.B. (2008). $\mathcal{H}_2$ optimal tuning algorithms for controller with fixed structure. *Automation and Remote Control* (to appear)

Zhou, K., Doyle, J.C. & Glover, K. (1996). *Robust and Optimal Control*. Prentice Hall, New York

11

A Sampled-data Regulator using Sliding Modes and Exponential Holder for Linear Systems

B. Castillo-Toledo[1], S. Di Gennaro[2] and A. Loukianov[1]
[1]*Centro de Investigación y de Estudios Avanzados del I.P.N, Unidad Guadalajara,*
[3]*Department of Electrical Engineering and Information and Center of Excellence DEWS, University of L'Aquila*
[1]*México,* [3]*Italy*

Abstract

In a general command tracking and disturbance rejection problem, it is known that a sampled-data controller using zero-order hold may only guarantee asymptotic tracking at the sampling instances, but in general cannot guarantee the absence of ripples between the sampling instants. In this paper, a discrete robust regulator and a sampled-data robust regulator using slide modes techniques and exponential holder are presented. In particular, it is shown that the controller proposed for the sampled-data system ensures asymptotic tracking when applied to the continuous-time system.

1. Introduction

The extensive use of digital computers has introduced a great flexibility on the implementation of control laws but has also, in some cases, given rise to some problems related to the dynamic behavior to the coupling of continuous-time systems with digital devices via A/D and D/A converters. In fact, when a control law is implemented via digital devices, two ways are possible. The first is to design a continuous control law and use sufficiently small sampling periods with respect to the plant dynamics, to approximate by a discrete system the original continuous controller. The second approach consists in discretizing the plant dynamics and to design a digital control law on the basis of the sampled measurements. The output of the digital controller is then converted to continuous signal generally using zero orders holders. This second solution is in general more adequate since some of the structural properties may be ensured, even if only at the sampling instants, since in the intersampling time the system is in open-loop. In particular, for nonconstant reference signals, a digital control law applied via zero order holders to a continuous time system may cause the presence of ripple in the output tracking error signal. This means that the asymptotic output tracking is guaranteed only at the sampling instants, where the steady-state output error is zero. This can be explained by the fact that a necessary and sufficient condition for guaranteeing a ripple-free tracking is that an internal model of the reference and/or disturbance is present in the controller structure ([2], [3], [5], [11]). Clearly, when using zero-order holders, it is not possible to reconstruct the internal model, except for the constant signals.

For sampled-data linear systems, in [5] among others, a hybrid controller was presented; pointing out that a continuous internal model is necessary and sufficient to provide ripple-free response. Along the same lines, in [4], a hybrid robust controller consisting of a discrete-time linear controller and an analog linear immersion which guarantees a ripple free behavior was presented. In [6] a more general setting using a so-called exponential holder for nonlinear systems was presented.
Based on these ideas, in this work we present a ripple-free sampled-data robust regulator with sliding modes control scheme for linear systems. We formulate the design of a robust controller on the basis of sampling a continuous-time linear systems and then introducing the sliding mode approach, which permits to guarantee the stabilization property relaxing the requirements of the existence of a linear stabilizing control law and using the exponential holder to guarantee the existence of the internal model inside the controller structure... The paper is organized as follows: in Section 2 we give some preliminaries on the robust regulator by sliding modes techniques, while in Section 3 we introduce the main result of the paper. Section 4 is devoted to an illustrative example and finally, some conclusions are drawn.

2. Basic results on Robust Regulation

A central problem in control theory is that of manipulating the inputs of a system in such a way that the outputs track, at least asymptotically, a defined reference signals, preserving at the same time some desired stability property of the close-loop system. In [14], a discontinuous regulator using a sliding modes control technique is proposed, where the underlying idea is to design a sliding surface on which the dynamics of the system are constrained to evolve by means of a discontinuous control law, instead of designing a continuous stabilizing feedback, as in the case of the classical regulator problem. The sliding surface is constructed with the steady-state surface, and the state of the system is forced to reach the sliding surface in finite time with a sliding control.
To precise the ideas, let us consider a continuous-time linear system described by

$$\dot{x}(t) = Ax(t) + Bu(t) + Pw(t) \tag{1}$$

$$\dot{w}(t) = Sw(t) \tag{2}$$

$$e(t) = Cx(t) - Rw(t) \tag{3}$$

where $u \in \Re^m$ is the input signal, $x \in \Re^n$ is the state of the system, $w \in \Re^p$ represents the state of an external signal generator, described by (2), which provides the reference and/or perturbation signals. Equation (3) describes the output tracking error $e \in \Re^q$ defined as the difference between the system output and the reference signal.
For this system, the mentioned problem has been treated under different approaches, among which is the regulator theory by sliding modes techniques. In general terms, this problem consists in finding a submanifold (the steady state submanifold) on which the output tracking error is zeroed, as well as an input signal (the steady state input) which makes this submanifold invariant and attractive. The sliding regulator problem approach has been studied in the linear case ([Louk:99],[Louk:99b]).

Since we are concerned with a discrete controller, the discretization of the continuous system (1)-(3) can be described by

$$\begin{aligned} x_{k+1} &= A_d x_k + B_d u_k + P_d w_k \\ w_{k+1} &= S_d w_k \\ e_k &= C x_k - R w_k \end{aligned}$$

where

$$A_d = e^{\delta A} = \sum_{i=0}^{\infty} \frac{\delta^i}{i!} A^i;$$

$$B_d = \int_0^{\delta} e^{sA} B ds = \sum_{i=0}^{\infty} \frac{\delta^i}{i!} A^{i-1} B;$$

$$S_d = e^{\delta S} = \sum_{i=0}^{\infty} \frac{\delta^i}{i!} S^i;$$

$$C_d = C; R_d = R; P_d = \int_0^{\delta} e^{sA} P ds = \sum_{i=0}^{\infty} \frac{\delta^{i+1}}{(i+1)!} P_i;$$

where P_i can be computed iteratively from

$$P_0 = P; P_i = AP_{i-1} + PS^i; i = 1, 2, ...$$

The classical **Robust Regulator Problem with Measurement of the Output** for system (1)-(3) consists in finding a dynamic controller

$$\begin{aligned} \dot{\xi}(t) &= F\xi(t) + Ge(t) \\ u &= H_e \xi(t) \end{aligned}$$

such that the following requirements hold:

S) The equilibrium point $(x, \xi) = (0, 0)$ of the closed loop system without disturbances

$$\begin{aligned} \dot{x}(t) &= Ax(t) + BH_e \xi(t) \\ \dot{\xi}(t) &= F\xi(t) + GCx(t) \end{aligned}$$

is exponentially stable.

R) For each initial condition (x_0, w_0, ξ_0) , the dynamics of the system

$$\begin{aligned}
\dot{x}(t) &= Ax(t) + BH_e\xi(t) + Pw(t) \\
\dot{\xi}(t) &= F\xi(t) + G(Cx(t) - Rw(t)) \\
\dot{w}(t) &= Sw(t)
\end{aligned}$$

satisfy that

$$\lim_{t\to\infty} e(t) = 0.$$

A solution to this problem can be found in [1]. This solution is stated in terms of the existence of mappings $x_{ss} = \Pi w; \xi_{ss} = \Sigma w$ satisfying the Francis equations

$$\begin{aligned}
\Pi S &= A\Pi + BH_e\Sigma + P \\
\Sigma S &= F\Sigma \\
0 &= C\Pi - R
\end{aligned} \tag{4}$$

for all admissible values of the systems parameters. More precisely, the solution can be stated in terms of the existence of mappings $x_{ss} = \Pi w, u_{ss} = \Gamma w$ solving the equations

$$\Pi S = A\Pi + B\Gamma + P \tag{5}$$

$$0 = C\Pi - R \tag{6}$$

from which we reckon

$$\Sigma = \begin{pmatrix} \Gamma \\ \Gamma S \\ \vdots \\ \Gamma S^{q-1} \\ -a_0\Gamma - a_1\Gamma S - .... - a_{q-1}\Gamma S^{q-1} \end{pmatrix}$$

where the polynomial

$$s^q + a_{q-1}s^{q-1} + ... + a_1 s + a_0 = 0$$

is the characteristic polynomial of S. The mapping $x_{ss} = \Pi w$ represents the steady state zero output subspace and $u_{ss} = \Gamma w$ is the steady-state input which make invariant that subspace. This steady-state input can be generated, independently of the values of the parameters of the system and thanks to the Cayley-Hamilton Theorem, by the linear dynamical system

$$\dot{\eta} = \Phi \eta \tag{7a}$$

$$u_{ss} = H\eta \tag{7b}$$

where $\Phi = diag\{\Phi_1, \ldots \Phi_m\}; H = diag\{H_1, \ldots, H_m\}$ and

$$\Phi_i = \begin{pmatrix} 0 & 1 & 0 & \cdots & \\ 0 & 0 & 1 & \cdots & 0 \\ \vdots & \vdots & \vdots & \ddots & \vdots \\ 0 & 0 & 0 & \cdots & 1 \\ -a_0 & -a_1 & -a_2 & \cdots & -a_{q-1} \end{pmatrix};$$

$$H_i = (1 \quad 0 \quad \cdots \quad 0)_{1\times q}.$$

Defining the transformation $z_1 = x - \Pi w; z_2 = \eta,$ the system can be rewritten as

$$\dot{z}_1 = Az_1 - BHz_2 + Bu \tag{8}$$

$$\dot{z}_2 = \Phi z_2 \tag{9}$$

$$e(t) = \begin{bmatrix} C & 0 \end{bmatrix} \begin{bmatrix} z_1 \\ z_2 \end{bmatrix} \tag{10}$$

Finally, a controller which solves the problem can be constructed as an observer for system (8)-(9), namely

$$\begin{aligned} \dot{\xi}_1 &= (A_0 - G_1 C_0)\xi_1 - B_0 H \xi_2 + B_0 u + G_1 e \\ \dot{\xi}_2 &= -G_2 C_0 \xi_1 + \Phi \xi_2 + G_2 e \\ u &= K\xi_1 + H\xi_2 \end{aligned} \tag{11}$$

where A_0, B_0, C_0 are the nominal values of the matrices of the system (1)-(3) and K and G_1, G_2 make stable the matrices $(A_0 + B_0 K)$ and

$$\begin{pmatrix} A_0 & -B_0 H \\ 0 & \Phi \end{pmatrix} - \begin{pmatrix} G_1 \\ G_2 \end{pmatrix} \begin{pmatrix} C_0 & 0 \end{pmatrix}. \tag{12}$$

When dealing with controllers implemented via digital devices and zero order holders, the sampled data version of the controller could render unstable the closed-loop system. In this work we will take the approach of designing a hybrid controller consisting in two parts: a discrete sliding mode controller ensuring the stabilization of the closed-loop system, and a continuous part containing the internal model dynamics (internal model) obtained from the continuous model.

3. The Continuous Sliding Robust Regulator

Analogously to the case of the Robust Regulator Problem, we formulate the ***Sliding Mode Robust Regulator Problem*** ([13], [14], [15]) as the problem of finding a sliding surface

$$\sigma = \sigma(\xi) = 0,\ \sigma = col(\sigma_1(\xi),...,\sigma_m(\xi)) \tag{13}$$

and a dynamic compensator

$$\dot{\xi} = g(\xi, e) \tag{14}$$

with the control action defined as

$$u_i = \begin{cases} u_i^+(\xi) & \sigma_i(\xi) > 0 \\ u_i^-(\xi) & \sigma_i(\xi) < 0 \end{cases}, \quad i = 1,...,m \tag{15}$$

where the mappings $u_i^+(\xi)$, $u_i^-(\xi)$ and $\sigma_i(\xi)$ are calculated in order to induce an asymptotic convergence to the sliding surface $\sigma_i(\xi) = 0$ and such that, for all admissible parameter values in a suitable neighborhood $\mathcal{P}$ of the nominal parameter vector, the following conditions hold:

(**SS** c) The equilibrium point $(x,\xi) = (0,0)$ of the closed-loop system is asymptotically stable.

(**SM** c) The sliding surface is attractive, namely the state of the closed loop system converges to the manifold $\sigma(\xi) = 0$.

(**SR** c) The output tracking error tends asymptotically to zero, namely

$$\lim_{t\to\infty} e(t) = 0$$

Now, to introduce the sliding mode approach into the regulator problem, we will chose the control input $u(t)$ as

$$u(t) = u_{slid} + u_{eq}$$

instead of $u(t) = K\xi_1 + H\xi_2$ as taken in the controller (11), where we impose that u_{eq} must be equal to $H\xi_2$ when $\sigma(\xi) = 0$. Note that the stabilizing part $K\xi_1$ will now be substituted by the term u_{slid} which will be calculated to make attractive the sliding surface.

To be more precise, let us consider the switching surface

$$\sigma = \begin{bmatrix} \Sigma & 0 \end{bmatrix} \xi = \Sigma \xi_1, \tag{16}$$

where $\sigma \in \Re^m$, $\Sigma \in \Re^{mxn}$ with $rank \quad \Sigma B_0 = m$.
Differentiating this function, and from the first equation of (11) we reckon

$$\begin{aligned} \dot{\sigma} = \Sigma \dot{\xi}_1 &= \Sigma[(A_0 - G_1 C_0)\xi_1 - B_0 H \xi_2 + B_0 u + G_1 e] \\ &= \Sigma(A_0 - G_1 C_0)\xi_1 - \Sigma B_0 H \xi_2 + \Sigma B_0 u + \Sigma G_1 e \end{aligned}$$

from which the equivalent control u_{eq} is obtained from the condition $\dot{\sigma} = 0$ as

$$u_{eq} = -(\Sigma B_0)^{-1} \Sigma \left[(A_0 - G_1 C_0)\xi_1 - B_0 H \xi_2 + G_1 e \right]$$

Defining the estimation errors as $\varepsilon_1 = z_1 - \xi_1$ and $\varepsilon_2 = z_2 - \xi_2$, we may substitute u_{eq} into equation (8) at the nominal values of the parameters to get the sliding motion dynamics

$$\dot{z}_1 = [I_n - B_0(\Sigma B_0)^{-1}\Sigma] A_0 z_1 + B_0(\Sigma B_0)^{-1}\Sigma(A_0 - G_1 C_0)\varepsilon_1 - B_0 H \varepsilon_2$$

where the estimation errors satisfy the dynamics

$$\begin{aligned} \dot{\varepsilon}_1 &= (A_0 - G_1 C_0)\varepsilon_1 - B_0 H \varepsilon_2 \\ \dot{\varepsilon}_2 &= -G_2 C_0 \varepsilon_1 + \Phi \varepsilon_2. \end{aligned}$$

Note that these dynamics are asymptotically stable thanks to the observability assumption of matrix (12).

Lemma 1. [14] *Define the operator* D *as* $D = (I_n - B(\Sigma B)^{-1}\Sigma)$ *. Then the relation*

$$D(A\Pi - \Pi S + P) = 0 \tag{17}$$

is true if and only if there exist matrices Π *and* Γ *such that*

$$A\Pi - \Pi S + P = B\Gamma. \tag{18}$$

Proof. The operator D is a projection operator along the rank of B over the null space of Σ [16], namely

$$\begin{aligned} DB &= (I_n - B(\Sigma B)^{-1}\Sigma)B = 0 \\ Dz_1 &= z_1 \quad \forall z_1 \in \aleph, \aleph = \{z_1 \in \Re^n \mid \Sigma z_1 = 0\} \end{aligned}$$

Thus, if condition (18) holds, then it follows that $D(A\Pi - \Pi S + P) = DB\Sigma = 0.$ Conversely, if condition (17) holds, then $(A\Pi - \Pi S + D)$ must be in the image of B this is, $(A\Pi - \Pi S + D) = B\Gamma$ for some matrix Γ. ■

A condition for the solution of the Sliding Mode Regulator Problem can be given in the following result.

Proposition 2. *Assume the following assumptions:*

H1) *The matrix* S *has all its eigenvalues on the imaginary axis*

H2) *The pair* (A_0, B_0) *is stabilizable*

H3) *The pair* $\begin{bmatrix} C_0 & 0 \end{bmatrix}, \begin{bmatrix} A_0 & -B_0 H \\ 0 & \Phi \end{bmatrix}$ *is observable.*

Then the Sliding Mode Regulator Problem is solvable if there exists a matrix Π *solving the equations*

$$A\Pi - \Pi S + P = -B\Gamma \tag{19}$$

$$C\Pi - R = 0 \tag{20}$$

for some matriz Γ, *and or all admissible values of the system parameters.*

Proof . Let us choose the control as

$$u = -Msign(\sigma) + u_{eq},$$

with $M = diag(m_i); m_i > 0,$ and $sign(\sigma) = [sign(\sigma_1), ..., sign(\sigma_m)]^T$. This control action guarantees a sliding mode motion on the surface $\sigma = 0.$ Then, assuming that the observer estimation error decays rapidly by appropriate choice of the gains G_1, G_2 we have that

$$\dot{z}_1 = DA_0 z_1 \,|_{\Sigma z_1 = 0}$$

Since the matrix Σ by assumption H2 can be chosen such that ΣB is invertible, and the $(n-m)$ eigenvalues of DA_0 can be arbitrarily placed in C^-, then $z_1(t) \to 0$ as $t \to \infty$ satisfying condition (**SS** $_c$). Now, since the tracking error equation is given by $e(t) = C_0 z_1(t),$ then it follows that $e(t)$ goes to zero asymptotically, satisfying condition (**SR** $_c$). ■

Note that when the state of the system is on the sliding surface, the control signal is exactly u_{eq} which in turn comes to be $u_{eq} = H\xi_2 = u_{ss}$, namely, the steady-state input. This steady -state input guarantees that the output tracking error stays at zero. This property will be used later.

4. A Sliding Robust Regulator for Discrete Systems

For the discrete case, the problem can be formulated in a similar way to the continuous case. To this end, let us consider the discretization of system (8)-(10), this is

$$\begin{bmatrix} z_{1,k+1} \\ z_{2,k+1} \end{bmatrix} = \begin{bmatrix} A_d & -\Lambda \\ 0 & \Phi_d \end{bmatrix} \begin{bmatrix} z_{1,k} \\ z_{2,k} \end{bmatrix} + \begin{bmatrix} B_d \\ 0 \end{bmatrix} u_k \tag{21}$$

$$e_k = \begin{bmatrix} C_d & 0 \end{bmatrix} \begin{bmatrix} z_{1,k} \\ z_{2,k} \end{bmatrix} \tag{22}$$

where

$$A_{d0} = e^{A_0 T}, \Lambda = \int_0^T e^{A\theta} B_0 H d\theta,\ C_{d0} = C_0$$
$$\Phi_d = e^{\Phi T}, u(kT+\theta) = u(kT);$$
$$B_{d0} = \int_0^T e^{A_0\theta} B_0 d\theta,\ 0 \le \theta \le T.$$

For this system, the Sliding Regulator Problem can be set as the problem of finding a sliding surface σ_k and a dynamic controller

$$\xi_{k+1} = F_d \xi_k + G_d e_k \tag{23}$$

$$u_k = \alpha_d(\xi_k, e_k) \tag{24}$$

such that, for all admissible parameter values in a suitable neighborhood $\mathcal{P}$ of the nominal parameter vector, the following conditions hold:

(**SS**$_d$) The equilibrium point $(x,\xi) = (0,0)$ of the closed-loop system is asymptotically stable.

(**SM**$_d$) The sliding surface is attractive, namely the state of the closed loop system converges to the manifold $\sigma_k(\xi_k) = 0$.

(**SR**$_d$) For each initial condition (x_0, w_0, ξ_0), the dynamics of the closed-loop system

$$x_{k+1} = A_d x_k + B_d \alpha_d(\xi_k, e_k) + P w_k$$
$$\xi_{k+1} = F\xi_k + G(C_d x_k - R_d w_k)$$
$$w_{k+1} = S_d w_k$$

where $S_d = e^{ST}$ guarantees that $\lim_{k\to\infty} e_k = 0.$

Assume the following conditions hold:

(**H1**$_d$) All the eigenvalues of matrix S_d lie on the unitary circle.

($\mathbf{H2}_d$) The pair $\{A_{d0}, B_{d0}\}$ is stabilizable,

($\mathbf{H3}_d$) There exists a solution Π_d, Γ_d to the regulator equations

$$\Pi_d S_d = A_d \Pi_d + B_d \Gamma_d + P_d \tag{25}$$

$$0 = C_d \Pi_d - R_d \tag{26}$$

($\mathbf{H4}_d$) The pair $\begin{bmatrix} C_{d0} & 0 \end{bmatrix}, \begin{bmatrix} A_{d0} & -\Lambda \\ 0 & \Phi_d \end{bmatrix}$ is observable.

Then, a classic robust regulator can be constructed as

$$\begin{aligned} \xi_{1,k+1} &= (A_{d0} - G_{d1} C_{d0}) \xi_{1,k} - \Lambda \xi_{2,k} + B_{d0} u_k + G_{d1} e_k \\ \xi_{2,k+1} &= -G_{d2} C_{d0} \xi_{1,k} + \Phi_d \xi_{2,k} + G_{d2} e_k \\ u_k &= K_d \xi_{1,k} + H \xi_{2,k} \end{aligned} \tag{27}$$

where K_d and G_{d1}, G_{d2} make stable the matrices $(A_{d0} + B_{d0} K_d)$ and

$$\begin{pmatrix} A_{d0} & -\Lambda \\ 0 & \Phi_d \end{pmatrix} - \begin{pmatrix} G_{d1} \\ G_{d2} \end{pmatrix} \begin{pmatrix} C_{d0} & 0 \end{pmatrix}. \tag{28}$$

respectively.
For the Discrete Sliding Regulator Problem, we can chose a sliding surface

$$\sigma_k = \begin{bmatrix} \Sigma_d & 0 \end{bmatrix} \xi_k = \Sigma_d \xi_{1,k}, \tag{29}$$

and calculate the equivalent control. The following result, which can be proved similarly to the continuous case, gives a solution to the Discrete Sliding Regulator Problem:

Proposition 3. *Assume that assumptions* $H1_d$ *through* $H4_d$ *hold. Then the Discrete Sliding Regulator Problem is solvable. Moreover, the controller solving the problem can be chosen as*

$$u_k = u_{eq,k} = -(\Sigma_d B_{d0})^{-1} \Sigma_d \left[(A_{d0} - G_{d1} C_{d0}) \xi_{1,k} - \Lambda \xi_{2,k} + G_{d1} e_k \right].$$

Proof. Calculating

$$\begin{aligned} \sigma_{k+1} &= \Sigma_d \xi_{1,k+1} \\ &= \Sigma_d [(A_{d0} - G_{d1} C_{d0}) \xi_{1,k} - \Lambda \xi_{2,k} + B_{d0} u_k + G_{d1} e_k] \end{aligned}$$

we can calculate the equivalent control from the condition $\sigma_{k+1} = 0,$ namely:

$$u_{eq,k} = -(\Sigma_d B_{d0})^{-1} \Sigma_d \left[(A_{d0} - G_{d1} C_{d0}) \xi_{1,k} - \Lambda \xi_{2,k} + G_{d1} e_k \right].$$

Note that this control makes also the sliding surface attractive, since the same control guarantees that $\sigma_{k+j} = 0$ for $j \geqslant 1$. Now, substituting u_{eq} in the first equation of (21) we obtain

$$z_{1,k+1} = [I_n - B_{d0}(\Sigma_d B_{d0})^{-1}\Sigma_d]A_{d0}z_{1,k} + B_{d0}(\Sigma_d B_{d0})^{-1}\Sigma_d(A_{d0} - G_{d1}C_{d0})\varepsilon_{1,k} - \Lambda\varepsilon_{2,k}$$

where $\epsilon_{1,k} = z_{1,k} - \xi_{1,k}$; $\epsilon_{2,k} = z_{2,k} - \xi_{2,k}$. As in the continuos case, if the gains G_{d1}, G_{d2} are appropriately chosen, the estimation errors $\epsilon_{1,k}$ and $\epsilon_{2,k}$ will converge to zero and then

$$z_{1,k+1} = DA_{d0}z_{1,k}$$

where $D = [I_n - B_{d0}(\Sigma_d B_{d0})^{-1}\Sigma_d]$. Since the matrix Σ_d by assumption H2$_d$ can be chosen such that $\Sigma_d B_{d0}$ is invertible, and the *(n-m)* eigenvalues of DA_{d0} can be arbitrarily placed inside the unitary circle, then $z_{1,k} \to 0$ as $k \to \infty$ satisfying condition (**SS**$_d$). Now, since the tracking error equation is given by $e_k = C_{d0}z_{1,k}$, then it follows that e_k goes to zero asymptotically, satisfying condition (**SR**$_d$). ■

Note that when the state of the system is on the sliding surface, the control signal is exactly u_{eq} which in turn comes to be $u_{eq} = H\xi_2 = u_{ss}$, namely, the steady-state input.

Again note that when the solution of the system is on the sliding surface, the control signal is exactly u_{eq} which in turn, since $\Lambda = B_{d0}H$, comes to be

$$u_{eq} = (\Sigma_d B_{d0})^{-1}\Sigma_d \Lambda \xi_{2,k} = H\xi_{2,k},$$

namely, the steady-state input.

Clearly, this controller guarantees zero output tracking error only at the sampling instants, but not at the intersampling. To force the output tracking error to converge to zero also in the intersampling time, in the following section we will formulate the a ripple-free sliding regulator problem.

5. A Ripple-Free Sliding Robust Regulator for Sampled Data Linear Systems

From the previous discussion it is clear that implementing a Sliding Mode Robust Regulator for the discretization of the continuous linear system, this will guarantee only that the output tracking error will be zeroed only at the sampling instant. In order to eliminate the possible ripple, it is necessary to reproduce the internal model (7) from its discrete time realization. To do this, we note that the solution of (7) can be written as $\xi(t) = e^{\Phi t}\xi(0)$, and setting $t = kT + \theta$ with $\theta \in [0, T)$ we have

$$\xi(k\delta+\theta)=e^{\Phi(k\delta+\theta)}\xi(0)=e^{\Phi\theta}e^{\Phi kT}\xi(0)$$
$$=e^{\Phi\theta}\xi(kT)$$
$$u_{ss}(kT+\theta)=H\xi(kT+\theta)=He^{\Phi\theta}\xi(kT)$$

which describe *exactly* the behavior also in the intersampling. The term $e^{\Phi\theta}$ is known as the ***exponential holder***.
We can now formulate the **Ripple-Free Sliding Robust Regulator Problem** as the problem of finding a sliding surface

$$\sigma_k=\Sigma\xi_k \tag{30}$$

and a dynamic controller

$$\xi_{k+1}=F\xi_k+Ge_k \tag{31}$$

$$u(kT+\theta)=\alpha\left(\xi_k,\theta,e_k\right); \tag{32}$$
$$0\le\theta\le T.$$

such that, for all admissible parameter values in a suitable neighborhood $\mathcal{P}$ of the nominal parameter vector, the following conditions hold:

(**SS** r **)** The equilibrium point $\left(x_k,\xi_k\right)=\left(0,0\right)$ of the system in closed-loop is asymptotically stable.

(**SM** r) The sliding surface is attractive, namely the state of the closed loop system converges to the manifold $\sigma_k(\xi_k)=0.$

(**SR** r **)** For each initial condition $\left(x_0,w_0,\xi_0\right)$, the dynamics of the closed-loop system

$$\dot{x}(t)=Ax(t)+B\alpha\left(\xi_k,\theta,e_k\right)+Pw(t)$$
$$\xi_{k+1}=F\xi_k+G(C_dx_k-R_dw_k)$$
$$\dot{w}(t)=Sw(t)$$

guarantees that

$$\lim_{t\to\infty}e(t)=0.$$

In order to solve the Ripple-Free Sliding Robust Regulator Problem, the following assumptions will be considered:

H1) The matrix S has all its eigenvalues on imaginary axis

H2) The pair (A_0,B_0) is stabilizable

H3) The equations (5), (6) have solution Π,Γ for all admissible values of the system parameters.

H4) The pair $\begin{bmatrix} C_d & 0 \end{bmatrix}$, $\begin{bmatrix} A_d & -M_d \\ 0 & \Phi_d \end{bmatrix}$ is detectable, where $M_d = \int_0^T e^{A_0(T-\theta)} B_0 H e^{\Phi\theta} d\theta.$

For this case, and taking the previous results, we now state the following result.

Theorem 4. *Let us assume assumptions H1) to H4) hold. Then the* ***RFSRRP*** *is solvable. Moreover, the controller which solves the problem is given by*

$$\begin{aligned} \xi_{1,k+1} &= (A_{d0} - G_{d1}C_{d0})\xi_{1,k} - M_d\xi_{2,k} + B_{d0}u_k + G_{d1}e_k \\ \xi_{2,k+1} &= -G_{d2}C_{d0}\xi_{1,k} + \Phi_d\xi_{2,k} + G_{d2}e_k \\ u_k &= -(\Sigma_d B_{d0})^{-1}\Sigma_d\left[(A_{d0} - G_{d1}C_{d0})\xi_{1,k} - B_{d0}He^{\Phi\theta}\xi_{2,k} + G_{d1}e_k\right] \end{aligned} \tag{33}$$

Proof. In order to implement the discretized controller, we consider again the transformed continuous system

$$\dot{z}_1 = Az_1 - BHz_2 + Bu \tag{34}$$

$$\dot{z}_2 = \Phi z_2 \tag{35}$$

$$e(t) = \begin{bmatrix} C & 0 \end{bmatrix}\begin{bmatrix} z_1 \\ z_2 \end{bmatrix} \tag{36}$$

$$\dot{w} = Sw. \tag{37}$$

Substituting u_k in the equation (34) gives:

$$\dot{z}_1 = Az_1 - BHz_2 - B(\Sigma_d B_{d0})^{-1}\Sigma_d \times \\ \left[(A_{d0} - G_{d1}C_{d0})\xi_{1,k} - B_{d0}He^{\Phi\theta}\xi_{2,k} + G_{d1}e_k\right]$$

whose discretization, together with that of (35) is be given by

$$\begin{aligned} z_{1,k+1} &= [I_n - B_{d0}(\Sigma_d B_{d0})^{-1}\Sigma_d]A_{d0}z_{1,k} + \\ &+ B_{d0}(\Sigma_d B_{d0})^{-1}\Sigma_d(A_{d0} - G_{d1}C_{d0})\varepsilon_{1,k} - \Lambda\varepsilon_{2,k} \\ z_{2,k+1} &= \Phi_d z_{2.k}. \end{aligned}$$

As in the case of discrete sliding regulator, an observer may be constructed as

$$\begin{aligned} \xi_{1,k+1} &= (A_{d0} - G_{d1}C_{d0})\xi_{1,k} - M_d\xi_{2,k} + B_{d0}u_k + G_{d1}e_k \\ \xi_{2,k+1} &= -G_{d2}C_{d0}\xi_{1,k} + \Phi_d\xi_{2,k} + G_{d2}e_k. \end{aligned}$$

Defining a switching function as

$$\sigma_k = \begin{bmatrix}\Sigma_d & 0\end{bmatrix}\xi_k = \Sigma_d \xi_{1,k}$$

and proceeding as in the discrete case, we may show that by a proper choice of the gains $G_{d1,}G_{d2}$, the estimation errors converge to zero and the matrix $DA_d z_k$ where $D = [I_n - B_{d0}(\Sigma_d B_{d0})^{-1}\Sigma_d]$ has all the eigenvalues inside the unitary circle. Thus $e_k \to 0$ when $k \to \infty$. To see that the error is eliminated also during the interval $kT < \theta \le (k+1)T$, $k = 0,1,2,\ldots$, we observe that when $e_k = 0,$ the control law u_k is

$$\begin{aligned} u(kT+\theta) &= He^{\Phi\theta}\xi_{2,k} \\ &= H\xi_2 \end{aligned}$$

which is exactly the continuous steady-state input needing to zeroing the continuous output tracking error, so requirement SR $_r$ is also fulfilled. ■

6. An illustrative example

Consider the model of a DC motor given by:

$$\begin{aligned} \frac{dw_m}{dt} &= \frac{k_t}{J} i_a - \frac{\tau_1}{J} \\ \frac{di_a}{dt} &= -\frac{\lambda_0}{L} w_m - \frac{R}{L} i_a + \frac{1}{L} u \end{aligned}$$

where i_a is the armature current, w_m is the shaft speed, R is armature resistance, λ_o is the back-EMF constant, τ_1 is the load torque, u is the terminal voltage, J is the inertia of the motor, rotor and load, L is the armature inductance and k_t is the torque constant. Defining $x_1 = w_m$ and $x_2 = i_a$, and assuming that τ_1 is a known constant we have:

$$\begin{bmatrix} \dot{x}_1 \\ \dot{x}_2 \end{bmatrix} = \begin{bmatrix} 0 & \frac{k_t}{J} \\ -\frac{\lambda_0}{L} & -\frac{R}{L} \end{bmatrix} \begin{bmatrix} x_1 \\ x_2 \end{bmatrix} + \begin{bmatrix} 0 \\ \frac{1}{L} \end{bmatrix} u + \begin{bmatrix} -\frac{\tau}{J} \\ 0 \end{bmatrix}$$

$$\dot{w} = Sw$$

where $w=\left(w_1,w_2,w_3\right)^T$, $S=\begin{bmatrix}0&0&0\\0&0&\alpha\\0&-\alpha&0\end{bmatrix}$, $y=x_1,\ y_{ref}=w_2$, $w_1=\tau_1$ and

$L=1mH$, $R=0.5\Omega$, $J=0.001Kgm^2$, $\lambda_o=0.001V\times s\times rad^{-1}$, $\beta=0.01Nm\times s\times rad^{-1}$, $k_t=0.008NmA^{-1}$.

From this, we can calculate

$$\Phi=\begin{bmatrix}0&1&0\\0&0&1\\-a_0&-a_1&-a_2\end{bmatrix}, a_0=0, a_1=\alpha^2, a_2=0.$$

Discretizing the system with a sampling of *T=0.3 s* and choosing a reference $y_{ref}=0.1\sin(5t)$, the discrete robust controller with no exponential holder is constructed with:

$$F_d=\begin{bmatrix}-0.5399&1.0201&0&0&0\\0.0645&-0.1218&0&0&0\\-0.8072&0&0&1&0\\1.3671&0&0&0&1\\1.3775&0&1&-1.1414&1.1414\end{bmatrix}$$

$$G_d=\begin{bmatrix}1.802&0.1481&0.8072&-1.3671&-1.3775\end{bmatrix}^T$$

where

$$\Sigma_d=\begin{bmatrix}0.1194&1\end{bmatrix}, A_d=\begin{bmatrix}0.9996&2.2284\\-0.00027&0.8603\end{bmatrix}$$

$$B_d=\begin{bmatrix}0.343&0.279\end{bmatrix}^T, C_d=\begin{bmatrix}1&0\end{bmatrix}, H=\begin{bmatrix}1&0&0\end{bmatrix}$$

As is shown in Figure 1, as expected for the Discrete Sliding Regulator, the output tracking error is zero at the sampling instant, but different from zero in the intersampling times. Constructing now the controller (33) with an exponential holder we obtain

$$G_d=\begin{bmatrix}1.802&0.156&1.199&-0.992&-35.054\end{bmatrix}^T$$

$$F_d = \begin{bmatrix} -0.531 & 1.0201 & 0 & 0 & 0 \\ 0.0634 & -0.1218 & 0 & 0 & 0 \\ -1.1993 & 0 & 1 & 0.1994 & 0.0371 \\ 0.9922 & 0 & 0 & 0.0707 & 0.1994 \\ 35.0536 & 0 & 0 & -4.9874 & 0.0707 \end{bmatrix}$$

where

$$e^{\Phi\theta} = \begin{bmatrix} 1 & 0.2\sin(5\theta) & -0.04\cos(5\theta)+0.04 \\ 0 & \cos(5\theta) & 0.2\sin(5\theta) \\ 0 & -5\sin(5\theta) & \cos(5\theta) \end{bmatrix}$$

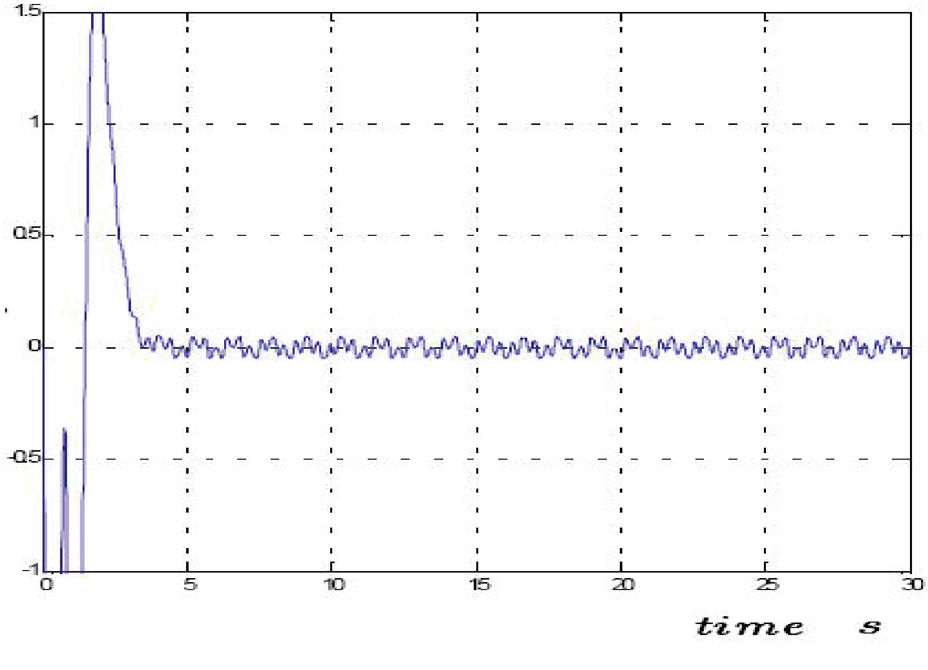

Figure 1. Output tracking error for the Discrete Sliding Robust Regulator

As shown in Figure 2, the sliding discretized controller with exponential holder present a remarkable performance guaranteeing zero output trackin error also in the intersampling.

Finally, variations on the values of the parameters ranging up to $\pm 25\%$ for R and $\pm 12\%$ for L were introduced. As may be observed in Figure 3, the controller is able to cope with these variations, maintaining the asymptotic tracking property as well.

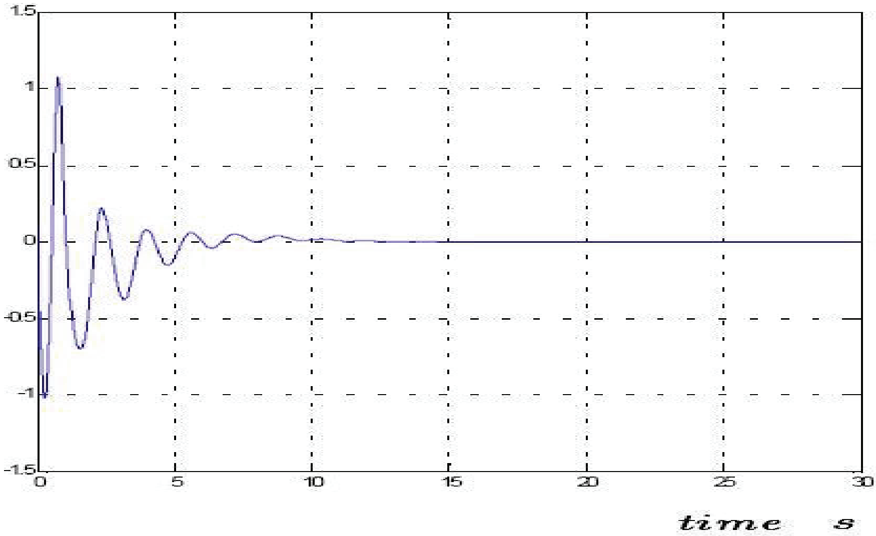

Figure 2. Output tracking error for the Ripple-Free Slidng Robust Regulator

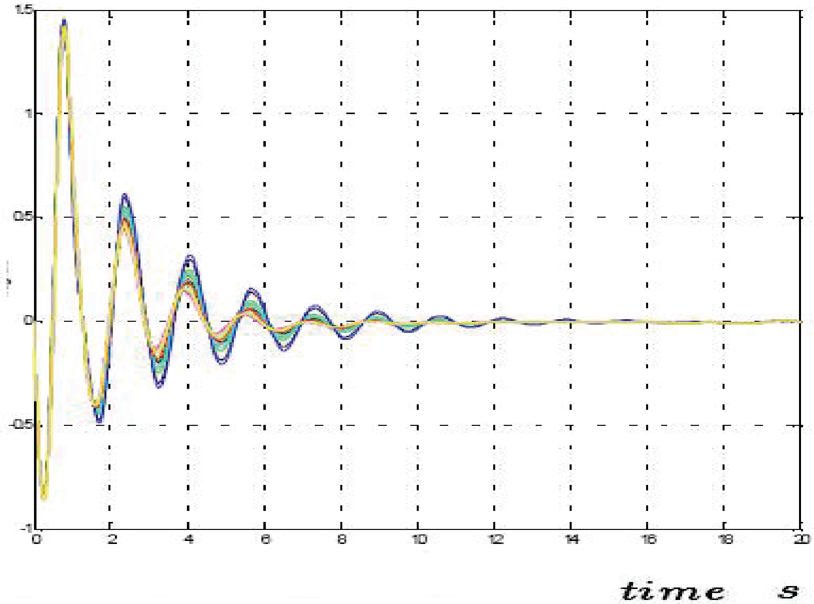

Figure 3. Output tracking error for the Ripple-Free Slidng Robust Regulator with parametric variations

7. Conclusions

In this paper, we presented an extensión to the Continuous Sliding Robust Regulator to the Dicrete case. A Ripple-Free Sliding Robust Regulator which guarantees that the output tracking error is zeroed not only at the sampling instants, but also in the intersampling behavior was alsoformulated and a solution was obtained. The controller has two components: one of them depending of the discrete dynamics of the system, and the other containing the internal model of the reference and/or perturbations generator. This feature allows the implementation of the controller on a digital device. An illustrative example shows the performance of the presented scheme.

8. Bibliography

Isidori, A., (1995), *Nonlinear Control System*. Third Edition. Ed. Springer-Verlag. [1]

Francis, B. A. and Wonham, W. M., (1976), The internal model principle of control theory. *Automatica*. Vol. 12. pp. 457-465. [2]

Francis, B.A. (1977), The linear multivariable regulator problem. SIAM J. *Control Optimiz*., Vol. 15, pp. 486-505. [3]

Yung-Chun, W., Nie-Zen, Y. (1994). A Ripple Free Sampled-Data Robust Servomechanism Controller Using Exponential Hold. *IEEE Transactions on Automatic Control*, Vol. 39, No. 6, pp. 1287-1291. [4]

Franklin, G. F. & Emami-Naeini, A. (1986), Design of Ripple Free Multivariable Robust Servomechanism, *IEEE Trans. Aut. Control*, Vol. AC-31, No. 7, pp. 661-664. [5]

Castillo-Toledo, B., Di Gennaro, S., Monaco, S. & Normand-Cyrot (1997), On regulation under sampling, *EEE Trans. Aut. Control*, Vol. 42, No. 6, pp. 864-868. [6]

Kabamba, P. T. (1987), Control of Linear Systems using generalized sample-data hold funtions, *IEEE Trans. Aut. Control*, Vol. AC-32, No. 9, pp. 772-782. [7]

Loukianov, Alexander G., Castillo-Toledo, B. and García, R. (1999) , Output Regulation in Sliding Mode , *Proc.of the American Control Conference*, pp. 1037-1041. [8]

Castillo-Toledo, B., and Di Gennaro, S. (2002), On the nonlinear ripple free sampled-data robust regulator. *Eur. J. of Contr*., Vol. 8, pp. 44- 55. [9]

Castillo-Toledo, B., and Obregon-Pulido, G. (2003). Guaranteeing asymptotic zero intersampling tracking error via a discretized regulator and exponential holder for nonlinear systems, *J. App. Reserch & Tech*. 1, pp. 203-214. [10]

Yamamoto, A., A function space approach to sampled data control systems and tracking problems, *IEEE Trans Aut. Control* (1994); 350(4), pp 703-712 [11]

Utkin, V.I. (1981), Sliding modes in control and optimization (in Russian), *Nauka*. Moscow. [12]

Loukianov, A.., Castillo-Toledo, B. and García, R. (1999) , On the sliding mode regulator problem, *Proc. of the 14th IFAC World Congress*, pp. 61-66. [13]

Utkin V., Castillo-Toledo B., Loukianov A., Espinoza-Guerra O.(2002), On robust VSS nonlinear servomechanism problem, in Variable Structure Systems: Towards the 21st Century, Springer Verlag, *Lecture Notes in Control and Information Scie ncies*, vol. 274, Berlín, , X. Yu and J-X. Xu Eds., pp. 343-363. ISBN 3 540 42965 4 [14]

V. Utkin, A. Loukianov , Castillo-Toledo B., , and J. Rivera (2004), Sliding mode regulador design, in Variable Structure Systems: from Principles to implementation, The Institution of Electrical Engineers, *IEE Control Engineering Series*, vol. 66, Sabanovi A., Fridman L and Spurgeon S. Eds., , pp. 19-44, ISBN 0 86341 350 1 [15]

El-Chesawi, O.M.E., Zinober, A.S.I., Billings, S.A. (1983), Analysis and design of variable structure systems using a geometric approach. *International Journal of Control* 38, pp. 657-671. [16]